

UNIVERSITY COLLEGE LONDON

PHD THESIS

**Efficient computation and applications of
the Calderón projector**

Matthew W. Scroggs

supervised by

Prof. Erik BURMAN & Prof. Timo BETCKE

January 20, 2020

I, Matthew William Scroggs confirm that the work presented in this thesis is my own. Where information has been derived from other sources, I confirm that this has been indicated in the thesis.

Signed _____

Date _____

ABSTRACT

The boundary element method (BEM) is a numerical method for the solution of partial differential equations through the discretisation of associated boundary integral equations. BEM formulations are commonly derived from properties of the Calderón projector, a blocked operator containing four commonly used boundary integral operators. In this thesis, we look in detail at the Calderón projector, derive and analyse a novel use of it to impose a range of boundary conditions, and look at how it can be efficiently computed. Throughout, we present computations made using the open-source software library Bempp, many features of which have been developed as part of this PhD.

We derive a method for weakly imposing boundary conditions on BEM, inspired by Nitsche’s method for finite element methods. Formulations for Laplace problems with Dirichlet, Neumann, Robin, and mixed boundary conditions are derived and analysed. For Robin and mixed boundary conditions, the resulting formulations are simpler than standard BEM formulations, and convergence at a similar rate to standard methods is observed.

As a more advanced application of this method, we derive a BEM formulation for Laplace’s equation with Signorini contact conditions. Using the weak imposition framework allows us to naturally impose this more complex boundary condition; the ability to do this is a significant advantage of this work. These formulations are derived and analysed, and numerical results are presented.

Using properties of the Calderón projector, methods of operator preconditioning for BEM can be derived. These formulations involve the product of boundary operators. We present the details of a discrete operator algebra that allows the easy calculation of these products on the discrete level. This operator algebra allows for the easy implementation of various formulations of Helmholtz and Maxwell problems, including regularised combined field formulations that are immune to ill-conditioning near eigenvalues that are an issue for other formulations.

We conclude this thesis by looking at weakly imposing Dirichlet and mixed Dirichlet–Neumann boundary condition on the Helmholtz equation. The theory for Laplace problems is extended to apply to Helmholtz problems, and an application to wave scattering from multiple scatterers is presented.

IMPACT STATEMENT

The work completed for this PhD has included development of the open-source Python boundary element method (BEM) library Bempp. Some components of this PhD—such as the implementation of an operator algebra, or the numerical investigation of preconditioning strategies—has been directly software related; other components have been more theoretical, but have been accompanied by numerical results computed using this library. As this library is open-source, it allows the research presented here to have a wide impact in both academia and industry.

The main Bempp paper [70] has received 139 citations [38] since its publication in 2015, suggesting a large userbase of the software within the academic community. All the developments presented in this thesis are accompanied by developments to the library, and example scripts on `bempp.com`. Through these, other researchers working on BEM have easy access to the results of the research presented here, allowing this work to have a quick and far-reaching impact.

Alongside the impact within academia, the inclusion of the results of this research in Bempp also has an impact outside academia. In the past few years, there have been a number of commercial collaborations involving Bempp, with companies interested in using the software for specific problems that they are interested in solving.

ACKNOWLEDGEMENTS

Note: the thankees in each section (except family) are sorted in reverse alphabetical order by surname.

I would like to start by thanking my supervisors Erik Burman and Timo Betcke for their unlimited patience, support and encouragement over the past few years, and without whom I would most certainly not be about to become a doctor.

I would like to thank Antigoni Kleanthous, Dave Hewett, and Stefan Frei for their numerous collaborations and discussions over the past few years; Garth Wells, Elwin van 't Wout, Chris Richardson, Mihai Nechita, Andrea Moiola for many helpful comments and conversations; and Wojciech Śmigaj for his work on the original version of BEM++ without which much of this PhD work would not be possible. I would like to thank Iain Smears and Ivan Graham for their helpful comments and feedback on this thesis.

I would like to thank the Department of Mathematics at UCL for all its support over the past few years. In particular, I would like to thank Helen Wilson and Robb McDonald for being the two most excellent heads of department ever; Luciano Rila for throwing more outreach and teaching opportunities my way than I ever thought possible; Helen Higgins for single-handedly keeping the entire department running; and Sukh Thiara, Sam Hopkins, Kate Fraser, Soheni Francis, and Harry Donnelly for (among more important duties) dealing with my inability to fill in forms correctly or on time.

I would like to thank Mart, Adam, Olly, Belgin, Huda, Grace, Niki, Sean, TD, Sam, and Jeanne, among others, for numerous cups of tea, cakes, lunches, and Chalky distractions.

Outside work, I would like to thank Alan for her love and support; and her, Adam (again) and Mike for so many dinners, board games, and singalongs of *Now is the Month of Maying*. Finally, I would like to thank Mum, Dad, Hannah, Jamie, Isla, Ben, Ricky, and Timber for being such a supportive family.



Figure 0: Thanks Timber. Timber.

CONTENTS

Introduction	13
1 Preliminaries	17
1.1 Function spaces	17
1.1.1 Scalar function spaces	18
1.1.2 Vector function spaces	20
1.2 Partial differential equations	22
1.3 Boundary integral operators	24
1.3.1 Laplace’s equation and the Helmholtz Equation	25
1.3.2 Laplace’s equation	28
1.3.3 The Helmholtz equation	29
1.3.4 Maxwell’s equations	30
1.4 Properties of the Calderón projector	33
2 A discrete algebra for Calderón operators and its implementation	37
2.1 Abstract formulation	39
2.2 Software implementation of an operator algebra	43
2.2.1 Grid functions	44
2.2.2 Operators	45
2.2.3 Operations on operators and grid functions	45
2.2.4 Preconditioning	46
2.2.5 Blocked operators	47
2.3 Laplace’s equation and the Helmholtz equation	48
2.3.1 Discrete spaces	48
2.3.2 Stable discretisation of the multitrace operator	52
2.3.3 Numerical results for Laplace’s equation	56
2.3.4 Numerical results for the Helmholtz equation	57
2.4 Maxwell’s equations	60
2.4.1 The electric field integral equation (EFIE)	61
2.4.2 The magnetic field integral equation (MFIE)	62
2.4.3 The combined field integral equation (CFIE)	63
2.4.4 Discrete spaces	63
2.4.5 Stable discretisation of the multitrace operator	69
2.4.6 Implementational Details	72
2.4.7 Numerical results	72
3 Weak imposition of boundary conditions	79
3.1 Weak imposition of boundary conditions on Laplace’s equation	80
3.1.1 Dirichlet boundary condition	82
3.1.2 Neumann boundary condition	83
3.1.3 Mixed Dirichlet–Neumann boundary condition	84

3.1.4	Robin conditions	85
3.2	Analysis of the Laplace single domain problem	86
3.2.1	Application of the theory to the Dirichlet problem	90
3.2.2	Application of the theory to the Neumann problem	93
3.2.3	Application of the theory to the mixed Dirichlet–Neumann problem	95
3.2.4	Application of the theory to the Robin problem	97
3.3	Numerical results	101
3.3.1	Dirichlet boundary conditions	101
3.3.2	Mixed Dirichlet–Neumann boundary conditions	106
3.3.3	Robin boundary conditions	111
4	Weak imposition of Signorini boundary conditions	117
4.1	Weak imposition of Signorini boundary conditions on Laplace’s equation	118
4.1.1	Signorini boundary conditions	119
4.1.2	Mixed Dirichlet and contact boundary conditions	120
4.2	Analysis of the weak imposition of Signorini boundary conditions	120
4.3	Numerical results	126
4.3.1	Numerical results on the unit cube	128
4.3.2	Numerical results on the unit sphere	133
5	Weak imposition of boundary conditions on the Helmholtz equation	137
5.1	Derivation of weakly imposed boundary conditions for the Helmholtz equation	137
5.1.1	Dirichlet boundary condition	138
5.1.2	Mixed Dirichlet–Neumann boundary condition	139
5.2	Analysis of weakly imposed boundary conditions for the Helmholtz equation	139
5.2.1	Application of the theory to the Helmholtz Dirichlet problem	146
5.2.2	Application of the theory to the Helmholtz mixed Dirichlet–Neumann problem	150
5.3	Numerical results for the Helmholtz equation	154
5.3.1	Dirichlet and mixed Dirichlet–Neumann problems	154
5.3.2	Application to multiple scatterers	158
5.4	Concluding remarks	160
	Concluding remarks	163
	Appendices	165
	A Notation	167
	B Convergence results for functions on the dual grid	173
B.1	Order 0 dual spaces, $\text{DUAL}_h^0(\Gamma)$	173
B.2	Order 1 dual spaces, $\text{DUAL}_h^1(\Gamma)$	180
	C Weak imposition of BCs with dual discrete spaces	183
	References	188

INTRODUCTION

For many problems arising from scientific and industrial applications, there is no known method for finding the analytic solution. In such situations, fast numerical methods capable of finding a solution to an acceptable level of accuracy are very important. The finite element method (FEM) and boundary element method (BEM) are two numerical methods that are widely used to solve PDE problems. We focus on their use for 3D problems.

Both FEM and BEM work by discretising the problem and solving a finite dimensional problem that is an approximation of the continuous problem. For FEM, the entire domain on which the PDE is posed is discretised, most commonly by splitting the domain into tetrahedra and solving an associated variational problem.

For BEM, only the boundary of the domain is discretised, most commonly by approximating the surface with flat triangles. The PDE is then written as a variational boundary integral equation, and an approximate solution is sought in the space spanned by basis functions defined on the triangles.

In order to form the boundary integral equation that is used in BEM, some knowledge of the Green's function of the underlying problem is required. This limits the variety of problems that BEM is capable of solving. FEM does not have this problem, and is capable of solving a wider variety of PDE problems.

As BEM only requires the discretisation of the boundary, it is capable of solving problems on unbounded exterior domains. This is a major advantage of BEM over FEM: such problems can be approached using FEM—for example by imposing an artificial boundary far from the object with suitable boundary conditions—but FEM is not well suited to such problems.

Additionally, generating a triangulation of a surface is in general easier than generating a tetrahedration of a domain, especially for more complicated domains. On top of this, a triangulation of the boundary of a domain will contain fewer elements, leading to smaller discrete systems that must be solved when using BEM.

When using FEM, the matrices arising from the discrete system are sparse. BEM, however, leads to dense matrices, which are more expensive to store and compute with. It is essential therefore that matrix compression techniques such as hierarchical matrices [40, 12] or fast multiple methods [36] to overcome this disadvantage of BEM.

When solving a problem, there are a number of different BEM formulations that could be used. The Calderón projector is a blocked operator that, when applied to a solution

of the problem, returns the same solution. It is common to derive the different BEM formulations from this property, and formulations often arise from taking one row of the Calderón projector. In this thesis, we instead look at applications of the full Calderón projector.

We will focus on solving the following three PDEs.

$$\begin{array}{ll} \text{Laplace's equation} & -\Delta u = 0, \\ \text{The Helmholtz equation} & -\Delta u - k^2 u = 0, \\ \text{Maxwell's equations} & \mathbf{curl\,curl}\, \mathbf{e} = k^2 \mathbf{e}. \end{array}$$

Laplace's equation is the steady-state heat equation: if the distribution of heat in a region is not changing over time, and the region contains no heat sources, then it must be a solution of Laplace's equation.

Laplace's equation is used in electrostatics to find an electric field in a source-free region [35]. As an electric field \mathbf{e} is curl-free, it can be represented as the gradient of a potential function u ,

$$\mathbf{e} = \nabla u.$$

Using Gauss's law for electric fields,

$$\nabla \cdot \mathbf{e} = -\frac{\rho}{\epsilon_0},$$

and that fact that $\rho = 0$ in a source-free region, we conclude that u must be a solution of Laplace's equation.

The Helmholtz equation is a time-harmonic version of the wave equation, and can be derived from the wave equation by assuming that the solution is separable. The Helmholtz equation models acoustic waves travelling through a medium. The unknown u represents the amplitude of the wave. The equation features the wavenumber k ; for homogeneous media, k is constant and BEM can effectively solve the problem.

BEM is commonly used to solve Helmholtz scattering problems, as these involve an incident wave scattering off a small object contained in a large, or infinite, medium. For such problems, BEM's ability to rephrase a problem in an infinite domain as a problem on the boundary of the scatterer is a great advantage.

Maxwell's equations describe the behaviour of electromagnetic waves for more general problems than those for which they can be modelled by Laplace's equation. Again the wavenumber k appears in the equation: for Maxwell problems, the wavenumber is defined to be $k := \omega \sqrt{\epsilon_0 \mu_0}$, where ω is frequency, ϵ_0 is the electric permeability, and μ_0 is the magnetic permeability.

BEM is commonly used to solve electromagnetic scattering problems, as the method has the same advantages as in the Helmholtz case. For Maxwell problems, however, there are additional significant theoretical and computational challenges. One of the greatest

challenges is the ill-conditioning of linear systems arising from the formulations, making effective preconditioning essential.

Alongside the theoretical developments presented here, work has been carried out developing Bempp, an open-source BEM Python library [70, 68]. The aim of this library is to allow the user to implement BEM for a wide range of problems by writing code that closely resembles the mathematical formulation without having to see all the technical details of the implementation. Throughout this thesis, we present the results of numerical simulations carried out using this library, and in chapter 2 we discuss the development of a discrete operator algebra within the library and its implementational advantages.

Before we look at BEM in detail, we begin by presenting some preliminary material in chapter 1. In section 1.1, we define the function spaces which will be used throughout. In section 1.2 we discuss Laplace’s equation, the Helmholtz equation, and Maxwell’s equation in more detail and look at the function spaces in which their solutions live. The boundary integral equations that we will discretise will be written using boundary integral operators; these operators will be defined and some of their properties will be given in section 1.3. In section 1.4, we look in more detail at the Calderón projector and many of its important properties.

The formulations derived in chapters 3 to 5 involve combinations of the Calderón and multitrace operators, and other blocked operators. In chapter 2, we discuss the implementation of a discrete operator algebra within Bempp, that allows the easy computation of such operator combinations. This chapter first focusses on Laplace’s equation and the Helmholtz equation (section 2.3), then looks at this operator algebra for Maxwell’s equations (section 2.4). For each PDE, it is important that the discrete spaces involved in the operator products form stable dual pairings. For Laplace’s equation and the Helmholtz equation, we use the dual spaces defined in section 2.3.1 for this. For Maxwell’s equations, we define the finite dimensional spaces that we will use in section 2.4.4, including Buffa–Christiansen dual basis functions that are an integral part of the implementation of Calderón preconditioning, a form of operator preconditioning for Maxwell’s equations.

Nitsche’s method [60] is a popular method for weakly imposing boundary condition when using FEM. In chapter 3, we look at a method for weakly imposing boundary conditions on BEM inspired by Nitsche’s method. This method involves writing the boundary conditions as a penalty function, then adding a suitably weighted form of this penalty to the Calderón projector. In section 3.1, we derive formulations for Laplace problems with weakly imposed Dirichlet, Neumann, mixed Dirichlet–Neumann, and Robin conditions. In section 3.2, we present analysis of this method and prove *a priori* error bounds. In section 3.3, we present some numerical results for this method.

As this method of weak imposition uses the full Calderón projector, as opposed to using one row of it as in a standard method, it leads to discrete systems that are approximately twice as large as those arising from standard methods. For simpler problems—such pure Dirichlet or pure Neumann problems—this means that the method will be more computationally expensive and not competitive. For more complex problems, however, this

method has advantages over standard methods—such as the increased simplicity of the formulations—while presenting a computational cost comparable to standard methods.

In chapter 4, we look at how this method of weak imposition can be used to impose Signorini contact conditions. In section 4.1, we derive a formulation for Laplace’s equation with Signorini conditions. We analyse this formulation in section 4.2 and present some numerical results in section 4.3.

In chapter 5, we look at the weak imposition of boundary conditions for Helmholtz problems. In section 5.1, we derive formulations for Dirichlet and mixed Dirichlet–Neumann problems. In section 5.2, we analyse these formulations and in section 5.3 we present some numerical results, including in section 5.3.2 an application to problems involving multiple scatterers.

We finish with some concluding remarks, including a discussion of areas of possible future work.

CHAPTER 1

PRELIMINARIES

In this chapter, we look at the function spaces in which the problems are well-defined (section 1.1), and define the integral operators that will appear in our BEM formulations (section 1.3). Throughout this thesis, we use the following notation for the domains of our problems. This notation is summarised in figure 1.1.

Let $\Omega^- \subset \mathbb{R}^3$ be a bounded Lebesgue-measurable domain with boundary Γ . We assume that Γ consists of a finite number of smooth faces that meet at non-degenerate edges and corners: more precisely, we assume that there is a polyhedron $\tilde{\Gamma}$ and a bijective function

$$\sigma : \tilde{\Gamma} \rightarrow \Gamma, \quad (1.1)$$

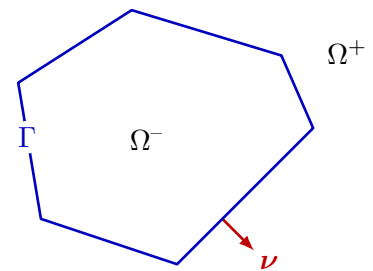


Figure 1.1: Ω^- , Ω^+ , Γ and ν .

such that σ and σ^{-1} are Lipschitz continuous [39]. This is a reasonable assumption from the point of view of BEM, as we will consider discrete problems on meshed surfaces. Let $\Omega^+ := \mathbb{R}^3 \setminus \Omega^-$. Let ν be the normal to the surface Γ pointing outwards from Ω^- . When ambiguous, we will use $\nu_{\mathbf{x}}$ to signify the normal to the surface at the point $\mathbf{x} \in \Gamma$.

— 1.1 —

FUNCTION SPACES

We begin by defining the function spaces in which the problems are well-posed. For Laplace and Helmholtz problems, we will use spaces of scalar functions $f : \mathbb{R}^3 \rightarrow \mathbb{C}$. These are defined in section 1.1.1 For Maxwell problems, we will use spaces of vector functions $\mathbf{f} : \mathbb{R}^3 \rightarrow \mathbb{C}^3$. These are defined in section 1.1.2

It is important that we correctly describe the traces spaces on Γ for the solutions of the PDEs we are looking to solve. The description of these spaces is particularly difficult for Maxwell's equations [78, 18, 17, 19, 15]. In this section, we summarise without proof some of the results of these papers, as they form the foundations of much that is presented later.

Throughout, we adopt the convention of using bold lowercase symbols for vector functions (\mathbf{f} , $\boldsymbol{\phi}$, etc) and bold uppercase symbols for spaces of vector functions (\mathbf{H} , \mathbf{L} , etc); and non-bold lowercase symbols for scalar functions (f , ϕ , etc) and non-bold uppercase

symbols for spaces of scalar functions (H , L , etc).

— 1.1.1 —

SCALAR FUNCTION SPACES

We now proceed to define the scalar function spaces that will be used for Laplace and Helmholtz problems. The main references for this section are [55, chapter 3], [73, chapter 2] and [33].

We define the space of square integrable functions on the interior domain Ω^- by

$$L^2(\Omega^-) := \left\{ f : \Omega^- \rightarrow \mathbb{C} \mid f \text{ is Lebesgue measurable and } \int_{\Omega^-} |f|^2 < \infty \right\}. \quad (1.2)$$

This is a Hilbert space with inner product

$$\langle f, g \rangle_{\Omega^-} := \int_{\Omega^-} f \bar{g}. \quad (1.3)$$

Let $u \in L^1_{\text{loc}}(\Omega^-) := \{ f : \Omega^- \rightarrow \mathbb{C} \mid f \text{ is Lebesgue measurable and } \int_K |f| < \infty \text{ for all compact } K \subset \Omega^- \}$. If there exists $v \in L^1_{\text{loc}}(\Omega^-)$ such that

$$\int_{\Omega^-} v(\mathbf{x}) \phi(\mathbf{x}) \, d\mathbf{x} = - \int_{\Omega^-} u(\mathbf{x}) \frac{\partial \phi}{\partial x_i}(\mathbf{x}) \, d\mathbf{x}, \quad (1.4)$$

for all $\phi \in C_0^\infty(\Omega^-)$, then v is the weak derivative of u with respect to x_i . For $s \in \mathbb{N}$, we define the Sobolev space $H^s(\Omega^-)$ to be the space of functions whose weak derivatives of order up to s exist and are square integrable, ie

$$H^s(\Omega^-) := \{ f \in L^2(\Omega^-) \mid \forall \alpha \text{ s.t. } |\alpha| \leq s, D^\alpha f \in L^2(\Omega^-) \}, \quad (1.5)$$

where $\alpha = (\alpha_1, \alpha_2, \alpha_3)$ is a multi-index, ie

$$|\alpha| := \alpha_1 + \alpha_2 + \alpha_3, \quad D^\alpha := \frac{\partial^{|\alpha|}}{\partial x^{\alpha_1} \partial y^{\alpha_2} \partial z^{\alpha_3}}, \quad (1.6)$$

where $\frac{\partial}{\partial x}$, $\frac{\partial}{\partial y}$, and $\frac{\partial}{\partial z}$ denote weak derivatives. Taking $s = 0$, we see that $H^0(\Omega^-) = L^2(\Omega^-)$.

For any differential operator, op , we define the space

$$H^s(\text{op}, \Omega^-) := \{ f \in H^s(\Omega^-) \mid \text{op } f \in L^2(\Omega^-) \}, \quad (1.7)$$

where $\text{op } u$ is understood weakly. In particular, we will use the space $H^1(\Delta, \Omega^-)$.

In the unbounded exterior domain Ω^+ , we define the space of locally square integrable functions by

$$L^2_{\text{loc}}(\Omega^+) := \left\{ f : \Omega^+ \rightarrow \mathbb{C} \mid \int_K |f|^2 < \infty \text{ for all compact } K \subset \Omega^+ \right\}, \quad (1.8)$$

and note that for the bounded domain Ω^- , $L^2(\Omega^-) = L^2_{\text{loc}}(\Omega^-)$. We then define the spaces $H^s_{\text{loc}}(\Omega^+)$ and $H^s_{\text{loc}}(\text{op}, \Omega^+)$, for $s \in \mathbb{N}$, as above with $L^2_{\text{loc}}(\Omega^+)$ in the place of $L^2(\Omega^-)$.

The boundary integral formulations of our PDEs will use the Dirichlet (D) and Neumann (N) traces of functions on the boundary. For sufficiently smooth functions p and q , we define these by

$$\gamma_{\text{D}}^{\pm} p(\mathbf{x}) := \lim_{\Omega^{\pm} \ni \mathbf{x}' \rightarrow \mathbf{x} \in \Gamma} p(\mathbf{x}'), \quad \gamma_{\text{N}}^{\pm} q(\mathbf{x}) := \lim_{\Omega^{\pm} \ni \mathbf{x}' \rightarrow \mathbf{x} \in \bar{\Gamma}} \nabla q(\mathbf{x}') \cdot \boldsymbol{\nu}_{\mathbf{x}}, \quad (1.9)$$

where the superscripts $-$ and $+$ denote the interior and exterior traces, respectively, and $\bar{\Gamma}$ is the set of all points on Γ that are interior to a face of Γ . These definitions can be extended to all functions $p \in H^1_{\text{loc}}(\Omega^{\pm})$ and $q \in H^1_{\text{loc}}(\Delta, \Omega^{\pm})$ to give continuous traces, as given in the following lemma.

Lemma 1.1. *The traces*

$$\gamma_{\text{D}}^{\pm} : H^1_{\text{loc}}(\Omega^{\pm}) \rightarrow H^{1/2}(\Gamma) \quad (1.10)$$

are continuous and surjective. The traces

$$\gamma_{\text{N}}^{\pm} : H^1_{\text{loc}}(\Delta, \Omega^{\pm}) \rightarrow H^{-1/2}(\Gamma) \quad (1.11)$$

are continuous.

Proof. [73, theorems 2.21 and 2.22], [31], [55, chapter 3]. \square

In what follows, we need the average $\{\cdot\}_{\Gamma}$, and jump, $[[\cdot]]_{\Gamma}$ of these traces, defined as

$$\{\gamma_{*}\}_{\Gamma} f := \frac{1}{2}(\gamma_{*}^{+} f + \gamma_{*}^{-} f), \quad [[\gamma_{*}]]_{\Gamma} f := \gamma_{*}^{+} f - \gamma_{*}^{-} f. \quad (1.12)$$

We define $L^2(\Gamma)$ to be the space of square integrable functions on the boundary, ie

$$L^2(\Gamma) := \left\{ f : \Gamma \rightarrow \mathbb{C} \mid \int_{\Gamma} |f|^2 < \infty \right\}, \quad (1.13)$$

with the inner product defined, for $v, w \in L^2(\Gamma)$, by

$$\langle v, w \rangle_{\Gamma} := \int_{\Gamma} vw. \quad (1.14)$$

We define the Sobolev space $H^{1/2}(\Gamma)$ by

$$H^{1/2}(\Gamma) := \gamma_{\text{D}}^{-} (H^1(\Omega^-)) = \{\gamma_{\text{D}}^{-} p : p \in H^1(\Omega^-)\}, \quad (1.15)$$

with associated norm

$$\|v\|_{H^{1/2}(\Gamma)} := \left(\|v\|_{L^2(\Gamma)}^2 + \int_{\Gamma} \int_{\Gamma} \frac{|v(\mathbf{x}) - v(\mathbf{y})|^2}{|\mathbf{x} - \mathbf{y}|^3} d\mathbf{x} d\mathbf{y} \right)^{\frac{1}{2}}. \quad (1.16)$$

We define the space $H^{-1/2}(\Gamma)$ to be the dual space of $H^{1/2}(\Gamma)$.

— 1.1.2 —

VECTOR FUNCTION SPACES

We now proceed to define the vector spaces that we will use when solving Maxwell's equations. The main references for this section are [20] and [56].

Similar to the scalar case, we define

$$\mathbf{L}^2(\Omega^-) := \left\{ \mathbf{f} : \Omega^- \rightarrow \mathbb{C}^3 \mid \int_{\Omega^-} |\mathbf{f}|^2 < \infty \right\}, \quad (1.17)$$

$$\mathbf{H}^s(\Omega^-) := \{ \mathbf{f} \in \mathbf{L}^2(\Omega^-) \mid \forall \alpha \text{ s.t. } |\alpha| \leq s, D^\alpha \mathbf{f} \in \mathbf{L}^2(\Omega^-) \}, \quad \text{for } s \in \mathbb{N}. \quad (1.18)$$

The space $\mathbf{L}^2(\Omega^-)$ is a Hilbert space with inner product

$$\langle \mathbf{f}, \mathbf{g} \rangle_{\mathbf{L}^2(\Omega^-)} := \int_{\Omega^-} \mathbf{f} \cdot \bar{\mathbf{g}}. \quad (1.19)$$

Let \mathbf{op} be a vector differential operator and op be a scalar differential operator. We define

$$\mathbf{H}(\mathbf{op}, \Omega^-) := \{ \mathbf{u} \in \mathbf{L}^2(\Omega^-) : \mathbf{op} \mathbf{u} \in \mathbf{L}^2(\Omega^-) \}, \quad (1.20)$$

$$\mathbf{H}(\text{op}, \Omega^-) := \{ \mathbf{u} \in \mathbf{L}^2(\Omega^-) : \text{op} \mathbf{u} \in \mathbf{L}^2(\Omega^-) \}, \quad (1.21)$$

noting here that when $s = 0$ it is conventional to write \mathbf{H} instead of \mathbf{H}^0 . In particular, we will later use the spaces $\mathbf{H}(\mathbf{curl}, \Omega^-)$, $\mathbf{H}(\mathbf{curl}^2, \Omega^-)$, and $\mathbf{H}(\text{div}, \Omega^-)$.

As in the scalar case, on the unbounded domain Ω^+ , we define the space of locally square integrable functions by

$$\mathbf{L}_{\text{loc}}^2(\Omega^+) := \left\{ \mathbf{f} : \Omega^+ \rightarrow \mathbb{C}^3 \mid \int_K |\mathbf{f}|^2 < \infty \text{ for all compact } K \subset \Omega^+ \right\}, \quad (1.22)$$

and note that for the bounded domain Ω^- , $\mathbf{L}_{\text{loc}}^2(\Omega^-) = \mathbf{L}^2(\Omega^-)$. We then define the corresponding spaces $\mathbf{H}_{\text{loc}}^s(\Omega^+)$, $\mathbf{H}_{\text{loc}}(\mathbf{op}, \Omega^+)$, and $\mathbf{H}_{\text{loc}}(\text{op}, \Omega^+)$ as above with $\mathbf{L}^2(\Omega^-)$ replaced by $\mathbf{L}_{\text{loc}}^2(\Omega^+)$.

To define the necessary function spaces on the surface Γ , we first define the tangential (\mathbf{t}), Neumann (\mathbf{N}), and normal ($\mathbf{\nu}$) traces on Γ . These are defined, for $\mathbf{p} \in \mathbf{H}_{\text{loc}}(\mathbf{curl}, \Omega^\pm)$,

$\mathbf{q} \in \mathbf{H}_{\text{loc}}(\mathbf{curl}^2, \Omega^\pm)$, and $\mathbf{r} \in \mathbf{H}_{\text{loc}}(\text{div}, \Omega^\pm)$, by

$$\gamma_t^\pm \mathbf{p}(\mathbf{x}) := \lim_{\Omega^\pm \ni \mathbf{x}' \rightarrow \mathbf{x} \in \Gamma} \mathbf{p}(\mathbf{x}') \times \boldsymbol{\nu}_{\mathbf{x}}, \quad (1.23)$$

$$\gamma_{N,k}^\pm \mathbf{q}(\mathbf{x}) := \frac{1}{ik} \gamma_t^\pm \mathbf{curl} \mathbf{q}(\mathbf{x}), \quad (1.24)$$

$$\gamma_\nu^\pm \mathbf{r}(\mathbf{x}) := \lim_{\Omega^\pm \ni \mathbf{x}' \rightarrow \mathbf{x} \in \Gamma} \mathbf{r}(\mathbf{x}') \cdot \boldsymbol{\nu}_{\mathbf{x}}, \quad (1.25)$$

where the superscripts $-$ and $+$ denote the interior and exterior traces, respectively. Note that in our definition $\gamma_{N,k}^\pm$ contains an additional factor of i , which does not appear in [20]. The interpretation is that if we normalise the magnetic permittivity and electric permeability to 1, this definition of $\gamma_{N,k}^\pm$ is the tangential trace of the magnetic field data.

In what follows we need the average $\{\cdot\}_\Gamma$, and jump, $\llbracket \cdot \rrbracket_\Gamma$ of these traces, defined as

$$\{\gamma_*\}_\Gamma \mathbf{f} := \frac{1}{2} (\gamma_*^+ \mathbf{f} + \gamma_*^- \mathbf{f}), \quad \llbracket \gamma_* \rrbracket_\Gamma \mathbf{f} := \gamma_*^+ \mathbf{f} - \gamma_*^- \mathbf{f}. \quad (1.26)$$

We define $\mathbf{L}_t^2(\Gamma)$ to be the space of square integrable tangential vector functions on the boundary, ie

$$\mathbf{L}_t^2(\Gamma) := \{\mathbf{u} \in \mathbf{L}^2(\Gamma) : \mathbf{u} \cdot \boldsymbol{\nu} = 0\}. \quad (1.27)$$

We define the tangential trace space, $\mathbf{H}_\times^{1/2}(\Gamma)$, as in [20, definition 1] by

$$\mathbf{H}_\times^{1/2}(\Gamma) := \gamma_t^-(\mathbf{H}^1(\Omega^-)) = \{\gamma_t^- \mathbf{u} : \mathbf{u} \in \mathbf{H}^1(\Omega^-)\}. \quad (1.28)$$

The dual of this space with respect to the antisymmetric product,

$$\langle \mathbf{a}, \mathbf{b} \rangle_\tau := \int_\Gamma \mathbf{a} \cdot (\boldsymbol{\nu} \times \mathbf{b}), \quad \text{for } \mathbf{a}, \mathbf{b} \in \mathbf{L}_t^2(\Gamma). \quad (1.29)$$

is denoted by $\mathbf{H}_\times^{-1/2}(\Gamma)$.

If Γ is smooth, we define the scalar surface divergence, div_Γ , of $\mathbf{u} \in \gamma_t^-(\mathbf{H}(\mathbf{curl}, \Omega^-))$ to be the 2D divergence of \mathbf{u} at each point on Γ . For $\mathbf{u} \in \mathbf{H}_{\text{loc}}(\mathbf{curl}, \Omega^\pm)$, we may deduce from the definitions of div_Γ , \mathbf{curl} , γ_ν and γ_t that

$$\text{div}_\Gamma(\gamma_t^\pm \mathbf{u}) = \gamma_\nu^\pm(\mathbf{curl} \mathbf{u}). \quad (1.30)$$

Due to the assumption that Γ consists of a finite number of smooth faces, we may let $\Gamma = \bigcup_{j=1}^\theta \Gamma^j$, where $\Gamma^1, \dots, \Gamma^\theta$ are smooth. For a function $\mathbf{u} \in \gamma_t^-(\mathbf{C}^\infty(\overline{\Omega^-}))$, the scalar surface divergence of \mathbf{u} is defined by

$$\text{div}_\Gamma \mathbf{u} := \begin{cases} \text{div}_j \mathbf{u}^j & \text{on } \Gamma^j \\ (\mathbf{u}^j \cdot \boldsymbol{\nu}^{jj} + \mathbf{u}^i \cdot \boldsymbol{\nu}^{ji}) \delta_{ij} & \text{on } \overline{\Gamma^j} \cap \overline{\Gamma^i}, \end{cases} \quad (1.31)$$

where \mathbf{u}^j is the restriction of \mathbf{u} to the face Γ^j , $\boldsymbol{\nu}^{ij}$ is the outward pointing tangential normal to Γ^i restricted to the edge $\overline{\Gamma^i} \cap \overline{\Gamma^j}$, div_j is the two dimensional divergence computed on the face Γ^i , and δ_{ij} is the Dirac delta distribution with support on the edge $\overline{\Gamma^i} \cap \overline{\Gamma^j}$. By density, this definition can be extended to $\mathbf{u} \in \mathbf{H}_\times^{-1/2}(\Gamma)$. We now define the space of surface-div-conforming functions by

$$\mathbf{H}_\times^{-1/2}(\operatorname{div}_\Gamma, \Gamma) := \{\boldsymbol{\mu} \in \mathbf{H}_\times^{-1/2}(\Gamma) : \operatorname{div}_\Gamma \boldsymbol{\mu} \in H^{-1/2}(\Gamma)\}. \quad (1.32)$$

The scalar surface curl may be defined [19], for $\mathbf{u} \in \mathbf{H}_\times^{-1/2}(\Gamma)$, by

$$\operatorname{curl}_\Gamma(\mathbf{u}) := \operatorname{div}_\Gamma(\mathbf{u} \times \boldsymbol{\nu}), \quad (1.33)$$

and the space of surface-curl-conforming functions by

$$\mathbf{H}_\times^{-1/2}(\operatorname{curl}_\Gamma, \Gamma) := \{\boldsymbol{\nu} \times \boldsymbol{\mu} : \boldsymbol{\mu} \in \mathbf{H}_\times^{-1/2}(\operatorname{div}_\Gamma, \Gamma)\}. \quad (1.34)$$

The following lemma gives important properties of the trace operators.

Lemma 1.2. *The traces*

$$\gamma_t^\pm : \mathbf{H}_{\operatorname{loc}}(\mathbf{curl}, \Omega^\pm) \rightarrow \mathbf{H}_\times^{-1/2}(\operatorname{div}_\Gamma, \Gamma) \quad (1.35)$$

$$\text{and } \gamma_{N,k}^\pm : \mathbf{H}_{\operatorname{loc}}(\mathbf{curl}^2, \Omega^\pm) \rightarrow \mathbf{H}_\times^{-1/2}(\operatorname{div}_\Gamma, \Gamma) \quad (1.36)$$

are continuous and surjective.

Proof. See [19, theorem 4.1] and [20, Lemma 3]. \square

The antisymmetric dual form $\langle \cdot, \cdot \rangle_\tau$ defined in (1.29) is intimately connected with the space $\mathbf{H}_\times^{-1/2}(\operatorname{div}_\Gamma, \Gamma)$. In [19, Lemma 5.6] it is shown that the space $\mathbf{H}_\times^{-1/2}(\operatorname{div}_\Gamma, \Gamma)$ is self-dual with respect to $\langle \cdot, \cdot \rangle_\tau$. Another interpretation of $\langle \cdot, \cdot \rangle_\tau$ is as the standard \mathbf{L}^2 dual between the spaces $\mathbf{H}_\times^{-1/2}(\operatorname{div}_\Gamma, \Gamma)$ and $\mathbf{H}_\times^{-1/2}(\operatorname{curl}_\Gamma, \Gamma)$ since $\boldsymbol{\psi} \in \mathbf{H}_\times^{-1/2}(\operatorname{curl}_\Gamma, \Gamma)$ if and only if $\boldsymbol{\psi} = \boldsymbol{\nu} \times \boldsymbol{\xi}$ for some $\boldsymbol{\xi} \in \mathbf{H}_\times^{-1/2}(\operatorname{div}_\Gamma, \Gamma)$.

— 1.2 —

PARTIAL DIFFERENTIAL EQUATIONS

We will consider three PDEs: Laplace's equation, the Helmholtz equation and Maxwell's equations. In this section, we look at each of these equations and the spaces in which we will look for their solutions.

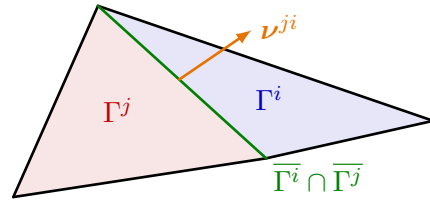


Figure 1.2: Defining the surface divergence.

LAPLACE'S EQUATION

To solve Laplace's equation, we look for $u \in H_{\text{loc}}^1(\Delta, \Omega^\pm)$ such that

$$-\Delta u = 0 \quad \text{in } \Omega^\pm. \quad (1.37a)$$

For exterior problems, we require an additional condition at infinity to ensure that the problem has a unique solution,

$$u(\mathbf{x}) \rightarrow 0 \quad \text{as } |\mathbf{x}| \rightarrow \infty. \quad (1.37b)$$

Both the interior and exterior Laplace problems will be provided with boundary conditions of the following form.

$$u = g_D \quad \text{on } \Gamma_D, \quad (1.37c)$$

$$\frac{\partial u}{\partial \boldsymbol{\nu}} = g_N \quad \text{on } \Gamma_N, \quad (1.37d)$$

$$\frac{\partial u}{\partial \boldsymbol{\nu}} = \frac{1}{\varepsilon}(g_D - u) + g_N \quad \text{on } \Gamma_R, \quad (1.37e)$$

$$u \leq g_C \quad \text{and} \quad \frac{\partial u}{\partial \boldsymbol{\nu}} \leq \psi_C \quad \text{on } \Gamma_C, \quad (1.37f)$$

$$\left(\frac{\partial u}{\partial \boldsymbol{\nu}} - \psi_C \right) \left(u - g_C \right) = 0 \quad \text{on } \Gamma_C, \quad (1.37g)$$

for some $g_N \in H^{-1/2}(\Gamma_N \cup \Gamma_R)$, $g_D \in H^{1/2}(\Gamma_D \cup \Gamma_R)$, $g_C \in H^{1/2}(\Gamma_C)$, $\psi_C \in H^{-1/2}(\Gamma_C)$, and $\varepsilon > 0$. Here, Γ has been split into four parts: the Dirichlet part Γ_D , the Neumann part Γ_N , the Robin part Γ_R , and the Signorini part Γ_C . We call problems where the entire boundary is equal to one of these parts Dirichlet, Neumann, Robin and Signorini problems respectively.

THE HELMHOLTZ EQUATION

To solve the Helmholtz equation, we look for $u \in H_{\text{loc}}^1(\Delta, \Omega^\pm)$ satisfying

$$-\Delta u - k^2 u = 0 \quad \text{in } \Omega^\pm, \quad (1.38a)$$

where $k \in \mathbb{R}$ is the wavenumber of the problem.

For exterior problems, we again require a condition at infinity to ensure that the problem has a unique solution. We write the total exterior wave as the sum of the incident and scattered wave, $u^{\text{tot}} = u^{\text{scat}} + u^{\text{inc}}$. The Sommerfeld radiation condition at infinity is

then imposed on the scattered wave to ensure a unique solution,

$$\frac{\partial u^{\text{scat}}}{\partial |\mathbf{x}|} - iku^{\text{scat}} = o(|\mathbf{x}|^{-1}) \quad \text{as } |\mathbf{x}| \rightarrow \infty. \quad (1.38b)$$

Both the interior and exterior problems will be provided with boundary conditions of the same form as Laplace problems.

MAXWELL'S EQUATIONS

To solve Maxwell's equations, we look for $\mathbf{e} \in \mathbf{H}_{\text{loc}}^1(\mathbf{curl}, \Omega^\pm)$ such that

$$\mathbf{curl} \mathbf{curl} \mathbf{e} = k^2 \mathbf{e} \quad \text{in } \Omega^\pm, \quad (1.39a)$$

where $k = \omega \sqrt{\epsilon_0 \mu_0}$ denotes the wavenumber of the problem, with ω denoting the frequency and ϵ_0 and μ_0 the electric permeability and magnetic permittivity.

As in the Helmholtz case, for exterior problems we split the total field into the incident and scattered fields, $\mathbf{e}^{\text{tot}} = \mathbf{e}^{\text{scat}} + \mathbf{e}^{\text{inc}}$. We impose the Silver–Müller conditions at infinity on the scattered field,

$$|\mathbf{x}| \left(\mathbf{curl} \mathbf{e}^{\text{scat}} \times \frac{\mathbf{x}}{|\mathbf{x}|} - ik \mathbf{e}^{\text{scat}} \right) \rightarrow \mathbf{0} \quad \text{as } |\mathbf{x}| \rightarrow \infty. \quad (1.39b)$$

Both the interior and exterior Maxwell problems will be provided with boundary conditions of the following form.

$$\mathbf{e} \times \boldsymbol{\nu} = \mathbf{g}_D \quad \text{on } \Gamma_D, \quad (1.39c)$$

$$(\mathbf{curl} \mathbf{e}) \times \boldsymbol{\nu} = \mathbf{g}_N \quad \text{on } \Gamma_N, \quad (1.39d)$$

for some $\mathbf{g}_N, \mathbf{g}_D \in \mathbf{H}_\times^{-1/2}(\text{div}_\Gamma, \Gamma)$. Here, Γ has been split into two parts: the Dirichlet part Γ_D and the Neumann part Γ_N . Problems where the entire boundary is equal to one of these parts are called Dirichlet and Neumann respectively.

— 1.3 —

BOUNDARY INTEGRAL OPERATORS

The boundary element method (BEM) has two key ingredients: a representation formula and a boundary integral equation. The representation formula describes how to reconstruct the function u in $\Omega^\pm \setminus \Gamma$ using an unknown function on the boundary Γ . The boundary integral equation can be used to find this unknown function. BEM involves discretising the boundary integral equations in order to find an approximation of the unknown boundary function.

In this section, we define the potential operators that we will use to write representation formulae, and the boundary operators that we will use to write boundary integral equations. We also summarise some important properties of these operators.

— 1.3.1 —

LAPLACE'S EQUATION AND THE HELMHOLTZ EQUATION

We begin by considering Laplace and Helmholtz problems, where the unknown is a scalar function.

We define the Green's function of a PDE to be the solution of the PDE with the Dirac delta function on the right hand side. The Green's function for the Laplace operator in \mathbb{R}^3 is

$$G(\mathbf{x}, \mathbf{y}) = \frac{1}{4\pi|\mathbf{x} - \mathbf{y}|}, \quad (1.40)$$

as

$$\Delta_{\mathbf{x}}G(\mathbf{x}, \mathbf{y}) = \delta(\mathbf{x} - \mathbf{y}). \quad (1.41)$$

The Green's function for the Helmholtz operator in \mathbb{R}^3 is given by

$$G(\mathbf{x}, \mathbf{y}) = \frac{e^{ik|\mathbf{x}-\mathbf{y}|}}{4\pi|\mathbf{x} - \mathbf{y}|}. \quad (1.42)$$

In this thesis, we focus on problems in \mathbb{R}^3 . Similar methods can be used for problems in \mathbb{R}^2 , in which case the Green's functions in \mathbb{R}^2 should be used. The Green's function for the Laplace operator in \mathbb{R}^2 is defined by

$$G(\mathbf{x}, \mathbf{y}) = -\log|\mathbf{x} - \mathbf{y}|/2\pi, \quad (1.43)$$

and the Green's function for the Helmholtz operator in \mathbb{R}^2 is defined by

$$G(\mathbf{x}, \mathbf{y}) = \frac{i}{4}H_0^{(1)}(k|\mathbf{x} - \mathbf{y}|), \quad (1.44)$$

where $H_0^{(1)}$ is a Hankel function of the first kind.

—

POTENTIAL OPERATORS

In the standard fashion (see eg [73, chapter 6]), we define the single layer potential operator, $\mathcal{V} : H^{-1/2}(\Gamma) \rightarrow H_{\text{loc}}^1(\Omega^\pm)$, and the double layer potential operator, $\mathcal{K} : H^{1/2}(\Gamma) \rightarrow$

$H_{\text{loc}}^1(\Omega^\pm)$, for $v \in H^{1/2}(\Gamma)$, $\mu \in H^{-1/2}(\Gamma)$, and $\mathbf{x} \in \Omega^\pm \setminus \Gamma$ by

$$(\mathcal{V}\mu)(\mathbf{x}) := \int_{\Gamma} G(\mathbf{x}, \mathbf{y})\mu(\mathbf{y}) \, d\mathbf{y}, \quad (1.45)$$

$$(\mathcal{K}v)(\mathbf{x}) := \int_{\Gamma} \frac{\partial G(\mathbf{x}, \mathbf{y})}{\partial \nu_{\mathbf{y}}} v(\mathbf{y}) \, d\mathbf{y}, \quad (1.46)$$

if μ and v are regular enough, then we extend these definition to the whole of $H^{1/2}(\Gamma)$ and $H^{-1/2}(\Gamma)$ by completion.

We recall that if the Dirichlet and Neumann traces of a function $u \in H_{\text{loc}}^1(\Delta, \Omega^\pm)$ that is a solution to either Laplace's equation (1.37a) or the Helmholtz equation (1.38a) are known, then the potentials (1.45) and (1.46) may be used to reconstruct the function in Ω^\pm using the following relation.

$$u = \mathcal{K}(\llbracket \gamma_{\text{D}} u \rrbracket_{\Gamma}) - \mathcal{V}(\llbracket \gamma_{\text{N}} u \rrbracket_{\Gamma}). \quad (1.47)$$

By taking this relation first with $\tilde{u}(\mathbf{x}) = \begin{cases} u(\mathbf{x}) & \mathbf{x} \in \Omega^- \\ 0 & \mathbf{x} \in \Omega^+ \end{cases}$ for a given Laplace or Helmholtz

solution in Ω^- , $u(x) \in H^1(\Omega^-)$ we arrive at the following representation formula for interior problems,

$$u = -\mathcal{K}(\gamma_{\text{D}}^- u) + \mathcal{V}(\gamma_{\text{N}}^- u). \quad (1.48)$$

Similarly, taking $\tilde{u}(\mathbf{x}) = \begin{cases} u(\mathbf{x}) & \mathbf{x} \in \Omega^+ \\ 0 & \mathbf{x} \in \Omega^- \end{cases}$ for a given Laplace or Helmholtz solution in

Ω^+ , $u(x) \in H^1(\Omega^+)$ gives the following representation formula for exterior problems,

$$u = \mathcal{K}(\gamma_{\text{D}}^+ u) - \mathcal{V}(\gamma_{\text{N}}^+ u). \quad (1.49)$$

BOUNDARY OPERATORS

Next, we define the single layer, double layer, adjoint double layer, and hypersingular boundary integral operators, $\mathbf{V} : H^{-1/2}(\Gamma) \rightarrow H^{1/2}(\Gamma)$, $\mathbf{K} : H^{1/2}(\Gamma) \rightarrow H^{1/2}(\Gamma)$, $\mathbf{K}' : H^{-1/2}(\Gamma) \rightarrow H^{-1/2}(\Gamma)$, and $\mathbf{W} : H^{1/2}(\Gamma) \rightarrow H^{-1/2}(\Gamma)$, for $\mathbf{x} \in \Gamma$, $v \in H^{1/2}(\Gamma)$ and $\mu \in H^{-1/2}(\Gamma)$ and by

$$(\mathbf{K}v)(\mathbf{x}) := \{\gamma_{\text{D}} \mathcal{K}v\}_{\Gamma}(\mathbf{x}), \quad (\mathbf{V}\mu)(\mathbf{x}) := \{\gamma_{\text{D}} \mathcal{V}\mu\}_{\Gamma}(\mathbf{x}), \quad (1.50a)$$

$$(\mathbf{W}v)(\mathbf{x}) := -\{\gamma_{\text{N}} \mathcal{K}v\}_{\Gamma}(\mathbf{x}), \quad (\mathbf{K}'\mu)(\mathbf{x}) := \{\gamma_{\text{N}} \mathcal{V}\mu\}_{\Gamma}(\mathbf{x}), \quad (1.50b)$$

as given in [73, chapter 6]. Additionally, we define the identity operator, Id , that maps every function to itself.

The following jump conditions can be derived [73, sections 6.2 to 6.4].

$$\llbracket \gamma_D \rrbracket_{\Gamma} \mathcal{V} = \llbracket \gamma_N \rrbracket_{\Gamma} \mathcal{K} = 0, \quad \llbracket \gamma_N \rrbracket_{\Gamma} \mathcal{V} = -\llbracket \gamma_D \rrbracket_{\Gamma} \mathcal{K} = -\text{Id}. \quad (1.51)$$

Combining (1.50) and (1.51) gives

$$\gamma_D^+ \mathcal{V} = \mathbf{V}, \quad \gamma_N^+ \mathcal{V} = -\frac{1}{2} \text{Id} + \mathbf{K}', \quad (1.52)$$

$$\gamma_D^+ \mathcal{K} = \frac{1}{2} \text{Id} + \mathbf{K}, \quad \gamma_N^+ \mathcal{K} = -\mathbf{W}, \quad (1.53)$$

for the exterior traces and

$$\gamma_D^- \mathcal{V} = \mathbf{V}, \quad \gamma_N^- \mathcal{V} = \frac{1}{2} \text{Id} + \mathbf{K}', \quad (1.54)$$

$$\gamma_D^- \mathcal{K} = -\frac{1}{2} \text{Id} + \mathbf{K}, \quad \gamma_N^- \mathcal{K} = -\mathbf{W}, \quad (1.55)$$

for the interior traces.

These results are only true almost everywhere. Results that are true everywhere can be given in terms of a factor σ , as defined in [73, (6.11)], that is equal to $\frac{1}{2}$ almost everywhere. In what follows, we present results that hold almost everywhere. As we will be integrating these identities over the boundary, this will not cause any issues.

Taking both traces of (1.48), we see that if $u \in H^1(\Omega^-)$ is a solution of Laplace or Helmholtz in Ω^- , then it satisfies

$$\gamma_D^- u = (\frac{1}{2} \text{Id} - \mathbf{K}) \gamma_D^- u + \mathbf{V} \gamma_N^- u, \quad (1.56)$$

$$\gamma_N^- u = (\frac{1}{2} \text{Id} + \mathbf{K}') \gamma_N^- u + \mathbf{W} \gamma_D^- u. \quad (1.57)$$

To simplify the notation, we write u in the place of $\gamma_D^- u$ and define $\lambda := \gamma_N^- u$. This leads to the following equations for the interior problem.

$$u = (\frac{1}{2} \text{Id} - \mathbf{K})u + \mathbf{V}\lambda, \quad (1.58)$$

$$\lambda = (\frac{1}{2} \text{Id} + \mathbf{K}')\lambda + \mathbf{W}u. \quad (1.59)$$

Doing the same for (1.49), with a function $u \in H_{\text{loc}}^1(\Omega^+)$ that is a solution of Laplace or Helmholtz in Ω^+ and writing u in the place of $\gamma_D^+ u$ and defining $\lambda := \gamma_N^+ u$, leads to the following equations for the exterior problem.

$$u = (\frac{1}{2} \text{Id} + \mathbf{K})u - \mathbf{V}\lambda, \quad (1.60)$$

$$\lambda = (\frac{1}{2} \text{Id} - \mathbf{K}')\lambda - \mathbf{W}u. \quad (1.61)$$

We define the interior Calderón projector by

$$\mathbf{C}^- := \begin{bmatrix} \frac{1}{2} \text{Id} - \mathbf{K} & \mathbf{V} \\ \mathbf{W} & \frac{1}{2} \text{Id} + \mathbf{K}' \end{bmatrix}, \quad (1.62)$$

and the exterior Calderón projector by

$$C^+ := \begin{bmatrix} \frac{1}{2}\text{Id} + K & -V \\ -W & \frac{1}{2}\text{Id} - K' \end{bmatrix}, \quad (1.63)$$

We may then rewrite (1.58) to (1.61) as

$$C^- \begin{bmatrix} u \\ \lambda \end{bmatrix} = \begin{bmatrix} u \\ \lambda \end{bmatrix} \quad \text{and} \quad C^+ \begin{bmatrix} u \\ \lambda \end{bmatrix} = \begin{bmatrix} u \\ \lambda \end{bmatrix}. \quad (1.64)$$

Additionally, we define the multitrace operator by

$$A := \begin{bmatrix} -K & V \\ W & K' \end{bmatrix}, \quad (1.65)$$

and we may write $C^- = \frac{1}{2}\text{Id} + A$ and $C^+ = \frac{1}{2}\text{Id} - A$.

— 1.3.2 —

LAPLACE'S EQUATION

For Laplace problems, the following coercivity results are known for the single layer and hypersingular operators in \mathbb{R}^3 when Γ is the boundary of a Lipschitz domain, as defined in [73, definition 2.1].

Lemma 1.3 (Coercivity of V). *There exists $\alpha_V > 0$ such that*

$$\alpha_V \|\mu\|_{H^{-1/2}(\Gamma)}^2 \leq \langle V\mu, \mu \rangle_\Gamma, \quad \forall \mu \in H^{-1/2}(\Gamma). \quad (1.66)$$

Proof. [73, theorem 6.22]. □

Lemma 1.4 (Coercivity of W). *There exists $\alpha_W > 0$ such that*

$$\alpha_W \|v\|_{H^{1/2}(\Gamma)}^2 \leq \langle Wv, v \rangle_\Gamma, \quad \forall v \in H_*^{1/2}(\Gamma), \quad (1.67)$$

where $H_*^{1/2}(\Gamma)$ denotes the set of functions $v \in H^{1/2}(\Gamma)$ such that $\bar{v} = 0$, where $\bar{v} := \frac{\langle v, 1 \rangle_\Gamma}{\langle 1, 1 \rangle_\Gamma}$ is the average value of v . From this it follows that

$$\alpha_W |v|_{H_*^{1/2}(\Gamma)}^2 \leq \langle Wv, v \rangle_\Gamma, \quad \forall v \in H^{1/2}(\Gamma), \quad (1.68)$$

where $|\cdot|_{H_*^{1/2}(\Gamma)}$ is defined, for $v \in H^{1/2}(\Gamma)$, by $|v|_{H_*^{1/2}(\Gamma)} := \|v - \bar{v}\|_{H^{1/2}(\Gamma)}$.

Proof. [73, theorem 6.24]. □

The following boundedness results are also known.

Lemma 1.5 (Boundedness). *There exist $C_V, C_K, C'_K, C_W > 0$ such that*

$$i) \quad \|\mathbf{V}\mu\|_{H^{1/2}(\Gamma)} \leq C_V \|\mu\|_{H^{-1/2}(\Gamma)} \quad \forall \mu \in H^{-1/2}(\Gamma), \quad (1.69)$$

$$ii) \quad \|\mathbf{K}v\|_{H^{1/2}(\Gamma)} \leq C_K \|v\|_{H^{1/2}(\Gamma)} \quad \forall v \in H^{1/2}(\Gamma), \quad (1.70)$$

$$iii) \quad \|\mathbf{K}'\mu\|_{H^{-1/2}(\Gamma)} \leq C'_K \|\mu\|_{H^{-1/2}(\Gamma)} \quad \forall \mu \in H^{-1/2}(\Gamma), \quad (1.71)$$

$$iv) \quad \|\mathbf{W}v\|_{H^{-1/2}(\Gamma)} \leq C_W \|v\|_{H^{1/2}(\Gamma)} \quad \forall v \in H^{1/2}(\Gamma). \quad (1.72)$$

Proof. [73, sections 6.2–6.5]. □

It is also known [73, lemma 6.6] that for all $\mu \in H^{-1/2}(\Gamma)$, the function

$$u_\mu^\mathcal{V} := \mathcal{V}\mu \quad (1.73)$$

satisfies $-\Delta u_\mu^\mathcal{V} = 0$ in $\Omega^- \cup \Omega^+$ and

$$\|u_\mu^\mathcal{V}\|_{H^1(\Omega^-)} \leq c \|\mu\|_{H^{-1/2}(\Gamma)}. \quad (1.74)$$

Similarly, for the double layer potential there holds [73, lemma 6.10] that for all $v \in H^{1/2}(\Gamma)$, the function

$$u_v^\mathcal{K} := \mathcal{K}v \quad (1.75)$$

satisfies $-\Delta u_v^\mathcal{K} = 0$ in $\Omega^- \cup \Omega^+$ and

$$\|u_v^\mathcal{K}\|_{H^1(\Omega^-)} \leq c \|v\|_{H^{1/2}(\Gamma)}. \quad (1.76)$$

— 1.3.3 —

THE HELMHOLTZ EQUATION

For Helmholtz problems, the following results involving Gårding's inequalities are known for the single layer and hypersingular operators in \mathbb{R}^3 .

Lemma 1.6 (Gårding's inequality for \mathbf{V}). *There exists a compact operator $\mathbf{C} : H^{-1/2}(\Gamma) \rightarrow H^{1/2}(\Gamma)$ and $\alpha_V > 0$ such that*

$$\alpha_V \|\mu\|_{H^{-1/2}(\Gamma)}^2 \leq \langle \mathbf{V}\mu, \mu \rangle_\Gamma + \langle \mathbf{C}\mu, \mu \rangle_\Gamma, \quad \forall \mu \in H^{-1/2}(\Gamma). \quad (1.77)$$

Proof. [73, theorem 6.40]. □

Lemma 1.7 (Gårding's inequality for \mathbf{W}). *There exists a compact operator $\mathbf{C} : H^{1/2}(\Gamma) \rightarrow H^{-1/2}(\Gamma)$ and $\alpha_W > 0$ such that*

$$\alpha_W \|v\|_{H^{1/2}(\Gamma)}^2 \leq \langle \mathbf{W}v, v \rangle_\Gamma + \langle \mathbf{C}v, v \rangle_\Gamma, \quad \forall v \in H_*^{1/2}(\Gamma), \quad (1.78)$$

where $H_*^{1/2}(\Gamma)$ is defined as in lemma 1.4.

Proof. This follows by applying the proof of [73, theorem 6.40] to the hypersingular operator. \square

The following boundedness results are also known.

Lemma 1.8 (Boundedness). *There exist $C_V, C_K, C'_K, C_W > 0$ such that*

$$i) \quad \|V\mu\|_{H^{1/2}(\Gamma)} \leq C_V \|\mu\|_{H^{-1/2}(\Gamma)} \quad \forall \mu \in H^{-1/2}(\Gamma), \quad (1.79)$$

$$ii) \quad \|Kv\|_{H^{1/2}(\Gamma)} \leq C_K \|v\|_{H^{1/2}(\Gamma)} \quad \forall v \in H^{1/2}(\Gamma), \quad (1.80)$$

$$iii) \quad \|K'\mu\|_{H^{-1/2}(\Gamma)} \leq C'_K \|\mu\|_{H^{-1/2}(\Gamma)} \quad \forall \mu \in H^{-1/2}(\Gamma), \quad (1.81)$$

$$iv) \quad \|Wv\|_{H^{-1/2}(\Gamma)} \leq C_W \|v\|_{H^{1/2}(\Gamma)} \quad \forall v \in H^{1/2}(\Gamma). \quad (1.82)$$

Proof. [73, sections 6.2–6.5 and 6.9]. \square

Following the proof of [73, lemmas 6.6 and 6.10], it can be shown that for all $v \in H^{1/2}(\Gamma)$ and $\mu \in H^{-1/2}(\Gamma)$, the functions

$$u_\mu^\mathcal{V} := \mathcal{V}\mu \quad (1.83)$$

$$u_v^\mathcal{K} := \mathcal{K}v \quad (1.84)$$

satisfy $-\Delta u_\mu^\mathcal{V} - k^2 u_\mu^\mathcal{V} = 0$ and $-\Delta u_v^\mathcal{K} - k^2 u_v^\mathcal{K} = 0$ in $\Omega^- \cup \Omega^+$.

— 1.3.4 —

MAXWELL'S EQUATIONS

For Maxwell problems, we use the Green's function for the Helmholtz operator. In \mathbb{R}^3 , this is defined, as above, by

$$G(\mathbf{x}, \mathbf{y}) = \frac{e^{ik|\mathbf{x}-\mathbf{y}|}}{4\pi|\mathbf{x}-\mathbf{y}|}. \quad (1.85)$$

—

POTENTIAL OPERATORS

We define the electric and magnetic potential operators (see [20]), $\mathcal{E}, \mathcal{H} : \mathbf{H}_\times^{-1/2}(\operatorname{div}_\Gamma, \Gamma) \rightarrow \mathbf{H}_{\operatorname{loc}}(\operatorname{curl}^2, \Omega^+ \cup \Omega^-)$, by

$$\mathcal{E}(\mathbf{p})(\mathbf{x}) := ik \int_\Gamma \mathbf{p}(\mathbf{y}) G(\mathbf{x}, \mathbf{y}) \, d\mathbf{y} - \frac{1}{ik} \nabla_{\mathbf{x}} \int_\Gamma \operatorname{div}_\Gamma \mathbf{p}(\mathbf{y}) G(\mathbf{x}, \mathbf{y}) \, d\mathbf{y}, \quad (1.86)$$

$$\mathcal{H}(\mathbf{p})(\mathbf{x}) := \operatorname{curl}_{\mathbf{x}} \int_\Gamma \mathbf{p}(\mathbf{y}) G(\mathbf{x}, \mathbf{y}) \, d\mathbf{y}. \quad (1.87)$$

The definition of the electric potential operator, \mathcal{E} , used here differs from that used in [20] by a factor of i , corresponding to the modified definition of $\gamma_{N,k}^\pm$.

With the electric and magnetic field operators we obtain the following representation formula [20, section 4]: If $\mathbf{e} \in \mathbf{H}_{\text{loc}}(\mathbf{curl}^2, \Omega^+ \cup \Omega^-)$ is a solution of Maxwell's equations, then

$$\mathbf{e}(\mathbf{x}) = -\mathcal{H}(\llbracket \gamma_t \rrbracket_{\Gamma} \mathbf{e})(\mathbf{x}) - \mathcal{E}(\llbracket \gamma_{N,k} \rrbracket_{\Gamma} \mathbf{e})(\mathbf{x}). \quad (1.88)$$

Once the jumps of the traces of the solution are known or estimated on Γ , the representation formula (1.88) can be used to find the solution at points in Ω^{\pm} . As in the scalar case, we can take $\mathbf{e}(\mathbf{x}) = \begin{cases} \mathbf{e}(\mathbf{x}) & \mathbf{x} \in \Omega^- \\ \mathbf{0} & \mathbf{x} \in \Omega^+ \end{cases}$, and $\mathbf{e}(\mathbf{x}) = \begin{cases} \mathbf{e}(\mathbf{x}) & \mathbf{x} \in \Omega^+ \\ \mathbf{0} & \mathbf{x} \in \Omega^- \end{cases}$, to derive the following representation formula for interior problems,

$$\mathbf{e}(\mathbf{x}) = \mathcal{H}(\gamma_t^- \mathbf{e})(\mathbf{x}) + \mathcal{E}(\gamma_{N,k}^- \mathbf{e})(\mathbf{x}). \quad (1.89)$$

and the following representation formula for exterior problems,

$$\mathbf{e}(\mathbf{x}) = -\mathcal{H}(\gamma_t^+ \mathbf{e})(\mathbf{x}) - \mathcal{E}(\gamma_{N,k}^+ \mathbf{e})(\mathbf{x}). \quad (1.90)$$

It is also known [20, equation (29)] that for all $\mathbf{f} \in \mathbf{H}_{\times}^{-1/2}(\text{div}_{\Gamma}, \Gamma)$, the functions

$$\mathbf{e}_{\mathbf{f}}^{\mathcal{E}} := \mathcal{E} \mathbf{f} \quad (1.91)$$

$$\mathbf{e}_{\mathbf{f}}^{\mathcal{H}} := \mathcal{H} \mathbf{f} \quad (1.92)$$

satisfy $\mathbf{curl} \mathbf{curl} \mathbf{e}_{\mathbf{f}}^{\mathcal{E}} - k^2 \mathbf{e}_{\mathbf{f}}^{\mathcal{E}} = 0$ and $\mathbf{curl} \mathbf{curl} \mathbf{e}_{\mathbf{f}}^{\mathcal{H}} - k^2 \mathbf{e}_{\mathbf{f}}^{\mathcal{H}} = 0$.

BOUNDARY OPERATORS

Taking traces of the electric and magnetic field potential operators we arrive at the electric boundary operator, $\mathbf{E} : \mathbf{H}_{\times}^{-1/2}(\text{div}_{\Gamma}, \Gamma) \rightarrow \mathbf{H}_{\times}^{-1/2}(\text{div}_{\Gamma}, \Gamma)$, and the magnetic boundary operator, $\mathbf{H} : \mathbf{H}_{\times}^{-1/2}(\text{div}_{\Gamma}, \Gamma) \rightarrow \mathbf{H}_{\times}^{-1/2}(\text{div}_{\Gamma}, \Gamma)$. These are defined by

$$\mathbf{E} := \{\gamma_t\}_{\Gamma} \mathcal{E}, \quad \mathbf{H} := \{\gamma_t\}_{\Gamma} \mathcal{H}. \quad (1.93)$$

Additionally, we define the identity operator, Id , that maps every function to itself. Because of the symmetry between electric and magnetic fields, the average Neumann traces can be written in terms of \mathbf{E} and \mathbf{H} as follows:

$$\{\gamma_{N,k}\}_{\Gamma} \mathcal{E} = \mathbf{H}, \quad \{\gamma_{N,k}\}_{\Gamma} \mathcal{H} = -\mathbf{E}. \quad (1.94)$$

The following jump conditions can be derived [20, theorem 7].

$$\llbracket \gamma_t \rrbracket_{\Gamma} \mathcal{E} = \llbracket \gamma_{N,k} \rrbracket_{\Gamma} \mathcal{H} = 0, \quad \llbracket \gamma_{N,k} \rrbracket_{\Gamma} \mathcal{E} = \llbracket \gamma_t \rrbracket_{\Gamma} \mathcal{H} = -\text{Id}. \quad (1.95)$$

Combining (1.93) to (1.95) gives

$$\gamma_t^+ \mathcal{E} = \mathbf{E}, \quad \gamma_{N,k}^+ \mathcal{E} = -\frac{1}{2} \text{Id} + \mathbf{H}, \quad (1.96)$$

$$\gamma_t^+ \mathcal{H} = -\frac{1}{2} \text{Id} + \mathbf{H}, \quad \gamma_{N,k}^+ \mathcal{H} = -\mathbf{E}, \quad (1.97)$$

for the exterior traces and

$$\gamma_t^- \mathcal{E} = \mathbf{E}, \quad \gamma_{N,k}^- \mathcal{E} = \frac{1}{2} \text{Id} + \mathbf{H}, \quad (1.98)$$

$$\gamma_t^- \mathcal{H} = \frac{1}{2} \text{Id} + \mathbf{H}, \quad \gamma_{N,k}^- \mathcal{H} = -\mathbf{E}, \quad (1.99)$$

for the interior traces.

To simplify the notation, we write \mathbf{e} in the place of $\gamma_t^\pm \mathbf{e}$ and define $\mathbf{h} := \gamma_{N,k}^\pm \mathbf{e}$. By taking both traces of (1.89), we arrive at the following equations for the interior problem.

$$\mathbf{e} = (\frac{1}{2} \text{Id} + \mathbf{H})\mathbf{e} + \mathbf{E}\mathbf{h}, \quad (1.100)$$

$$\mathbf{h} = (\frac{1}{2} \text{Id} + \mathbf{H})\mathbf{h} - \mathbf{E}\mathbf{e}. \quad (1.101)$$

Doing the same for the (1.90) leads to the following equations for the exterior problem.

$$\mathbf{e} = (\frac{1}{2} \text{Id} - \mathbf{H})\mathbf{e} - \mathbf{E}\mathbf{h}, \quad (1.102)$$

$$\mathbf{h} = (\frac{1}{2} \text{Id} - \mathbf{H})\mathbf{h} + \mathbf{E}\mathbf{e}. \quad (1.103)$$

We define the exterior and interior Calderón projectors, C^+ and C^- , as follows.

$$C^+ := \begin{bmatrix} \frac{1}{2} \text{Id} - \mathbf{H} & -\mathbf{E} \\ \mathbf{E} & \frac{1}{2} \text{Id} - \mathbf{H} \end{bmatrix}, \quad (1.104)$$

$$C^- := \begin{bmatrix} \frac{1}{2} \text{Id} + \mathbf{H} & \mathbf{E} \\ -\mathbf{E} & \frac{1}{2} \text{Id} + \mathbf{H} \end{bmatrix}. \quad (1.105)$$

We may then rewrite (1.100) to (1.103) as

$$C^- \begin{bmatrix} \mathbf{e} \\ \mathbf{h} \end{bmatrix} = \begin{bmatrix} \mathbf{e} \\ \mathbf{h} \end{bmatrix} \quad \text{and} \quad C^+ \begin{bmatrix} \mathbf{e} \\ \mathbf{h} \end{bmatrix} = \begin{bmatrix} \mathbf{e} \\ \mathbf{h} \end{bmatrix}. \quad (1.106)$$

We define the multitrace operator \mathbf{A} by

$$\mathbf{A} := \begin{bmatrix} \mathbf{H} & \mathbf{E} \\ -\mathbf{E} & \mathbf{H} \end{bmatrix}, \quad (1.107)$$

and we may write $C^- = \frac{1}{2} \text{Id} + \mathbf{A}$ and $C^+ = \frac{1}{2} \text{Id} - \mathbf{A}$.

For Maxwell problems, the following boundedness results are known.

Lemma 1.9 (Boundedness). *There exist $C_E, C_H > 0$ such that*

$$i) \quad \|\mathbf{E}\mathbf{f}\|_{\mathbf{H}_\times^{-1/2}(\text{div}_\Gamma, \Gamma)} \leq C_E \|\mathbf{f}\|_{\mathbf{H}_\times^{-1/2}(\text{div}_\Gamma, \Gamma)} \quad \forall \mathbf{f} \in \mathbf{H}_\times^{-1/2}(\text{div}_\Gamma, \Gamma), \quad (1.108)$$

$$ii) \quad \|\mathbf{H}\mathbf{f}\|_{\mathbf{H}_\times^{-1/2}(\text{div}_\Gamma, \Gamma)} \leq C_H \|\mathbf{f}\|_{\mathbf{H}_\times^{-1/2}(\text{div}_\Gamma, \Gamma)} \quad \forall \mathbf{f} \in \mathbf{H}_\times^{-1/2}(\text{div}_\Gamma, \Gamma). \quad (1.109)$$

Proof. [20, corollary 2]. □

— 1.4 —

PROPERTIES OF THE CALDERÓN PROJECTOR

In this section, we present a number of important properties of the Calderón projector as introduced in the previous section. The results presented in this section are valid for the Calderón projector in both the vector and scalar cases. We define the product space

$$\mathbb{V} = \begin{cases} H^{1/2}(\Gamma) \times H^{-1/2}(\Gamma) & \text{for Laplace and Helmholtz problems,} \\ \left[\mathbf{H}_\times^{-1/2}(\text{div}_\Gamma, \Gamma) \right]^2 & \text{for Maxwell problems,} \end{cases} \quad (1.110)$$

and note that in each case $\mathbf{C}^\pm : \mathbb{V} \rightarrow \mathbb{V}$.

We saw in the previous section that if $(a, b) \in \mathbb{V}$ is the trace data of an interior solution, then

$$\mathbf{C}^- \begin{bmatrix} a \\ b \end{bmatrix} = \begin{bmatrix} a \\ b \end{bmatrix}; \quad (1.111)$$

and if $(a, b) \in \mathbb{V}$ is the trace data of an exterior solution, then

$$\mathbf{C}^+ \begin{bmatrix} a \\ b \end{bmatrix} = \begin{bmatrix} a \\ b \end{bmatrix}. \quad (1.112)$$

Using the definitions of the Calderón projectors, we see that $\text{Id} - \mathbf{C}^- = \mathbf{C}^+$ and $\text{Id} - \mathbf{C}^+ = \mathbf{C}^-$. Using this, we see that if $(a, b) \in \mathbb{V}$ is the trace data of an interior solution, then

$$\mathbf{C}^+ \begin{bmatrix} a \\ b \end{bmatrix} = 0; \quad (1.113)$$

and if $(a, b) \in \mathbb{V}$ is the trace data of an exterior solution, then

$$\mathbf{C}^- \begin{bmatrix} a \\ b \end{bmatrix} = 0. \quad (1.114)$$

If a and b are the traces of a solution of the problem, we call (a, b) a pair of Cauchy data. The following lemma shows that applying the Calderón projector to any pair of functions leads to a pair of Cauchy data.

Lemma 1.10. *Given any arbitrary $(a, b) \in \mathbb{V}$, the product*

$$\mathbf{C}^\pm \begin{bmatrix} a \\ b \end{bmatrix} \tag{1.115}$$

defines a compatible pair of Cauchy data for the interior or exterior problem.

Proof. By (1.73), (1.75) and (1.83) for Laplace, (1.83) for Helmholtz, and (1.91) and (1.92) for Maxwell, we see that applying one of the representation formulae (1.48), (1.49), (1.89) and (1.90) to the functions (a, b) leads to a solution of the problem.

By the definition of the Calderón projector for each problem, $\mathbf{C}^\pm \begin{bmatrix} a \\ b \end{bmatrix}$ is the traces of this solution, and is therefore a pair of Cauchy data. \square

Combining (1.111) and (1.112) and lemma 1.10, we conclude that

$$(\mathbf{C}^-)^2 = \mathbf{C}^- \quad \text{and} \quad (\mathbf{C}^+)^2 = \mathbf{C}^+. \tag{1.116}$$

Using the second identity and the representation $\mathbf{C}^+ = \frac{1}{2}\text{Id} - \mathbf{A}$ we obtain

$$\mathbf{A}^2 = \frac{1}{4}\text{Id}. \tag{1.117}$$

This relationship is crucial for preconditioning numerical methods based on the Calderón projector, as we will see in chapter 2, and any discretisation scheme should preserve this property.

— — —

Now that you've finished reading chapter 1, why not take a break and fill figure 1.3 with hot liquid before reading on.

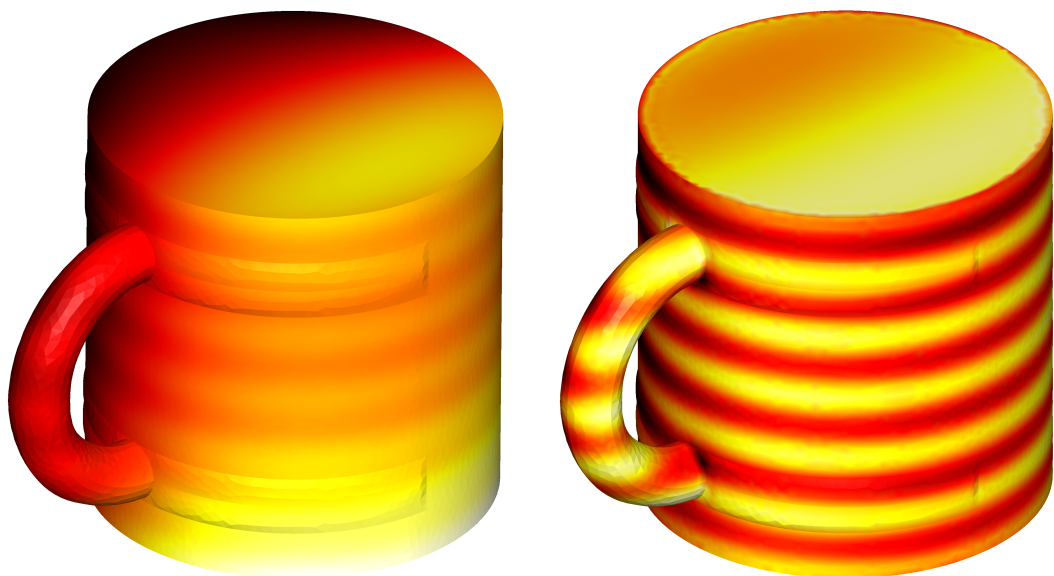


Figure 1.3: The results w_h (left) and η_h (right) of applying the interior Calderón projector for Laplace to the functions $v_h(\mathbf{x}) = (1 + z^2)^{-1} + \sin(y)$ and $\mu_h(\mathbf{x}) = \cos(3\pi z)$ on a mug. By lemma 1.10, these are a pair of compatible Cauchy data.

CHAPTER 2

A DISCRETE ALGEBRA FOR CALDERÓN OPERATORS AND ITS IMPLEMENTATION

The methods that we will present in chapters 3 to 5 are all based on properties of the Calderón projector and multitrace operator, as defined in (1.62), (1.63), (1.65), (1.104), (1.105) and (1.107). It is therefore important that the properties of these operators that we presented in chapter 1 are preserved—or approximately preserved—following discretisation. In this chapter, we look at how a discrete operator algebra can be designed that allows for easy computation with discrete operators, for example forming the product of operators, without the user having to directly interact with the technicalities of the implementation.

Suppose we want to compute

$$\mathbf{K}^2 v, \tag{2.1}$$

where $\mathbf{K} : H^{1/2}(\Gamma) \rightarrow H^{1/2}(\Gamma)$ is the double layer boundary operator, as defined in (1.50), and $v \in H^{1/2}(\Gamma)$. Defining

$$w := \mathbf{K}v, \tag{2.2}$$

we can rewrite (2.1) as

$$\mathbf{K}w. \tag{2.3}$$

Multiplying (2.2) by a test function $\mu \in H^{-1/2}(\Gamma)$, integrating over Γ , then discretising leads to

$$\langle \mathbf{K}v_h, \mu_h \rangle_\Gamma = \langle w_h, \mu_h \rangle_\Gamma. \tag{2.4}$$

Defining \mathbf{v}_h to be the vector of coefficients of the discrete approximation v_h of v , ie

$$\mathbf{v}_h = \begin{pmatrix} c_1 \\ c_2 \\ \vdots \\ c_n \end{pmatrix}, \quad \text{and} \quad v \approx v_h = \sum_{i=1}^n c_i \phi_i, \tag{2.5}$$

where $\{\phi_1, \phi_2, \dots, \phi_n\}$ is the basis of discrete space containing v_h ; and defining \mathbf{w}_h and $\boldsymbol{\mu}_h$ to be the vectors of coefficients of the discrete approximations of w and μ , we may write

(2.4) as

$$\mathbf{K}_1 \mathbf{v}_h = \mathbf{M} \mathbf{w}_h, \quad (2.6)$$

where \mathbf{K}_1 is a discretisation of the operator \mathbf{K} , and \mathbf{M} is the mass matrix defined by

$$[\mathbf{M}]_{i,j} = \langle \phi_j, \psi_i \rangle_\Gamma, \quad (2.7)$$

where $\{\phi_1, \phi_2, \dots, \phi_n\}$ is the basis of the space containing w_h , ie the range space of \mathbf{K} ; and $\{\psi_1, \psi_2, \dots, \psi_n\}$ is the basis of the space containing the test function μ_h .

Discretising (2.3) and using (2.6), leads to

$$\mathbf{K}_2 \mathbf{M}^{-1} \mathbf{K}_1 \mathbf{v}_h, \quad (2.8)$$

where \mathbf{K}_2 is a discretisation of the operator \mathbf{K} (which may or may not be equal to \mathbf{K}_1 , depending on the discrete spaces used).

Suppose now that we want to compute

$$\mathbf{A}^2 \begin{bmatrix} v \\ \mu \end{bmatrix}, \quad (2.9)$$

where \mathbf{A} is the multitrace operator mapping from the product Hilbert space \mathbb{V} into itself, and $(v, \mu) \in \mathbb{V}$. Proceeding as above, we arrive at the discretisation

$$\mathbf{A}_2 \mathbf{M}^{-1} \mathbf{A}_1 \begin{bmatrix} \mathbf{v}_h \\ \boldsymbol{\mu}_h \end{bmatrix}, \quad (2.10)$$

where \mathbf{A}_1 and \mathbf{A}_2 are discretisations of the multitrace operator \mathbf{A} (which may or may not be equal depending on the discretisation spaces used); \mathbf{v}_h and $\boldsymbol{\mu}_h$ are the vectors of coefficients, as above; and \mathbf{M} is the blocked diagonal mass matrix

$$\begin{bmatrix} \mathbf{M}_1 & 0 \\ 0 & \mathbf{M}_2 \end{bmatrix}, \quad (2.11)$$

where \mathbf{M}_1 and \mathbf{M}_2 are mass matrices between the appropriate discrete spaces.

In order to compute (2.8) or (2.10), we have to assemble the three matrices, compute the coefficients $(\mathbf{v}_h, \boldsymbol{\mu}_h)$, then evaluate $\mathbf{K}_2 \mathbf{M}^{-1} \mathbf{K}_1$ or $\mathbf{A}_2 \mathbf{M}^{-1} \mathbf{A}_1$ applied to these coefficients. Ideally we would not have to deal with these implementational details, and could just write the following code.

```
op1 = operator(...)
op2 = operator(...)
v = function(...)
mu = function(...)
result = op2 * op1 * [v,mu]
```

Here, the `*` operator has been overloaded to detect that two discrete operators are being

multiplied, and so the inverse mass matrix in (2.8) or (2.10) is applied automatically.

In order for this code snippet to work and the mass matrix \mathbf{M} to be assembled automatically, either the implementation of the operator product needs to be aware of the test space of `op1` and domain space of `op2`, or the software definition of these operators need to contain information about their range spaces. In this chapter, we will follow the latter approach by defining the notion of the strong form of a Galerkin discretisation and demonstrate its benefits.

Operator preconditioning [44, 75] involves applying an operator to the equation on the continuous level, then discretising the result. Our efficient implementation of this relies heavily on the discrete operator algebra, and the discretisation of these products of operators is the main justification of the developments in this chapter. Calderón preconditioning [27, 2] is a type of operator preconditioning whose efficacy is derived from properties of the Calderón projector, and is commonly used to precondition Maxwell’s equations. In addition to these operator preconditioning methods, we look in this chapter at mass matrix preconditioning, where an inverse mass matrix is applied to both sides after discretisation.

A theoretical framework for operator preconditioning was proposed in [44], where it was shown that in order to obtain well conditioned discrete problems, the discrete spaces used must form inf-sup stable dual pairings. In this chapter, we define the basis functions that define standard polynomial spaces, plus div- and curl-conforming Raviart–Thomas [65], Nédélec [57], and Rao–Wilton–Glisson [64] spaces. These standard spaces, however, do not provide inf-sup stable dual pairings, and so we additionally define dual spaces on the barycentric dual grid. In [16], it was shown that these barycentric spaces form inf-sup stable dual pairings with the standard spaces, allowing us to stably discretise the operator products we desire.

An implementation of a product algebra based on this idea is contained in Bempp. Initial steps towards a Bempp operator algebra were briefly described in [70] as part of a general library overview. The formalism introduced here is based on Riesz mappings between dual spaces. A nice introduction in the context of Galerkin discretisations is given in [48].

This chapter is based on the material in [68, 10].

— 2.1 —

ABSTRACT FORMULATION

In this section, we present an abstract framework for the representation of operator products and their discretisation, and look at the properties of the discrete spaces that this approach requires.

Let $A : \mathcal{H}_A^{\text{dom}} \rightarrow \mathcal{H}_A^{\text{ran}}$ and $B : \mathcal{H}_B^{\text{dom}} \rightarrow \mathcal{H}_B^{\text{ran}}$ be operators mapping between Hilbert

spaces. We assume that $\mathcal{H}_A^{\text{ran}} \subset \mathcal{H}_B^{\text{dom}}$, so that the product

$$g = \mathbf{B}Af \quad (2.12)$$

is well defined in $\mathcal{H}_B^{\text{ran}}$. Defining the function $q = Af$, the operator product (2.12) can equivalently be written as

$$q = \mathbf{A}f \quad (2.13a)$$

$$g = \mathbf{B}q. \quad (2.13b)$$

We begin by looking at (2.13a). In order to write this as a variational equation, we must define a space $\mathcal{H}_A^{\text{dual}}$ that is dual to $\mathcal{H}_A^{\text{ran}}$ and a dual pairing $\langle \cdot, \cdot \rangle_A : \mathcal{H}_A^{\text{ran}} \times \mathcal{H}_A^{\text{dual}} \rightarrow \mathbb{C}$. We may then write (2.13a) in variational form as

$$\langle \mathbf{A}f, \mu \rangle_A = \langle q, \mu \rangle_A \quad \forall \mu \in \mathcal{H}_A^{\text{dual}}. \quad (2.14a)$$

Similarly, we may write (2.13b) in variational form as

$$\langle \mathbf{B}q, \eta \rangle_B = \langle g, \eta \rangle_B \quad \forall \eta \in \mathcal{H}_B^{\text{dual}}. \quad (2.14b)$$

We now introduce the finite dimensional subspaces

$$\begin{aligned} \mathcal{H}_{h,A}^{\text{dom}} &:= \text{span}\{\phi_{i,A}^{\text{dom}}\} \subset \mathcal{H}_A^{\text{dom}}, & \mathcal{H}_{h,B}^{\text{dom}} &:= \text{span}\{\phi_{i,B}^{\text{dom}}\} \subset \mathcal{H}_B^{\text{dom}}, \\ \mathcal{H}_{h,A}^{\text{ran}} &:= \text{span}\{\phi_{i,A}^{\text{ran}}\} \subset \mathcal{H}_A^{\text{ran}}, & \mathcal{H}_{h,B}^{\text{ran}} &:= \text{span}\{\phi_{i,B}^{\text{ran}}\} \subset \mathcal{H}_B^{\text{ran}}, \\ \mathcal{H}_{h,A}^{\text{dual}} &:= \text{span}\{\phi_{i,A}^{\text{dual}}\} \subset \mathcal{H}_A^{\text{dual}}, & \mathcal{H}_{h,B}^{\text{dual}} &:= \text{span}\{\phi_{i,B}^{\text{dual}}\} \subset \mathcal{H}_B^{\text{dual}}, \end{aligned}$$

and discretise (2.14) to obtain

$$\mathbf{A}\mathbf{f}_h = \mathbf{M}_A\mathbf{q}_h, \quad (2.15a)$$

$$\mathbf{B}\mathbf{q}_h = \mathbf{M}_B\mathbf{g}_h, \quad (2.15b)$$

where

$$[\mathbf{A}]_{i,j} = \left\langle \mathbf{A}\phi_{j,A}^{\text{dom}}, \phi_{i,A}^{\text{dual}} \right\rangle_A, \quad (2.16a)$$

$$[\mathbf{M}_A]_{i,j} = \left\langle \phi_{j,A}^{\text{ran}}, \phi_{i,A}^{\text{dual}} \right\rangle_A, \quad (2.16b)$$

$$[\mathbf{B}]_{i,j} = \left\langle \mathbf{B}\phi_{j,B}^{\text{dom}}, \phi_{i,B}^{\text{dual}} \right\rangle_B, \quad (2.16c)$$

$$[\mathbf{M}_B]_{i,j} = \left\langle \phi_{j,B}^{\text{ran}}, \phi_{i,B}^{\text{dual}} \right\rangle_B, \quad (2.16d)$$

and the vectors \mathbf{f}_h , \mathbf{q}_h and \mathbf{g}_h are vectors of coefficients of approximation of the functions

f , q and q in the discrete spaces. Combining both equations we obtain

$$\mathbf{g}_h = \mathbf{M}_B^{-1} \mathbf{B} \mathbf{M}_A^{-1} \mathbf{A} \mathbf{f}_h. \quad (2.17)$$

Motivated by this, we define the discrete weak and strong forms of an operator as follows.

Definition 2.1. *We define the discrete weak form of an operator \mathbf{A} to be \mathbf{A} , as defined in (2.16a).*

Definition 2.2. *We define the discrete strong form of an operator \mathbf{A} to be*

$$\mathbf{A}^S := \mathbf{M}_A^{-1} \mathbf{A}, \quad (2.18)$$

where \mathbf{A} is the discrete weak form of \mathbf{M}_A is defined in (2.16b).

The matrix \mathbf{M}_A^{-1} represents a map from the discrete dual space $\mathcal{H}_{h,A}^{\text{dual}}$ into the space $\mathcal{H}_{h,A}^{\text{ran}}$, and so the strong form \mathbf{A}^S represents a discretisation of \mathbf{A} whose discrete domain and range are the subspaces of the domain and range of the operator \mathbf{A} . We now define the product of two discrete operators as follows.

Definition 2.3. *Given two operators \mathbf{A} and \mathbf{B} and their discrete weak forms \mathbf{A} and \mathbf{B} , we define their product by*

$$\mathbf{B} \odot \mathbf{A} := \mathbf{B} \mathbf{A}^S. \quad (2.19)$$

The product $\mathbf{B} \odot \mathbf{A}$ represents the discrete weak form of the product $\mathbf{B}\mathbf{A}$; the discrete strong form of $\mathbf{B}\mathbf{A}$ is given by $\mathbf{B}^S \odot \mathbf{A}$.

We note that the direct discretisation $\left\langle \mathbf{B} \mathbf{A} \phi_{j,A}^{\text{dom}}, \phi_{i,B}^{\text{dual}} \right\rangle_B$ is usually not identical to the product $\mathbf{B} \odot \mathbf{A}$ as the latter is computed as the solution of the operator system (2.14) whose discretisation error also depends on the space $\mathcal{H}_{h,A}^{\text{ran}}$ and the corresponding discrete dual. However, the discretisation of the operator product $\mathbf{B}\mathbf{A}$ can rarely be computed directly and solving (2.14) is usually the only possibility to evaluate this product.

In order to compute the discrete weak form, the implementation of an operator must be aware of the discrete domain and dual spaces; to compute the discrete strong form, the implementation operator must additionally be aware of the discrete range space. Providing these three spaces will allow our implementation to compute the product of two operators using the strong form as in definition 2.3.

The evaluation of the discrete strong form of an operator \mathbf{A} requires computing the inverse of the mass matrix \mathbf{M}_A , and so in order to form a stable discretisation of operator products, we need the condition number of \mathbf{M}_A to remain bounded as the mesh parameter h is reduced.

Let $\|\cdot\|_{\mathcal{H}_A^{\text{ran}}}$ be a norm defined on the space $\mathcal{H}_A^{\text{ran}}$, and define the norm $\|\cdot\|_{\mathcal{H}_A^{\text{dual}}}$, for $\phi_h^{\text{dual}} \in \mathcal{H}_A^{\text{dual}}$, by

$$\left\| \phi_h^{\text{dual}} \right\|_{\mathcal{H}_A^{\text{dual}}} = \sup_{\phi_h^{\text{ran}} \in \mathcal{H}_A^{\text{ran}}} \frac{\langle \phi_h^{\text{ran}}, \phi_h^{\text{dual}} \rangle_A}{\left\| \phi_h^{\text{ran}} \right\|_{\mathcal{H}_A^{\text{ran}}}}. \quad (2.20)$$

In order to show that the condition number of the mass matrix remains bounded as h is reduced, we make the following assumptions.

Assumption 2.1 (inf-sup condition). *There exists an h -independent constant $c_A > 0$ such that*

$$\sup_{\phi_h^{\text{dual}} \in \mathcal{H}_{h,A}^{\text{dual}}} \frac{\langle \phi_h^{\text{ran}}, \phi_h^{\text{dual}} \rangle_A}{\|\phi_h^{\text{dual}}\|_{\mathcal{H}_A^{\text{dual}}}} \geq c_A \|\phi_h^{\text{ran}}\|_{\mathcal{H}_A^{\text{ran}}}, \quad \forall \phi_h^{\text{ran}} \in \mathcal{H}_{h,A}^{\text{ran}}.$$

Assumption 2.2. *Let*

$$\begin{aligned} \phi_h^{\text{ran}} &= \sum_i p_i^{\text{ran}} \phi_i^{\text{ran}} \in \mathcal{H}_{h,A}^{\text{ran}}, & \phi_h^{\text{dual}} &= \sum_i p_i^{\text{dual}} \phi_i^{\text{dual}} \in \mathcal{H}_{h,A}^{\text{dual}}, \\ \mathbf{p}_{h,\text{ran}} &= \begin{pmatrix} p_1^{\text{ran}} \\ \vdots \\ p_n^{\text{ran}} \end{pmatrix} \in \mathbb{R}^n, & \mathbf{p}_{h,\text{dual}} &= \begin{pmatrix} p_1^{\text{dual}} \\ \vdots \\ p_n^{\text{dual}} \end{pmatrix} \in \mathbb{R}^n. \end{aligned}$$

There exist h -independent constants $a \in \mathbb{R}$, and $c_{\text{ran}}, C_{\text{ran}}, c_{\text{dual}}, C_{\text{dual}} > 0$ such that

$$\begin{aligned} c_{\text{ran}} h^a \|\phi_h^{\text{ran}}\|_{\mathcal{H}_A^{\text{ran}}} &\leq \|\mathbf{p}_{h,\text{ran}}\|_2 \leq C_{\text{ran}} h^a \|\phi_h^{\text{ran}}\|_{\mathcal{H}_A^{\text{ran}}}, \\ c_{\text{dual}} h^{-a} \|\phi_h^{\text{dual}}\|_{\mathcal{H}_A^{\text{dual}}} &\leq \|\mathbf{p}_{h,\text{dual}}\|_2 \leq C_{\text{dual}} h^{-a} \|\phi_h^{\text{dual}}\|_{\mathcal{H}_A^{\text{dual}}}, \end{aligned}$$

where $\|\cdot\|_2$ is the 2-norm of a vector.

Assumption 2.2 will hold for the Sobolev norms that we will use as long as the discretisations are quasi-uniform (see eg [34, lemma 9.7]).

Using these assumptions, we now prove, following [44], that the condition number of the matrix \mathbf{M}_A is bounded by a constant.

Lemma 2.1. *If assumptions 2.1 and 2.2 hold, then the spectral condition number of the matrix \mathbf{M}_A defined in (2.16b) satisfies*

$$\kappa(\mathbf{M}_A) \leq c'_A,$$

from some h -independent constant c'_A .

Proof. Let $\phi_h^{\text{ran}} \in \mathcal{H}_{h,A}^{\text{ran}}$. By assumption 2.1, we see that

$$\sup_{\phi_h^{\text{dual}} \in \mathcal{H}_{h,A}^{\text{dual}}} \frac{\langle \phi_h^{\text{ran}}, \phi_h^{\text{dual}} \rangle_A}{\|\phi_h^{\text{dual}}\|_{\mathcal{H}_A^{\text{dual}}} \|\phi_h^{\text{ran}}\|_{\mathcal{H}_A^{\text{ran}}}} \geq c_A. \quad (2.21)$$

Define $\mathbf{p}_{h,\text{ran}}$ and $\mathbf{p}_{h,\text{dual}}$ as in assumption 2.2. By the definition of \mathbf{M}_A and assumption 2.2, we see that

$$c_A \leq \frac{1}{C_{\text{dual}} C_{\text{ran}}} \sup_{\mathbf{p}_{h,\text{dual}} \in \mathbb{R}^n} \frac{\mathbf{p}_{h,\text{dual}}^T \mathbf{M}_A \mathbf{p}_{h,\text{ran}}}{\|\mathbf{p}_{h,\text{dual}}\|_2 \|\mathbf{p}_{h,\text{ran}}\|_2}. \quad (2.22)$$

Let σ_n be the smallest eigenvalue of M_A , and let $\mathbf{p}_{h,\text{ran}} = \mathbf{v}_n$ be the corresponding eigenvector. Applying this gives

$$\begin{aligned} c_A &\leq \frac{\sigma_n}{C_{\text{dual}}C_{\text{ran}}} \sup_{\mathbf{p}_{h,\text{dual}} \in \mathbb{R}^n} \frac{\mathbf{p}_{h,\text{dual}}^T \mathbf{v}_n}{\|\mathbf{p}_{h,\text{dual}}\|_2 \|\mathbf{v}_n\|_2} \\ &= \frac{\sigma_n}{C_{\text{dual}}C_{\text{ran}}}. \end{aligned} \quad (2.23)$$

Taking σ_1 to be the largest eigenvalue of M_A , and \mathbf{v}_1 to be the corresponding eigenvector, we see that

$$\begin{aligned} \sigma_1 &= \sigma_1 \sup_{\mathbf{p}_{h,\text{dual}} \in \mathbb{R}^n} \frac{\mathbf{p}_{h,\text{dual}}^T \mathbf{v}_1}{\|\mathbf{p}_{h,\text{dual}}\|_2 \|\mathbf{v}_1\|_2} \\ &= \sup_{\mathbf{p}_{h,\text{dual}} \in \mathbb{R}^n} \frac{\mathbf{p}_{h,\text{dual}}^T M_A \mathbf{v}_1}{\|\mathbf{p}_{h,\text{dual}}\|_2 \|\mathbf{v}_1\|_2} \\ &\leq \sup_{\mathbf{p}_{h,\text{ran}} \in \mathbb{R}^n} \sup_{\mathbf{p}_{h,\text{dual}} \in \mathbb{R}^n} \frac{\mathbf{p}_{h,\text{dual}}^T M_A \mathbf{p}_{h,\text{ran}}}{\|\mathbf{p}_{h,\text{dual}}\|_2 \|\mathbf{p}_{h,\text{ran}}\|_2} \\ &\leq \frac{1}{C_{\text{dual}}C_{\text{ran}}} \sup_{\phi_h^{\text{ran}} \in \mathcal{H}_{h,A}^{\text{ran}}} \sup_{\phi_h^{\text{dual}} \in \mathcal{H}_{h,A}^{\text{dual}}} \frac{\langle \phi_h^{\text{ran}}, \phi_h^{\text{dual}} \rangle_A}{\|\phi_h^{\text{dual}}\|_{\mathcal{H}_A^{\text{dual}}} \|\phi_h^{\text{ran}}\|_{\mathcal{H}_A^{\text{ran}}}} \\ &= \frac{1}{C_{\text{dual}}C_{\text{ran}}} \sup_{\phi_h^{\text{dual}} \in \mathcal{H}_{h,A}^{\text{dual}}} \frac{1}{\|\phi_h^{\text{dual}}\|_{\mathcal{H}_A^{\text{dual}}}} \sup_{\phi_h^{\text{ran}} \in \mathcal{H}_{h,A}^{\text{ran}}} \frac{\langle \phi_h^{\text{ran}}, \phi_h^{\text{dual}} \rangle_A}{\|\phi_h^{\text{ran}}\|_{\mathcal{H}_A^{\text{ran}}}} \\ &= \frac{1}{C_{\text{dual}}C_{\text{ran}}}. \end{aligned} \quad (2.24)$$

Combining (2.23) and (2.24), we obtain

$$\kappa(M_A) = \frac{\sigma_1}{\sigma_n} \quad (2.25)$$

$$\leq \frac{1}{c_A C_{\text{dual}} C_{\text{ran}} c_{\text{dual}} c_{\text{ran}}} \quad (2.26)$$

$$=: c'_A. \quad (2.27)$$

□

— 2.2 —

SOFTWARE IMPLEMENTATION OF AN OPERATOR ALGEBRA

Based on the definition of a discrete product algebra for Galerkin discretisations, we can now discuss the software implementation. Two concepts are crucial: namely that of a *grid function*, which represents functions defined on a grid; and that of an *operator*, which maps grid functions from a discrete domain space into a discrete range space.

— 2.2.1 —

GRID FUNCTIONS

We start with the description of a grid function. Let $\phi_h \in \mathcal{H}_h$, and let \mathbf{p}_h be the vector of coefficients of ϕ_h , as defined in assumption 2.2. A basic grid function object is defined by the discrete function space, \mathcal{H}_h , and a vector of coefficients on the space, \mathbf{p}_h . In Bempp, this can be done as follows.

```
fun = bempp.api.GridFunction(space, coefficients=...)
```

However, for practical purposes this is not always sufficient. Consider the following situation. Let \mathbf{E} be the electric field integral operator (1.93), let $\mathbf{f} \in \mathbf{H}_\times^{-1/2}(\text{div}_\Gamma, \Gamma)$, and suppose we want the function $\mathbf{g} := \mathbf{E}\mathbf{f}$. On the discrete level, the vector of coefficients \mathbf{g}_h is given by $\mathbf{g}_h = \mathbf{E}^S \mathbf{f}_h = \mathbf{M}_E^{-1} \mathbf{E} \mathbf{f}_h$, where \mathbf{f}_h is the vector of coefficients of \mathbf{f} , \mathbf{E}^S and \mathbf{E} are the discrete strong and weak forms of \mathbf{E} , and \mathbf{M}_E is the mass matrix between the range and dual of \mathbf{E} .

If the spaces used the discretise \mathbf{E} are not inf-sup stable, then by lemma 2.1 the mass matrix \mathbf{M}_E may have be strongly ill-conditioned. In this case, we also allow the definition of a grid function purely through the vector of coefficients on the dual space. This can be done as follows.

```
fun = bempp.api.GridFunction(space, dual_space=..., projections=...)
```

Associated with these two constructors are two methods that extract the vectors of coefficients or projections.

```
coeffs = fun.coefficients()
proj = fun.projections(dual_space)
```

If the grid function is initialised with a coefficient vector, then the first operation just returns this vector, and the second operation sets up the corresponding mass matrix \mathbf{M} and returns the vector $\mathbf{M} * \text{coeffs}$.

If the grid function is initialised with a vector of projections and a corresponding dual space, then the first operation returns the solution of a linear system if the space and dual space have the same number of degrees of freedom. Otherwise, an exception is thrown. If the `projections` method is called and the given dual space is identical to the original dual space on initialisation, the vector `projections` is returned. Otherwise, first a conversion to coefficient form via a call to `coefficients` is attempted.

This dual representation of a grid function via either a vector of coefficients or a vector of projections makes it possible to represent functions in many standard situations, where a conversion between coefficients and projections is mathematically not possible and not necessary for the formulation of a problem.

— 2.2.2 —

OPERATORS

In finite element discretisation libraries, the definition of an operator typically requires an underlying weak form, a domain space and a test space. However, to support the operator algebra introduced in section 2.1, the range space is also required. Hence, we represent a constructor for a boundary operator in the following form.

```
op = operator(domain, range_, dual_to_range, ...)
```

Here, the objects `domain`, `range_` and `dual_to_range` describe the finite dimensional domain, range and dual spaces. The space `range_` has the trailing underscore to avoid conflict with Python's internal `range` function. Each operator provides the following two methods.

```
discrete_weak_form = op.weak_form()
discrete_strong_form = op.strong_form()
```

The first one returns the standard discrete weak form (definition 2.1) while the second one returns the discrete strong form (definition 2.2). The `discrete_weak_form` and `discrete_strong_form` are objects that provide at least a matrix-vector routine to multiply a vector with the corresponding discrete operator. The multiplication with the inverse of the mass matrix in the strong form is implemented via the computation of an LU decomposition and solving the associated linear system.

As discretising an operator is expensive, the weak form is computed when the method `weak_form()` is first called and then cached. Similarly, the LU decomposition necessary for the strong form is computed only once and then cached.

— 2.2.3 —

OPERATIONS ON OPERATORS AND GRID FUNCTIONS

With this framework the multiplication `op * fun` of a boundary operator `op` with a grid function `fun` can be elegantly described in the following way:

```
result_fun = bempp.api.GridFunction(
    space=op.range_,
    dual_space=op.dual_to_range,
    projections=op.weak_form() * fun.coefficients)
```

Alternatively, we could have more simply presented the result as

```
result_fun = bempp.api.GridFunction(
    space=op.range_,
    coefficients=op.strong_form() * fun.coefficients)
```

However, the latter is only valid when there is a stable mass matrix transformation available that could map from the discrete dual space to the discrete range space.

The internal implementation of the product of two operators is equally simple in this framework. Given two operators `op1` and `op2`, the `weak_form()` method of the product `op1 ⊙ op2`, which can be obtained in python by writing `op1 * op2`, is defined as follows.

```
def weak_form():
    return op1.weak_form() * op2.strong_form()
```

Correspondingly, the strong form of the product is implemented as:

```
def strong_form():
    return op1.strong_form() * op2.strong_form()
```

Internally, the product of two discrete operators provides a matrix-vector routine that successively applies the two operators to a given vector. If `op1` and `op2` implement caching then an actual discretisation of a weak form is only performed once, and the product of the two operators is performed with almost no overhead.

It is easy to wrap standard iterative solvers (such as those in SciPy [46]) to support this operator algebra. For example, the definition of such a GMRES routine is as follows.

```
def gmres(A, b, ...):
    from scipy.sparse import linalg
    x, info = linalg.gmres(A.weak_form(), b.projections(A.dual_to_range), ...)
    return GridFunction(A.domain, coefficients=x), info
```

The weak form of the operator `A` and the projection of the function `b` onto its dual space are computed, then these are handed over to SciPy. The solution is then returned as a `GridFunction`.

The full Bempp GMRES implementation provides, among other options, a keyword attribute `use_strong_form`. If this is set to `True`, then inside the GMRES routine the solution is computed as

```
x, info = linalg.gmres(A.strong_form(), b.coefficients)
```

This corresponds to mass matrix preconditioning and comes naturally as part of this algebra.

— 2.2.4 —

PRECONDITIONING

The implementation of this operator algebra allows for the easy implementation of operator preconditioning methods, and mass matrix preconditioning.

Suppose we want to solve $Au = f$, where A is an operator, f is a known function, and u is unknown. The discrete weak form of this equation is

$$Au_h = M_A f_h. \tag{2.28}$$

The mass matrix preconditioned form of this equation corresponds to taking its discrete

strong form,

$$M_A^{-1} \mathbf{A} \mathbf{u}_h = \mathbf{f}_h, \quad (2.29)$$

$$\text{or } \mathbf{A}^S \mathbf{u}_h = \mathbf{f}_h. \quad (2.30)$$

Operator preconditioning arises from applying an operator on the continuous level, then discretising. For example, the operator \mathbf{B} can be applied to give the equation $\mathbf{B} \mathbf{A} u = \mathbf{B} f$. The weak form of this equation is

$$\mathbf{B} M_A^{-1} \mathbf{A} \mathbf{u}_h = M_B \mathbf{f}_h, \quad (2.31)$$

$$\text{or } \mathbf{B} \odot \mathbf{A} \mathbf{u}_h = M_B \mathbf{f}_h. \quad (2.32)$$

This is the operator preconditioned formulation. Typically, an operator \mathbf{A} is preconditioned with an operator of the opposite order [75], for example the hypersingular operator \mathbf{W} may be used to precondition the single-layer operator \mathbf{V} , as in (2.47).

Calderón preconditioning, a form of operator preconditioning derived from properties of the Calderón projector and commonly used for Maxwell problems is discussed in section 2.4.

— 2.2.5 —

BLOCKED OPERATORS

The operator algebra defined in Bempp can also be used for blocked systems of operators. Suppose we want to solve a Laplace Dirichlet problem using the weak imposition formulation (3.14) that we will derive in chapter 3. In strong form, this formulation can be written as

$$\left(\mathbf{A} + \begin{bmatrix} \frac{1}{2} \text{Id} & 0 \\ \beta_D \text{Id} & -\frac{1}{2} \text{Id} \end{bmatrix} \right) \begin{bmatrix} u \\ \lambda \end{bmatrix} = \begin{bmatrix} g_D \\ \beta_D g_D \end{bmatrix}. \quad (2.33)$$

The code to solve this system takes the following form.

```

beta = ...
A = bempp.api.operators.boundary.laplace.multitrace_operator(...)
D = bempp.api.BlockedOperator(2,2)
D[0,0] = 0.5 * bempp.api.operators.boundary.sparse.identity(...)
D[1,0] = beta * bempp.api.operators.boundary.sparse.identity(...)
D[1,1] = -0.5 * bempp.api.operators.boundary.sparse.identity(...)
g = bempp.api.GridFunction(...)
solution, info = bempp.api.gmres(A+D, [g, beta * g], use_strong_form=True)

```

The implementation of GMRES in this case will compute the strong form of each block of the blocked operator, and pass the results and the coefficients of each `GridFunction` to SciPy. The solution will then be split, and a list of `GridFunction` objects will be returned.

The keyword argument `use_strong_form` has been used to apply mass matrix precon-

ditioning. In this case, the mass matrix preconditioner is a blocked diagonal matrix, and so the preconditioned discrete system is

$$\begin{bmatrix} \mathbf{M}_{\mathbf{K}}^{-1} & 0 \\ 0 & \mathbf{M}_{\mathbf{K}'}^{-1} \end{bmatrix} \left(\mathbf{A} + \begin{bmatrix} \frac{1}{2}\mathbf{M}_{11} & 0 \\ \beta_{\mathbf{D}}\mathbf{M}_{21} & -\frac{1}{2}\mathbf{M}_{22} \end{bmatrix} \right) \begin{bmatrix} \mathbf{u}_h \\ \boldsymbol{\lambda}_h \end{bmatrix} = \begin{bmatrix} \mathbf{M}_{\mathbf{K}}^{-1} & 0 \\ 0 & \mathbf{M}_{\mathbf{K}'}^{-1} \end{bmatrix} \begin{bmatrix} \mathbf{g}_h \\ \beta_{\mathbf{D}}\mathbf{g}_h \end{bmatrix}, \quad (2.34)$$

where $\mathbf{M}_{\mathbf{K}}$ and $\mathbf{M}_{\mathbf{K}'}$ are the mass matrices between the range and dual spaces of the top left and bottom right blocks of \mathbf{A} respectively, and all the other terms are discretisations of the terms in (2.33).

— 2.3 —

LAPLACE'S EQUATION AND THE HELMHOLTZ EQUATION

In this section, we look at specific implementation details and applications of the discrete operator algebra for Laplace's equation and the Helmholtz equation. First, we must define the finite dimensional spaces of piecewise polynomials that we will use to discretise the formulations we present.

— 2.3.1 —

DISCRETE SPACES

We introduce a family of conforming, shape regular triangulations of Γ , $\{\mathcal{T}_h\}_{h>0}$, indexed by the largest element diameter of the mesh, h . We let T_1, \dots, T_o be the triangles in the triangulation \mathcal{T}_h . We assume that the triangulations are fitted to the different boundary sets $\Gamma_{\mathbf{D}}$, $\Gamma_{\mathbf{R}}$ and $\Gamma_{\mathbf{N}}$.

—

PIECEWISE POLYNOMIAL SPACES

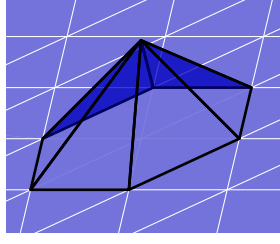
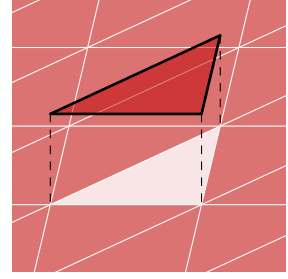
We define the space of continuous polynomial functions by

$$\mathbf{P}_h^k := \{v_h \in C^0(\Gamma) : v_h|_{T_i} \in \mathbb{P}_k(T_i), \text{ for every } T_i \in \mathcal{T}_h\},$$

where $\mathbb{P}_k(T_i)$ denotes the space of polynomials of order less than or equal to k on T_i .

Typically, we will take $k = 1$ and use the space of continuous piecewise linear functions. We can write $\mathbf{P}_h^1 = \text{span}\{\phi_1, \dots, \phi_n\}$, where for $i = 1, \dots, n$, ϕ_i is the function that is linear within each triangle and

$$\phi_i(\mathbf{v}_j) = \begin{cases} 1 & i = j \\ 0 & i \neq j \end{cases} \quad \text{for } j = 1, \dots, n, \quad (2.35)$$

Figure 2.1: An example basis function $\phi_i \in \mathbb{P}_h^1(\Gamma)$.Figure 2.2: An example basis function $\psi_i \in \text{DP}_h^0(\Gamma)$.

where $\mathbf{v}_1, \dots, \mathbf{v}_n$ are the vertices in the triangulation \mathcal{T}_h . An example basis function is shown in figure 2.1.

We define the space of discontinuous polynomial functions by

$$\text{DP}_h^l := \{v_h \in L^2(\Gamma) : v_h|_T \in \mathbb{P}_l(T), \text{ for every } T \in \mathcal{T}_h\}.$$

Typically, we will take $l = 0$ and use the space of piecewise constant functions. We can write $\text{DP}_h^0 = \text{span}\{\psi_1, \dots, \psi_o\}$, where

$$\psi_i(\mathbf{x}) = \begin{cases} 1 & \mathbf{x} \in T_i \\ 0 & \text{otherwise} \end{cases} \quad \text{for } j = 1, \dots, o. \quad (2.36)$$

where T_1, \dots, T_o are the triangles in the triangulation \mathcal{T}_h . An example basis function is shown in figure 2.2.

We observe that $\mathbb{P}_h^k \subset H^{1/2}(\Gamma)$ and $\text{DP}_h^l \subset L^2(\Gamma)$. The following approximation properties of these finite dimensional spaces are known.

Lemma 2.2. $\forall \mu \in H^s(\Gamma)$,

$$\inf_{\eta_h \in \text{DP}_h^0(\Gamma)} \|\mu - \eta_h\|_{H^{-1/2}(\Gamma)} \lesssim h^{\xi+1/2} \|\mu\|_{H^\xi(\Gamma)} \quad (2.37)$$

$$\inf_{\eta_h \in \text{DP}_h^0(\Gamma)} \|\mu - \eta_h\|_{L^2(\Gamma)} \lesssim h^\xi \|\mu\|_{H^\xi(\Gamma)}, \quad (2.38)$$

where $\xi = \min(1, s)$.

Proof. [73, theorem 10.4]. □

Lemma 2.3. $\forall v \in H^s(\Gamma)$,

$$\inf_{w_h \in \mathbb{P}_h^1(\Gamma)} \|v - w_h\|_{H^{1/2}(\Gamma)} \lesssim h^{\zeta-1/2} \|v\|_{H^\zeta(\Gamma)} \quad (2.39)$$

$$\inf_{w_h \in \mathbb{P}_h^1(\Gamma)} \|v - w_h\|_{L^2(\Gamma)} \lesssim h^\zeta \|v\|_{H^\zeta(\Gamma)}, \quad (2.40)$$

where $\zeta = \min(2, s)$.

Proof. [73, theorem 10.9]. □

DUAL POLYNOMIAL SPACES

In addition to the polynomial spaces described above, we will also use polynomial spaces defined on the dual grid. As shown in figure 2.3, the dual grid is defined by barycentrically refining each triangle in the grid: a straight line is drawn from each vertex to the midpoint of the opposite side, splitting each triangle into six smaller triangles. The elements of the dual grid are then made up of all the triangles in the refined grid that are attached to a given vertex in the original grid.

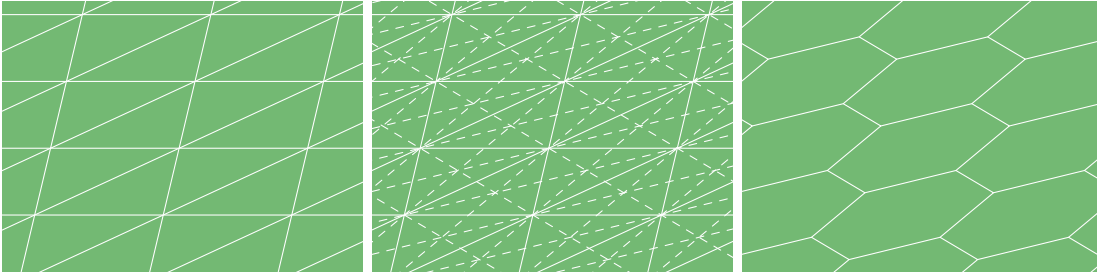


Figure 2.3: A grid (left), the barycentric refinement of the grid (centre), and the dual grid (right).

We define $\text{DUAL}_h^0(\Gamma)$ to be the space of piecewise constant functions on the dual grid. We observe that $\text{DUAL}_h^0(\Gamma) \subset L^2(\Gamma)$.

We can write $\text{DUAL}_h^0(\Gamma) = \text{span}\{\chi_1, \dots, \chi_n\}$, where χ_i is defined to be equal to 1 on one polygon in the dual grid and 0 otherwise. An example basis function is shown in figure 2.4.

We note that in the majority of cases—for example if the surface is curved, or has edges between flat faces—then the triangles that make up the dual grid polygons will not form a flat surface. In this case the elements of the dual grid are defined to be the union of these triangles and so will not be flat.

This space forms a inf-sup stable dual pairing with the space of continuous linear functions $\text{P}_h^1(\Gamma)$, as given in the following result. The space pairing $\text{P}_h^1(\Gamma) \times \text{DUAL}_h^0(\Gamma)$ therefore satisfies assumption 2.1.

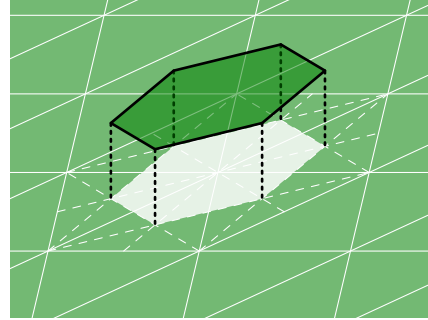


Figure 2.4: An example basis function $\chi_i \in \text{DUAL}_h^0(\Gamma)$.

Proposition 2.1. *There exists $C > 0$ such that*

$$\inf_{v_h \in \text{P}_h^1(\Gamma)} \sup_{\mu_h \in \text{DUAL}_h^0(\Gamma)} \frac{\int_{\Gamma} v_h \mu_h}{\|v_h\|_{L^2(\Gamma)} \|\mu_h\|_{L^2(\Gamma)}} \geq \frac{1}{C}. \quad (2.41)$$

Proof. [72, lemma 3.1]. □

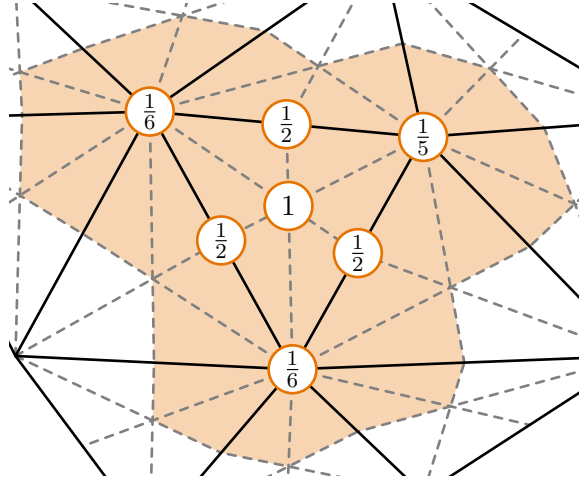


Figure 2.6: The coefficients used to define a function $\xi_i \in \text{DUAL}_h^1(\Gamma)$ in terms of functions in $\text{P}_h^1(\Gamma)$ on the barycentrically refined grid. The support of ξ_i is shaded in orange.

Let T_i be a triangle in the non-refined coarse grid. Let ξ_i be a piecewise linear function on the barycentrically refined grid such that, for each vertex \tilde{v}_j in the barycentrically refined grid,

$$\xi_i(\tilde{v}_j) = \begin{cases} 1 & \tilde{v}_j \text{ is the barycentre of } T_i, \\ \frac{1}{2} & \tilde{v}_j \text{ is the midpoint of an edge of } T_i, \\ \frac{1}{o_j} & \tilde{v}_j \text{ is one of the vertices of } T_i, \\ 0 & \text{otherwise,} \end{cases} \quad (2.42)$$

where o_j is the number of triangles in the non-refined coarse grid that have a vertex at the point \tilde{v}_j . An example such function is shown in figure 2.5, and some example coefficients are shown in figure 2.6.

We define $\text{DUAL}_h^1(\Gamma)$ to be the space of piecewise linear functions spanned by the basis functions ξ_1, \dots, ξ_o . We observe that $\text{DUAL}_h^1(\Gamma) \subset H^{1/2}(\Gamma)$.

The space was defined in [16], as a space that forms a inf-sup stable dual pairing with the space of piecewise constant functions $\text{DP}_h^0(\Gamma)$, as given in the following result. The space pairing $\text{DUAL}_h^1(\Gamma) \times \text{DP}_h^0(\Gamma)$ therefore satisfies assumption 2.1.

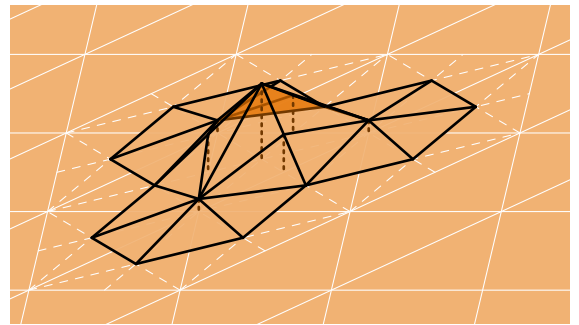


Figure 2.5: An example basis function $\xi_i \in \text{DUAL}_h^1(\Gamma)$.

Proposition 2.2. *There exists $C > 0$ such that*

$$\inf_{\mu_h \in \text{DP}_h^0} \sup_{v_h \in \text{DUAL}_h^1} \frac{\int_{\Gamma} \mu_h v_h}{\|\mu_h\|_{L^2(\Gamma)} \|v_h\|_{L^2(\Gamma)}} \geq \frac{1}{C}. \quad (2.43)$$

Proof. [16, proposition 3.9]. □

The following approximation properties of the spaces $\text{DUAL}_h^0(\Gamma)$ and $\text{DUAL}_h^1(\Gamma)$ can be proven.

Lemma 2.4. *For all $v, \mu \in H^s(\Gamma)$,*

$$\begin{aligned} \inf_{\eta_h \in \text{DUAL}_h^0(\Gamma)} \|\mu - \eta_h\|_{H^{-1/2}(\Gamma)} &\lesssim h^{\xi+1/2} \|\mu\|_{H^\xi(\Gamma)} \\ \inf_{w_h \in \text{DUAL}_h^1(\Gamma)} \|v - w_h\|_{H^{1/2}(\Gamma)} &\lesssim h^{\zeta-1/2} \|v\|_{H^\zeta(\Gamma)} \end{aligned}$$

where $\xi = \min(\frac{1}{2}, s)$ and $\zeta = \min(\frac{3}{2}, s)$.

Proof. Proof of these results can be found in appendix B. □

Typically, we will use the space $\text{DUAL}_h^0(\Gamma)$ to approximate the normal derivative $\lambda = \gamma_N u$ of the solution u . When Γ is smooth, the normal ν will be continuous across edges, and we will expect order 1 convergence due to corollary B.1.

In [16], a space of divergence-conforming vector functions on the dual grid was also defined. We will examine this space in more detail in section 2.4.4.

— 2.3.2 —

STABLE DISCRETISATION OF THE MULTITRACE OPERATOR

In section 1.4, we derived some important properties of the Calderón projectors and multitrace operator, including $\mathbf{A}^2 = \frac{1}{4}\text{Id}$, $[\mathbf{C}^\pm]^2 = \mathbf{C}^\pm$. In order to preserve these properties on the discrete level, we look to discretise these operators in a stable way, so that the mass matrices involved in squaring these operators satisfy assumption 2.1.

As well as the application to the formulations that we examine in chapters 3 to 5, it is common to derive methods of operator preconditioning [75, 44] from these identities. The stable discretisation of the Calderón operators provides an easy implementation of such preconditioning methods.

Denote by

$$\mathbf{A} := \begin{bmatrix} -\mathbf{K} & \mathbf{V} \\ \mathbf{W} & \mathbf{K}' \end{bmatrix}, \tag{2.44}$$

the discretisation of the operator \mathbf{A} , as defined in (1.65). Here, \mathbf{K} , \mathbf{V} , \mathbf{W} , and \mathbf{K}' are discretisations of the double layer, single layer, hypersingular, and adjoint double layer boundary operators (respectively).

In order for this discretisation to be able to be multiplied by itself, we must choose the discrete spaces so that the mass matrix mappings formed in the product are stable, satisfying assumption 2.1. A choice of spaces for the operators that achieves this goal is shown in the table below.

Matrix	Operator	Domain	Range	Dual to Range
\mathbf{K}	Double layer	$P_h^1(\Gamma)$	$P_h^1(\Gamma)$	$\text{DUAL}_h^0(\Gamma)$
\mathbf{V}	Single layer	$\text{DUAL}_h^0(\Gamma)$	$P_h^1(\Gamma)$	$\text{DUAL}_h^0(\Gamma)$
\mathbf{W}	Hypersingular	$P_h^1(\Gamma)$	$\text{DUAL}_h^0(\Gamma)$	$P_h^1(\Gamma)$
\mathbf{K}'	Adjoint double layer	$\text{DUAL}_h^0(\Gamma)$	$\text{DUAL}_h^0(\Gamma)$	$P_h^1(\Gamma)$

These choices of spaces lead to all mass matrices in the discretisation of \mathbf{A}^2 being the $P_h^1(\Gamma)$ – $\text{DUAL}_h^0(\Gamma)$ pairing, that were shown in proposition 2.1 to satisfy assumption 2.1.

In some cases, for example when weakly imposing boundary conditions on the cube as in chapter 3, it is undesirable to use the space $\text{DUAL}_h^0(\Gamma)$ as the domain of the single layer operator due to this space's lower order convergence properties (lemma 2.4). In cases such as this, it may be more desirable to the following discretisation spaces.

Matrix	Operator	Domain	Range	Dual to Range
\mathbf{K}	Double layer	$P_h^1(\Gamma)$	$P_h^1(\Gamma)$	$\text{DUAL}_h^0(\Gamma)$
\mathbf{V}	Single layer	$\text{DP}_h^0(\Gamma)$	$P_h^1(\Gamma)$	$\text{DUAL}_h^0(\Gamma)$
\mathbf{W}	Hypersingular	$P_h^1(\Gamma)$	$\text{DP}_h^0(\Gamma)$	$\text{DUAL}_h^1(\Gamma)$
\mathbf{K}'	Adjoint double layer	$\text{DP}_h^0(\Gamma)$	$\text{DP}_h^0(\Gamma)$	$\text{DUAL}_h^1(\Gamma)$

Later, in chapter 3 and appendix C, we will look at using this second discretisation of \mathbf{A} , as the domains of all the operators involved have good convergence orders (lemmas 2.2 and 2.3), while mass matrix preconditioning can be effectively applied as all the dual products are stable (propositions 2.1 and 2.2).

Using the Bempp library, the stable Laplace multitrace operator defined in the first table may be created using the following lines of Python.

```
from bempp.api.operators.boundary import laplace
multitrace = laplace.multitrace_operator(grid, spaces="dual")
```

The stable multitrace operator for Helmholtz may be created using the following lines.

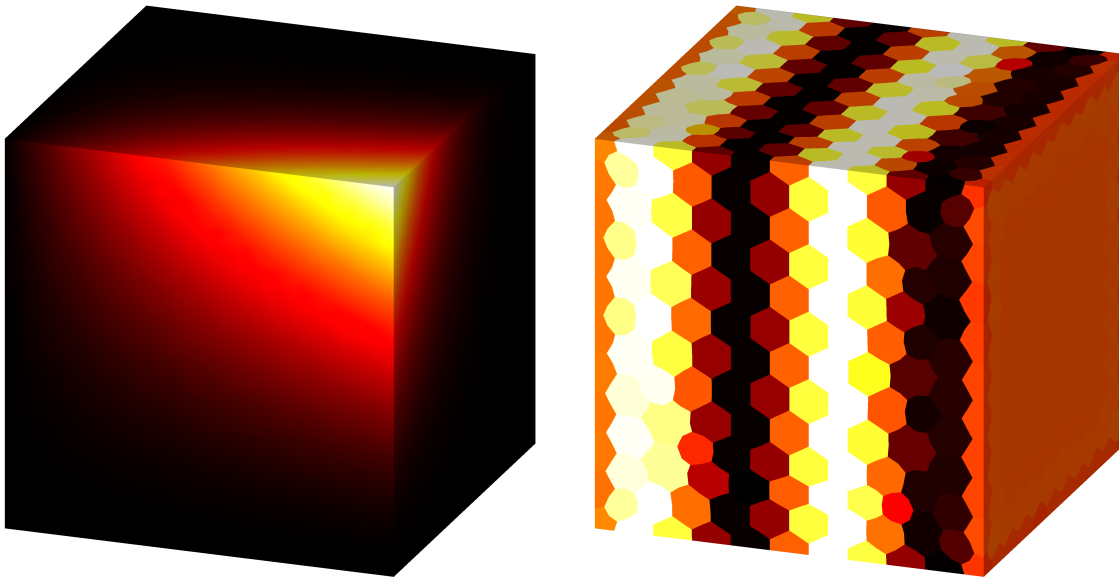
```
from bempp.api.operators.boundary import helmholtz
multitrace = helmholtz.multitrace_operator(grid, k, spaces="dual")
```

We may then create the interior Calderón projector with the following lines.

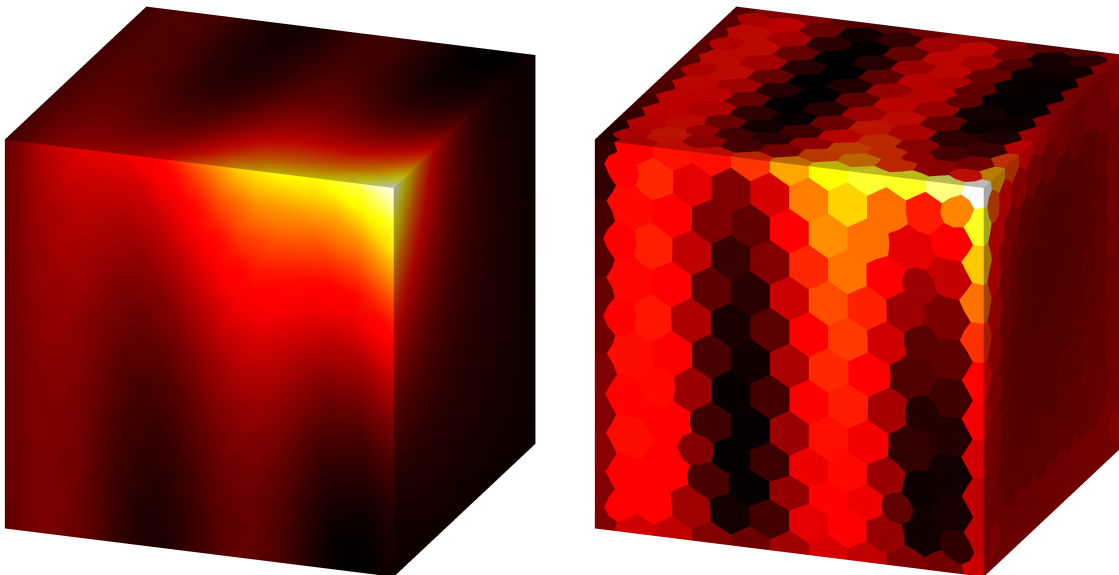
```
from bempp.api.operators.boundary import sparse
identity = sparse.multitrace_identity(grid, spaces="dual")
calderon = 0.5 * identity + multitrace
```

Now that we have a stable discretisation of the Calderón projector, we can look at how its properties on the continuous level carry across to the discrete level.

The result of applying the Calderón projector to any two functions is a pair of compatible Cauchy data, as shown in lemma 1.10. Figure 2.7b shows the result of applying the Calderón projector to the functions $f(\mathbf{x}) = xy^2z^3$ and $g(\mathbf{x}) = \sin(4\pi x)$.



(a) Approximations of $f(\mathbf{x}) = xyz^3$ in $P_h^1(\Gamma)$ (left) and $g(\mathbf{x}) = \sin(4\pi x)$ in $DUAL_h^0(\Gamma)$ (right) on a discretised cube with 1468 faces.



(b) The result of applying the Calderón projector to the functions in figure 2.7a. These functions are (up to discretisation error) valid interior Laplace Cauchy data.

Figure 2.7: Visualisation of the Calderón projector applied to non-compatible Cauchy data.

```

import bempp.api
from bempp.api.operators.boundary import laplace
from bempp.api.operators.boundary import sparse
import numpy as np

grid = bempp.api.shapes.cube(h=0.1)
multitrace = laplace.multitrace_operator(grid, spaces='dual')
identity = sparse.multitrace_identity(grid, spaces='dual')

calderon = 0.5 * identity + multitrace

def f(x, n, domain_index, result):
    result[0] = x[0] * x[1]**2 * x[2]**3

def g(x, n, domain_index, result):
    result[0] = np.sin(np.pi*4*x[0])

v = bempp.api.GridFunction(
    space=calderon.domain_spaces[0],
    fun=f,
    dual_space=calderon.dual_to_range_spaces[0])

mu = bempp.api.GridFunction(
    space=calderon.domain_spaces[1],
    fun=g,
    dual_space=calderon.dual_to_range_spaces[1])

traces_1 = calderon * [v, mu]
traces_2 = calderon * traces_1

v_error = (traces_2[0] - traces_1[0]).l2_norm() / traces_1[0].l2_norm()
mu_error = (traces_2[1] - traces_1[1]).l2_norm() / traces_1[1].l2_norm()

```

Figure 2.8: Applying the Calderón projector to the functions $f(\mathbf{x}) = xy^2z^3$ and $g(\mathbf{x}) = \sin(4\pi x)$, and computing the error between the application of $[C^-]^2$ and C^- to this data. The error `v_error` is 1.03×10^{-3} and the error `mu_error` is 1.17×10^{-2} .

As we saw in section 1.4, we know that $[\mathbf{C}^-]^2 = \mathbf{C}^-$, and so applying the Calderón projector a second time to the result should leave the result unchanged. The full Python example code for this calculation is given in figure 2.20. `traces_1` and `traces_2` should agree up to discretisation error, and indeed, the error `v_error` in the Dirichlet component is 1.03×10^{-3} and the error `mu_error` in the Neumann component is 1.17×10^{-2} .

— 2.3.3 —

NUMERICAL RESULTS FOR LAPLACE'S EQUATION

In this section, we look at how the implementation of the discrete operator algebra can be used to precondition Laplace's equation. As a model problem, we take $g_D(\mathbf{x}) := e^{x+\sqrt{y}}$ and $\Omega = \{\mathbf{x} \in \mathbb{R} : |\mathbf{x}| < 1\}$ and consider the single layer formulation of an interior Laplace problem: Find $\lambda \in H^{-1/2}(\Gamma)$ such that

$$\langle \mathbf{V}\lambda, \mu \rangle_\Gamma = \langle (\tfrac{1}{2}\mathbf{Id} + \mathbf{K})g_D, \mu \rangle_\Gamma \quad \forall \mu \in H^{-1/2}(\Gamma). \quad (3.59)$$

It is a common preconditioning strategy [75] to precondition this equation with an operator of the opposite order. In this case, (3.59) can be preconditioned with the operator \mathbf{W} to give the problem: Find $\lambda \in H^{-1/2}(\Gamma)$ such that

$$\langle \mathbf{W}\mathbf{V}\lambda, v \rangle_\Gamma = \langle \mathbf{W}(\tfrac{1}{2}\mathbf{Id} + \mathbf{K})g_D, v \rangle_\Gamma \quad \forall v \in H^{1/2}(\Gamma). \quad (2.45)$$

We discretise (2.45) and (3.59) using $P_h^1(\Gamma) \subset H^{1/2}(\Gamma)$ and $\text{DUAL}_h^0(\Gamma) \subset H^{-1/2}(\Gamma)$, leading to the following discrete problems.

$$\mathbf{V}\lambda_h = (\tfrac{1}{2}\mathbf{M}_K + \mathbf{K})\mathbf{g}_h \quad (2.46)$$

$$\mathbf{W}\mathbf{M}_K^{-1}\mathbf{V}\lambda_h = \mathbf{W}\mathbf{M}_K^{-1}(\tfrac{1}{2}\mathbf{M}_K + \mathbf{K})\mathbf{g}_h. \quad (2.47)$$

Alternatively, we could take the discrete strong form of each equation, leading to the following mass matrix preconditioned discrete problems.

$$\mathbf{M}_K^{-1}\mathbf{V}\lambda_h = \mathbf{M}_K^{-1}(\tfrac{1}{2}\mathbf{M}_K + \mathbf{K})\mathbf{g}_h \quad (2.48)$$

$$\mathbf{M}_W^{-1}\mathbf{W}\mathbf{M}_K^{-1}\mathbf{V}\lambda_h = \mathbf{M}_W^{-1}\mathbf{W}\mathbf{M}_K^{-1}(\tfrac{1}{2}\mathbf{M}_K + \mathbf{K})\mathbf{g}_h. \quad (2.49)$$

The number of GMRES iterations required to solve (2.46) to (2.49) to a tolerance of 1×10^{-5} (the default tolerance used in SciPy [46]) in the vector 2-norm as h is reduced are shown in figure 2.9. Here, it can be seen that the number of iterations taken to solve the operator preconditioned systems (2.47) and (2.49) (red circles) remain low as h decreases while the number of iterations taken to solve the unpreconditioned systems (2.46) and (2.48) (orange triangles) gradually increase.

For both the unpreconditioned and the operator preconditioned systems (dashed lines), applying mass matrix preconditioning reduces the number of GMRES iterations.

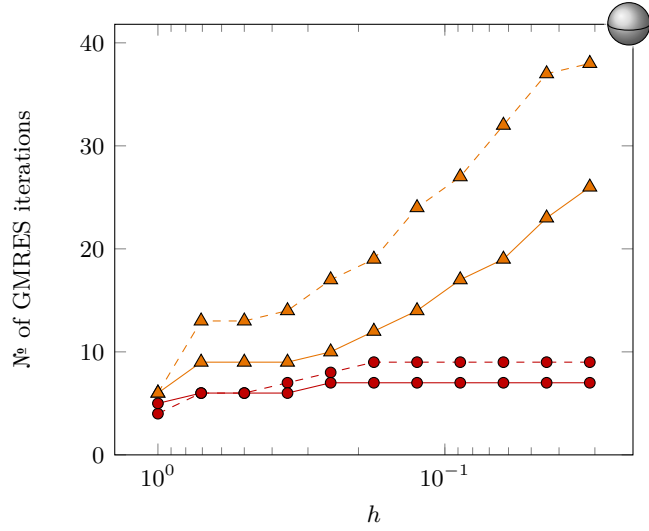


Figure 2.9: The number of GMRES iterations taken to solve the Laplace problems (2.46) (dashed orange triangles), (2.47) (dashed red circles), (2.48) (orange triangles), and (2.49) (red circles), to a tolerance of 1×10^{-5} for the problem on the interior of a unit sphere.

— 2.3.4 —

NUMERICAL RESULTS FOR THE HELMHOLTZ EQUATION

Next, we look at solving Helmholtz wave scattering problems. We let $\Omega^- = \{\mathbf{x} \in \mathbb{R}^3 : |\mathbf{x}| < 1\}$ be the unit sphere and $\Omega^+ = \mathbb{R} \setminus \Omega^-$, and let $u^{\text{inc}}(\mathbf{x}) = e^{i\mathbf{k}\mathbf{x}\cdot\mathbf{d}}$ be an incident wave, where $\mathbf{d} = (\frac{1}{\sqrt{3}}, \frac{1}{\sqrt{3}}, \frac{1}{\sqrt{3}})$ is the direction of wave propagation. This wave satisfies $-\Delta u^{\text{inc}} - k^2 u^{\text{inc}} = 0$.

In this section we consider the sound-soft scattering problem,

$$-\Delta u^{\text{scat}} - k^2 u^{\text{scat}} = 0 \quad \text{in } \Omega^+, \quad (1.38a)$$

$$u^{\text{tot}} = 0 \quad \text{on } \Gamma \quad (2.50)$$

$$\frac{\partial u^{\text{scat}}}{\partial |\mathbf{x}|} - ik u^{\text{scat}} = o(|\mathbf{x}|^{-1}) \quad \text{as } |\mathbf{x}| \rightarrow \infty, \quad (1.38b)$$

The solution u^{tot} of (1.38a) can be represented by the following representation formula [28].

$$u^{\text{tot}} - u^{\text{inc}} = \mathcal{K}u - \mathcal{V}\lambda, \quad (2.51)$$

where $u = \gamma_{\text{D}}^+ u^{\text{tot}}$ and $\lambda = \gamma_{\text{N}}^+ u^{\text{tot}}$.

Taking the Dirichlet trace of (2.51) gives

$$\left(\frac{1}{2}\text{Id} - \mathcal{K}\right)u + \mathcal{V}\lambda = \gamma_{\text{D}}^+ u^{\text{inc}}, \quad (2.52)$$

and taking the Neumann trace gives

$$Wu + (\tfrac{1}{2}\text{Id} + K')\lambda = \gamma_N^+ u^{\text{inc}}. \quad (2.53)$$

For sound-soft scattering, (2.52) leads to the formulation: Find $\lambda \in H^{-1/2}(\Gamma)$ such that

$$\langle V\lambda, \mu \rangle_\Gamma = \langle \gamma_D^+ u^{\text{inc}}, \mu \rangle_\Gamma \quad \forall \mu \in H^{-1/2}(\Gamma); \quad (2.54)$$

and (2.53) leads to the formulation: Find $\lambda \in H^{-1/2}(\Gamma)$ such that

$$\langle (\tfrac{1}{2}\text{Id} + K')\lambda, v \rangle_\Gamma = \langle \gamma_N^+ u^{\text{inc}}, v \rangle_\Gamma \quad \forall v \in H^{1/2}(\Gamma). \quad (2.55)$$

As in the previous section, we can apply operator preconditioning to (2.54) to obtain the formulation: Find $\lambda \in H^{-1/2}(\Gamma)$ such that

$$\langle WV\lambda, v \rangle_\Gamma = \langle W\gamma_D^+ u^{\text{inc}}, v \rangle_\Gamma \quad \forall v \in H^{1/2}(\Gamma). \quad (2.56)$$

We can combine (2.54) and (2.55) to obtain a combined formulation: Find $\lambda \in H^{-1/2}(\Gamma)$ such that

$$\langle (RV + \eta(\tfrac{1}{2}\text{Id} + K'))\lambda, v \rangle_\Gamma = \langle R\gamma_D^+ u^{\text{inc}} + \eta\gamma_N^+ u^{\text{inc}}, v \rangle_\Gamma \quad \forall v \in H^{1/2}(\Gamma), \quad (2.57)$$

where $R : H^{1/2}(\Gamma) \rightarrow H^{-1/2}(\Gamma)$ is an operator. Following [14], we take $R = W_{k/2}$ (the hypersingular operator with wavenumber $\frac{k}{2}$) and $\eta = i$. This choice is made so that the resulting operator on the left-hand side of (2.57) is a compact perturbation of the identity [14, theorem 2.1].

Figure 2.10 shows the number of GMRES iterations taken to solve the sound-soft Helmholtz model problem to a tolerance of 1×10^{-5} using the formulation (2.54) with (orange triangles) and without (dashed orange triangles) mass matrix preconditioning, and the operator preconditioned formulation (2.56) with (red circles) and without (dashed red circles) mass matrix preconditioning. As for the Laplace problem, we see that the number of iterations taken to solve the unpreconditioned formulation (2.54) gradually rises as h decreases, while the number of iterations taken to solve the operator preconditioned system (2.55) remains low. For this formulation, mass matrix preconditioning appears to be almost as effective as operator preconditioning.

In figure 2.11, we compare the number of iterations taken to solve the operator preconditioned formulation (2.56) (red circles) with the number taken to solve the formulation (2.55) (blue squares) and the combined formulation (2.57) as h is reduced. For each formulation, the number of iterations remains low as the grid is refined.

When k^2 coincides with an eigenvalue of the exterior Laplace problem, then the Helmholtz problem (1.38a) does not have a unique solution. Near these eigenvalues, the

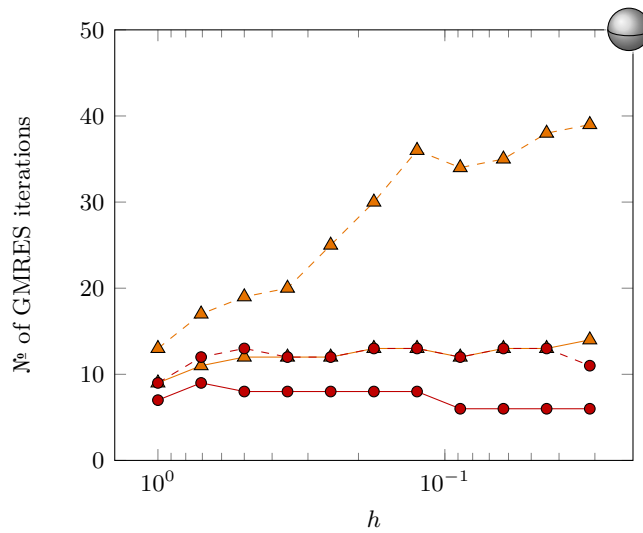


Figure 2.10: The number of GMRES iterations taken to solve the sound-soft Helmholtz problem using the unpreconditioned formulation (2.54) with (orange triangles) and without (dashed orange triangles) mass matrix preconditioning, and the operator preconditioned formulation Helmholtz problem (2.56) with (red circles) and without (dashed red circles) mass matrix preconditioning to a tolerance of 1×10^{-5} for the problem on the exterior of a unit sphere. The differences between value of the solutions obtained are small and decrease as the grid is refined.

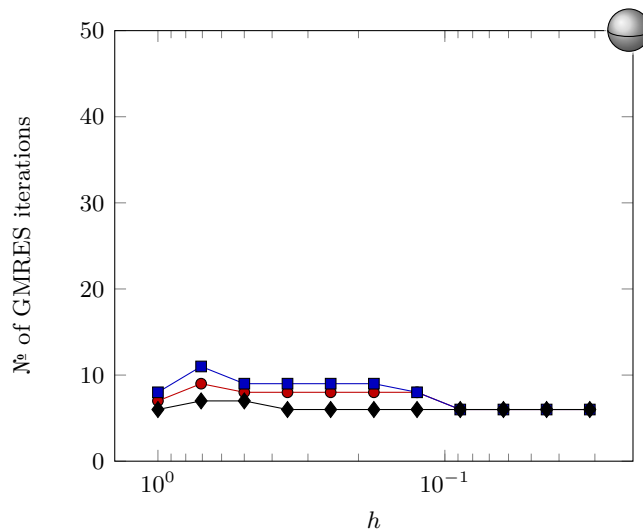


Figure 2.11: The number of GMRES iterations taken to solve the sound-soft Helmholtz problem with $k = 2$ using the formulations (2.56) (red circles), (2.55) (blue squares), and (2.57) (black diamonds) to a tolerance of 1×10^{-5} for the problem on the interior of a unit sphere. Again, the differences between value of the solutions obtained are small and decrease as the grid is refined.

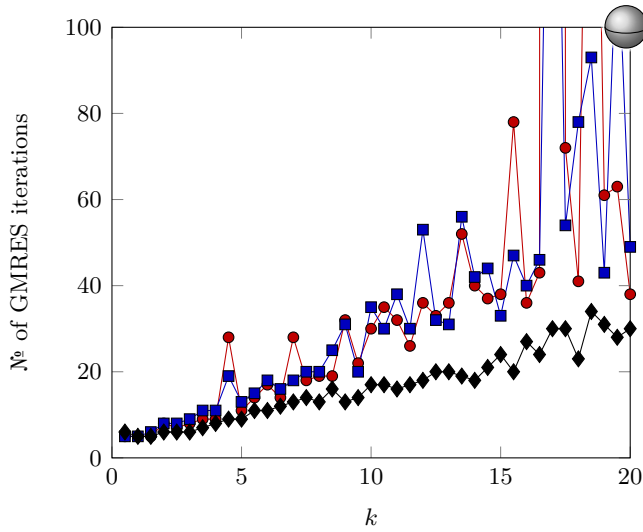


Figure 2.12: The number of GMRES iterations taken to solve the sound-soft Helmholtz problem as k is increased using the formulations (2.56) (red circles), (2.55) (blue squares), and (2.57) (black diamonds) to a tolerance of 1×10^{-5} for the problem on the interior of a unit sphere with $h = 0.1$ (3206 edges).

formulations (2.55) and (2.56) become ill-conditioned. Figure 2.12 shows the number of GMRES iterations required for these formulations as k is varied. Near $k = 17$, there is an eigenvalue of the Laplace problem, and so the number of iterations sharply increases.

The combined formulation (2.57), however, is immune to these eigenvalues. As figure 2.12 shows, the number of iterations required by this formulation remains bounded as k is increased.

— 2.4 —

MAXWELL'S EQUATIONS

Before looking at uses of the discrete operator algebra for Maxwell's equation, we must first look at the use of BEM for Maxwell's equations in more detail. In particular, we focus on the simulation of wave scattering phenomena by solving an exterior Maxwell problem (1.39) with zero Dirichlet boundary conditions (1.39c):

$$\mathbf{curl} \mathbf{curl} \mathbf{e}^{\text{tot}} = k^2 \mathbf{e}^{\text{tot}} \quad \text{in } \Omega^+, \quad (1.39a)$$

$$\mathbf{e}^{\text{tot}} \times \boldsymbol{\nu} = \mathbf{0} \quad \text{on } \Gamma, \quad (1.39c)$$

$$|\mathbf{x}| \left(\mathbf{curl} \mathbf{e}^{\text{scat}} \times \frac{\mathbf{x}}{|\mathbf{x}|} - ik \mathbf{e}^{\text{scat}} \right) \rightarrow \mathbf{0} \quad \text{as } |\mathbf{x}| \rightarrow \infty, \quad (1.39b)$$

where \mathbf{e}^{inc} is the incident field, \mathbf{e}^{scat} is the scattered field, and $\mathbf{e}^{\text{tot}} = \mathbf{e}^{\text{scat}} + \mathbf{e}^{\text{inc}}$ is the total field. The incident field \mathbf{e}^{inc} satisfies $\mathbf{curl} \mathbf{curl} \mathbf{e}^{\text{inc}} = k^2 \mathbf{e}^{\text{inc}}$, and is commonly taken to be a plane wave given by $\mathbf{e}^{\text{inc}} = \mathbf{p} e^{ik\mathbf{x}\cdot\mathbf{d}}$, where \mathbf{p} is a non-zero vector representing the polarisation of the wave and \mathbf{d} is a unit vector perpendicular to \mathbf{p} that gives the direction

of the plane wave.

There are three widely used boundary integral formulations of this problem: the electric field (EFIE), magnetic field (MFIE) and combined field (CFIE) integral equations. Each of these integral equations comes in two forms: direct and indirect. The direct forms are derived by taking trace of representation formula (1.88); the indirect forms are derived by representing the solution in terms of a non-physical unknown, as in (1.91) and (1.92), then taking the traces of this representation.

In this section, we present the integral equations in the form

$$\mathbf{B}\boldsymbol{\rho} = \mathbf{C}\boldsymbol{\gamma}_t^+ \mathbf{e}^{\text{inc}}, \quad (2.58)$$

where $\boldsymbol{\rho}$ is unknown, and \mathbf{B} and \mathbf{C} are boundary operators. We call this the strong form of the equation. In order discretise and solve the equations, we will write them in the form: Find $\boldsymbol{\rho} \in \mathbf{H}_\times^{-1/2}(\text{div}_\Gamma, \Gamma)$ such that

$$\langle \mathbf{B}\boldsymbol{\rho}, \boldsymbol{\mu} \rangle_\tau = \langle \mathbf{C}\boldsymbol{\gamma}_t^+ \mathbf{e}^{\text{inc}}, \boldsymbol{\mu} \rangle_\tau \quad \forall \boldsymbol{\mu} \in \mathbf{H}_\times^{-1/2}(\text{div}_\Gamma, \Gamma). \quad (2.59)$$

This form is called the weak or variational form of the equation.

— 2.4.1 —

THE ELECTRIC FIELD INTEGRAL EQUATION (EFIE)

The EFIE is widely used in applications for low-frequency scattering from closed and open surfaces. To derive the direct EFIE, we begin with the representation formula (1.88), and take $\mathbf{e}(\mathbf{x}) = \begin{cases} \mathbf{e}^{\text{scat}}(\mathbf{x}) & \text{if } \mathbf{x} \in \Omega^+ \\ \mathbf{0} & \text{if } \mathbf{x} \in \Omega^- \end{cases}$. Using the boundary condition (1.39c), this leads to the following representation formula in Ω^+ .

$$\begin{aligned} \mathbf{e}^{\text{scat}} &= -\mathcal{H}\boldsymbol{\gamma}_t^+ \mathbf{e}^{\text{scat}} - \mathcal{E}\boldsymbol{\gamma}_{N,k}^+ \mathbf{e}^{\text{scat}} \\ &= \mathcal{H}\boldsymbol{\gamma}_t^+ \mathbf{e}^{\text{inc}} - \mathcal{E}\boldsymbol{\pi}, \end{aligned} \quad (2.60)$$

where $\boldsymbol{\pi} := \boldsymbol{\gamma}_{N,k}^+ \mathbf{e}^{\text{scat}}$. Taking the tangential trace of this representation formula leads to the strong form direct EFIE,

$$\mathbf{E}\boldsymbol{\pi} = (\tfrac{1}{2}\text{Id} + \mathbf{H})\boldsymbol{\gamma}_t^+ \mathbf{e}^{\text{inc}}. \quad (2.61)$$

To derive the indirect EFIE, we represent the scattered field in terms of a non-physical unknown $\boldsymbol{\lambda} \in \mathbf{H}_\times^{-1/2}(\text{div}_\Gamma, \Gamma)$, as in (1.91),

$$\mathbf{e}^{\text{scat}} = -\mathcal{E}\boldsymbol{\lambda}. \quad (2.62)$$

Taking the tangential trace of this representation leads to the indirect EFIE,

$$\mathbf{E}\boldsymbol{\lambda} = \boldsymbol{\gamma}_t^+ \mathbf{e}^{\text{inc}}. \quad (2.63)$$

— CALDERÓN PRECONDITIONING

By itself the EFIE is ill-conditioned, making either direct solvers or efficient preconditioning necessary. The identity (1.117) provides an efficient preconditioning strategy: from the top-left block of $\mathbf{A}^2 = \frac{1}{4}\text{Id}$, it follows that $\mathbf{E}^2 = -\frac{1}{4}\text{Id} + \mathbf{H}^2$.

The eigenvalues of \mathbf{E} accumulate at 0 and ∞ making discretisations of this operator highly ill-conditioned. However, the operator \mathbf{H} is compact on smooth surfaces [58, Section 5.5], and so the eigenvalues of \mathbf{E}^2 accumulate at $-\frac{1}{4}$. This means that we can expect discretisations of \mathbf{E}^2 to be well-conditioned. By applying the operator \mathbf{E} to (2.61), we obtain the Calderón preconditioned direct EFIE,

$$\mathbf{E}^2 \boldsymbol{\pi} = \mathbf{E}(\frac{1}{2}\text{Id} + \mathbf{H})\boldsymbol{\gamma}_t^+ \mathbf{e}^{\text{inc}}. \quad (2.64)$$

By doing the same to (2.63), we obtain the Calderón preconditioned indirect EFIE,

$$\mathbf{E}^2 \boldsymbol{\lambda} = \mathbf{E}\boldsymbol{\gamma}_t^+ \mathbf{e}^{\text{inc}}. \quad (2.65)$$

— 2.4.2 —

THE MAGNETIC FIELD INTEGRAL EQUATION (MFIE)

The MFIE is a valid formulation on closed domains. Its advantage compared to the EFIE is that on smooth domains, it is a compact perturbation of the identity operator and therefore well suited to iterative solvers. However, the robust implementation of the MFIE on non-smooth domains requires the use of the stable pairing of discrete spaces [30] satisfying assumption 2.1. These discrete spaces will be discussed in more detail in section 2.4.4.

The direct MFIE is derived from (2.60) by taking the Neumann trace. This leads to the strong form of the direct MFIE,

$$(\mathbf{H} + \frac{1}{2}\text{Id}) \boldsymbol{\pi} = -\mathbf{E}\boldsymbol{\gamma}_t^+ \mathbf{e}^{\text{inc}}. \quad (2.66)$$

To derive the indirect MFIE, we represent the scattered field in terms of a non-physical unknown $\boldsymbol{\xi} \in \mathbf{H}_{\times}^{-1/2}(\text{div}_{\Gamma}, \Gamma)$, as in (1.92),

$$\mathbf{e}^{\text{scat}} = -\mathcal{H}\boldsymbol{\xi}. \quad (2.67)$$

Taking the tangential trace of this representation leads to the indirect MFIE,

$$(\mathbf{H} - \frac{1}{2}\text{Id}) \boldsymbol{\lambda} = \boldsymbol{\gamma}_t^+ \mathbf{e}^{\text{inc}}. \quad (2.68)$$

— 2.4.3 —

THE COMBINED FIELD INTEGRAL EQUATION (CFIE)

While the EFIE and MFIE are efficient for low-frequency Maxwell problems, they lead to break-down close to interior resonances. The CFIE is immune to breakdown at resonances and is therefore particularly suitable for high-frequency scattering problems.

Here, we focus on the direct CFIE and the stable version of it derived in [29]. This is derived from the representation formula (2.60): this representation formula leads to both the direct EFIE (2.61) and the direct MFIE (2.66). Applying a regularising operator \mathbf{R} to the EFIE then adding the MFIE [29] leads to the strong form of the direct CFIE,

$$(-\mathbf{R}\mathbf{E} + \frac{1}{2}\text{Id} + \mathbf{H}) \boldsymbol{\pi} = -\mathbf{R}(\frac{1}{2}\text{Id} + \mathbf{H})\boldsymbol{\gamma}_t^+ \mathbf{e}^{\text{inc}} - \mathbf{E}\boldsymbol{\gamma}_t^+ \mathbf{e}^{\text{inc}}. \quad (2.69)$$

Frequently, the EFIE component is multiplied with a complex scalar. This is not necessary here, as in our implementation the electric field operator itself is already scaled with i . A common choice for the regularisation operator is $\mathbf{R} = \mathbf{E}_{ik}$, the electric field integral operator with wavenumber ik .

Another construction of the CFIE based on the use of the BC spaces that we will look at in section 2.4.4 was presented in [5]. In particular, the treatment of the MFIE component in that paper differs from the proposed formulation in this section.

— 2.4.4 —

DISCRETE SPACES

In the previous section, we derived boundary integral equations for Maxwell problems. In order to approximately solve these equations, we first write them in weak form and discretise them.

In general, the integral equations in the previous section can be written in weak form as: Find $\boldsymbol{\rho} \in \mathbf{H}_\times^{-1/2}(\text{div}_\Gamma, \Gamma)$ such that

$$\langle \mathbf{B}\boldsymbol{\rho}, \boldsymbol{\mu} \rangle_\tau = \langle \mathbf{D}\boldsymbol{\gamma}_t^+ \mathbf{e}^{\text{inc}}, \boldsymbol{\mu} \rangle_\tau \quad \forall \boldsymbol{\mu} \in \mathbf{H}_\times^{-1/2}(\text{div}_\Gamma, \Gamma). \quad (2.70)$$

This can be written using the L^2 inner product $\langle \cdot, \cdot \rangle_\Gamma$ as: Find $\boldsymbol{\rho} \in \mathbf{H}_\times^{-1/2}(\text{div}_\Gamma, \Gamma)$ such that

$$\langle \mathbf{B}\boldsymbol{\rho}, \boldsymbol{\eta} \rangle_\Gamma = \langle \mathbf{D}\boldsymbol{\gamma}_t^+ \mathbf{e}^{\text{inc}}, \boldsymbol{\eta} \rangle_\Gamma \quad \forall \boldsymbol{\eta} \in \mathbf{H}_\times^{-1/2}(\text{curl}_\Gamma, \Gamma). \quad (2.71)$$

To discretise this, we take $\mathbf{V}_h \subset \mathbf{H}_\times^{-1/2}(\text{div}_\Gamma, \Gamma)$ and $\tilde{\mathbf{V}}_h \subset \mathbf{H}_\times^{-1/2}(\text{curl}_\Gamma, \Gamma)$, and solve the

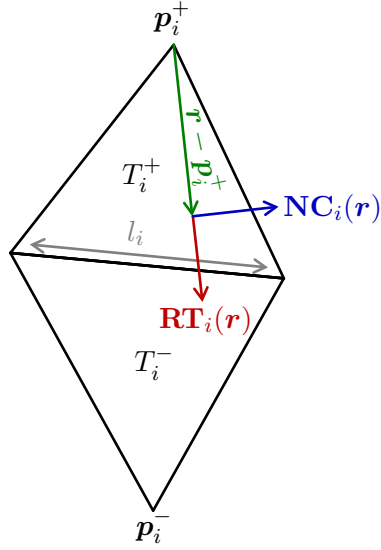


Figure 2.13: Two adjacent triangles on which Raviart–Thomas (RT) and Nédélec (NC) basis functions are defined.

finite dimensional problem: Find $\boldsymbol{\rho}_h \in \mathbf{V}_h$ such that

$$\langle \mathbf{B}\boldsymbol{\rho}_h, \boldsymbol{\eta}_h \rangle_\Gamma = \langle \mathbf{D}\boldsymbol{\gamma}_t^+ e^{\text{inc}}, \boldsymbol{\eta}_h \rangle_\Gamma \quad \forall \boldsymbol{\eta}_h \in \tilde{\mathbf{V}}_h. \quad (2.72)$$

In this section, we look at the basis functions we will use to define the finite dimensional subspaces of $\mathbf{H}_\times^{-1/2}(\text{div}_\Gamma, \Gamma)$ and $\mathbf{H}_\times^{-1/2}(\text{curl}_\Gamma, \Gamma)$.

Let \mathcal{T}_h be a triangulation of Γ into o piecewise flat triangular elements of diameter $\leq h$. Let T_j (for $j = 1, \dots, o$) be the triangular elements and let \mathbf{p}_i (for $i = 1, \dots, n$) be the vertices of the triangulation. Typically, we will define the basis functions of our finite dimensional subspaces to have support on a small group of triangles.

An overview of other bases that can be used to discretise $\mathbf{H}_\times^{-1/2}(\text{div}_\Gamma, \Gamma)$ and $\mathbf{H}_\times^{-1/2}(\text{curl}_\Gamma, \Gamma)$, as well as other spaces, can be found in [49].

RAVIART–THOMAS AND NÉDÉLEC BASIS FUNCTIONS

The most commonly used discretisations of the spaces $\mathbf{H}_\times^{-1/2}(\text{div}_\Gamma, \Gamma)$ and $\mathbf{H}_\times^{-1/2}(\text{curl}_\Gamma, \Gamma)$ are Raviart-Thomas (RT) div-conforming [65] and Nédélec (NC) curl-conforming [57] basis functions.

For the i th edge in a mesh, between two triangles T_i^+ and T_i^- , the order 0 RT basis function is defined by

$$\boldsymbol{\phi}_i(\mathbf{r}) := \begin{cases} \frac{1}{2A_i^+}(\mathbf{r} - \mathbf{p}_i^+) & \text{if } \mathbf{r} \in T_i^+ \\ -\frac{1}{2A_i^-}(\mathbf{r} - \mathbf{p}_i^-) & \text{if } \mathbf{r} \in T_i^- \\ \mathbf{0} & \text{otherwise} \end{cases}, \quad (2.73)$$

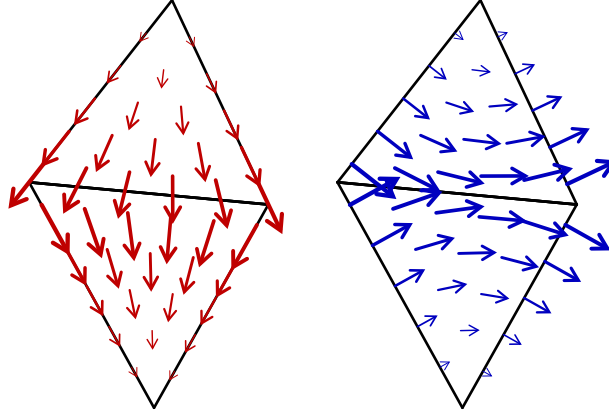


Figure 2.14: Div-conforming Raviart–Thomas (left) and curl-conforming Nédélec (right) order 0 basis functions.

where A_i^+ and A_i^- are the areas of T_i^+ and T_i^- , and \mathbf{p}_i^- and \mathbf{p}_i^+ are the corners of T_i^+ and T_i^- not on the shared edge, as shown in figure 2.13. For the same edge, the order 0 NC basis function may be defined by

$$\boldsymbol{\psi}_i(\mathbf{r}) := \boldsymbol{\nu} \times \boldsymbol{\phi}_i(\mathbf{r}). \quad (2.74)$$

Example RT and NC order 0 basis functions are shown in figure 2.14.

We let $\mathbf{RT}_h^0(\Gamma) = \text{span}\{\boldsymbol{\phi}_1, \dots, \boldsymbol{\phi}_m\}$ and $\mathbf{NC}_h^0(\Gamma) = \text{span}\{\boldsymbol{\psi}_1, \dots, \boldsymbol{\psi}_m\}$ be the function spaces spanned by these basis functions.

The RT basis functions are closely related to the Rao–Wilton–Glisson (RWG) basis functions presented in [64]. These are defined by

$$\boldsymbol{\zeta}_i(\mathbf{r}) := l_i \boldsymbol{\phi}_i(\mathbf{r}) = \begin{cases} \frac{l_i}{2A_i^+}(\mathbf{r} - \mathbf{p}_i^+) & \text{if } \mathbf{r} \in T_i^+ \\ -\frac{l_i}{2A_i^-}(\mathbf{r} - \mathbf{p}_i^-) & \text{if } \mathbf{r} \in T_i^- \\ \mathbf{0} & \text{otherwise} \end{cases}, \quad (2.75)$$

where l_i is the length of the shared edge, and all other terms are as above. We define the scaled curl-conforming dual basis functions of the RWG functions as

$$\boldsymbol{\varsigma}_i(\mathbf{r}) := l_i \boldsymbol{\psi}_i(\mathbf{r}) = \boldsymbol{\nu} \times \boldsymbol{\zeta}_i(\mathbf{r}). \quad (2.76)$$

We let $\mathbf{RWG}_h^0(\Gamma) = \text{span}\{\boldsymbol{\zeta}_1, \dots, \boldsymbol{\zeta}_m\}$ and $\mathbf{SNC}_h^0(\Gamma) = \text{span}\{\boldsymbol{\varsigma}_1, \dots, \boldsymbol{\varsigma}_m\}$ be the function spaces spanned by these basis functions.

In Bempp, the spaces $\mathbf{RT}_h^0(\Gamma)$, $\mathbf{NC}_h^0(\Gamma)$, $\mathbf{RWG}_h^0(\Gamma)$ and $\mathbf{SNC}_h^0(\Gamma)$ may be created with the following lines of Python.

```
rt_space = bempp.api.function_space(grid, "RT", 0)
nc_space = bempp.api.function_space(grid, "NC", 0)
rwg_space = bempp.api.function_space(grid, "RWG", 0)
snc_space = bempp.api.function_space(grid, "SNC", 0)
```

—

BUFFA–CHRISTIANSEN SPACES

The space of div-conforming RT functions has a subspace that is quasi-orthogonal to the space of curl-conforming Nédélec functions [27, section 3.1]. Due to this, the antisymmetric bilinear form, as defined in (1.29), on the discrete RT space is not inf-sup stable. The motivation for Buffa–Christiansen (BC) basis functions is to find a space of functions that are div-conforming but behave like curl-conforming functions, as this will recover inf-sup stability.

Following [16], we define this space by first taking the barycentric refinement of the grid. We pick an edge e_i in the unrefined coarse mesh, and we let \mathbf{v}_j and \mathbf{v}_k be the two vertices (in the coarse grid) that it joins. Let $\tilde{e}_{j_1}, \tilde{e}_{j_2}, \dots, \tilde{e}_{j_{2m_1}}$ be the edges in the barycentrically refined grid that meet the vertex \mathbf{v}_j , with \tilde{e}_{j_1} equal to half of the edge e_i , and the rest of the edges ordered in an anticlockwise direction. Similarly, let $\tilde{e}_{k_1}, \tilde{e}_{k_2}, \dots, \tilde{e}_{k_{2m_2}}$ be the edges in the barycentrically refined grid that meet the vertex \mathbf{v}_k , with \tilde{e}_{k_1} equal to half of the edge e_i , and the rest of the edges ordered in an anticlockwise direction. Finally, we let \tilde{e}_{i_1} and \tilde{e}_{i_2} be the two edges in the barycentrically refined grid that meet the midpoint of the edge e_i but are not part of the edge e_i . An example of this labelling of edges in this way is shown in figure 2.15.

We now define a basis function, $\boldsymbol{\xi}_i$, by

$$\boldsymbol{\xi}_i = \sum_{l=2}^{2m_2} \frac{m_2 + 1 - l}{2m_2} \tilde{\boldsymbol{\zeta}}_{k_l} - \sum_{l=2}^{2m_1} \frac{m_1 + 1 - l}{2m_1} \tilde{\boldsymbol{\zeta}}_{j_l} + \frac{1}{2} \tilde{\boldsymbol{\zeta}}_{i_1} + \frac{1}{2} \tilde{\boldsymbol{\zeta}}_{i_2}, \quad (2.77)$$

where $\tilde{\boldsymbol{\zeta}}_l$ are the RWG basis functions on the barycentrically refined grid, assumed to be directed in an anticlockwise direction around the two vertices, and pointing from \mathbf{v}_j towards \mathbf{v}_k on the edges \tilde{e}_{i_1} and \tilde{e}_{i_2} . Example coefficients used to define a basis function $\boldsymbol{\xi}_i$ are shown in figure 2.16.

For a BC basis function, $\boldsymbol{\xi}_i$, we may also define the rotated Buffa–Christiansen (RBC) basis function, in an analogous way to (2.74), by

$$\boldsymbol{\chi}_i(\mathbf{r}) := \boldsymbol{\nu} \times \boldsymbol{\xi}_i(\mathbf{r}). \quad (2.78)$$

Example BC and RBC basis functions are shown in figure 2.17.

We let $\mathbf{BC}_h^0(\Gamma) = \text{span}\{\boldsymbol{\xi}_1, \dots, \boldsymbol{\xi}_m\}$ and $\mathbf{RBC}_h^0(\Gamma) = \text{span}\{\boldsymbol{\chi}_1, \dots, \boldsymbol{\chi}_m\}$ be the function spaces spanned by these basis functions.

The following inf-sup stability result, expressed here using the antisymmetric product $\langle \cdot, \cdot \rangle_\tau$, is shown in [16].

Proposition 2.3. *There exists $C > 0$ such that*

$$\inf_{\boldsymbol{\mu} \in \mathbf{RWG}_h^0(\Gamma)} \sup_{\boldsymbol{\eta} \in \mathbf{BC}_h^0(\Gamma)} \frac{\langle \boldsymbol{\mu}, \boldsymbol{\eta} \rangle_\tau}{\|\boldsymbol{\mu}\|_{\mathbf{H}_x^{-1/2}(\text{div}, \Gamma)} \|\boldsymbol{\eta}\|_{\mathbf{H}_x^{-1/2}(\text{div}, \Gamma)}} \geq \frac{1}{C}. \quad (2.79)$$

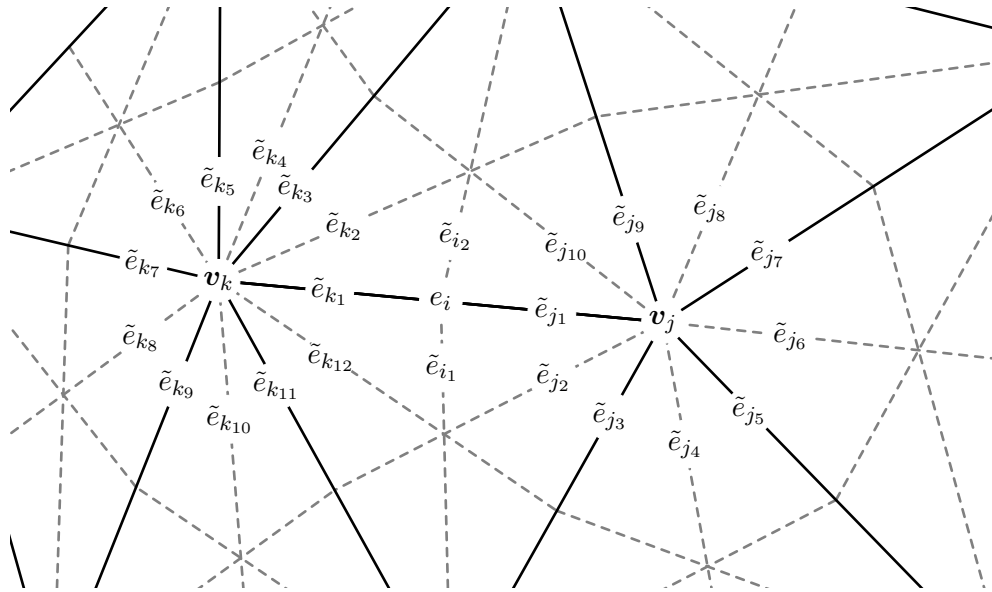


Figure 2.15: An example labelling of the edged used in the definition of the BC basis functions.

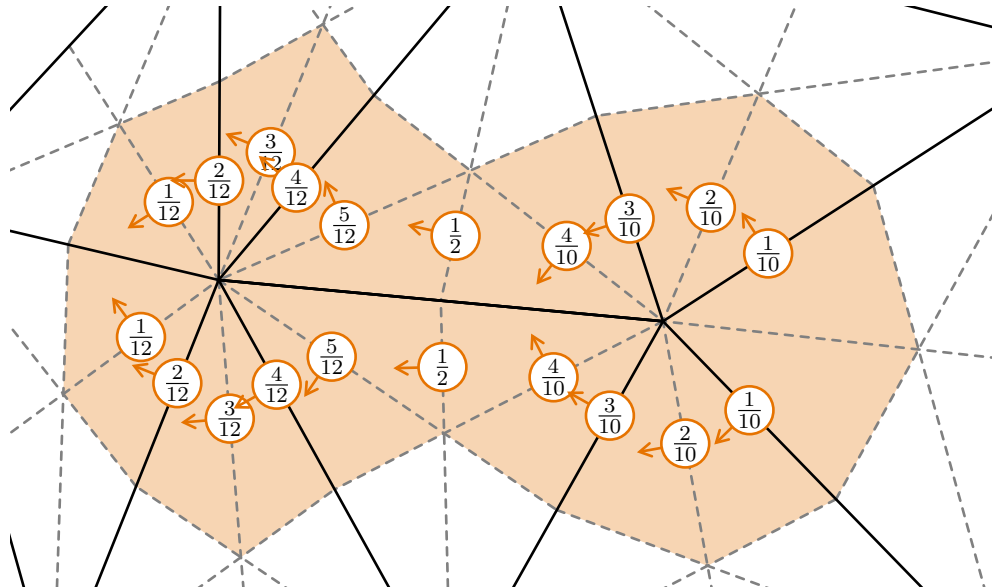


Figure 2.16: The coefficients used to define a BC basis function in terms of RWG basis functions on the barycentrically refined grid. The support of the BC function is shaded in orange.

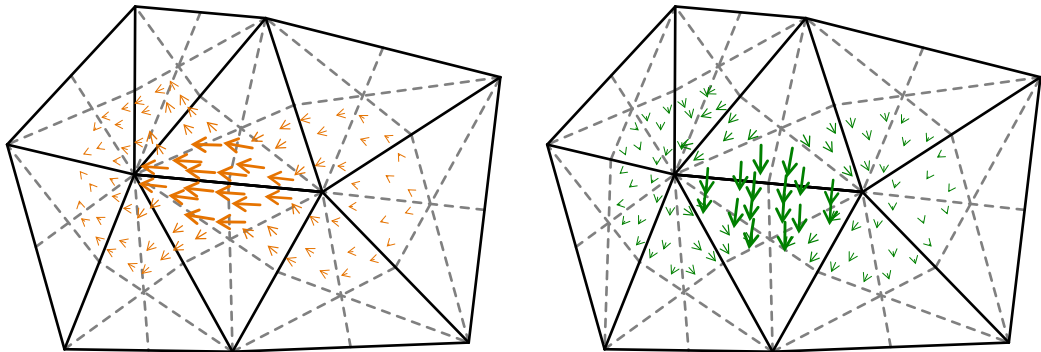


Figure 2.17: A div-conforming and quasicurl-conforming Buffa-Christansen basis function (left), and a curl-conforming and quasidiv-conforming rotated Buffa-Christansen basis function (right).

```

import numpy as np
import bempp.api
from bempp.api.operators.boundary.sparse import identity

grid = bempp.api.shapes.regular_sphere(3)
rwg_space = bempp.api.function_space(grid, "B-RWG", 0)
rbc_space = bempp.api.function_space(grid, "RBC", 0)
snc_space = bempp.api.function_space(grid, "B-SNC", 0)
id1 = identity(rwg_space, rwg_space, snc_space).weak_form()
id2 = identity(rwg_space, rwg_space, rbc_space).weak_form()

print(np.linalg.cond(bempp.api.as_matrix(id1).todense()))
print(np.linalg.cond(bempp.api.as_matrix(id2).todense()))

```

Figure 2.18: Computing the condition number of the $\mathbf{RWG}_h^0(\Gamma)$ – $\mathbf{SNC}_h^0(\Gamma)$ and the $\mathbf{RWG}_h^0(\Gamma)$ – $\mathbf{RBC}_h^0(\Gamma)$ mass matrices in Bempp. The values computed are 7.7×10^{17} and 3.60.

Proof. [16, proposition 3.14]. □

Using the L^2 inner product, this result can be written as follows.

Proposition 2.4. *There exists $C > 0$ such that*

$$\inf_{\mu \in \mathbf{RWG}_h^0(\Gamma)} \sup_{\eta \in \mathbf{RBC}_h^0(\Gamma)} \frac{\langle \mu, \eta \rangle_\Gamma}{\|\mu\|_{\mathbf{H}_x^{-1/2}(\text{div}, \Gamma)} \|\eta\|_{\mathbf{H}_x^{-1/2}(\text{curl}, \Gamma)}} \geq \frac{1}{C} \quad (2.80)$$

$$\inf_{\mu \in \mathbf{SNC}_h^0(\Gamma)} \sup_{\eta \in \mathbf{BC}_h^0(\Gamma)} \frac{\langle \mu, \eta \rangle_\Gamma}{\|\mu\|_{\mathbf{H}_x^{-1/2}(\text{curl}, \Gamma)} \|\eta\|_{\mathbf{H}_x^{-1/2}(\text{div}, \Gamma)}} \geq \frac{1}{C}. \quad (2.81)$$

In Bempp, the spaces $\mathbf{BC}_h^0(\Gamma)$ and $\mathbf{RBC}_h^0(\Gamma)$ spaces may be created with the following lines of Python.

```

bc_space = bempp.api.function_space(grid, "BC", 0)
rbc_space = bempp.api.function_space(grid, "RBC", 0)

```

We can use Bempp to compare the stability of dual pairings of the space $\mathbf{RWG}_h^0(\Gamma)$ with the spaces $\mathbf{SNC}_h^0(\Gamma)$ and $\mathbf{RBC}_h^0(\Gamma)$. The code in figure 2.18 computes the condition number of mass matrices on a regular sphere grid generated from the $\mathbf{RWG}_h^0(\Gamma)$ – $\mathbf{SNC}_h^0(\Gamma)$ pairing (id1) and the $\mathbf{RWG}_h^0(\Gamma)$ – $\mathbf{RBC}_h^0(\Gamma)$ pairing (id2).

For the condition number of id1 the code computes a value of 7.7×10^{17} and for the condition number of id2 it computes a value of 3.60. We note that in the definitions of the spaces in figure 2.18 we have used the identifiers **B-RWG** and **B-SNC** instead of **RWG** and **SNC**. The reason is that the RBC spaces are defined over barycentric refinements of the grid. So we need to tell also the other space definitions to internally use barycentric refinements of the grid (even though the actual spaces are defined on the coarse grid), which is done by prepending **B-** in the definitions.

— 2.4.5 —

STABLE DISCRETISATION OF THE MULTITRACE OPERATOR

As we did in section 2.3, we now look to discretise the multitrace operator A , so that the product A^2 can be stably computed on the discrete level. Denote by

$$A := \begin{bmatrix} \mathbf{H}_1 & \mathbf{E}_1 \\ -\mathbf{E}_2 & \mathbf{H}_2 \end{bmatrix}, \quad (2.82)$$

the discretisation of the operator A . Here, \mathbf{E}_1 and \mathbf{E}_2 are discretisations of electric field operators and \mathbf{H}_1 and \mathbf{H}_2 are discretisations of magnetic field operators. A choice of spaces for the operators is shown in the table below.

Matrix	Operator	Domain	Range	Dual to Range
\mathbf{H}_1	Magnetic	$\mathbf{RWG}_h^0(\Gamma)$	$\mathbf{RWG}_h^0(\Gamma)$	$\mathbf{RBC}_h^0(\Gamma)$
\mathbf{E}_1	Electric	$\mathbf{BC}_h^0(\Gamma)$	$\mathbf{RWG}_h^0(\Gamma)$	$\mathbf{RBC}_h^0(\Gamma)$
\mathbf{E}_2	Electric	$\mathbf{RWG}_h^0(\Gamma)$	$\mathbf{BC}_h^0(\Gamma)$	$\mathbf{SNC}_h^0(\Gamma)$
\mathbf{H}_2	Magnetic	$\mathbf{BC}_h^0(\Gamma)$	$\mathbf{BC}_h^0(\Gamma)$	$\mathbf{SNC}_h^0(\Gamma)$

These choices of spaces lead to all mass matrices in the discretisation of A^2 being the invertible $\mathbf{RWG}_h^0(\Gamma)$ – $\mathbf{RBC}_h^0(\Gamma)$ or $\mathbf{BC}_h^0(\Gamma)$ – $\mathbf{SNC}_h^0(\Gamma)$ pairings. This choice of spaces is based on representing the tangential trace with an RWG space and the Neumann trace with a BC space. Alternatively, one could use a BC space for the electric component and an RWG space for the magnetic component. This would lead to a discretisation in which \mathbf{E}_1 and \mathbf{E}_2 are swapped and \mathbf{H}_1 and \mathbf{H}_2 are swapped.

Using the Bempp library, the stable multitrace operator may be created using the following lines of Python.

```
from bempp.api.operators.boundary import maxwell
multitrace = maxwell.multitrace_operator(grid, k)
```

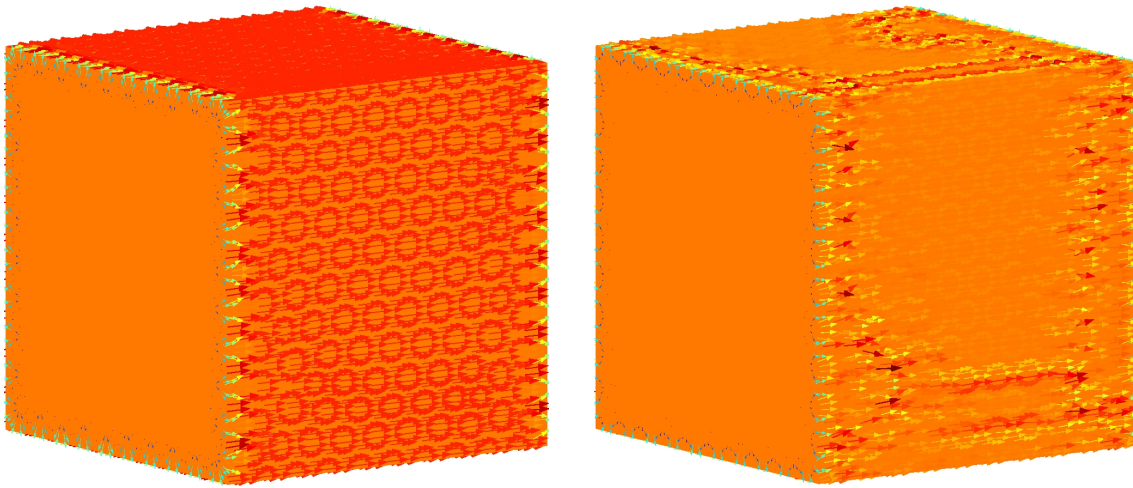
We may then create the exterior Calderón projector with the following lines.

```
from bempp.api.operators.boundary import sparse
identity = sparse.multitrace_identity(grid, spaces="maxwell")
calderon = 0.5 * identity - multitrace
```

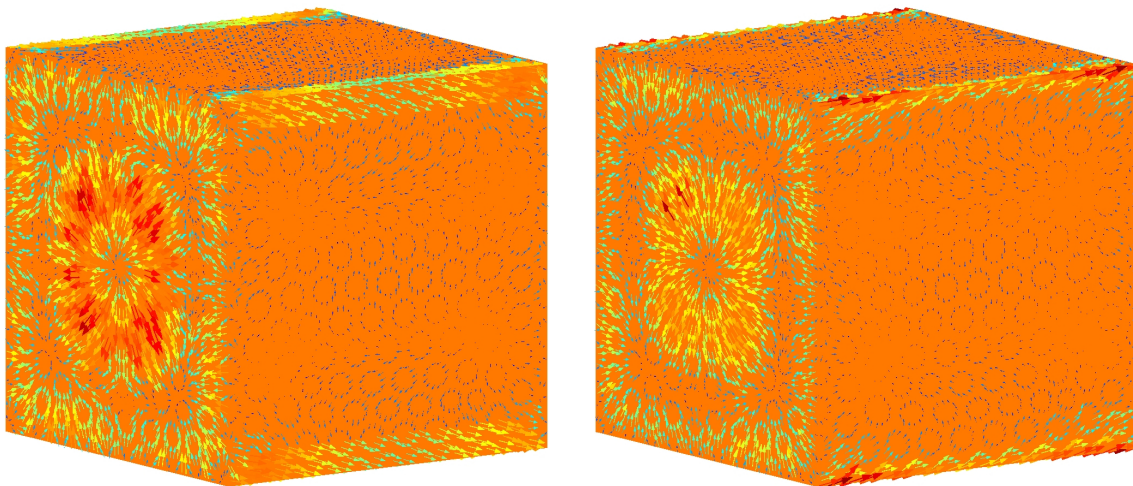
Now that we have a stable discretisation of the Calderón projector, we can look at how its properties on the continuous level carry across to the discrete level.

The result of applying the Calderón projector to any two tangential functions is a pair of compatible Cauchy data, as shown in lemma 1.10. Figure 2.19 shows the result of applying the Calderón projector to the tangential traces of the constant vector $(1, 0, 0)$.

As we saw in section 1.4, we know that $[C^+]^2 = C^+$, and so applying the Calderón projector a second time to the result should leave the result unchanged. The full Python



(a) Approximations of the tangential trace of $(1, 0, 0)$ in RWG (left) and BC (right) spaces on a discretised cube with 2202 edges.



(b) The result of applying the Calderón projector to the functions in figure 2.19a. These functions are (up to discretisation error) valid exterior Maxwell Cauchy data.

Figure 2.19: Visualisation of the Calderón projector applied to the function $(1, 0, 0)$. The Python code used to do this is given in figure 2.20, where it is confirmed by applying the Calderón projector a second time that the functions in figure 2.19b are indeed Maxwell Cauchy data.

```

import bempp.api
from bempp.api.operators.boundary import maxwell
from bempp.api.operators.boundary import sparse
import numpy as np

k = 2

grid = bempp.api.shapes.cube(h=0.1)
multitrace = maxwell.multitrace_operator(grid, k)
identity = sparse.multitrace_identity(grid, spaces='maxwell')

calderon = 0.5 * identity - multitrace

def tangential_trace(x, n, domain_index, result):
    result[:] = np.cross(np.array([1, 0, 0]), n)

electric_trace = bempp.api.GridFunction(
    space=calderon.domain_spaces[0],
    fun=tangential_trace,
    dual_space=calderon.dual_to_range_spaces[0])

magnetic_trace = bempp.api.GridFunction(
    space=calderon.domain_spaces[1],
    fun=tangential_trace,
    dual_space=calderon.dual_to_range_spaces[1])

traces_1 = calderon * [electric_trace, magnetic_trace]
traces_2 = [C^+]^2 * traces_1
electric_error = (traces_2[0] - traces_1[0]).l2_norm() / traces_1[0].l2_norm()
magnetic_error = (traces_2[1] - traces_1[1]).l2_norm() / traces_1[1].l2_norm()

```

Figure 2.20: Applying the Calderón projector to the tangential trace of the constant vector $(1, 0, 0)$ for the electric and magnetic trace, and computing the error in the magnetic and electric trace between the application of $[C^+]^2$ and C^+ to this trace data. The error `electric_error` in the electric component is 9.8×10^{-3} and the error `magnetic_error` in the magnetic component is 7.4×10^{-3} .

example code for this calculation is given in figure 2.20. `traces_1` and `traces_2` should agree up to discretisation error, and indeed, the error `electric_error` in the electric component is 9.8×10^{-3} and the error `magnetic_error` in the magnetic component is 7.4×10^{-3} .

— 2.4.6 —

IMPLEMENTATIONAL DETAILS

The discrete multitrace operator \mathbf{A} consists of the two magnetic field operator discretisations \mathbf{H}_1 and \mathbf{H}_2 , and the two electric field operator discretisations \mathbf{E}_1 and \mathbf{E}_2 . In practice, we only create two operators $\tilde{\mathbf{E}}$, and $\tilde{\mathbf{H}}$, using RWG basis functions on the barycentrically refined grid. Let $\tilde{\mathbf{M}}$ be the L^2 mass matrix associated with this RWG space, defined by

$$\tilde{M}_{ij} = \int_{\Gamma} \zeta_i \cdot \zeta_j, \quad (2.83)$$

where ζ_i is the i th RWG basis function on the barycentrically refined grid. Let now \mathbf{M}_{RWG} be the mass matrix obtained from trial functions in the RWG space on the barycentrically refined grid, and test functions from the original RWG space on the coarse grid. We correspondingly define the mass matrix \mathbf{M}_{BC} with test functions from the BC space on the original coarse grid. The operators \mathbf{E}_i , and \mathbf{H}_i , $i = 1, 2$, are now given as

$$\mathbf{H}_1 = \mathbf{M}_{\text{BC}} \tilde{\mathbf{M}}^{-1} \tilde{\mathbf{H}} \tilde{\mathbf{M}}^{-1} \mathbf{M}_{\text{RWG}}^{\text{T}}, \quad \mathbf{E}_1 = \mathbf{M}_{\text{BC}} \tilde{\mathbf{M}}^{-1} \tilde{\mathbf{H}} \tilde{\mathbf{M}}^{-1} \mathbf{M}_{\text{BC}}^{\text{T}}, \quad (2.84a)$$

$$\mathbf{H}_2 = \mathbf{M}_{\text{RWG}} \tilde{\mathbf{M}}^{-1} \tilde{\mathbf{H}} \tilde{\mathbf{M}}^{-1} \mathbf{M}_{\text{BC}}^{\text{T}}, \quad \mathbf{E}_2 = \mathbf{M}_{\text{RWG}} \tilde{\mathbf{M}}^{-1} \tilde{\mathbf{H}} \tilde{\mathbf{M}}^{-1} \mathbf{M}_{\text{RWG}}^{\text{T}}. \quad (2.84b)$$

We note that due to the definitions of the rotated spaces, the mass matrices \mathbf{M}_{SNC} and \mathbf{M}_{RBC} are equal to \mathbf{M}_{RWG} and \mathbf{M}_{BC} , and so the mass matrices on the left can be written using non-rotated spaces.

In [2], a similar construction of the matrices is suggested. The difference is that their permutation matrices that represent the basis functions on the coarse mesh in terms of basis functions on the barycentric refinement are stated explicitly.

The implicit construction here has the advantage that it is independent of the particular space. All that is needed is the ability to construct mass matrices, which is often already available. A potential performance pitfall is the application of the mass matrix inverse of $\tilde{\mathbf{M}}$ for each matrix vector product with \mathbf{E}_i or \mathbf{E}_j . We automatically precompute the LU decomposition of $\tilde{\mathbf{M}}$. Even for fairly large meshes this is done in a few seconds.

— 2.4.7 —

NUMERICAL RESULTS

In this section, we present code snippets showing how to use Bempp to solve the EFIE (2.63), Calderón preconditioned EFIE (2.65), MFIE (2.68), and CFIE (2.69), and present

```

import bempp.api
import numpy as np

from bempp.api.operators.boundary.maxwell import multitrace_operator
from bempp.api.operators.potential.maxwell import electric_field

grid = ...
k = ...

def incident_field(x):
    return np.array([np.exp(1j * k * x[2]),
                    0. * x[2], 0. * x[2]])

def tangential_trace(x, n, domain_index, result):
    result[:] = np.cross(incident_field(x), n, axis=0)
    multitrace = multitrace_operator(grid, k)
    bc_space = multitrace.range_spaces[1]
    snc_space = multitrace.dual_to_range_spaces[1]

    grid_fun = bempp.api.GridFunction(
        bc_space, fun=tangential_trace,
        dual_space=snc_space)

E2 = -multitrace[1, 0]
E1 = multitrace[0, 1]
op = E1 * E2
rhs = E1 * grid_fun

sol, info = bempp.api.linalg.gmres(op, rhs, use_strong_form=True)
eval_points = ...
efie_pot = electric_field(sol.space, eval_points, k)
field = -efie_pot * sol

```

Figure 2.21: Code snippet to solve the Calderón preconditioned EFIE.

some comparisons between the three equations. The difference in the performance of the direct and indirect formulations is small; in this section we focus on the indirect formulations, although similar results would be found for the direct formulations. In each of the examples in this section, we set Bempp’s GMRES parameter `use_strong_form` to `True`, enabling mass matrix preconditioning.

To discretise the EFIE, it is typical to use RWG/SNC trial and dual spaces to discretise the operator \mathbf{E} . These match the spaces we used for the discretisation of \mathbf{E}_2 above, so we use this discretisation here.

For the Calderón preconditioned EFIE, we multiply the discrete strong form of \mathbf{E}_2 with the operator \mathbf{E}_1 . This coincides with the product that is formed in the bottom left block when the discretisation of \mathbf{A}^2 is formed using the discretisation of \mathbf{A} above. In figure 2.21 we show the Bempp implementation of the Calderón preconditioned indirect EFIE.

To discretise the MFIE, we use RWG spaces for the domain and range space and RBC spaces for the dual space, as we did above when discretising \mathbf{H}_1 . This space choice is necessary to ensure a stable discretisation [30]. The MFIE can be implemented as shown in the code snippet in figure 2.22.

```

from bempp.api.operators.potential.maxwell import magnetic_field

calderon = ...
tangential_trace = ...
rwg_space = calderon.domain_spaces[0]
rbc_space = calderon.dual_to_range_spaces[0]

rhs = bempp.api.GridFunction(
    rwg_space, fun=tangential_trace,
    dual_space=rbc_space)
op = -calderon[0, 0]
sol, info = bempp.api.linalg.gmres(op, rhs, use_strong_form=True)

eval_points = ...
mfie_pot = magnetic_field(sol.space, eval_points, k)
field = -mfie_pot * sol

```

Figure 2.22: Code snippet for the implementation of the MFIE in Bempp.

For the CFIE, we use an RWG space for the unknown Neumann trace $\boldsymbol{\pi}$. Hence, we swap \boldsymbol{E}_1 and \boldsymbol{E}_2 , and \boldsymbol{H}_1 and \boldsymbol{H}_2 in the discretisation of the Calderón projector as discussed in section 2.4.5. It follows that we discretise \mathbf{H} and \mathbf{E} on the left-hand side of (2.69) with \boldsymbol{H}_1 and \boldsymbol{E}_2 . The operator \boldsymbol{E}_2 maps from RWG into BC, while \boldsymbol{H}_1 maps from RWG into RWG. We therefore require a discretisation of \mathbf{R} that maps from the BC space to the RWG space. We could for example choose the operator \boldsymbol{E}_1 , but this operator is not injective at interior electric eigenvalues. The solution is to choose \boldsymbol{E}_1 based on the wavenumber ik , instead of k (see [29]). On the right-hand side of the CFIE, we discretise \mathbf{H} with \boldsymbol{H}_2 and \mathbf{E} with \boldsymbol{E}_1 to stay compatible with the corresponding direct EFIE and direct MFIE formulations. We can easily implement this in the framework of Bempp with the code snippet in figure 2.23.

In this section, we compare these methods using three test problems: The first test problem is the problem where Ω^- is the unit sphere, $\boldsymbol{e}^{\text{inc}} = [e^{ikz}, 0, 0]$ is the incident wave, and $k = 2$. The second test problem is the problem where Ω^- is the NASA almond benchmarking shape (the almond, as defined in [82], is approximately 0.25 units long, 0.1 units wide, and 0.03 units tall), $\boldsymbol{e}^{\text{inc}} = [0, 0, e^{ikx}]$ is the incident wave, and $k = 20\pi$. The third test problem is the problem where Ω^- is a level 1 Menger sponge, $\boldsymbol{e}^{\text{inc}} = \boldsymbol{p}e^{ikd\cdot\boldsymbol{x}}$ with $\boldsymbol{p} = [-1, 2, 0]$ is the incident wave, and $k = 5$. The solutions of the second and third problems, computed using the Calderón preconditioned EFIE, are shown in figure 2.24

For the problem on the sphere, we discretise EFIE, Calderón preconditioned EFIE, MFIE, and CFIE on a series of triangular grids with different levels of refinement. The number of GMRES iterations required to solve the linear system arising from each equation are shown in figure 2.25.

Here, it can be seen that Calderón preconditioning is highly effective for the EFIE: the number of iterations required to solve the EFIE (orange triangles) rises quickly as the grid is refined, but the number required to solve the preconditioned EFIE (red circles) remains below 10. Due to the ill-conditioning of the standard EFIE, it is not a feasible to use it

```

multitrace = ...
multitrace_scaled = ...
identity = ...
tangential_trace = ...

rwg_space = multitrace.domain_spaces[0]
snc_space = multitrace.dual_to_range_spaces[1]
bc_space = multitrace.domain_spaces[1]
rbc_space = multitrace.dual_to_range_spaces[0]

calderon = 0.5 * identity + multitrace
grid_fun = bempp.api.GridFunction(
    bc_space, fun=tangential_trace,
    dual_space=snc_space)

R = multitrace_scaled[0, 1]
E1 = multitrace[0, 1]
E2 = -multitrace[1, 0]
mfie1 = calderon[0, 0]
mfie2 = calderon[1, 1]

rhs = -R * mfie2 * grid_fun - E1 * grid_fun
op = -R * E2 + mfie1
sol, info = bempp.api.linalg.gmres(op, rhs, use_strong_form=True)

```

Figure 2.23: Code snippet for the implementation of the CFIE in Bempp.

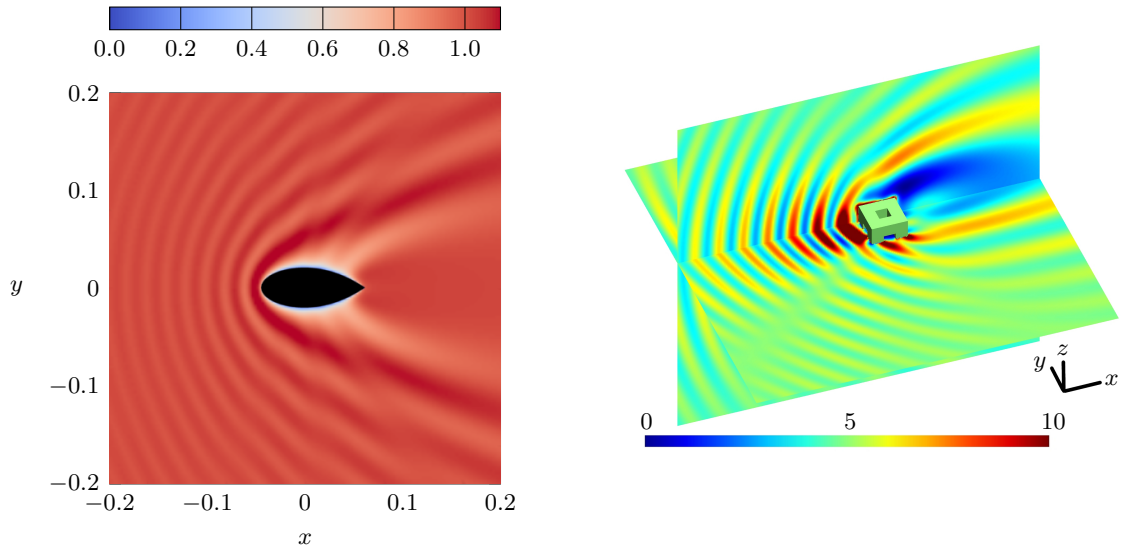


Figure 2.24: Slice at $z = 0$ of squared electric field density of the wave $\mathbf{e}^{\text{inc}} = [0, 0, e^{ikx}]$, with $k = 20\pi$, scattering off the NASA almond, computed using the indirect Calderón preconditioned EFIE discretised on a grid with 2442 edges (left); and slices at $z = 0.5$ and $y = 0.5$ of squared electric field density of the wave $\mathbf{e}^{\text{inc}} = \mathbf{p}e^{ik\mathbf{d}\cdot\mathbf{x}}$, with $\mathbf{p} = [-1, 2, 0]$, $\mathbf{d} = [\frac{2}{\sqrt{5}}, \frac{1}{\sqrt{5}}, 0]$, and $k = 5$ scattering off a level 1 Menger sponge, computed using the indirect Calderón preconditioned EFIE discretised on a grid with 4680 edges (right).

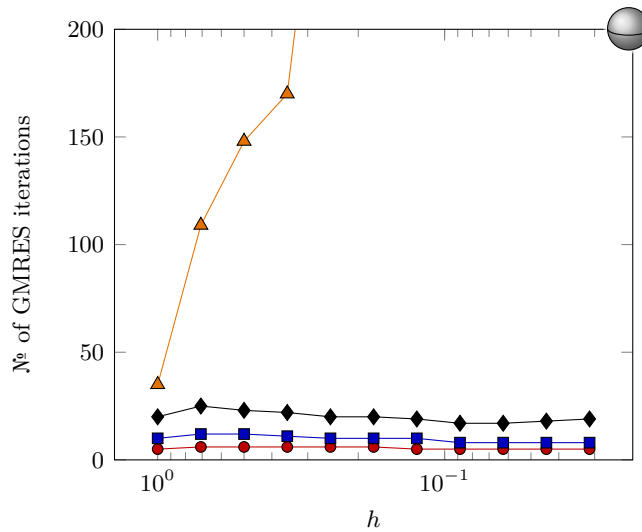


Figure 2.25: The number of GMRES iterations taken to solve the EFIE (orange triangles), Calderón preconditioned EFIE (red circles), MFIE (blue squares), and CFIE (black diamonds) to a tolerance of 1×10^{-5} for scattering from the unit sphere. Each equation has had mass matrix preconditioning applied.

to solve actual problems, and so we exclude it from all further examples. In what follows, all mentions of the EFIE refer to the Calderón preconditioned EFIE.

In figure 2.25, it can be seen that the MFIE and CFIE are both well-conditioned. The EFIE has the lowest iteration count, but in many cases the MFIE will be the most efficient method: this is due to each iteration of the EFIE requiring two applications of a boundary operator, while the MFIE only requires one per iteration.

The EFIE and MFIE are more efficient than the CFIE for low frequency problems, but they are both prone to ill-conditioning near interior resonances. This can be seen in figure 2.26, which shows the GMRES iteration counts for the EFIE (red circles), MFIE (blue squares), and CFIE (black diamonds) for the problem on the unit sphere as the wavenumber k is increased. Close to $k = 12.5$ there is an interior resonance of the sphere. In the neighbourhood of this, the numbers of iterations taken to solve the EFIE and MFIE increase rapidly. The number of iterations taken to solve the CFIE, however, remains bounded, as the CFIE formulation used here is immune to these resonances. For this reason, the CFIE is more suitable for higher frequency problems.

The convergence of the GMRES residuals for the problems on the NASA Almond (discretised using a grid with 2442 edges) and the Menger sponge (discretised using a grid with 4680 edges) are shown in figure 2.27. As for the problem on the sphere, it can be seen that the EFIE converges in the lowest number of iterations. Again we note that the MFIE may still be the most efficient method, as the EFIE and CFIE require multiple boundary operator applications per iteration.

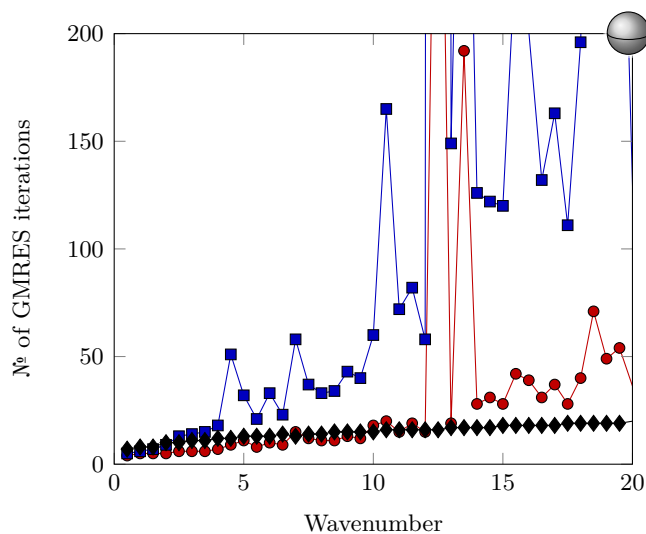


Figure 2.26: The number of GMRES iterations needed to solve the Calderón preconditioned EFIE (red circles), MFIE (blue squares) and CFIE (black diamonds), for the problem on the unit sphere with 4809 grid edges as the wavenumber increases. Close to $k = 12.5$ there is an interior resonance, which causes the number of iterations for the EFIE and MFIE to explode, while the CFIE's iteration count stays small.

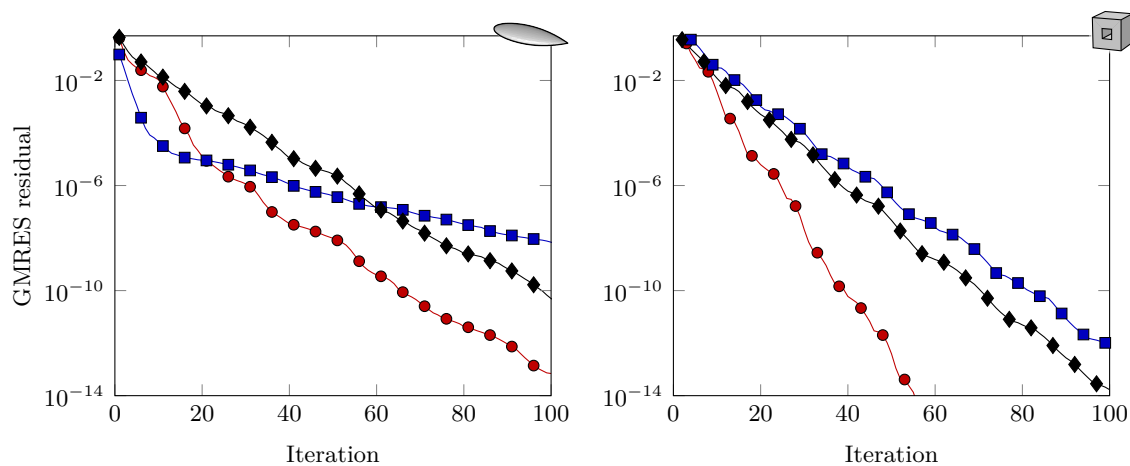


Figure 2.27: The convergence of the GMRES residual for the problem on a NASA almond (left) and a level 1 Menger sponge (right) for the Calderón preconditioned EFIE (red circles), MFIE (blue squares), and CFIE (black diamonds).

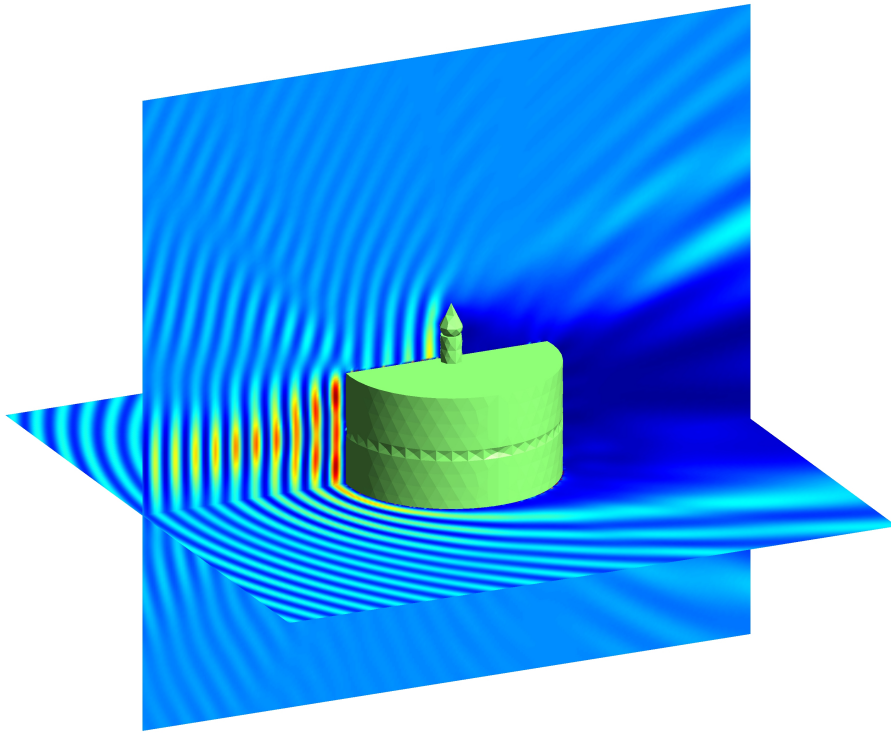


Figure 2.28: Slices of the squared electric field density of the wave $e^{\text{inc}} = [0, 0, e^{ikx}]$, with $k = 8$, scattering off a perfectly conducting cake, computed using the Calderón preconditioned EFIE discretised on a grid with 3225 edges.

Now that you've finished reading chapter 2, why not take a break and have a slice of figure 2.28 before reading on.

CHAPTER 3

WEAK IMPOSITION OF BOUNDARY CONDITIONS

Weak imposition of boundary conditions has been very successful in the context of finite element methods. In particular, Nitsche’s method [60] has recently received increased interest in the scientific computation community. This chapter discusses how the idea behind this type of method can be applied in the context of boundary element methods to impose different types of boundary condition in a unified framework.

Weak imposition of boundary conditions here means that neither the Dirichlet trace nor the Neumann trace is imposed exactly, instead an h -dependent boundary condition is imposed that is weighted in such a way that optimal error estimates may be derived and the exact boundary condition is recovered in the asymptotic limit. Methods based on Nitsche’s method have been successfully utilised for boundary element method domain decomposition problems, where they have been used to impose interface conditions at 1D interfaces between segments of 2D screens embedded in 3D space [37, 24]. Our approach instead focusses on imposing boundary conditions on the 2D boundary of a single domain problem through the addition of penalty terms to a general formulation written in terms of the multitrace operator, in a similar vein to the method discussed in [3] for the finite element method.

The use of systems of boundary integral equations for problems with mixed boundary conditions is quite classical [32, 77, 80, 81]. While these papers require the assembly of boundary operators on subsets of the boundary mesh, the penalty method proposed in this chapter requires only the addition of sparse mass matrices to the multitrace operator assembled on the entire mesh. In addition to the greater simplicity of the resulting formulation, this method has the advantage that the sparse penalty terms only affect the entries in the matrix for near interactions: this gives the resulting system a structure that can be utilised when designing effective preconditioners.

This approach may not be competitive in the simple case of pure Dirichlet or Neumann conditions due to the increase in the number of unknowns. Therefore the main focus of this work is on more complex situations.

The proposed framework is flexible and allows for the design of a range of different methods depending on the choice of weights and residuals. We will present a sample of possible methods with the ambition of showing the versatility of the framework rather than claiming that for each case the choices are optimal.

While the present chapter focuses on weak imposition of boundary conditions through Nitsche type coupling for BEM, ultimately the goal is to develop a framework for complex BEM/BEM and FEM/BEM multiphysics coupling situations. Existing approaches here are often built upon FETI and BETI type methods [50, 51]. While BETI is usually formulated in terms of Steklov–Poincaré operators, the framework proposed in this chapter builds directly upon Calderón projectors of the subdomains.

For the method proposed in the present work the multi-domain coupling will take a form similar to that using Nitsche’s method in the FEM/FEM coupling setting of [8]; see also the FEM/BEM coupling of [23] where a Nitsche’s method for the coupling was proposed, using the Steklov-Poincaré operator for the BEM system.

An important application area for the presented weak imposition of boundary conditions are inverse problems with unknown boundary conditions. Since the boundary condition only enters through a sparse operator this can be easily updated in each step of a solver iteration, while the boundary integral operators only need to be computed once. In particular, for reconstruction of the coefficient in a Robin condition (see eg [45] for a finite element approach and [6] for a detailed analysis of the stability of this problem), the robustness with respect to the coefficient of the present method is an advantage.

This chapter is based on the material in [9].

— 3.1 —

WEAK IMPOSITION OF BOUNDARY CONDITIONS ON LAPLACE’S EQUATION

In this chapter, we focus on the interior Laplace problem (1.37): Find $u \in H^1(\Delta, \Omega^-)$ such that

$$-\Delta u = 0 \quad \text{in } \Omega^-, \quad (1.37a)$$

$$u = g_D \quad \text{on } \Gamma_D, \quad (1.37c)$$

$$\frac{\partial u}{\partial \boldsymbol{\nu}} = g_N \quad \text{on } \Gamma_N, \quad (1.37d)$$

$$\frac{\partial u}{\partial \boldsymbol{\nu}} = \frac{1}{\varepsilon}(g_D - u) + g_N \quad \text{on } \Gamma_R. \quad (1.37e)$$

We assume for simplicity that the boundaries between Γ_D , Γ_N and Γ_R coincide with edges between the faces of Γ . We assume that $g_D \in H^{1/2}(\Gamma_D \cup \Gamma_R)$ and $g_N \in L^2(\Gamma_N \cup \Gamma_R)$. Observe that, by the Lax–Milgram lemma, there exists a unique solution to (1.37). We assume that $u \in H^{3/2+\epsilon}(\Omega^-)$ for some $\epsilon > 0$.

This section will focus on four model cases: non-homogeneous Dirichlet conditions, non-homogeneous Neumann conditions, mixed Dirichlet–Neumann boundary conditions, and Robin conditions of the form (1.37e).

For the Robin boundary condition, we will use the ideas of Juntunen and Stenberg [47]. A salient feature of this type of imposition of the Robin condition is that it is robust under singular perturbations. Indeed regardless of the Robin coefficient, the conditioning of the resulting system matrix is no worse than for the Neumann or the Dirichlet problem.

To quantify the two traces we introduce the product space

$$\mathbb{V} := H^{1/2}(\Gamma) \times (H^{-1/2}(\Gamma) \cap L^2(\Gamma_N \cup \Gamma_R)).$$

The additional regularity on the flux variable is required later when imposing Neumann and Robin conditions. We also introduce the associated norm, defined for $(v, \mu) \in \mathbb{V}$ by

$$\|(v, \mu)\|_{\mathbb{V}} := \|v\|_{H^{1/2}(\Gamma)} + \|\mu\|_{H^{-1/2}(\Gamma)}.$$

For a more compact notation, we introduce the Calderón form, defined for $(w, \eta), (v, \mu) \in \mathbb{V}$ by

$$\mathcal{C}[(w, \eta), (v, \mu)] := \langle (\frac{1}{2}\text{Id} - \mathbf{K})w, \mu \rangle_{\Gamma} + \langle \mathbf{V}\eta, \mu \rangle_{\Gamma} + \langle (\frac{1}{2}\text{Id} + \mathbf{K}')\eta, v \rangle_{\Gamma} + \langle \mathbf{W}w, v \rangle_{\Gamma}. \quad (3.2)$$

We may then rewrite the Calderón identities (1.58) and (1.59) as

$$\mathcal{C}[(u, \lambda), (v, \mu)] = \langle u, \mu \rangle_{\Gamma} + \langle \lambda, v \rangle_{\Gamma}, \quad (3.3)$$

where $(u, \lambda) \in \mathbb{V}$ is the solution of the problem.

We will also frequently use the multitrace form, defined for $(w, \eta), (v, \mu) \in \mathbb{V}$ by

$$\mathcal{A}[(w, \eta), (v, \mu)] := -\langle \mathbf{K}w, \mu \rangle_{\Gamma} + \langle \mathbf{V}\eta, \mu \rangle_{\Gamma} + \langle \mathbf{K}'\eta, v \rangle_{\Gamma} + \langle \mathbf{W}w, v \rangle_{\Gamma}. \quad (3.4)$$

Using this, we may rewrite (3.3) as

$$\mathcal{A}[(u, \lambda), (v, \mu)] = \frac{1}{2} \langle u, \mu \rangle_{\Gamma} + \frac{1}{2} \langle \lambda, v \rangle_{\Gamma}. \quad (3.5)$$

Using the results in lemmas 1.3 to 1.5, we obtain the continuity and coercivity of \mathcal{A} .

Lemma 3.1 (Continuity). *There exists $C > 0$ such that*

$$|\mathcal{A}[(w, \eta), (v, \mu)]| \leq C \|(w, \eta)\|_{\mathbb{V}} \|(v, \mu)\|_{\mathbb{V}} \quad \forall (w, \eta), (v, \mu) \in \mathbb{V}.$$

Proof. Use the results (iii) and (iv) from lemma 1.5. □

Lemma 3.2 (Coercivity). *There exists $\alpha > 0$ such that*

$$\alpha \left(|v|_{H_*^{1/2}(\Gamma)}^2 + \|\mu\|_{H^{-1/2}(\Gamma)}^2 \right) \leq \mathcal{A}[(v, \mu), (v, \mu)] \quad \forall (v, \mu) \in \mathbb{V}.$$

Proof. Use the coercivity of \mathbf{V} and \mathbf{W} from lemmas 1.3 and 1.4 and let $\alpha = \min(\alpha_{\mathbf{W}}, \alpha_{\mathbf{V}})$. □

We now proceed to derive boundary integral formulations of the problem (1.37), that we will then discretise to arrive at BEM formulations. Let $(u, \lambda) \in \mathbb{V}$ be the solution of the problem we are solving, and let $(v, \mu) \in \mathbb{V}$. We assume that the boundary condition may be written as

$$R_\Gamma(u, \lambda) = 0. \quad (3.6)$$

The idea that we will exploit in the following is simply to add a suitably weighted weak form of this constraint to the Calderón form (3.3). Formally, this leads to an expression of the form

$$C[(u, \lambda), (v, \mu)] = \langle u, \mu \rangle_\Gamma + \langle \lambda, v \rangle_\Gamma + \langle R_\Gamma(u, \lambda), \beta_1 v + \beta_2 \mu \rangle_\Gamma, \quad (3.7)$$

or equivalently

$$\mathcal{A}[(u, \lambda), (v, \mu)] = \frac{1}{2} \langle u, \mu \rangle_\Gamma + \frac{1}{2} \langle \lambda, v \rangle_\Gamma + \langle R_\Gamma(u, \lambda), \beta_1 v + \beta_2 \mu \rangle_\Gamma, \quad (3.8)$$

where β_1 and β_2 are problem-dependent scaling operators that will be chosen as a function of the physical parameters in order to obtain robustness of the method.

— 3.1.1 —

DIRICHLET BOUNDARY CONDITION

In this section, we assume that $\Gamma_D \equiv \Gamma$ and consider the resulting Dirichlet problem. We choose $\beta_1 = \beta_D^{1/2}$, $\beta_2 = \beta_D^{-1/2}$, where β_D will be identified with a mesh-dependent penalty parameter, and

$$R_{\Gamma_D}(u, \lambda) := \beta_D^{1/2}(g_D - u) \quad (3.9)$$

where $g_D \in H^{1/2}(\Gamma)$ is the Dirichlet data.

Inserting this into (3.8), we obtain

$$\mathcal{A}[(u, \lambda), (v, \mu)] = \frac{1}{2} \langle u, \mu \rangle_\Gamma + \frac{1}{2} \langle \lambda, v \rangle_\Gamma + \left\langle \beta_D^{1/2}(g_D - u), \beta_D^{1/2}v + \beta_D^{-1/2}\mu \right\rangle_\Gamma. \quad (3.10)$$

Rearranging leads to the formulation

$$\mathcal{A}[(u, \lambda), (v, \mu)] - \frac{1}{2} \langle \lambda, v \rangle_{\Gamma_D} + \frac{1}{2} \langle u, \mu \rangle_{\Gamma_D} + \langle \beta_D u, v \rangle_{\Gamma_D} = \langle g_D, \beta_D v + \mu \rangle_{\Gamma_D}. \quad (3.11)$$

The boundary condition $u = g_D$ only enters this formulation through the definition of R_{Γ_D} , and is not used in the rearrangement. A number of alternative formulations could be obtained by differently incorporating this condition, but we use this one here as it represents the general formulation (3.5) that has only been modified by the addition of a penalty function, and so this derivation method can be used for a wide range boundary conditions. We also follow this same derivation method for the other problems in this chapter, and also for the problems in chapters 4 and 5. One can compare (3.11) with the

classical (non-symmetric) Nitsche's method by formally identifying λ with $\partial_\nu u$ and μ with $\partial_\nu v$ (up to the multiplicative factor $\frac{1}{2}$).

For a more compact notation, we introduce the boundary operator associated with the non-homogeneous Dirichlet condition

$$\mathcal{B}_D[(u, \lambda), (v, \mu)] := -\frac{1}{2} \langle \lambda, v \rangle_{\Gamma_D} + \frac{1}{2} \langle u, \mu \rangle_{\Gamma_D} + \langle \beta_D u, v \rangle_{\Gamma_D}, \quad (3.12)$$

and the operator associated with the right hand side

$$\mathcal{L}_D(v, \mu) := \langle g_D, \beta_D v + \mu \rangle_{\Gamma_D}. \quad (3.13)$$

Using these and (3.11), we arrive at the following problem: Find $(u, \lambda) \in \mathbb{V}$ such that

$$\mathcal{A}[(u, \lambda), (v, \mu)] + \mathcal{B}_D[(u, \lambda), (v, \mu)] = \mathcal{L}_D(v, \mu) \quad \forall (v, \mu) \in \mathbb{V}. \quad (3.14)$$

If we set $\beta_D = 0$ in (3.12) and (3.13), we obtain a penalty-free formulation for the Dirichlet problem.

— 3.1.2 —

NEUMANN BOUNDARY CONDITION

In this section, we assume that $\Gamma_N \equiv \Gamma$ and consider the resulting Neumann problem. We choose $\beta_1 = \beta_N^{-1/2}$, $\beta_2 = \beta_N^{1/2}$, and define

$$R_{\Gamma_N}(u, \lambda) := \beta_N^{1/2} (g_N - \lambda), \quad (3.15)$$

where $g_N \in L^2(\Gamma_N)$, with $\int_\Gamma g_N = 0$, is the Neumann data.

Proceeding as in the Dirichlet case, we obtain the formulation

$$\mathcal{A}[(u, \lambda), (v, \mu)] - \frac{1}{2} \langle u, \mu \rangle_{\Gamma_N} + \frac{1}{2} \langle \lambda, v \rangle_{\Gamma_N} + \langle \beta_N \lambda, \mu \rangle_{\Gamma_N} = \langle g_N, \beta_N \mu + v \rangle_{\Gamma_N}. \quad (3.16)$$

Defining

$$\mathcal{B}_N[(u, \lambda), (v, \mu)] := -\frac{1}{2} \langle u, \mu \rangle_{\Gamma_N} + \frac{1}{2} \langle \lambda, v \rangle_{\Gamma_N} + \langle \beta_N \lambda, \mu \rangle_{\Gamma_N}, \quad (3.17)$$

$$\mathcal{L}_N(v, \mu) := \langle g_N, \beta_N \mu + v \rangle_{\Gamma_N}, \quad (3.18)$$

we may write this as the variational problem: Find $(u, \lambda) \in \mathbb{V}^*$ such that

$$\mathcal{A}[(u, \lambda), (v, \mu)] + \mathcal{B}_N[(u, \lambda), (v, \mu)] = \mathcal{L}_N(v, \mu) \quad \forall (v, \mu) \in \mathbb{V}^*. \quad (3.19)$$

Here, we use the space $\mathbb{V}^* := H_*^{1/2}(\Gamma_N) \times L^2(\Gamma_N)$, as the solution to the Neumann problem can only be determined up to a constant, so we include the extra condition that $\bar{u} = 0$.

If we set $\beta_N = 0$ in (3.17) and (3.18), we obtain a penalty-free formulation for the

Neumann problem. In this case, we may take $\mathbb{V} = H_*^{1/2}(\Gamma_N) \times H^{-1/2}(\Gamma_N)$ and $g_N \in H^{-1/2}(\Gamma_N)$.

When $\beta_N > 0$, observe that for the terms imposing the Neumann condition to be well defined, we need $\lambda \in L^2(\Gamma_N)$. This can be avoided by replacing β_N with a regularising operator $R : H^{-1/2}(\Gamma_N) \rightarrow H^{1/2}(\Gamma_N)$. For example, we could take $R = \beta_V \mathbf{V}$, where $\beta_V \in \mathbb{R}$ and \mathbf{V} is the single layer boundary operator on Γ_N . This formulation with the operator R is given in [76, (3.10) and (3.11)], where it was derived using a domain decomposition approach where a Robin condition was used to weakly impose a Neumann condition.

The resulting formulations using β_N are in general easier to analyse, since they give control of λ on the Neumann boundary in the natural norm $\|\lambda\|_{H^{-1/2}(\Gamma_N)}$.

— 3.1.3 —

MIXED DIRICHLET–NEUMANN BOUNDARY CONDITION

We now consider the case of mixed Dirichlet–Neumann boundary conditions, when $\Gamma = \Gamma_D \cup \Gamma_N$. We note that in this case, and in the Robin case, we take $\mathbb{V} = H^{1/2}(\Gamma) \times L^2(\Gamma)$.

Let R_{Γ_D} and R_{Γ_N} be defined by (3.9) and (3.15). Using the abstract form (3.8), we obtain

$$\begin{aligned} \mathcal{A}[(u, \lambda), (v, \mu)] &= \frac{1}{2} \langle u, \mu \rangle_{\Gamma} + \frac{1}{2} \langle \lambda, v \rangle_{\Gamma} \\ &\quad + \left\langle R_{\Gamma_D}(u, \lambda), \beta_D^{1/2} v + \beta_D^{-1/2} \mu \right\rangle_{\Gamma_D} + \left\langle R_{\Gamma_N}(u, \lambda), \beta_N^{-1/2} v + \beta_N^{1/2} \mu \right\rangle_{\Gamma_N}. \end{aligned} \quad (3.20)$$

Developing (3.20), and defining

$$\begin{aligned} \mathcal{B}_{\text{ND}}[(u, \lambda), (v, \mu)] &:= \frac{1}{2} \langle u, \mu \rangle_{\Gamma_D} - \frac{1}{2} \langle \lambda, v \rangle_{\Gamma_D} + \langle \beta_D u, v \rangle_{\Gamma_D} \\ &\quad + \frac{1}{2} \langle \lambda, v \rangle_{\Gamma_N} - \frac{1}{2} \langle u, \mu \rangle_{\Gamma_N} + \langle \beta_N \lambda, \mu \rangle_{\Gamma_N}, \end{aligned} \quad (3.21)$$

$$\mathcal{L}_{\text{ND}}(v, \mu) := \langle g_D, \beta_D v + \mu \rangle_{\Gamma_D} + \langle g_N, \beta_N \mu + v \rangle_{\Gamma_N}, \quad (3.22)$$

we arrive the variational formulation: Find $(u, \lambda) \in \mathbb{V}$ such that

$$\mathcal{A}[(u, \lambda), (v, \mu)] + \mathcal{B}_{\text{ND}}[(u, \lambda), (v, \mu)] = \mathcal{L}_{\text{ND}}(v, \mu) \quad \forall (v, \mu) \in \mathbb{V}. \quad (3.23)$$

If we set $\beta_D = 0$ and $\beta_N = 0$ in (3.21) and (3.22), we obtain a penalty-free formulation for the mixed Dirichlet–Neumann problem. By taking $\Gamma_N = \emptyset$ or $\Gamma_D = \emptyset$, formulations for both Dirichlet and Neumann problems can be obtained from (3.23).

— 3.1.4 —

ROBIN CONDITIONS

For simplicity, we consider the case where $\Gamma = \Gamma_R$. Considering the Robin condition (1.37e), we may write, for some $\varepsilon > 0$,

$$R_{\Gamma_R}(u, \lambda) := \beta_R^{1/2} \left(\varepsilon^{1/2}(g_N - \lambda) + \varepsilon^{-1/2}(g_D - u) \right). \quad (3.24)$$

This function is a linear combination of the Dirichlet and the Neumann conditions.

$$R_{\Gamma_R}(u, \lambda) = \alpha_D R_{\Gamma_D}(u, \lambda) + \alpha_N R_{\Gamma_N}(u, \lambda), \quad (3.25)$$

where $\alpha_N = \beta_R^{1/2} \beta_N^{-1/2} \varepsilon^{1/2}$ and $\alpha_D = \beta_R^{1/2} \beta_D^{-1/2} \varepsilon^{-1/2}$.

We take $\beta_1 = \beta_R^{1/2}$ and $\beta_2 = \beta_R^{-1/2}$, and look for a term of the form

$$\left\langle \phi R_{\Gamma_R}(u, \lambda), \beta_R^{1/2} v + \beta_R^{-1/2} \mu \right\rangle_{\Gamma_R}, \quad (3.26)$$

where the ϕ and β_R must have the following properties to ensure that the formulation degenerates into the formulation for the Dirichlet and Neumann problems as $\varepsilon \rightarrow 0$ and $\varepsilon \rightarrow \infty$.

$$\begin{array}{llll} \beta_R \rightarrow \beta_D, & \alpha_D \phi \rightarrow 1, & \text{and} & \alpha_N \phi \rightarrow 0 & \text{as } \varepsilon \rightarrow 0, \\ \beta_R \rightarrow \beta_N^{-1}, & \alpha_N \phi \rightarrow 1, & \text{and} & \alpha_D \phi \rightarrow 0 & \text{as } \varepsilon \rightarrow \infty. \end{array}$$

It is straightforward to verify that these conditions are satisfied for the choices

$$\phi := \frac{\varepsilon^{1/2}}{\varepsilon \beta_R + 1}, \quad (3.27)$$

$$\beta_R := \frac{\varepsilon \beta_N^{-1} + \beta_D}{\varepsilon + 1}. \quad (3.28)$$

Later, we will use $\beta_D = \beta h^{-1}$ and $\beta_N = \beta h$, where β is a constant, as in the mixed Dirichlet–Neumann case.

Collecting the above considerations, we arrive at the formulation

$$\begin{aligned} \mathcal{A}[(u, \lambda), (v, \mu)] &= \frac{1}{2} \langle u, \mu \rangle_{\Gamma} + \frac{1}{2} \langle \lambda, v \rangle_{\Gamma} \\ &+ \left\langle \varepsilon(g_N - \lambda) + (g_D - u), \frac{\beta_R}{\varepsilon \beta_R + 1} v + \frac{1}{\varepsilon \beta_R + 1} \mu \right\rangle_{\Gamma_R}. \end{aligned} \quad (3.29)$$

Taking $\varepsilon \rightarrow 0$, we recover the Dirichlet formulation (3.11); and taking $\varepsilon \rightarrow \infty$ results in the Neumann formulation (3.16).

By introducing

$$\begin{aligned} \mathcal{B}_R[(u, \lambda), (v, \mu)] := & \frac{1}{2} \left\langle \frac{\varepsilon\beta_R - 1}{\varepsilon\beta_R + 1} \lambda, v \right\rangle_{\Gamma_R} - \frac{1}{2} \left\langle \frac{\varepsilon\beta_R - 1}{\varepsilon\beta_R + 1} u, \mu \right\rangle_{\Gamma_R} \\ & + \left\langle \frac{\varepsilon}{\varepsilon\beta_R + 1} \lambda, \mu \right\rangle_{\Gamma_R} + \left\langle \frac{\beta_R}{\varepsilon\beta_R + 1} u, v \right\rangle_{\Gamma_R} \end{aligned}$$

and

$$\mathcal{L}_R(v, \mu) := \left\langle g_D + \varepsilon g_N, \frac{\beta_R}{\varepsilon\beta_R + 1} v + \frac{1}{\varepsilon\beta_R + 1} \mu \right\rangle_{\Gamma_R},$$

we may write this as the variational problem: Find $(u, \lambda) \in \mathbb{V}$ such that

$$\mathcal{A}[(u, \lambda), (v, \mu)] + \mathcal{B}_R[(u, \lambda), (v, \mu)] = \mathcal{L}_R(v, \mu) \quad \forall (v, \mu) \in \mathbb{V}. \quad (3.30)$$

— 3.2 —

ANALYSIS OF THE LAPLACE SINGLE DOMAIN PROBLEM

All the methods introduced in section 3.1 are written as the sum of the multitrace operator \mathcal{A} and a boundary condition operator \mathcal{B} . We write this generally as: Find $(u, \lambda) \in \mathbb{V}$ such that

$$\mathcal{A}[(u, \lambda), (v, \mu)] + \mathcal{B}[(u, \lambda), (v, \mu)] = \mathcal{L}(v, \mu) \quad \forall (v, \mu) \in \mathbb{V}. \quad (3.31)$$

In this section, we analyse this general problem, then show that the analysis is applicable to the boundary conditions discussed in section 3.1.

We now introduce the discrete product space $\mathbb{V}_h := \mathbf{P}_h^k(\Gamma) \times \mathbf{DP}_h^l(\Gamma)$. The boundary element formulation of the generic problem (3.31) then takes the form: Find $(u_h, \lambda_h) \in \mathbb{V}_h$ such that

$$\mathcal{A}[(u_h, \lambda_h), (v_h, \mu_h)] + \mathcal{B}[(u_h, \lambda_h), (v_h, \mu_h)] = \mathcal{L}(v_h, \mu_h) \quad \forall (v_h, \mu_h) \in \mathbb{V}_h. \quad (3.32)$$

If we assume that $(u, \lambda) \in \mathbb{V}$ and $(u_h, \lambda_h) \in \mathbb{V}_h$ satisfy (3.31) and (3.32), it immediately follows that the following Galerkin orthogonality relation holds.

$$\mathcal{A}[(u - u_h, \lambda - \lambda_h), (v_h, \mu_h)] + \mathcal{B}[(u - u_h, \lambda - \lambda_h), (v_h, \mu_h)] = 0 \quad \forall (v_h, \mu_h) \in \mathbb{V}_h. \quad (3.33)$$

We also get the following representation formula for the approximation in Ω^- using (1.47).

$$\tilde{u}_h = -\mathcal{K}u_h + \mathcal{V}\lambda_h. \quad (3.34)$$

We will now proceed to derive some estimates for the solution of (3.32) and the reconstruction (3.34).

Let \mathbb{W} be a product Hilbert space for the primal and flux variables, such that $\mathbb{V}_h \subset \mathbb{W} \subset \mathbb{V}$. Let $\|\cdot\|_{\mathcal{B}}$ be a norm defined on \mathbb{W} , such that for all $(v, \mu) \in \mathbb{W}$, $\|(v, \mu)\|_{\mathcal{B}} \geq \|(v, \mu)\|_{\mathbb{V}}$.

To reduce the number of constants that appear, especially when proving that assumption 3.4 holds, we introduce the following notation.

- If $\exists C > 0$, independent of h , such that $a \leq Cb$, then we write $a \lesssim b$.
- If $a \lesssim b$ and $b \lesssim a$, then we write $a \approx b$.

For the abstract analysis, we will make use of the following standard assumptions.

Assumption 3.1 (Inf-sup condition). *There exists $\alpha > 0$ such that $\forall (v, \mu) \in \mathbb{W}$*

$$\alpha \|(v, \mu)\|_{\mathcal{B}} \leq \sup_{(w, \eta) \in \mathbb{W} \setminus \{0\}} \frac{\mathcal{A}[(v, \mu), (w, \eta)] + \mathcal{B}[(v, \mu), (w, \eta)]}{\|(w, \eta)\|_{\mathcal{B}}},$$

and $\forall (w, \eta) \in \mathbb{W} \setminus \{0\}$

$$\sup_{(v, \mu) \in \mathbb{W}} |\mathcal{A}[(v, \mu), (w, \eta)] + \mathcal{B}[(v, \mu), (w, \eta)]| > 0.$$

Assumption 3.2 (Discrete inf-sup stability). *There exists $\alpha > 0$ such that $\forall (v_h, \mu_h) \in \mathbb{V}_h$*

$$\alpha \|(v_h, \mu_h)\|_{\mathcal{B}} \leq \sup_{(w_h, \eta_h) \in \mathbb{V}_h \setminus \{0\}} \frac{\mathcal{A}[(v_h, \mu_h), (w_h, \eta_h)] + \mathcal{B}[(v_h, \mu_h), (w_h, \eta_h)]}{\|(w_h, \eta_h)\|_{\mathcal{B}}},$$

and $\forall (w_h, \eta_h) \in \mathbb{V}_h \setminus \{0\}$

$$\sup_{(v_h, \mu_h) \in \mathbb{V}_h} |\mathcal{A}[(v_h, \mu_h), (w_h, \eta_h)] + \mathcal{B}[(v_h, \mu_h), (w_h, \eta_h)]| > 0.$$

Assumption 3.3 (Continuity). *There exists an auxiliary norm $\|(v, \mu)\|_*$ defined on \mathbb{W} , and there exists $M > 0$ such that $\forall (w, \eta), (v, \mu) \in \mathbb{W}$*

$$|\mathcal{A}[(w, \eta), (v, \mu)] + \mathcal{B}[(w, \eta), (v, \mu)]| \leq M \|(w, \eta)\|_* \|(v, \mu)\|_{\mathcal{B}}$$

Assumption 3.4 (Approximation). $\forall (v, \mu) \in H^s(\Gamma) \times H^r(\Gamma)$,

$$\inf_{(w_h, \eta_h) \in \mathbb{V}_h} \|(v - w_h, \mu - \eta_h)\|_* \lesssim h^{\zeta-1/2} |v|_{H^\zeta(\Gamma)} + h^{\xi+1/2} |\mu|_{H^\xi(\Gamma)},$$

where $\zeta = \min(k+1, s)$, $\xi = \min(l+1, r)$, $s \geq \frac{1}{2}$ and $r \geq -\frac{1}{2}$.

Typically, we use approximation spaces with $k = l + 1$, where the polynomial spaces used for λ are one order lower than those for u , or spaces with $k = l$, where equal order spaces are used for both variables.

We note that if the form $\mathcal{A} + \mathcal{B}$ is coercive, that is there exists $\alpha > 0$ such that $\forall (v, \mu) \in \mathbb{W}$

$$\alpha \|(v, \mu)\|_{\mathcal{B}}^2 \leq \mathcal{A}[(v, \mu), (v, \mu)] + \mathcal{B}[(v, \mu), (v, \mu)],$$

then assumptions 3.1 and 3.2 hold.

We now proceed to prove some results about the abstract problem.

Proposition 3.1. *Assume that assumption 3.1 holds, then the linear system defined by (3.32) is invertible. If, in addition, we assume that*

- *assumption 3.3 holds,*
- *there exists $L > 0$ such that $\mathcal{L}(w, \eta) \leq L \|(w, \eta)\|_{\mathcal{B}} \quad \forall (w, \eta) \in \mathbb{W}$,*
- *and $\|\cdot\|_*$ is equivalent to $\|\cdot\|_{\mathcal{B}}$,*

then the formulation (3.31) admits a unique solution in \mathbb{W} .

Proof. Note that assumption 3.1 implies the inf-sup condition,

$$\inf_{(v, \mu) \in \mathbb{W} \setminus \{0\}} \sup_{(w, \eta) \in \mathbb{W} \setminus \{0\}} \frac{\mathcal{A}[(v, \mu), (w, \eta)] + \mathcal{B}[(v, \mu), (w, \eta)]}{\|(v, \mu)\|_{\mathcal{B}} \|(w, \eta)\|_{\mathcal{B}}} > 0. \quad (3.35)$$

Therefore we may apply the inf-sup theorem [59] [4, theorem 5.2.1]. \square

Proposition 3.2. *Assume that $(u, \lambda) \in \mathbb{V}$ is the solution to a boundary value problem of the form (1.37) satisfying the abstract form (3.31). Let $(u_h, \lambda_h) \in \mathbb{V}_h$ be the solution of (3.32). If assumptions 3.2 and 3.3 are satisfied then*

$$\|(u - u_h, \lambda - \lambda_h)\|_{\mathcal{B}} \leq \frac{M}{\alpha} \inf_{(v_h, \mu_h) \in \mathbb{V}_h} \|(u - v_h, \lambda - \mu_h)\|_*. \quad (3.36)$$

Proof. See [83, theorem 2]. \square

Corollary 3.1. *Let $(u, \lambda) \in H^s(\Gamma) \times H^r(\Gamma)$, for some $s \geq \frac{1}{2}$ and $r \geq -\frac{1}{2}$, satisfy the abstract form (3.31). Under the assumptions of proposition 3.2 and assumption 3.4,*

$$\|(u - u_h, \lambda - \lambda_h)\|_{\mathcal{B}} \lesssim h^{\zeta-1/2} |u|_{H^\zeta(\Gamma)} + h^{\xi+1/2} |\lambda|_{H^\xi(\Gamma)},$$

where $\zeta = \min(k + 1, s)$ and $\xi = \min(l + 1, r)$.

Proof. Apply assumption 3.4 to the right hand side of (3.36). \square

Proposition 3.3. *Assume that $(u, \lambda) \in \mathbb{V}$ is the solution to a boundary value problem of the form (1.37) satisfying the abstract form (3.31) and that the assumptions of proposition 3.2 are satisfied. Let $(u_h, \lambda_h) \in \mathbb{V}_h$. Let $\tilde{u} : \Omega^- \rightarrow \mathbb{R}$ be the reconstruction obtained using (1.47), with $u = \lambda$ and $u = u$; and $\tilde{u}_h : \Omega^- \rightarrow \mathbb{R}$ be the reconstruction obtained using (3.34). Then there holds*

$$\|\tilde{u} - \tilde{u}_h\|_{H^1(\Omega^-)} \lesssim \frac{M}{\alpha} \inf_{v_h, \mu_h \in \mathbb{V}_h} \|(u - v_h, \lambda - \mu_h)\|_*.$$

Proof. Using (1.73) and (1.75), we may write

$$\tilde{u} - \tilde{u}_h = (u_\lambda^{\mathcal{Y}} - u_{\lambda_h}^{\mathcal{Y}}) + (u_u^{\mathcal{K}} - u_{u_h}^{\mathcal{K}}).$$

Using the triangle inequality, we have

$$\|\tilde{u} - \tilde{u}_h\|_{H^1(\Omega^-)} \leq \|u_\lambda^{\mathcal{Y}} - u_{\lambda_h}^{\mathcal{Y}}\|_{H^1(\Omega^-)} + \|u_u^{\mathcal{K}} - u_{u_h}^{\mathcal{K}}\|_{H^1(\Omega^-)}. \quad (3.37)$$

By (1.74) and (1.76), there exist $c_1, c_2 > 0$ such that

$$\|u_\lambda^{\mathcal{Y}} - u_{\lambda_h}^{\mathcal{Y}}\|_{H^1(\Omega^-)} \leq c_1 \|\lambda - \lambda_h\|_{H^{-1/2}(\Gamma)}, \quad (3.38)$$

$$\|u_u^{\mathcal{K}} - u_{u_h}^{\mathcal{K}}\|_{H^1(\Omega^-)} \leq c_2 \|u - u_h\|_{H^{1/2}(\Gamma)}. \quad (3.39)$$

Collecting (3.37) to (3.39), we see that there exists $C > 0$ such that

$$\|\tilde{u} - \tilde{u}_h\|_{H^1(\Omega^-)} \leq C \|(\lambda - \lambda_h, u - u_h)\|_{\mathbb{V}} \leq C \|(\lambda - \lambda_h, u - u_h)\|_{\mathcal{B}}. \quad (3.40)$$

The statement now follows from proposition 3.2. \square

Corollary 3.2. *Under the same assumptions of proposition 3.3 and assumption 3.4,*

$$\|\tilde{u} - \tilde{u}_h\|_{H^1(\Omega^-)} \lesssim h^{\zeta-1/2} |u|_{H^\zeta(\Gamma)} + h^{\xi+1/2} |\lambda|_{H^\xi(\Gamma)},$$

where $\zeta = \min(k+1, s)$ and $\xi = \min(l+1, r)$.

Proof. Apply assumption 3.4 to (3.40) in the proof of proposition 3.3. \square

When $k = l + 1 = 1$, we may use the discrete product space $\mathbb{V}'_h = \text{DUAL}_h^1(\Gamma) \times \text{DUAL}_h^0(\Gamma)$ for the space containing the test functions (v_h, μ_h) and look to solve the following variant of (3.32): Find $(u_h, \lambda_h) \in \mathbb{V}_h$ such that

$$\mathcal{A}[(u_h, \lambda_h), (v'_h, \mu'_h)] + \mathcal{B}[(u_h, \lambda_h), (v'_h, \mu'_h)] = \mathcal{L}(v'_h, \mu'_h) \quad \forall (v'_h, \mu'_h) \in \mathbb{V}'_h. \quad (3.41)$$

In appendix C, we discuss how the results of this chapter could be applied to this variant. We note that by lemma 2.4, assumption 3.4 would not hold if we were looking for $u_h \in \text{DUAL}_h^1(\Gamma)$ or $\lambda_h \in \text{DUAL}_h^0(\Gamma)$, justifying our use of these spaces only for the test functions (v_h, μ_h) . On smooth domains, however, these spaces exhibit stronger approximation results so they could be used.

— 3.2.1 —

APPLICATION OF THE THEORY TO THE DIRICHLET PROBLEM

For the finite element spaces defined above, the Dirichlet problem takes the form: Find $(u_h, \lambda_h) \in \mathbb{V}_h$ such that

$$\mathcal{A}[(u_h, \lambda_h), (v_h, \mu_h)] + \mathcal{B}_D[(u_h, \lambda_h), (v_h, \mu_h)] = \mathcal{L}_D(v_h, \mu_h) \quad \forall (v_h, \mu_h) \in \mathbb{V}_h. \quad (3.42)$$

We introduce the following \mathcal{B}_D -norm.

$$\|(v, \mu)\|_{\mathcal{B}_D} := \|(v, \mu)\|_{\mathbb{V}} + \beta_D^{1/2} \|v\|_{L^2(\Gamma_D)}.$$

We let $\|\cdot\|_* = \|\cdot\|_{\mathcal{B}_D}$, and $\mathbb{W} = \mathbb{V}$. We now proceed to verify that assumptions 3.1 to 3.4 hold.

Proposition 3.4 (Coercivity). *Assumptions 3.1 and 3.2 are satisfied for the Dirichlet problem if $\exists \beta_{\min} > 0$, independent of h , such that $\beta_D > \beta_{\min}$.*

Proof. Using the fact that $|v|_{H_*^{1/2}(\Gamma_D)}^2 + \|\bar{v}\|_{L^2(\Gamma_D)}^2 \geq c \|v\|_{H^{1/2}(\Gamma_D)}^2$, where $\bar{v} := \frac{\langle v, 1 \rangle_{\Gamma}}{\langle 1, 1 \rangle_{\Gamma}}$ is the mean value of v , we deduce from lemma 3.2 that for every positive $\alpha' \leq \alpha$,

$$\alpha' \|(v, \mu)\|_{\mathbb{V}}^2 - c\alpha' \|\bar{v}\|_{L^2(\Gamma_D)}^2 \leq \mathcal{A}[(v, \mu), (v, \mu)] \quad \forall (v, \mu) \in \mathbb{W}.$$

Using the definition of \mathcal{B}_D , we see that

$$\mathcal{B}_D[(v, \mu), (v, \mu)] = \beta_D \langle v, v \rangle_{\Gamma_D} = \beta_D \|v\|_{L^2(\Gamma_D)}^2$$

Taking $\alpha' = \min(\alpha, \beta_{\min}/2)$, we see that

$$\begin{aligned} \mathcal{A}[(v, \mu), (v, \mu)] + \mathcal{B}_D[(v, \mu), (v, \mu)] &\geq \alpha' \|(v, \mu)\|_{\mathbb{V}}^2 + \left(1 - \frac{c\alpha'}{\beta_{\min}}\right) \beta_D \|v\|_{L^2(\Gamma_D)}^2 \\ &\geq \alpha'' \|(v, \mu)\|_{\mathcal{B}_D}^2, \end{aligned}$$

for some $\alpha'' > 0$, as we can take α' small enough for the final term to be positive. Therefore, in this case the form $\mathcal{A} + \mathcal{B}_D$ is coercive, and so assumptions 3.1 and 3.2 hold. \square

Proposition 3.5 (Inf-sup condition). *Assumptions 3.1 and 3.2 are satisfied for the Dirichlet problem with $\beta_D = 0$.*

Proof. Taking $w = v$ and $\eta = \mu + c\bar{v}$, where $\bar{v} := \frac{\langle v, 1 \rangle_{\Gamma}}{\langle 1, 1 \rangle_{\Gamma}}$ is the mean value of v , for some $c \in \mathbb{R}$ to be fixed, we obtain

$$\begin{aligned} L &:= \mathcal{A}[(v, \mu), (w, \eta)] + \mathcal{B}_D[(v, \mu), (w, \eta)] \\ &= \langle \mathbf{V}\mu, \mu \rangle_{\Gamma} + c \langle \mathbf{V}\mu, \bar{v} \rangle_{\Gamma} - c \langle \mathbf{K}v, \bar{v} \rangle_{\Gamma} + \langle \mathbf{W}v, v \rangle_{\Gamma} + \frac{c}{2} \langle v, \bar{v} \rangle_{\Gamma}. \end{aligned} \quad (3.43)$$

By lemmas 1.3 and 1.4, we know that

$$\langle \mathbf{V}\mu, \mu \rangle_\Gamma + \langle \mathbf{W}v, v \rangle_\Gamma \geq \alpha_V \|\mu\|_{H^{-1/2}(\Gamma)}^2 + \alpha_W |v|_{H_*^{1/2}(\Gamma)}^2. \quad (3.44)$$

By lemma 1.5, we see that

$$\begin{aligned} c |\langle \mathbf{V}\mu, \bar{v} \rangle_\Gamma| &\leq c \|\mathbf{V}\mu\|_{H^{1/2}(\Gamma)} \|\bar{v}\|_{H^{-1/2}(\Gamma)} \\ &\leq c C_V \|\mu\|_{H^{-1/2}(\Gamma)} \|\bar{v}\|_{H^{-1/2}(\Gamma)} \\ &= c C_V \|\mu\|_{H^{-1/2}(\Gamma)} \|\bar{v}\|_{L^2(\Gamma)}. \end{aligned}$$

Using the fact that for $a, b \geq 0$, $ab \leq (a^2 + b^2)/2$, we obtain

$$c |\langle \mathbf{V}\mu, \bar{v} \rangle_\Gamma| \leq \frac{c^2 C_V^2}{2\alpha_V} \|\bar{v}\|_{L^2(\Gamma)}^2 + \frac{\alpha_V}{2} \|\mu\|_{H^{-1/2}(\Gamma)}^2. \quad (3.45)$$

We note that $u = \bar{v}$ is a solution to (1.37), $\gamma_D^- \bar{v} = \bar{v}$ and $\gamma_N^- \bar{v} = 0$. Using this and applying (1.58), we see that $\forall \mu \in H^{-1/2}(\Gamma)$, $\langle \mathbf{K}\bar{v}, \mu \rangle_\Gamma = -\frac{1}{2} \langle \bar{v}, \mu \rangle_\Gamma$. Therefore, using $\mu = \bar{v}$,

$$\begin{aligned} c \langle \mathbf{K}v, \bar{v} \rangle_\Gamma &= c \langle \mathbf{K}(v - \bar{v}), \bar{v} \rangle_\Gamma + c \langle \mathbf{K}\bar{v}, \bar{v} \rangle_\Gamma \\ &= c \langle \mathbf{K}(v - \bar{v}), \bar{v} \rangle_\Gamma - \frac{c}{2} \langle \bar{v}, \bar{v} \rangle_\Gamma. \end{aligned}$$

Using the fact that $\|v - \bar{v}\|_{H^{1/2}(\Gamma)} = |v|_{H_*^{1/2}(\Gamma)}$, and proceeding in the same way as we did for the single layer term above, we obtain

$$c \langle \mathbf{K}v, \bar{v} \rangle_\Gamma \leq \frac{\alpha_W}{2} |v|_{H_*^{1/2}(\Gamma)}^2 + \frac{C_K^2 c^2}{2\alpha_W} \|\bar{v}\|_{L^2(\Gamma)}^2 - \frac{c}{2} \|\bar{v}\|_{L^2(\Gamma)}^2. \quad (3.46)$$

We also have that

$$\frac{c}{2} \langle v, \bar{v} \rangle_\Gamma = \frac{c}{2} \|\bar{v}\|_{L^2(\Gamma)}^2. \quad (3.47)$$

Taking $\alpha = \min(\alpha_V, \alpha_K)$ and $C = \max(C_V, C_K)$, and putting (3.44) to (3.47) together, we obtain

$$L \geq \frac{\alpha}{2} \|\mu\|_{H^{-1/2}(\Gamma)}^2 + \frac{\alpha}{2} |v|_{H_*^{1/2}(\Gamma)}^2 + \left(c - \frac{c^2 C^2}{\alpha} \right) \|\bar{v}\|_{L^2(\Gamma)}^2.$$

Letting $c = \frac{\alpha}{2C^2}$ gives

$$\begin{aligned} L &\geq \frac{\alpha}{2} \|\mu\|_{H^{-1/2}(\Gamma)}^2 + \frac{\alpha}{2} |v|_{H_*^{1/2}(\Gamma)}^2 + \frac{\alpha}{4C^2} \|\bar{v}\|_{L^2(\Gamma)}^2 \\ &\gtrsim \|\mu\|_{H^{-1/2}(\Gamma)}^2 + |v|_{H_*^{1/2}(\Gamma)}^2 + \|\bar{v}\|_{L^2(\Gamma)}^2. \end{aligned}$$

Finally, we show that

$$\begin{aligned}
\|(v, \mu)\|_{\mathbb{V}} &= \|v\|_{H^{1/2}(\Gamma)} + \|\mu\|_{H^{-1/2}(\Gamma)} \\
&\leq \|v - \bar{v}\|_{H^{1/2}(\Gamma)} + \|\bar{v}\|_{H^{1/2}(\Gamma)} + \|\mu\|_{H^{-1/2}(\Gamma)} \\
&= |v|_{H_*^{1/2}(\Gamma)} + \|\bar{v}\|_{L^2(\Gamma)} + \|\mu\|_{H^{-1/2}(\Gamma)}, \\
\|(w, \eta)\|_{\mathbb{V}} &\leq |v|_{H_*^{1/2}(\Gamma)} + \|\bar{v}\|_{L^2(\Gamma)} + \|\mu + c\bar{v}\|_{H^{-1/2}(\Gamma)} \\
&\leq |v|_{H_*^{1/2}(\Gamma)} + \|\bar{v}\|_{L^2(\Gamma)} + \|\mu\|_{H^{-1/2}(\Gamma)} + c\|\bar{v}\|_{H^{-1/2}(\Gamma)} \\
&\lesssim |v|_{H_*^{1/2}(\Gamma)} + \|\bar{v}\|_{L^2(\Gamma)} + \|\mu\|_{H^{-1/2}(\Gamma)}.
\end{aligned}$$

Therefore

$$\begin{aligned}
\|(v, \mu)\|_{\mathbb{V}} \|(w, \eta)\|_{\mathbb{V}} &\lesssim \|\mu\|_{H^{-1/2}(\Gamma)}^2 + |v|_{H_*^{1/2}(\Gamma)}^2 + \|\bar{v}\|_{L^2(\Gamma)}^2 \\
&\lesssim L.
\end{aligned}$$

We obtain the first part of assumption 3.1 by dividing through by $\|(w, \eta)\|_{\mathbb{V}}$ and taking the supremum.

To show the second part of assumption 3.1, we let $(w, \eta) \in \mathbb{W} \setminus \{0\}$ and proceed as follows.

$$\begin{aligned}
L &:= \sup_{(v, \mu) \in \mathbb{W}} |\mathcal{A}[(v, \mu), (w, \eta)] + \mathcal{B}_D[(v, \mu), (w, \eta)]| \\
&\geq \mathcal{A}[(w, \eta - \bar{w}), (w, \eta)] + \mathcal{B}_D[(w, \eta - \bar{w}), (w, \eta)] \\
&= -\langle \mathbf{K}'\bar{w}, w \rangle_{\Gamma} + \langle \mathbf{V}\eta, \eta \rangle_{\Gamma} - \langle \mathbf{V}\bar{w}, \eta \rangle_{\Gamma} + \langle \mathbf{W}w, w \rangle_{\Gamma} + \frac{1}{2} \langle \bar{w}, w \rangle_{\Gamma}.
\end{aligned}$$

This is of the same form as (3.43), so we proceed as above to obtain

$$L \gtrsim \|(v, \mu)\|_{\mathbb{V}} \|(w, \eta)\|_{\mathbb{V}}.$$

This is greater than zero for all $(w, \eta) \neq 0$, and so we have proven the second part of assumption 3.1.

Assumption 3.2 can be proven in the same way as above using the discrete space \mathbb{V}_h in the place of \mathbb{W} . \square

Proposition 3.6 (Continuity). *Assumption 3.3 is satisfied for the Dirichlet problem.*

Proof. Applying lemma 3.1, the relation

$$\langle \eta, v \rangle_{\Gamma} \leq \|\eta\|_{H^{-1/2}(\Gamma)} \|v\|_{H^{1/2}(\Gamma)},$$

and the Cauchy–Schwarz inequality,

$$\beta_D \langle w, v \rangle_{\Gamma} \leq \beta_D^{1/2} \|w\|_{L^2(\Gamma)} \beta_D^{1/2} \|v\|_{L^2(\Gamma)},$$

to the form $\mathcal{A} + \mathcal{B}_D$ yields the desired continuity result. \square

Proposition 3.7 (Approximation). *Assumption 3.4 is satisfied for the Dirichlet problem if $0 \leq \beta_D \lesssim h^{-1}$.*

Proof. Using standard approximation results (see eg [73, theorems 10.4 and 10.9]), we see that

$$\begin{aligned} \inf_{(w_h, \eta_h) \in \mathbb{V}_h} \|(v - w_h, \mu - \eta_h)\|_{\mathbb{V}} &= \inf_{w_h \in \mathbb{P}_h^k} \|v - w_h\|_{H^{1/2}(\Gamma)} + \inf_{\eta_h \in \mathbb{DP}_h^l} \|\mu - \eta_h\|_{H^{-1/2}(\Gamma)} \\ &\lesssim h^{\zeta-1/2} |v|_{H^\zeta(\Gamma)} + h^{\xi+1/2} |\mu|_{H^\xi(\Gamma)}, \\ \inf_{w_h \in \mathbb{P}_h^k} \|v - w_h\|_{L^2(\Gamma_D)} &\lesssim h^\zeta |v|_{H^\zeta(\Gamma)}. \end{aligned}$$

Applying these to the definition of $\|\cdot\|_*$ gives

$$\inf_{(w_h, \eta_h) \in \mathbb{V}_h} \|(v - w_h, \mu - \eta_h)\|_* \lesssim h^{\zeta-1/2} |v|_{H^\zeta(\Gamma)} + h^{\xi+1/2} |\mu|_{H^\xi(\Gamma)} + \beta_D^{1/2} h^\zeta |v|_{H^\zeta(\Gamma)}.$$

If $\beta_D = 0$, assumption 3.4 holds. If $0 < \beta_D \lesssim h^{-1}$, then $\beta_D^{1/2} h^\zeta \lesssim h^{\zeta-1/2}$, and so assumption 3.4 holds. \square

We have shown that assumptions 3.1 to 3.4 are satisfied. Additionally the extra assumptions in proposition 3.1 are satisfied, so we conclude that the results of propositions 3.1 to 3.3 and corollaries 3.1 and 3.2 apply to the Dirichlet problem. This is summarised in the following result.

Theorem 3.1. *The Dirichlet problem (3.14) has a unique solution $(u, \lambda) \in H^s(\Gamma) \times H^r(\Gamma)$, for some $s \geq \frac{1}{2}$ and $r \geq -\frac{1}{2}$. The discrete Dirichlet problem (3.42) is invertible. If $\exists \beta_{\min} > 0$ such that $\beta_{\min} < \beta_D \lesssim h^{-1}$ or $\beta_D = 0$, its solution $(u_h, \lambda_h) \in \mathbb{P}_h^k(\Gamma) \times \mathbb{DP}_h^l(\Gamma)$ satisfies*

$$\|(u - u_h, \lambda - \lambda_h)\|_{\mathcal{B}_D} \lesssim h^{\zeta-1/2} |u|_{H^\zeta(\Gamma)} + h^{\xi+1/2} |\lambda|_{H^\xi(\Gamma)},$$

where $\zeta = \min(k+1, s)$ and $\xi = \min(l+1, r)$. Additionally,

$$\|\tilde{u} - \tilde{u}_h\|_{H^1(\Omega^-)} \lesssim h^{\zeta-1/2} |u|_{H^\zeta(\Gamma)} + h^{\xi+1/2} |\lambda|_{H^\xi(\Gamma)},$$

where \tilde{u} and \tilde{u}_h are the solutions in Ω^- computed using (1.47).

— 3.2.2 —

APPLICATION OF THE THEORY TO THE NEUMANN PROBLEM

The Neumann problem takes the form: Find $(u_h, \lambda_h) \in \mathbb{V}_h^*$ such that

$$\mathcal{A}[(u_h, \lambda_h), (v_h, \mu_h)] + \mathcal{B}_N[(u_h, \lambda_h), (v_h, \mu_h)] = \mathcal{L}_N(v_h, \mu_h) \quad \forall (v_h, \mu_h) \in \mathbb{V}_h^*. \quad (3.48)$$

Here $\mathbb{V}_h^* := \mathbb{P}_h^k(\Gamma) \times \text{DP}_h^l(\Gamma)$ and $\mathbb{P}_h^k(\Gamma) := \{v \in \mathbb{P}_h^k : \bar{v} = 0\}$, where $\bar{v} := \frac{\langle v, 1 \rangle_\Gamma}{\langle 1, 1 \rangle_\Gamma}$ is the mean value of v .

We introduce the following \mathcal{B}_N -norm.

$$\|(v, \mu)\|_{\mathcal{B}_N} := \|(v, \mu)\|_{\mathbb{V}} + \beta_N^{1/2} \|\mu\|_{L^2(\Gamma_N)},$$

we let $\|\cdot\|_* = \|\cdot\|_{\mathcal{B}_N}$, and we let $\mathbb{W} = \mathbb{V}^*$.

We now proceed to verify that assumptions 3.1 to 3.4 hold.

Proposition 3.8 (Coercivity). *Assumptions 3.1 and 3.2 are satisfied for the Neumann problem with $\beta_N \geq 0$.*

Proof. As $v \in H_*^{1/2}(\Gamma_N)$, we may immediately apply lemmas 1.3 and 1.4 to show that the form is coercive. \square

Proposition 3.9 (Continuity). *Assumption 3.3 is satisfied for the Neumann problem.*

Proof. The proof is the same as in the Dirichlet case. \square

Proposition 3.10 (Approximation). *Assumption 3.4 is satisfied for the Neumann problem if $0 \leq \beta_N \lesssim h$.*

Proof. The proof is the same as in the Dirichlet case. \square

As in the Dirichlet case, the extra assumptions in proposition 3.1 are satisfied. We therefore conclude with the following result.

Theorem 3.2. *The Neumann problem (3.19) has a unique solution $(u, \lambda) \in H_*^s(\Gamma) \times H^r(\Gamma)$, for some $s \geq \frac{1}{2}$ and $r \geq 0$ if $\beta_N > 0$. If $\beta_N = 0$, this holds for some $r \geq -\frac{1}{2}$. The discrete Neumann problem (3.48) is invertible. If $0 \leq \beta_N \lesssim h$, its solution $(u_h, \lambda_h) \in \mathbb{P}_h^k(\Gamma) \times \text{DP}_h^l(\Gamma)$ satisfies*

$$\|(u - u_h, \lambda - \lambda_h)\|_{\mathcal{B}_N} \lesssim h^{\zeta-1/2} |u|_{H^\zeta(\Gamma)} + h^{\xi+1/2} |\lambda|_{H^\xi(\Gamma)},$$

where $\zeta = \min(k+1, s)$ and $\xi = \min(l+1, r)$. Additionally,

$$\|\tilde{u} - \tilde{u}_h\|_{H^1(\Omega^-)} \lesssim h^{\zeta-1/2} |u|_{H^\zeta(\Gamma)} + h^{\xi+1/2} |\lambda|_{H^\xi(\Gamma)},$$

where \tilde{u} and \tilde{u}_h are the solutions in Ω^- computed using (1.47).

— 3.2.3 —

APPLICATION OF THE THEORY TO THE MIXED
DIRICHLET–NEUMANN PROBLEM

For the mixed problem, the boundary element method takes the form: Find $(u_h, \lambda_h) \in \mathbb{V}_h$ such that

$$\mathcal{A}[(u_h, \lambda_h), (v_h, \mu_h)] + \mathcal{B}_{\text{ND}}[(u_h, \lambda_h), (v_h, \mu_h)] = \mathcal{L}_{\text{ND}}(v_h, \mu_h) \quad \forall (v_h, \mu_h) \in \mathbb{V}_h. \quad (3.49)$$

We now show that the assumptions for the abstract error estimate are satisfied for the formulation (3.49). First, we introduce the following norms.

$$\begin{aligned} \|(v, \mu)\|_{\mathcal{B}_{\text{ND}}} &:= \|(v, \mu)\|_{\mathbb{V}} + \beta_{\text{D}}^{1/2} \|v\|_{L^2(\Gamma_{\text{D}})} + \beta_{\text{N}}^{1/2} \|\mu\|_{L^2(\Gamma_{\text{N}})} \\ \|(v, \mu)\|_* &:= \|(v, \mu)\|_{\mathbb{V}} + \beta_{\text{D}}^{1/2} \|v\|_{L^2(\Gamma)} + \beta_{\text{N}}^{1/2} \|\mu\|_{L^2(\Gamma)}. \end{aligned}$$

We let $\mathbb{W} = H^{1/2}(\Gamma) \times L^2(\Gamma)$.

Observe that in this case the two norms are not the same, nor are they equivalent, so the below results cannot be used to prove existence of a unique solution to (3.23). Nevertheless, it is easy to verify that if the exact solution to the mixed Dirichlet–Neumann problem is in \mathbb{V} then it satisfies (3.23).

Proposition 3.11 (Coercivity). *Assumptions 3.1 and 3.2 are satisfied for the mixed Dirichlet–Neumann problem if $\exists \beta_{\text{min}} > 0$, independent of h , such that $\beta_{\text{D}} > \beta_{\text{min}}$.*

Proof. We obtain using lemma 3.2 that for $(v, \mu) \in \mathbb{W}$,

$$\begin{aligned} L &:= \mathcal{A}[(v, \mu), (v, \mu)] + \mathcal{B}_{\text{ND}}[(v, \mu), (v, \mu)] \\ &\geq \alpha \|\mu\|_{H^{-1/2}(\Gamma)}^2 + \alpha |v|_{H_*^{1/2}(\Gamma)}^2 + \beta_{\text{D}} \|v\|_{L^2(\Gamma_{\text{D}})}^2 + \beta_{\text{N}} \|\mu\|_{L^2(\Gamma_{\text{N}})}^2. \end{aligned}$$

Taking $\alpha' = \min(\alpha, \beta_{\text{min}}/2)$, we get

$$\begin{aligned} L &\geq \alpha' \|\mu\|_{H^{-1/2}(\Gamma)}^2 + \alpha' \left(|v|_{H_*^{1/2}(\Gamma)}^2 + \|v\|_{L^2(\Gamma_{\text{D}})}^2 \right) \\ &\quad + (\beta_{\text{D}} - \alpha') \|v\|_{L^2(\Gamma_{\text{D}})}^2 + \beta_{\text{N}} \|\mu\|_{L^2(\Gamma_{\text{N}})}^2. \end{aligned}$$

By [73, theorem 2.6], $\left(|v|_{H_*^{1/2}(\Gamma)}^2 + \|\cdot\|_{L^2(\Gamma_{\text{D}})}^2 \right)^{1/2}$ is an equivalent norm to $\|\cdot\|_{H^{1/2}(\Gamma)}$. Therefore

$$\begin{aligned} L &\geq \alpha' \|\mu\|_{H^{-1/2}(\Gamma)}^2 + c\alpha' \|v\|_{H^{1/2}(\Gamma)}^2 + \beta_{\text{D}} \left(1 - \frac{\alpha'}{\beta_{\text{min}}} \right) \|v\|_{L^2(\Gamma_{\text{D}})}^2 + \beta_{\text{N}} \|\mu\|_{L^2(\Gamma_{\text{N}})}^2 \\ &\geq C \left(\|\mu\|_{H^{-1/2}(\Gamma)}^2 + \|v\|_{H^{1/2}(\Gamma)}^2 + \beta_{\text{D}} \|v\|_{L^2(\Gamma_{\text{D}})}^2 + \beta_{\text{N}} \|\mu\|_{L^2(\Gamma_{\text{N}})}^2 \right), \end{aligned}$$

where $C = \min(\alpha', c\alpha', 1 - \frac{\alpha'}{\beta_{\text{min}}}, 1)$ and α' is chosen to be small enough that $1 - \frac{\alpha'}{\beta_{\text{min}}}$ is positive. Coercivity follows using the definition of $\|\cdot\|_{\mathcal{B}_{\text{ND}}}$. \square

Proposition 3.12 (Continuity). *Assumption 3.3 is satisfied for the mixed Dirichlet–Neumann problem if $\exists \beta_{\min} > 0$, independent of h , such that $\beta_{\text{D}}^{1/2} \beta_{\text{N}}^{1/2} > \beta_{\min}$.*

Proof. Using the fact that $\langle v, \mu \rangle_{\Gamma} = \langle v, \mu \rangle_{\Gamma_{\text{D}}} + \langle v, \mu \rangle_{\Gamma_{\text{N}}}$, we see that

$$\begin{aligned} \mathcal{B}_{\text{ND}}[(w, \eta), (v, \mu)] &= \frac{1}{2} \langle w, \mu \rangle_{\Gamma_{\text{D}}} - \frac{1}{2} \langle \eta, v \rangle_{\Gamma_{\text{D}}} + \beta_{\text{D}} \langle w, v \rangle_{\Gamma_{\text{D}}} \\ &\quad + \frac{1}{2} \langle \eta, v \rangle_{\Gamma_{\text{N}}} - \frac{1}{2} \langle w, \mu \rangle_{\Gamma_{\text{N}}} + \beta_{\text{N}} \langle \eta, \mu \rangle_{\Gamma_{\text{N}}} \\ &= \frac{1}{2} \langle w, \mu \rangle_{\Gamma} - \langle \eta, v \rangle_{\Gamma_{\text{D}}} + \beta_{\text{D}} \langle w, v \rangle_{\Gamma_{\text{D}}} \\ &\quad + \frac{1}{2} \langle \eta, v \rangle_{\Gamma} - \langle w, \mu \rangle_{\Gamma_{\text{N}}} + \beta_{\text{N}} \langle \eta, \mu \rangle_{\Gamma_{\text{N}}} \\ &\lesssim \frac{1}{2} \langle w, \mu \rangle_{\Gamma} - \beta_{\text{D}}^{1/2} \beta_{\text{N}}^{1/2} \langle \eta, v \rangle_{\Gamma_{\text{D}}} + \beta_{\text{D}} \langle w, v \rangle_{\Gamma_{\text{D}}} \\ &\quad + \frac{1}{2} \langle \eta, v \rangle_{\Gamma} - \beta_{\text{D}}^{1/2} \beta_{\text{N}}^{1/2} \langle w, \mu \rangle_{\Gamma_{\text{N}}} + \beta_{\text{N}} \langle \eta, \mu \rangle_{\Gamma_{\text{N}}}. \end{aligned}$$

Proceeding as in proposition 3.6 leads to the desired result. \square

Proposition 3.13 (Approximation). *Assumption 3.4 is satisfied for the mixed Dirichlet–Neumann problem if $0 < \beta_{\text{D}} \lesssim h^{-1}$ and $0 < \beta_{\text{N}} \lesssim h$.*

Proof. Proceeding as in the Dirichlet case, we see that

$$\begin{aligned} \inf_{(w_h, \eta_h) \in \mathbb{V}_h} \|(v - w_h, \mu - \eta_h)\|_* &\lesssim h^{\zeta-1/2} |v|_{H^{\zeta}(\Gamma)} + h^{\xi+1/2} |\mu|_{H^{\xi}(\Gamma)} \\ &\quad + \beta_{\text{D}}^{1/2} h^{\zeta} |v|_{H^{\zeta}(\Gamma)} + \beta_{\text{N}}^{1/2} h^{\xi} |\mu|_{H^{\xi}(\Gamma)} \end{aligned}$$

If $0 < \beta_{\text{D}} \lesssim h^{-1}$ and $0 < \beta_{\text{N}} \lesssim h$, then

$$\beta_{\text{D}}^{1/2} h^{\zeta} |v|_{H^{\zeta}(\Gamma)} + \beta_{\text{N}}^{1/2} h^{\xi} |\mu|_{H^{\xi}(\Gamma)} \lesssim h^{\zeta-1/2} |v|_{H^{\zeta}(\Gamma)} + h^{\xi+1/2} |\mu|_{H^{\xi}(\Gamma)},$$

and so assumption 3.4 holds. \square

Motivated by the bounds on β_{D} and β_{N} in this proposition, we will later take $\beta_{\text{D}} = \beta h^{-1}$ and $\beta_{\text{N}} = \beta h$, where β is a constant.

If $k = l$, $\beta_{\text{N}} \lesssim h^{-1}$, and the solution is smooth enough, then

$$\beta_{\text{N}}^{1/2} h^{\xi} = \beta_{\text{N}}^{1/2} h^{\zeta} \lesssim h^{\zeta-1/2}.$$

Therefore the same order of convergence will be observed when the bounds on β_{N} here and in the theorem below may be replaced by $\beta_{\text{N}} \lesssim h^{-1}$ without loss of convergence. In this case, both β_{N} and β_{D} may be taken to be constants independent of h .

We conclude that the best approximation result of proposition 3.2 and the error estimate of corollary 3.1 hold for the discrete solutions of (3.49), as given in the following theorem.

Theorem 3.3. *Let $(u, \lambda) \in H^s(\Gamma) \times H^r(\Gamma)$, for some $s \geq \frac{1}{2}$ and $r \geq 0$, be the unique solution to the mixed Dirichlet–Neumann problem. This solution satisfies (3.23). Let*

$(u_h, \lambda_h) \in \mathbf{P}_h^k(\Gamma) \times \mathbf{DP}_h^l(\Gamma)$ be the solution of (3.49). If $0 < \beta_D \lesssim h^{-1}$, $0 < \beta_N \lesssim h$ and $\exists \beta_{\min} > 0$ such that $\beta_D^{1/2} \beta_N^{1/2} > \beta_{\min}$ and $\beta_D > \beta_{\min}$, then

$$\|(u - u_h, \lambda - \lambda_h)\|_{\mathcal{B}_{\text{ND}}} \lesssim h^{\zeta-1/2} |u|_{H^\zeta(\Gamma)} + h^{\xi+1/2} |\lambda|_{H^\xi(\Gamma)},$$

where $\zeta = \min(k+1, s)$ and $\xi = \min(l+1, r)$.

If we set $\beta_D = 0$ and $\beta_N = 0$, we arrive at a penalty-free formulation for the mixed Dirichlet–Neumann problem. We conjecture based on numerical experiments that this result also holds for the penalty-free formulation. The analysis for this case would take a similar form as in the Dirichlet and Neumann penalty-free cases.

— 3.2.4 —

APPLICATION OF THE THEORY TO THE ROBIN PROBLEM

The formulation for Robin conditions was proposed in (3.30). To simplify the notation we introduce a function $\omega : \Gamma \rightarrow \mathbb{R}_+$ defined by

$$\omega(\mathbf{x}) := \frac{1}{\varepsilon(\mathbf{x})\beta_R(\mathbf{x}) + 1},$$

and we assume that ε and β_R are sufficiently regular so that

$$\omega \in W^{1,2}(\Gamma) \cap L^\infty(\Gamma). \quad (3.50)$$

This will be true if the mesh has some local quasi-uniformity and ε is smooth enough. Noting that

$$\omega - \frac{1}{2} = \frac{2 - (\varepsilon\beta_R + 1)}{2(\varepsilon\beta_R + 1)} = -\frac{1}{2} \frac{\varepsilon\beta_R - 1}{\varepsilon\beta_R + 1},$$

we may then write the operators \mathcal{B}_R and \mathcal{L}_R as

$$\mathcal{B}_R[(u, \lambda), (v, \mu)] = \langle (\omega - \frac{1}{2})u, \mu \rangle_{\Gamma_R} - \langle (\omega - \frac{1}{2})\lambda, v \rangle_{\Gamma_R} + \langle \omega\beta_R u, v \rangle_{\Gamma_R} + \langle \omega\varepsilon\lambda, \mu \rangle_{\Gamma_R}, \quad (3.51)$$

$$\mathcal{L}_R[(v, \mu)] = \langle (g_D + \varepsilon g_N)\omega, \beta_R v + \mu \rangle_{\Gamma_R}. \quad (3.52)$$

The boundary element method for the Robin problem reads: Find $(u_h, \lambda_h) \in \mathbb{V}_h$ such that

$$\mathcal{A}[(u_h, \lambda_h), (v_h, \mu_h)] + \mathcal{B}_R[(u_h, \lambda_h), (v_h, \mu_h)] = \mathcal{L}_R[(v_h, \mu_h)] \quad \forall (v_h, \mu_h) \in \mathbb{V}_h. \quad (3.53)$$

For the analysis the following technical lemmas will be useful.

Lemma 3.3. *If $\varphi \in W^{1,2}(\Gamma) \cap L^\infty(\Gamma)$ and $f \in H^{1/2}(\Gamma)$, then $\varphi f \in H^{1/2}(\Gamma)$ and*

$$\|\varphi f\|_{H^{1/2}(\Gamma)} \leq C \left(\|\varphi\|_{L^\infty(\Gamma)} + \|\varphi\|_{W^{1,2}(\Gamma)} \right) \|f\|_{H^{1/2}(\Gamma)}.$$

Proof. The proof is a consequence of [13, lemma 6] which shows that

$$\|\varphi f\|_{H^{1/2}(\Gamma)} \leq C \left(\|\varphi\|_{L^\infty(\Gamma)} \|f\|_{H^{1/2}(\Gamma)} + \|f\|_{L^4(\Gamma)} \|\varphi\|_{W^{1,2}(\Gamma)}^{1/2} \|\varphi\|_{L^\infty(\Gamma)}^{1/2} \right). \quad (3.54)$$

We then recall the Sobolev injection $\|f\|_{L^4(\Gamma)} \leq C \|f\|_{H^{1/2}(\Gamma)}$ from [33, theorem 6.7] and conclude using this result and an arithmetic-geometric inequality of the right hand side of (3.54). \square

Lemma 3.4. *If $f \in L^2(\Gamma)$, $\varphi \in L^2(\Gamma) \cap C^0(\Gamma)$ and $\varphi(\mathbf{x}) > 0$ for all $\mathbf{x} \in \Gamma$, then there exists $C > 0$ such that*

$$\|\varphi f\|_{L^2(\Gamma)}^2 \geq C \|f\|_{L^2(\Gamma)}^2.$$

Proof. Let $a = \inf_{\mathbf{x} \in \Gamma} \varphi(\mathbf{x})$. Since Γ is closed, there exists $\mathbf{y} \in \Gamma$ such that $\varphi(\mathbf{y}) = a$. Therefore $a > 0$. We now see that

$$\begin{aligned} \|\varphi f\|_{L^2(\Gamma)}^2 &= \int_{\Gamma} \varphi^2 f^2 \\ &\geq a^2 \int_{\Gamma} f^2 \\ &= C \|f\|_{L^2(\Gamma)}^2, \end{aligned}$$

where $C = a^2$. \square

We introduce the norm

$$\|(v, \mu)\|_{\mathcal{B}_R} := \|(v, \mu)\|_{\mathbb{W}} + \left\| (\varepsilon\omega)^{1/2} \mu \right\|_{L^2(\Gamma)} + \left\| (\omega\beta_R)^{1/2} v \right\|_{L^2(\Gamma)},$$

we let $\|\cdot\|_* = \|\cdot\|_{\mathcal{B}_R}$, and we let $\mathbb{W} = H^{1/2}(\Gamma) \times L^2(\Gamma)$. We note that if $\varepsilon \rightarrow 0$ or $\varepsilon \rightarrow \infty$, then $\|\cdot\|_{\mathcal{B}_R}$ converges to $\|\cdot\|_{\mathcal{B}_D}$ or $\|\cdot\|_{\mathcal{B}_N}$ respectively. We now proceed to show that assumptions 3.1 to 3.4 hold.

Proposition 3.14 (Coercivity). *Assumptions 3.1 and 3.2 are satisfied for the Robin problem.*

Proof. Let $(v, \mu) \in \mathbb{W}$, and let $L := \mathcal{A}[(v, \mu), (v, \mu)] + \mathcal{B}_R[(v, \mu), (v, \mu)]$. Using lemma 3.2, we see that

$$L \geq \alpha \|\mu\|_{H^{-1/2}(\Gamma)}^2 + \alpha \|v\|_{H^{1/2}(\Gamma)}^2 - \alpha \|v\|_{L^2(\Gamma)}^2 + \left\| (\varepsilon\omega)^{1/2} \mu \right\|_{L^2(\Gamma)}^2 + \left\| (\omega\beta_R)^{1/2} v \right\|_{L^2(\Gamma)}^2,$$

for any $\alpha \leq \min(\alpha_{\mathbb{V}}, \alpha_{\mathbb{W}})$.

By lemma 3.4, we have

$$-\alpha \|v\|_{L^2(\Gamma)}^2 \geq -\frac{\alpha}{C} \left\| (\omega\beta_R)^{1/2} v \right\|_{L^2(\Gamma)}^2. \quad (3.55)$$

Taking $\alpha = \min(\alpha_V, \alpha_W, C/2)$, we obtain

$$L \geq \alpha \|\mu\|_{H^{-1/2}(\Gamma)}^2 + \alpha \|v\|_{H^{1/2}(\Gamma)}^2 + \left\| (\varepsilon\omega)^{1/2} \mu \right\|_{L^2(\Gamma)}^2 + \frac{1}{2} \left\| (\omega\beta_R)^{1/2} v \right\|_{L^2(\Gamma)}^2,$$

Using the definition of $\|\cdot\|_{\mathcal{B}_R}$, we see that the form is coercive. \square

Proposition 3.15 (Continuity). *Assumption 3.3 is satisfied for the Robin problem if $\exists \beta_{\min} > 0$, independent of h , such that $\beta_R > \beta_{\min}$.*

Proof. Using lemma 3.3 and the fact that $\omega \in W^{1,2}(\Gamma) \cap L^\infty(\Gamma)$, we see that for $g \in H^{-1/2}(\Gamma)$ and $f \in H^{1/2}(\Gamma)$,

$$\langle \omega g, f \rangle_\Gamma \leq C \left(\|\omega\|_{L^\infty(\Gamma)} + \|\omega\|_{W^{1,2}(\Gamma)} \right) \|g\|_{H^{-1/2}(\Gamma)} \|f\|_{H^{1/2}(\Gamma)}.$$

Let $\varepsilon_{\min} := \inf_{\mathbf{x} \in \Gamma} \varepsilon(\mathbf{x})$. As in the proof of lemma 3.4, we see that $\varepsilon_{\min} > 0$. Hence,

$$-\frac{1}{2} < \omega - \frac{1}{2} < \frac{1}{\beta_{\min} \varepsilon_{\min} + 1},$$

and so

$$\left\| \omega - \frac{1}{2} \right\|_{L^\infty(\Gamma)} + \left\| \omega - \frac{1}{2} \right\|_{W^{1,2}(\Gamma)} < \max \left(\frac{1}{2}, \frac{1}{\beta_{\min} \varepsilon_{\min} + 1} \right) \left(\|1\|_{L^\infty(\Gamma)} + \|1\|_{W^{1,2}(\Gamma)} \right).$$

Applying these two results to the first two boundary terms in $\mathcal{B}_R[(w, \eta), (v, \mu)]$, we obtain

$$\left\langle \left(\omega - \frac{1}{2} \right) w, \mu \right\rangle_\Gamma - \left\langle \left(\omega - \frac{1}{2} \right) v, \eta \right\rangle_\Gamma \leq C \|(w, \eta)\|_{\mathbb{V}} \|(v, \mu)\|_{\mathbb{V}}.$$

By the Cauchy–Schwarz inequality, we obtain for the remaining terms

$$\begin{aligned} & \langle \omega \varepsilon \eta, \mu \rangle_\Gamma + \langle \omega \beta_R w, v \rangle_\Gamma \\ & \leq \left\| (\omega \varepsilon)^{1/2} \eta \right\|_{L^2(\Gamma)} \left\| (\omega \varepsilon)^{1/2} \mu \right\|_{L^2(\Gamma)} + \left\| (\omega \beta_R)^{1/2} w \right\|_{L^2(\Gamma)} \left\| (\omega \beta_R)^{1/2} v \right\|_{L^2(\Gamma)}. \end{aligned}$$

Collecting the terms, we then have

$$\mathcal{B}_R[(w, \eta), (v, \mu)] \lesssim \|(w, \eta)\|_{\mathcal{B}_R} \|(v, \mu)\|_{\mathcal{B}_R}.$$

\square

Proposition 3.16 (Approximation). *Assumption 3.4 is satisfied for the Robin problem if $\beta_R \approx h^{-1}$.*

Proof. First note that $\omega < 1$ and

$$\omega \varepsilon = \frac{\varepsilon}{\varepsilon \beta_R + 1} = \frac{1}{\beta_R + \frac{1}{\varepsilon}} < \frac{1}{\beta_R}.$$

Therefore,

$$\left\| (\omega\beta_R)^{1/2}v \right\|_{L^2(\Gamma)} \leq \beta_R^{1/2} \|v\|_{L^2(\Gamma)} \quad \text{and} \quad \left\| (\omega\varepsilon)^{1/2}\mu \right\|_{L^2(\Gamma)} \leq \beta_R^{-1/2} \|\mu\|_{L^2(\Gamma)}. \quad (3.56)$$

If $\beta_R \approx h^{-1}$, then assumption 3.4 can be shown to hold. \square

When using equal order approximation, the same order of convergence will be observed when the bounds on β_R here and in the theorem below may be replaced by $h \lesssim \beta_R \lesssim h^{-1}$ for sufficiently smooth solutions. Note that the condition $h^{-1} \lesssim \beta_R$ implies the existence of β_{\min} , as required by proposition 3.15. The condition $h \lesssim \beta_R$ does not imply this, so in this case the additional requirement that $\exists \beta_{\min} > 0$ such that $\beta_{\min} < \beta_R$ is necessary to ensure continuity.

Proposition 3.17. *The extra assumptions in proposition 3.1 are satisfied for the Robin problem.*

Proof. As a consequence of the coercivity and continuity above and observing that by the Cauchy–Schwarz inequality and the definition of ω , there exists C such that

$$\langle \omega(g_D + \varepsilon g_N), \beta_R v + \mu \rangle_\Gamma \leq C(\|g_D\|_{L^2(\Gamma)} + \|g_N\|_{L^2(\Gamma)}) \|(v, \mu)\|_{\mathcal{B}_R}$$

\square

We conclude that propositions 3.1 and 3.2 and corollaries 3.1 and 3.2 hold for the Robin problem. This is summarised in the following result.

Theorem 3.4. *The Robin problem (3.30) has a unique solution $(u, \lambda) \in H^s(\Gamma) \times H^r(\Gamma)$, for some $s \geq \frac{1}{2}$ and $r \geq 0$. The discrete Robin problem (3.53) is invertible. If $\beta_R \approx h^{-1}$, its solution $(u_h, \lambda_h) \in P_h^k(\Gamma) \times DP_h^l(\Gamma)$ satisfies*

$$\|(u - u_h, \lambda - \lambda_h)\|_{\mathcal{B}_R} \leq C \left(h^{\zeta-1/2} |u|_{H^\zeta(\Gamma)} + h^{\xi+1/2} |\lambda|_{H^\xi(\Gamma)} \right),$$

for some $C > 0$, where $\zeta = \min(k+1, s)$ and $\xi = \min(l+1, r)$. Additionally,

$$\|\tilde{u} - \tilde{u}_h\|_{H^1(\Omega^-)} \leq C \left(h^{\zeta-1/2} |u|_{H^\zeta(\Gamma)} + h^{\xi+1/2} |\lambda|_{H^\xi(\Gamma)} \right),$$

where \tilde{u} and \tilde{u}_h are the solutions in Ω^- computed using (1.47).

Again, we could set $\beta_R = 0$ to arrive at a penalty-free formulation for Robin problems. In this case, our numerical experiments show large errors for some values of the parameter ε , which leads us to conclude that this result does not hold for the penalty-free formulation.

As $\varepsilon \rightarrow 0$ and $\varepsilon \rightarrow \infty$, we obtain the Dirichlet and Neumann formulations analysed in sections 3.2.1 and 3.2.2. We expect the condition number of the discrete system for the Robin problem to be no worse than in either extreme case, and observe this in section 3.3.3.

— 3.3 —

NUMERICAL RESULTS

Drawing inspiration from [47], we define

$$\begin{aligned} u(x, y, z) &= \sin(\pi x) \sin(\pi y) \sinh(\sqrt{2}\pi z) \\ g_D(x, y, z) &= \sin(\pi x) \sin(\pi y) \sinh(\sqrt{2}\pi z), \\ g_N(x, y, z) &= \begin{pmatrix} \pi \cos(\pi x) \sin(\pi y) \sinh(\sqrt{2}\pi z) \\ \pi \sin(\pi x) \cos(\pi y) \sinh(\sqrt{2}\pi z) \\ \sqrt{2}\pi \sin(\pi x) \sin(\pi y) \cosh(\sqrt{2}\pi z) \end{pmatrix} \cdot \boldsymbol{\nu}. \end{aligned}$$

It is easy to check that for any bounded domain $\Omega^- \subset \mathbb{R}^3$ with boundary $\Gamma = \Gamma_D \cup \Gamma_N \cup \Gamma_R$ and any fixed $\varepsilon \in \mathbb{R}$, u is the solution of

$$-\Delta u = 0 \quad \text{in } \Omega^-, \quad (3.57a)$$

$$u = g_D \quad \text{on } \Gamma_D, \quad (3.57b)$$

$$\frac{\partial u}{\partial \boldsymbol{\nu}} = g_N \quad \text{on } \Gamma_N, \quad (3.57c)$$

$$\frac{\partial u}{\partial \boldsymbol{\nu}} = \frac{1}{\varepsilon}(u - g_D) + g_N \quad \text{on } \Gamma_R. \quad (3.57d)$$

In the examples presented here, we let Ω^- be the unit sphere or unit cube, and Γ its boundary. In the computations presented for the sphere, a series of approximations of the sphere by plane triangles are used.

To simplify the identification of the plots in this section, we follow a consistent labelling convention: plots for Dirichlet problems are shown in red, plots for mixed Dirichlet–Neumann problems are shown in blue, and plots for Robin problems are shown in green. Plots for methods shown for comparison are shown in grey. Additionally, at the top right corner of each plot either a cube or a sphere is drawn to indicate whether the plot shows results for the problem on the unit cube or the unit sphere.

— 3.3.1 —

DIRICHLET BOUNDARY CONDITIONS

First, we look at the case where $\Gamma = \Gamma_D$, in which the problem reduces to the Dirichlet problem:

$$-\Delta u = 0 \quad \text{in } \Omega^-, \quad (3.58a)$$

$$u = g_D \quad \text{on } \Gamma. \quad (3.58b)$$

For this problem, we compare the penalty method proposed in this chapter (3.42) to

the standard single layer formulation: Find $\lambda \in H^{-1/2}(\Gamma)$ such that

$$\langle \mathbf{V}\lambda, \mu \rangle_{\Gamma} = \langle (\tfrac{1}{2}\text{Id} + \mathbf{K})g_{\mathbf{D}}, \mu \rangle_{\Gamma} \quad \forall \mu \in H^{-1/2}(\Gamma), \quad (3.59)$$

discretised using the same space that λ_h is sought in in the penalty method

Figure 3.1 shows the convergence and iteration counts when $\beta_{\mathbf{D}} = 0.1$ and $k = l = 1$, and so we look for $(u_h, \lambda_h) \in \mathbf{P}_h^1(\Gamma) \times \mathbf{P}_h^1(\Gamma)$. We note that as h decreases, h^{-1} increases, so $0.1 \lesssim h^{-1}$. In the error plot (left), it can be seen that the penalty method proposed here gives comparable convergence to the standard method in a similar number of iterations. However, the system in the penalty method contains around twice the number of unknowns, and so each iteration will be more expensive.

The iteration count plot (right) shows the number of iterations taken to solve the non-preconditioned system (red diamonds), compared with the system with mass matrix preconditioning applied blockwise from the left (red circles). Mass matrix preconditioning greatly reduces the number of iterations required, and will be discussed in more detail in chapter 2. For the remainder of this chapter, we precondition all linear systems using mass matrix preconditioning.

For larger and more complex geometries, however, more specialised preconditioners are required. With systems of boundary element equations, it is common to use operator preconditioning or Calderón preconditioning [75, 16], where properties of the boundary operators at the continuous level are used to derive a preconditioned equation of a form known to be well conditioned. Calderón preconditioning for Maxwell problems is discussed in more detail in chapter 2. For the methods described in this chapter, it is not clear how to apply this approach, although further investigation of this warrants future work.

An alternative avenue of investigation leads to hierarchical LU based preconditioners, or even direct solvers of this type [7]. The penalty terms in this chapter are all sparse matrices that have non-zero entries only for neighbouring triangles, and so adding these terms only affects the entries in the matrix arising from near interactions; the far interactions—which are exactly those that are approximated in a hierarchical matrix (H-matrix) compression—are not affected by these terms. Therefore H-matrix methods can be applied to this method with few algorithmic changes required.

Figure 3.2 shows the dependence of the error and iteration count on the chosen value of $\beta_{\mathbf{D}}$, for a range of values of h . It can be seen that for the problem on the sphere, the number of iterations increases when $\beta_{\mathbf{D}}$ is above around 0.1, and the error increases when $\beta_{\mathbf{D}}$ is above 100. This motivates our earlier choice of 0.1 as the value of $\beta_{\mathbf{D}}$, although anything smaller than this appears to be a good choice of $\beta_{\mathbf{D}}$ for these problems.

We now let $k = l + 1 = 1$, and look for $(u_h, \lambda_h) \in \mathbf{P}_h^1(\Gamma) \times \text{DP}_h^0(\Gamma)$ or $(u_h, \lambda_h) \in \mathbf{P}_h^1(\Gamma) \times \text{DUAL}_h^0(\Gamma)$. Figure 3.3 shows the convergence and iteration counts in this case when $\beta_{\mathbf{D}} = 0.1$.

If we look for $(u_h, \lambda_h) \in \mathbf{P}_h^1(\Gamma) \times \text{DP}_h^0(\Gamma)$ (red squares) for the problem on the cube, we initially see the expected order $\frac{3}{2}$ convergence. This convergence however tails off

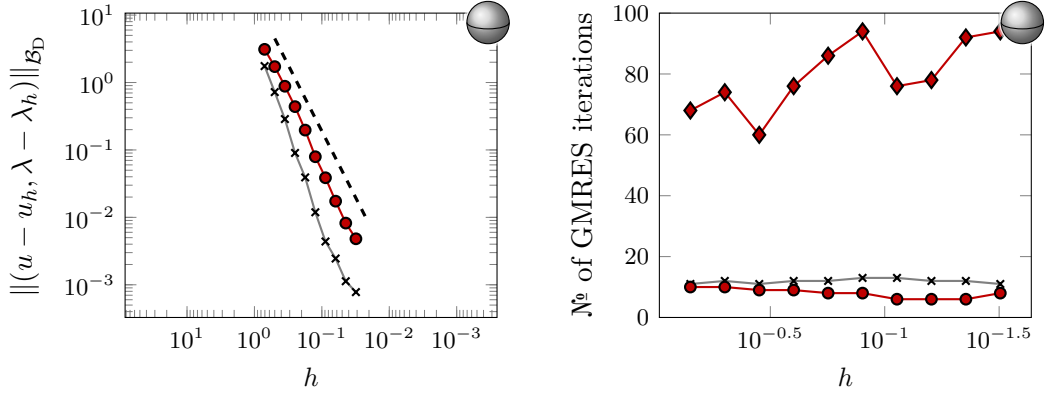


Figure 3.1: The convergence (left) and GMRES iteration counts (right) of the penalty method with $\beta_D = 0.1$ (red circles) compared to the standard single layer method (3.59) (grey crosses), for the Dirichlet problem on the unit sphere, with $(u_h, \lambda_h), (v_h, \mu_h) \in P_h^1(\Gamma) \times P_h^1(\Gamma)$. The iteration count plot shows the number of iterations taken to solve the mass matrix preconditioned system (red circles) and the non-preconditioned system (red diamonds). The dashed line shows order 2 convergence.

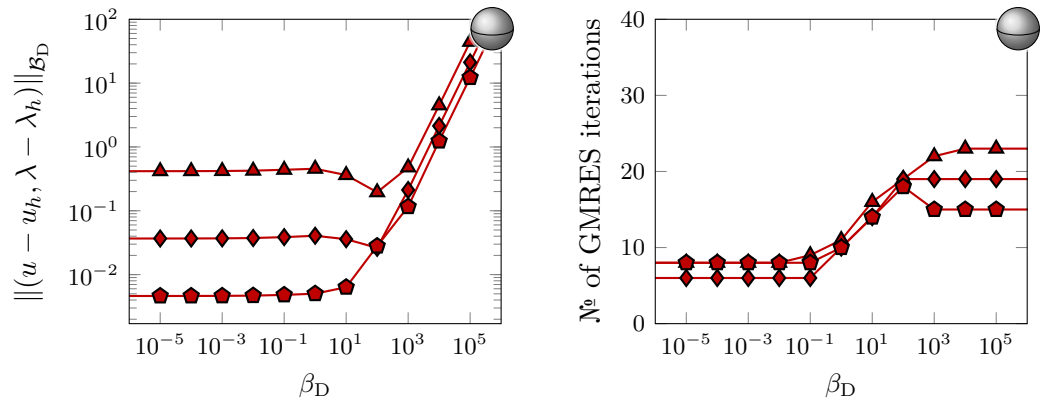


Figure 3.2: The dependence of the error (left) and iteration count (right) on the value of β_D for $h = 2^{-2}$ (red triangles), $h = 2^{-3.5}$ (red diamonds), and $h = 2^{-5}$ (red pentagons), for the Dirichlet problem on the unit sphere, with $(u_h, \lambda_h), (v_h, \mu_h) \in P_h^1(\Gamma) \times P_h^1(\Gamma)$.

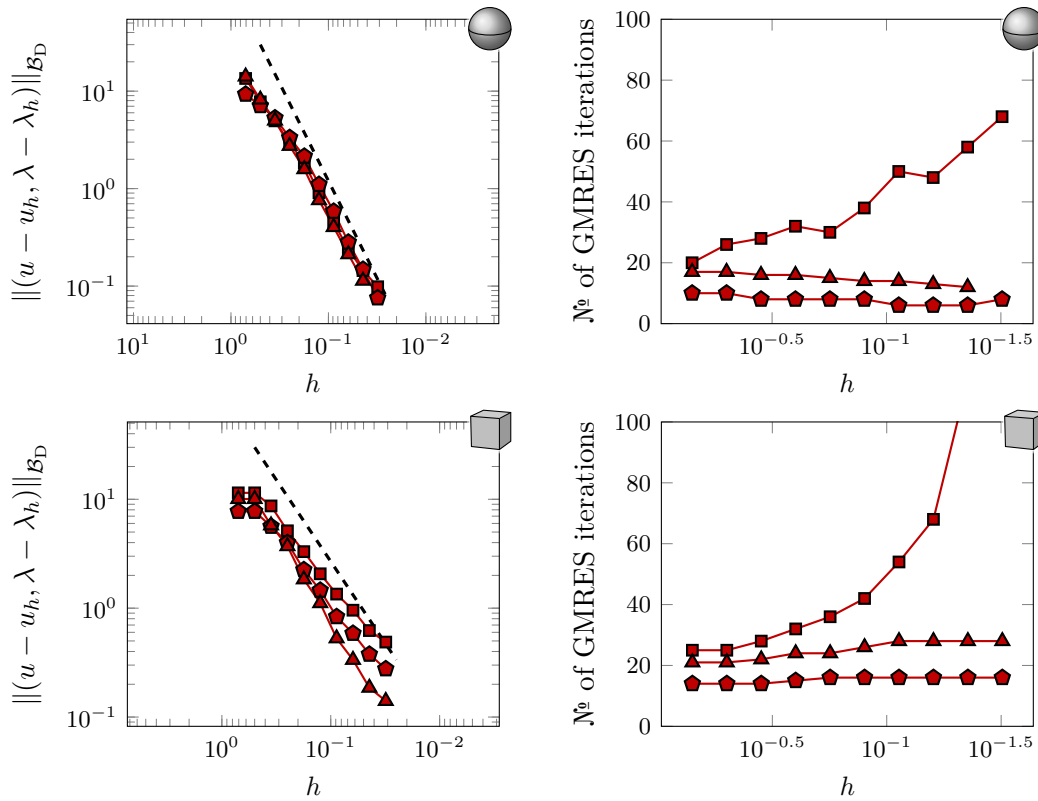


Figure 3.3: The convergence (left) and GMRES iteration counts (right) of the penalty method with $\beta_D = 0.1$ for the Dirichlet problem on the unit sphere (top) and cube (bottom), with $(u_h, \lambda_h), (v_h, \mu_h) \in P_h^1(\Gamma) \times DP_h^0(\Gamma)$ (red squares); $(u_h, \lambda_h), (v_h, \mu_h) \in P_h^1(\Gamma) \times DUAL_h^0(\Gamma)$ (red pentagons); and $(u_h, \lambda_h) \in P_h^1(\Gamma) \times DP_h^0(\Gamma)$ and $(v_h, \mu_h) \in DUAL_h^1(\Gamma) \times DUAL_h^0(\Gamma)$ (red triangles). The dashed lines show order 2 (top) and order $\frac{3}{2}$ (bottom) convergence.

as the linear system becomes more ill-conditioned, as evidenced by the rapidly increasing iteration count. For this choice of spaces, applying the mass matrix preconditioner involves inverting the non inf-sup stable $P_h^1(\Gamma)$ – $DP_h^0(\Gamma)$ pairing, leading to the preconditioner being ineffective and the ill-conditioning that we observe.

If we instead look for $(u_h, \lambda_h) \in P_h^1(\Gamma) \times DUAL_h^0(\Gamma)$ (red pentagons) for the problem on the cube, we obtain a better conditioned system, as the mass matrix preconditioner is based on the inf-sup stable $P_h^1(\Gamma)$ – $DUAL_h^0(\Gamma)$ pairing, but we see a lower order of convergence due to the lower order approximation result in lemma 2.4.

We can, however, obtain a well conditioned system that exhibits order $\frac{3}{2}$ convergence by looking for $(u_h, \lambda_h) \in P_h^1(\Gamma) \times DP_h^0(\Gamma)$ and testing with $(v_h, \mu_h) \in DUAL_h^1(\Gamma) \times DUAL_h^0(\Gamma)$. These choices mean that assumption 3.4 holds, as this only requires approximation results on the spaces in which we look for u_h and λ_h , while ensuring that all the dual pairings involved are the stable $P_h^1(\Gamma)$ – $DUAL_h^0(\Gamma)$ and $DP_h^0(\Gamma)$ – $DUAL_h^1(\Gamma)$ pairings. The order $\frac{3}{2}$ convergence obtained using this choice of spaces can be seen in figure 3.3 (red triangles). In what follows, we will only consider this choice of spaces for problems on the cube.

Figure 3.4, shows the error and iteration counts for the penalty-free method that can be derived by taking $\beta_D = 0$. In agreement with theorem 3.1, we see that the penalty-free

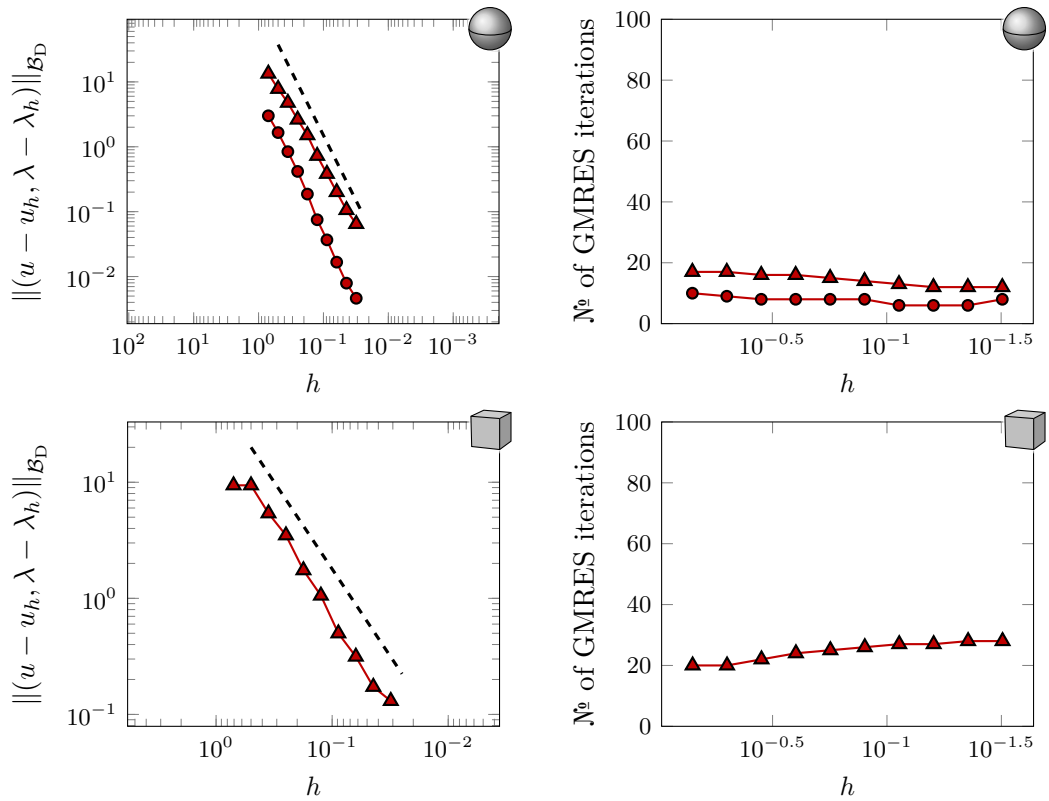


Figure 3.4: The convergence (left) and GMRES iteration counts (right) penalty-free method for the Dirichlet problem on the unit sphere (top) and cube (bottom), with $(u_h, \lambda_h), (v_h, \mu_h) \in P_h^1(\Gamma) \times P_h^1(\Gamma)$ (red circles); and $(u_h, \lambda_h) \in P_h^1(\Gamma) \times DP_h^0(\Gamma)$ and $(v_h, \mu_h) \in DUAL_h^1(\Gamma) \times DUAL_h^0(\Gamma)$ (red triangles). The dashed lines show order 2 (top) and order $\frac{3}{2}$ (bottom) convergence.

method converges at the same rate as the penalty method.

When discussing figure 3.1, we noted that although the penalty method has comparable convergence and a similar number of iterations to the standard method, the cost of each iteration will be higher. Additionally, the discrete systems for the penalty method are non-symmetric, so are solved using GMRES [66]. The discrete systems for the standard method (3.59) are symmetric, so CG [43] or MINRES [62] could be used: these methods are typically less expensive than GMRES. Overall, the penalty method is unlikely to be competitive for pure Dirichlet and Neumann problems.

— 3.3.2 —

MIXED DIRICHLET–NEUMANN BOUNDARY CONDITIONS

We now consider the case where $\Gamma = \Gamma_D \cup \Gamma_N$ and the problem reduces to a mixed Dirichlet–Neumann problem:

$$-\Delta u = 0 \quad \text{in } \Omega^-, \quad (3.60a)$$

$$u = g_D \quad \text{on } \Gamma_D, \quad (3.60b)$$

$$\frac{\partial u}{\partial \boldsymbol{\nu}} = g_N \quad \text{on } \Gamma_N. \quad (3.60c)$$

For the problem on the sphere, let $\Gamma_N := \{(x, y, z) \in \Gamma : x > 0\}$ and $\Gamma_D := \Gamma \setminus \Gamma_N$. For the problem on the cube, let $\Gamma_N := \{(x, y, z) \in \Gamma : z = 1\}$ and $\Gamma_D := \Gamma \setminus \Gamma_N$. We use the same g_D and g_N as above.

We compare the method proposed in this chapter with the standard method for mixed Dirichlet–Neumann problems [77, equation (3.2)]: Find $(u, \lambda) \in \tilde{H}^{1/2}(\Gamma_N) \times \tilde{H}^{-1/2}(\Gamma_D)$ such that

$$\begin{aligned} & \langle \mathbf{W}_{NN}u, v \rangle_\Gamma + \langle \mathbf{K}'_{DN}\lambda, v \rangle_\Gamma - \langle \mathbf{K}_{ND}u, \mu \rangle_\Gamma + \langle \mathbf{V}_{DD}\lambda, \mu \rangle_\Gamma \\ & = - \langle \mathbf{W}_{DN}g_D, v \rangle_\Gamma + \langle (\tfrac{1}{2}\text{Id} - \mathbf{K}'_{NN})g_N, v \rangle_\Gamma + \langle (\tfrac{1}{2}\text{Id} + \mathbf{K}_{DD})g_D, \mu \rangle_\Gamma - \langle \mathbf{V}_{ND}g_N, \mu \rangle_\Gamma \\ & \quad \forall (v, \mu) \in \tilde{H}^{1/2}(\Gamma_N) \times \tilde{H}^{-1/2}(\Gamma_D), \end{aligned} \quad (3.61)$$

where for a given boundary operator \mathbf{B} , \mathbf{B}_{ij} is the corresponding boundary operator with the integral taken over Γ_i and the point $\mathbf{x} \in \Gamma_j$. For example, \mathbf{V}_{ND} is defined by

$$[\mathbf{V}_{ND}f](\mathbf{x}) := \int_{\Gamma_N} f(\mathbf{y})G(\mathbf{x}, \mathbf{y}) \, d\mathbf{y} \quad \text{for } \mathbf{x} \in \Gamma_D. \quad (3.62)$$

We first let $k = l + 1 = 1$, and so look for $(u_h, \lambda_h) \in \mathbf{P}_h^1(\Gamma) \times \mathbf{DP}_h^0(\Gamma)$ or $\mathbf{P}_h^1(\Gamma) \times \mathbf{DUAL}_h^0(\Gamma)$. As motivated above by proposition 3.13, we set $\beta_D = \beta h^{-1}$ and $\beta_N = \beta h$, where β is a constant. The dependence of the error and iteration count on β is shown in figure 3.5. We observe that $\beta = 0.01$ is a reasonable choice for both problems, as this gives a small error and iteration count.

The convergence to the solution as we reduce h is shown in figure 3.6. On the both the sphere and the cube, we observe order 1.5 convergence when using spaces defined on the dual grid, the same rate of convergence as the standard method (3.61). We see that the iteration counts for the penalty method with $(u_h, \lambda_h), (v_h, \mu_h) \in \mathbf{P}_h^1(\Gamma) \times \mathbf{DP}_h^0(\Gamma)$ and the standard method both increase as h is reduced. When $(u_h, \lambda_h), (v_h, \mu_h) \in \mathbf{P}_h^1(\Gamma) \times \mathbf{DUAL}_h^0(\Gamma)$ (blue pentagons) or $(u_h, \lambda_h) \in \mathbf{P}_h^1(\Gamma) \times \mathbf{DP}_h^0(\Gamma)$ and $(v_h, \mu_h) \in \mathbf{DUAL}_h^1(\Gamma) \times \mathbf{DUAL}_h^0(\Gamma)$ (blue triangles), the iteration count remains low as h is reduced, and again we see the benefit of the stable dual pairing.

We next consider the case where $k = l = 1$. In this case, as remarked in section 3.2.3,

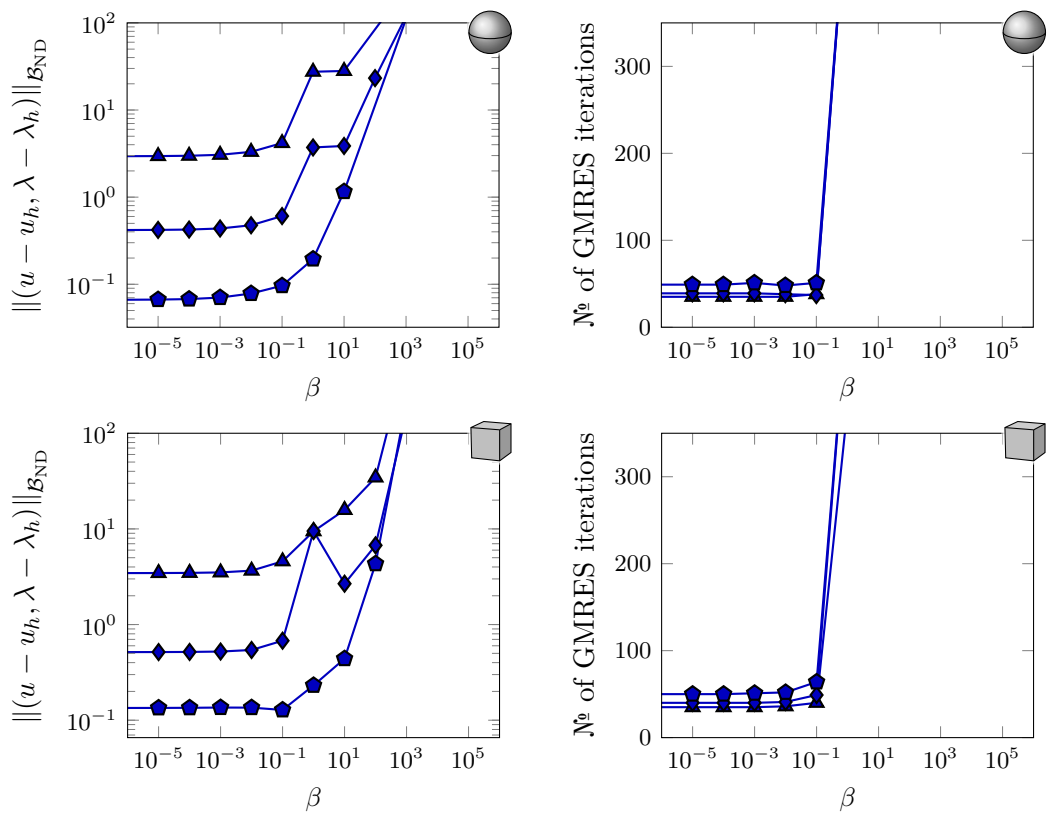


Figure 3.5: The dependence of the error (left) and iteration count (right) on the value of β for $h = 2^{-2}$ (blue triangles), $h = 2^{-3.5}$ (blue diamonds), and $h = 2^{-5}$ (blue pentagons), for the mixed Dirichlet–Neumann problem on the unit sphere (top) and unit cube (bottom), with $(u_h, \lambda_h) \in \mathbf{P}_h^1(\Gamma) \times \mathbf{DF}_h^0(\Gamma)$ and $(v_h, \mu_h) \in \mathbf{DUAL}_h^1(\Gamma) \times \mathbf{DUAL}_h^0(\Gamma)$. Here we use $\beta_{\text{D}} = \beta h^{-1}$ and $\beta_{\text{N}} = \beta h$.

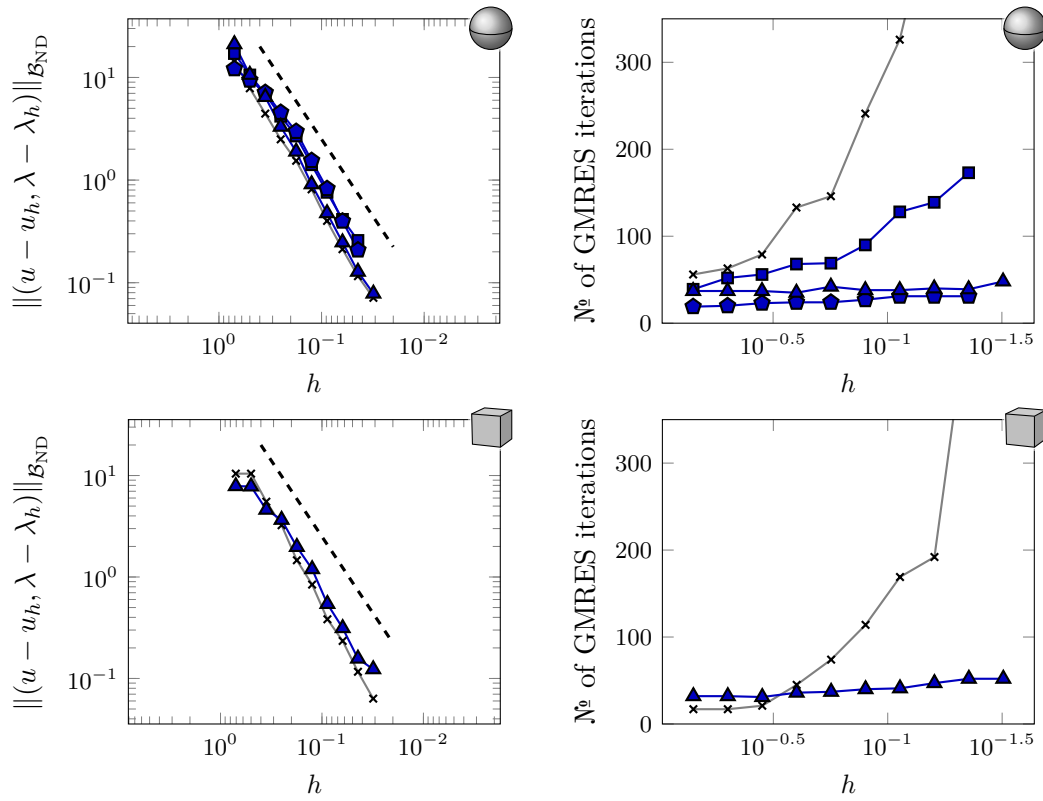


Figure 3.6: The convergence (left) and iterations counts (right) of the penalty method with $\beta = 0.01$ (blue) compared to the standard method (3.61) (grey crosses), for the mixed Dirichlet–Neumann problem on the unit sphere (top) and the unit cube (bottom), with $(u_h, \lambda_h), (v_h, \mu_h) \in P_h^1(\Gamma) \times DP_h^0(\Gamma)$ (blue squares); $(u_h, \lambda_h), (v_h, \mu_h) \in P_h^1(\Gamma) \times \text{DUAL}_h^0(\Gamma)$ (blue pentagons); and $(u_h, \lambda_h) \in P_h^1(\Gamma) \times DP_h^0(\Gamma)$ and $(v_h, \mu_h) \in \text{DUAL}_h^1(\Gamma) \times \text{DUAL}_h^0(\Gamma)$ (blue triangles). The dashed lines show order $\frac{3}{2}$ convergence. Here we use $\beta_{\text{D}} = \beta h^{-1}$ and $\beta_{\text{N}} = \beta h$.

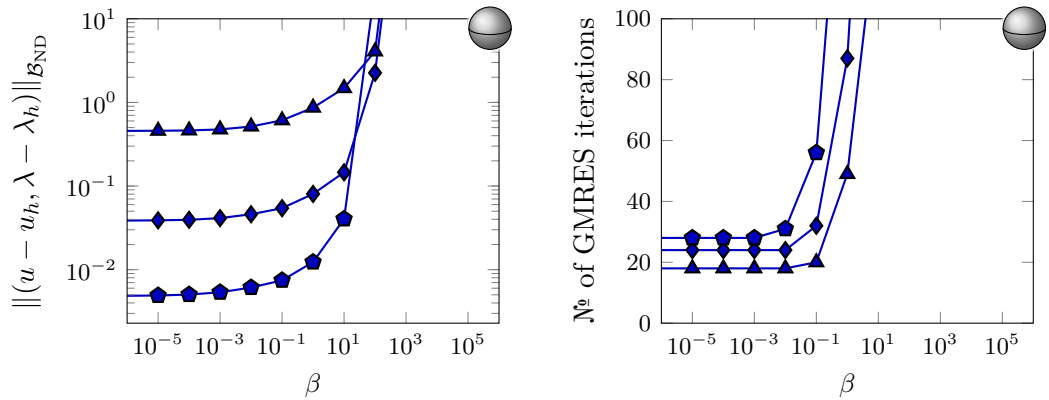


Figure 3.7: The dependence of the error (left) and iteration count (right) on the value of β for $h = 2^{-2}$ (blue triangles), $h = 2^{-3.5}$ (blue diamonds), and $h = 2^{-5}$ (blue pentagons), for the mixed Dirichlet–Neumann problem on the unit sphere, with $(u_h, \lambda_h), (v_h, \mu_h) \in P_h^1(\Gamma) \times P_h^1(\Gamma)$. Here we use $\beta_D = \beta_N = \beta$.

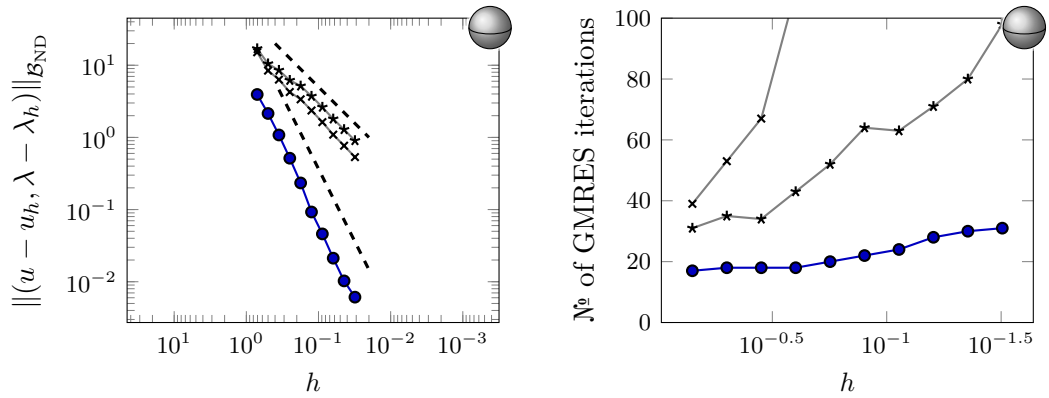


Figure 3.8: The convergence (left) and iterations counts (right) of the penalty method with $\beta = 0.01$ (blue circles) compared to the standard method (3.61) (grey crosses) and the method given in [32, equation (1.19)] (grey stars), for the mixed Dirichlet–Neumann problem on the unit sphere, with $(u_h, \lambda_h), (v_h, \mu_h) \in P_h^1(\Gamma) \times P_h^1(\Gamma)$. The dashed lines show order 2 and order 1 convergence. Here we use $\beta_D = \beta_N = \beta$.

we may replace the bound on β_N by $\beta_N \lesssim h^{-1}$, and so we may take both β_D and β_N to be constant: we set $\beta_D = \beta_N = \beta$. The dependence of the error and iteration count on β for this choice of parameters is shown in figure 3.7.

The convergence to the solution when $\beta = 0.01$ is shown in figure 3.8. It can be seen here that order 2 convergence is observed on the sphere, higher than the expected order 1.5 convergence, while the standard method (3.61) only achieves order 1 convergence when using $P_h^1(\Gamma)$ spaces. Additionally, the standard method requires more iterations than the penalty method. For this choice of discrete spaces, we also compared our method with the formulation given in [32, equation (1.19)]: this formulation is better conditioned than (3.61) but still achieves only order 1 convergence, and has a slightly higher error.

In figures 3.5 and 3.8, the error and iteration count remain steady as $\beta \rightarrow 0$. Figure 3.9 shows the error and iterations counts for the penalty-free method derived by setting $\beta = 0$. Here we see similar convergence to that observed for the penalty method. This leads us to conjecture that theorem 3.3 will hold when $\beta = 0$.

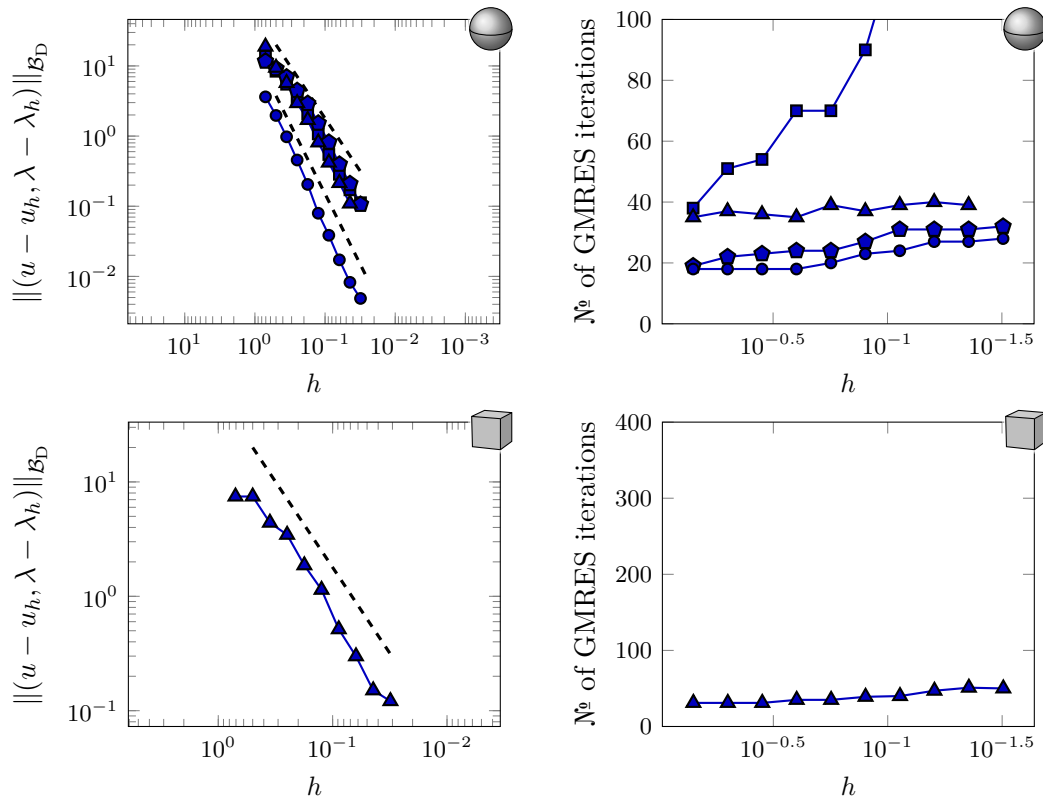


Figure 3.9: The convergence (left) and GMRES iteration counts (right) of the penalty-free method for the mixed Dirichlet–Neumann problem on the unit sphere (top) and cube (bottom), with $(u_h, \lambda_h), (v_h, \mu_h) \in P_h^1(\Gamma) \times P_h^1(\Gamma)$ (blue circles), $(u_h, \lambda_h), (v_h, \mu_h) \in P_h^1(\Gamma) \times DP_h^0(\Gamma)$ (blue squares), and $(u_h, \lambda_h), (v_h, \mu_h) \in P_h^1(\Gamma) \times DUAL_h^0(\Gamma)$ (blue pentagons) and $(u_h, \lambda_h) \in P_h^1(\Gamma) \times DP_h^0(\Gamma)$ and $(v_h, \mu_h) \in DUAL_h^1(\Gamma) \times DUAL_h^0(\Gamma)$ (blue triangles). The dashed lines show order 2 (top only) and order $\frac{3}{2}$ (both) convergence.

— 3.3.3 —

ROBIN BOUNDARY CONDITIONS

We now consider the case where $\Gamma = \Gamma_R$ and the problem reduces to a Robin problem:

$$-\Delta u = 0 \quad \text{in } \Omega^-, \quad (3.63a)$$

$$\frac{\partial u}{\partial \boldsymbol{\nu}} = \frac{1}{\varepsilon}(u - g_D) + g_N \quad \text{on } \Gamma, \quad (3.63b)$$

for some $\varepsilon \in \mathbb{R}$.

In this section, we compare the method proposed in this chapter with the method: Find $u \in H^{1/2}(\Gamma)$ such that

$$\langle \mathbb{W}u, v \rangle_\Gamma + \left\langle \frac{1}{\varepsilon} \left(\frac{1}{2} \text{Id} - \mathbf{K}' \right) u, v \right\rangle_\Gamma = \left\langle \left(\frac{1}{2} \text{Id} - \mathbf{K}' \right) \left(\frac{1}{\varepsilon} g_D + g_N \right), v \right\rangle_\Gamma \quad \forall v \in H^{1/2}(\Gamma). \quad (3.64)$$

Again, we begin letting $k = l + 1 = 1$. Here we use

$$\beta_R := \frac{\varepsilon \beta_N + \beta_D}{\varepsilon + 1},$$

where $\beta_D = \beta h^{-1}$ and $\beta_N = \beta h$, for some constant β , as in the mixed Dirichlet–Neumann case.

The dependence of the error and iteration count on both ε and β , on a grid with $h = 0.1$, is shown in figure 3.10. We see here that there are conditioning issues for a range of values ε when we look for $(u_h, \lambda_h) \in P_h^1(\Gamma) \times \text{DP}_h^0(\Gamma)$ and take $(v_h, \mu_h) \in P_h^1(\Gamma) \times \text{DP}_h^0(\Gamma)$ or $\text{DUAL}_h^1(\Gamma) \times \text{DUAL}_h^0(\Gamma)$. When β is small (but not too small), this ill-conditioning can be mostly avoided.

The convergence as h is reduced for $\varepsilon = \frac{1}{300}$, $\varepsilon = 1$, and $\varepsilon = 300$, and using $\beta = 0.01$, is shown in figure 3.11. In this case, order $\frac{3}{2}$ convergence is observed. Again, we see that when taking $(u_h, \lambda_h), (v_h, \mu_h) \in P_h^1(\Gamma) \times \text{DP}_h^0(\Gamma)$, the number of iterations grows as h is decreased, but when using the stable dual space pairing the number of iterations required remains low.

As in the mixed Dirichlet–Neumann case, when $k = l = 1$, we may replace the bound on β_N with $\beta_N \lesssim h^{-1}$ and we take $\beta_D = \beta_N = \beta$ for some constant β . The dependence of the error and iteration count on both β and ε is shown in figure 3.12. As in the previous case, $\beta = 0.01$ looks to be a suitable choice for the parameter.

The convergence as we reduce h for $\varepsilon = \frac{1}{300}$, $\varepsilon = 1$, and $\varepsilon = 300$, and using $\beta = 0.01$, is shown in figure 3.13. In this case, order 2 convergence is observed. For the method (3.64), the same order of convergence and errors of almost identical size are observed on the sphere. For the method (3.64), the number of iterations required to solve the system grows gradually as we reduce h . For the penalty method, the number of iterations remains close to constant.

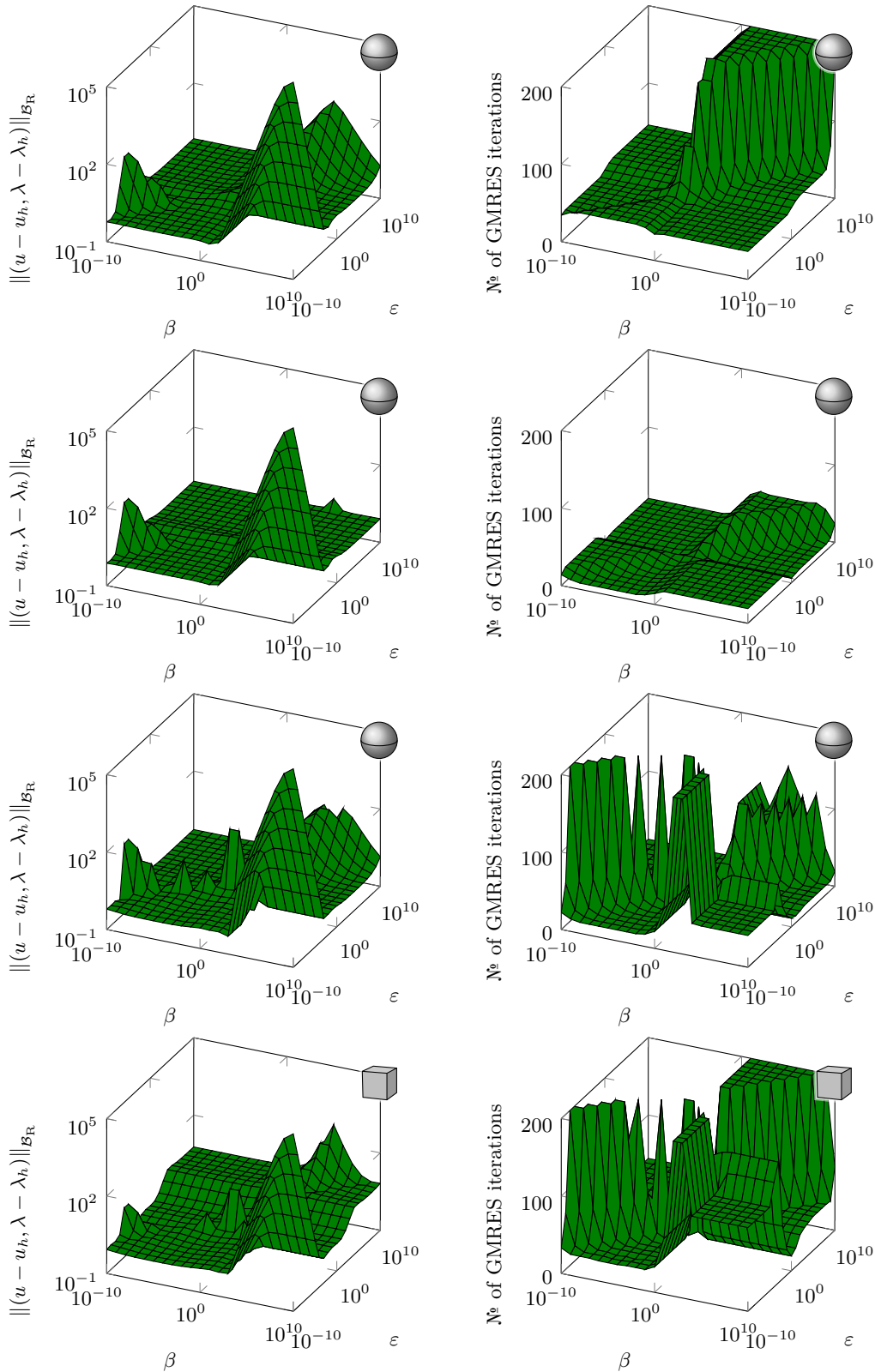


Figure 3.10: The dependence of the error on ε and β for the Robin problem on the unit sphere (first three rows) and unit cube (final row) with $h = 0.1$, with $(u_h, \lambda_h), (v_h, \mu_h) \in P_h^1(\Gamma) \times DP_h^0(\Gamma)$ (top row); $(u_h, \lambda_h), (v_h, \mu_h) \in P_h^1(\Gamma) \times DUAL_h^0(\Gamma)$ (second row); and $(u_h, \lambda_h) \in P_h^1(\Gamma) \times DP_h^0(\Gamma)$ and $(v_h, \mu_h) \in DUAL_h^1(\Gamma) \times DUAL_h^0(\Gamma)$ (final two rows). Here we use $\beta_D = \beta h^{-1}$ and $\beta_N = \beta h$.

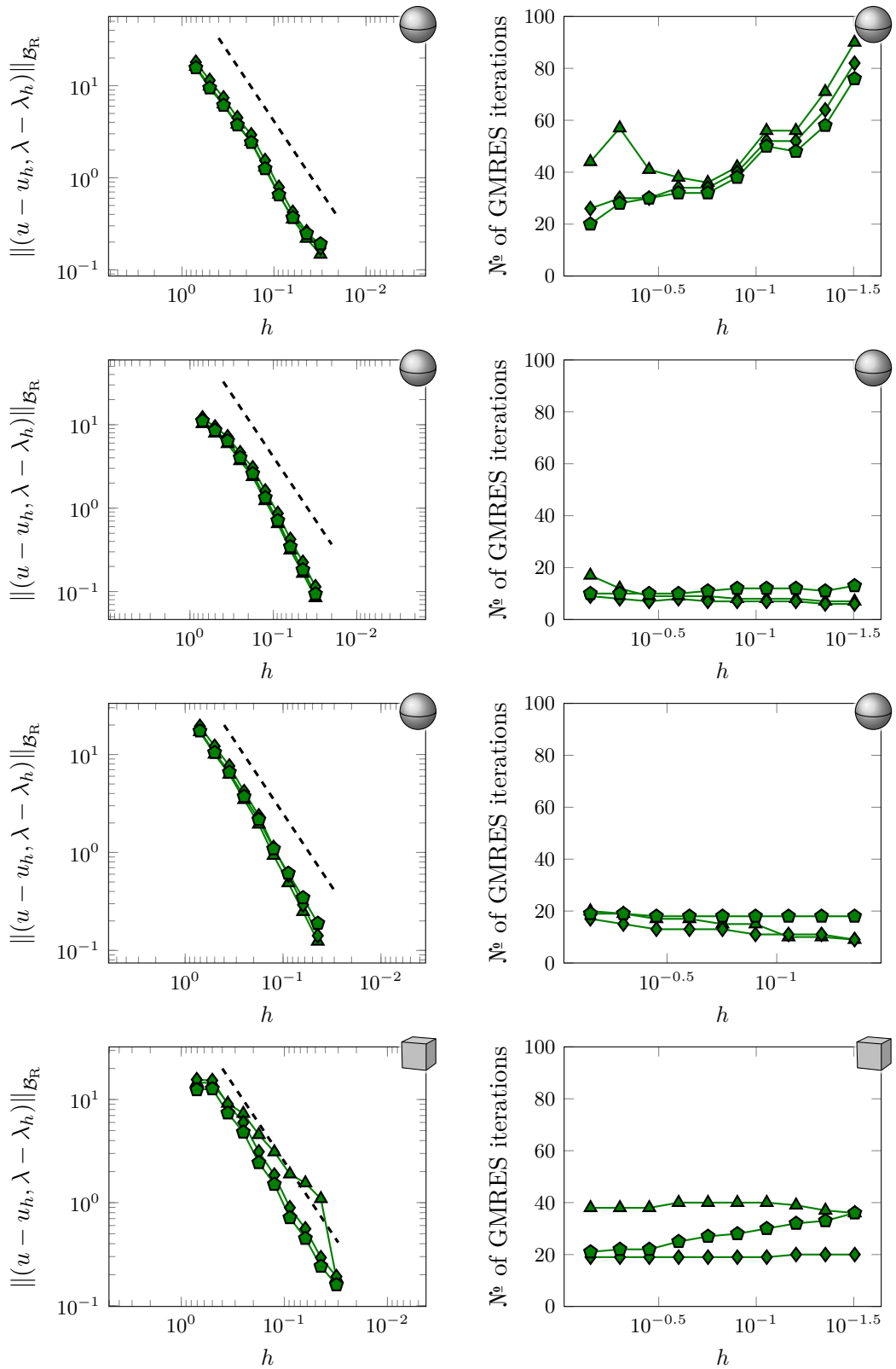


Figure 3.11: The convergence (left) and iteration counts (right) of the penalty method with $\beta = 0.01$ for the Robin problem with $\varepsilon = 300$ (green triangles), $\varepsilon = 1$ (green diamonds) and $\varepsilon = 1/300$ (green pentagons) on the unit sphere (first three rows) and the unit cube (final row), with $(u_h, \lambda_h), (v_h, \mu_h) \in P_h^1(\Gamma) \times DP_h^0(\Gamma)$ (top row); $(u_h, \lambda_h), (v_h, \mu_h) \in P_h^1(\Gamma) \times DUAL_h^0(\Gamma)$ (second row); and $(u_h, \lambda_h) \in P_h^1(\Gamma) \times DP_h^0(\Gamma)$ and $(v_h, \mu_h) \in DUAL_h^1(\Gamma) \times DUAL_h^0(\Gamma)$ (final two rows). The dashed lines show order $\frac{3}{2}$ convergence. Here we use $\beta_D = \beta h^{-1}$ and $\beta_N = \beta h$.

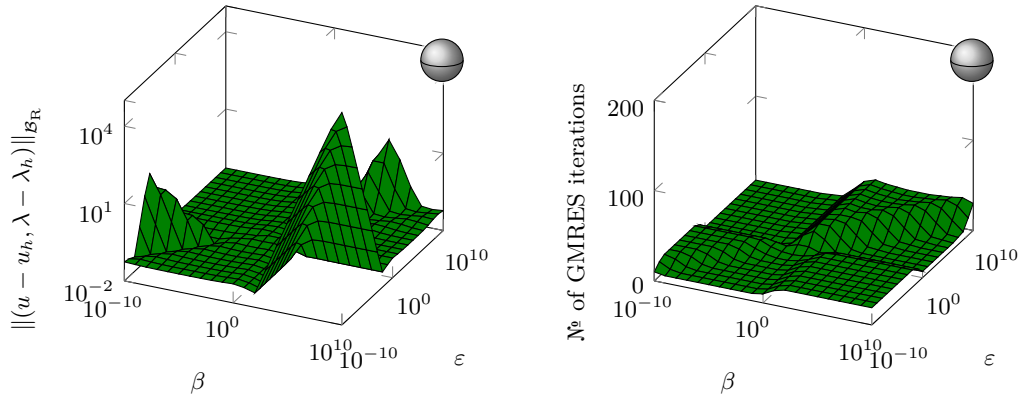


Figure 3.12: The dependence of the error on ϵ and β for the Robin problem on the unit sphere (top) and the unit cube (bottom) with $h = 0.1$, with $(u_h, \lambda_h), (v_h, \mu_h) \in P_h^1(\Gamma) \times P_h^1(\Gamma)$. Here we use $\beta_D = \beta_N = \beta$.

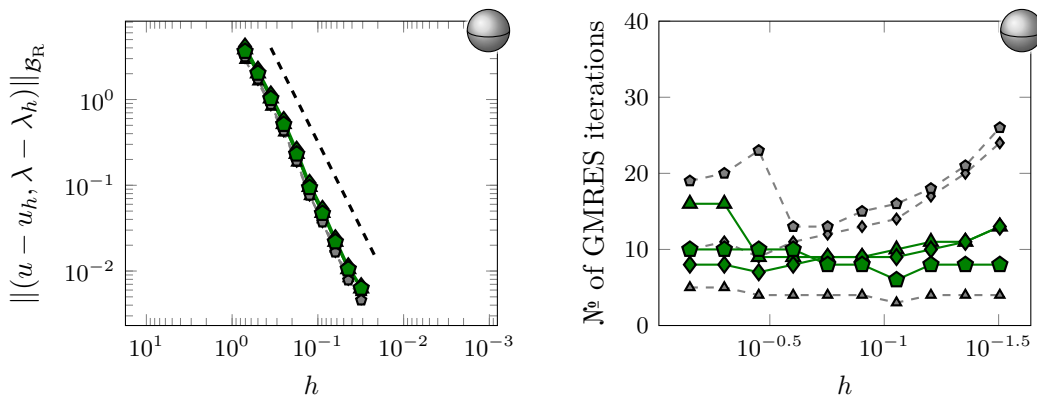


Figure 3.13: The convergence (left) and iteration counts (right) of the penalty method (green) with $\beta = 0.01$ compared to the method (3.64) (grey dashed), for the Robin problem with $\epsilon = 300$ (triangles), $\epsilon = 1$ (diamonds) and $\epsilon = 1/300$ (pentagons) on the unit sphere (top) and the unit cube (bottom), with $(u_h, \lambda_h), (v_h, \mu_h) \in P_h^1(\Gamma) \times P_h^1(\Gamma)$. The dashed line shows order 2 convergence. Here we use $\beta_D = \beta_N = \beta$.

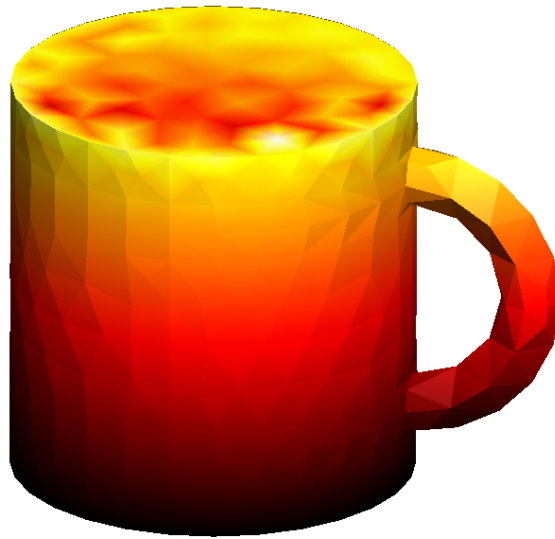


Figure 3.14: The solution, u_h , of a mixed Dirichlet–Neumann problem on the interior of a mug, solved using the penalty method with $\beta = 0.01$, with $(u_h, \lambda_h) \in P_h^1(\Gamma) \times DP_h^0(\Gamma)$ and $(v_h, \mu_h) \in \text{DUAL}_h^1(\Gamma) \times \text{DUAL}_h^0(\Gamma)$. The boundary conditions used are $\frac{\partial u}{\partial \nu} = y$ on the top of the mug and $u(\mathbf{x}) = z$ everywhere else.

Again, we could consider the penalty-free formulation for the Robin problem. However, figures 3.10 and 3.12 suggest that as $\beta \rightarrow 0$, the error increases for some values of ε . This increased error can also be observed in the numerical experiments we have run with $\beta = 0$. Hence in the Robin case, the penalty term is necessary and we expect that theorem 3.4 does not hold for $\beta_R = 0$.

— — —

Now that you’ve finished reading chapter 3, why not take a break and refill figure 3.14 with hot liquid before reading on.

CHAPTER 4

WEAK IMPOSITION OF SIGNORINI
BOUNDARY CONDITIONS

Signorini boundary conditions were first proposed by Antonio Signorini in 1959 [69] and are given by

$$u \leq g_C \quad \text{and} \quad \frac{\partial u}{\partial \nu} \leq \psi_C \quad \text{on } \Gamma_C, \quad (1.37f)$$

$$\left(\frac{\partial u}{\partial \nu} - \psi_C \right) (u - g_C) = 0 \quad \text{on } \Gamma_C. \quad (1.37g)$$

These conditions describe a contact problem, where u is the distance between the object and the obstacle at each point, $\frac{\partial u}{\partial \nu}$ is the force on the object due to contact. (1.37g) states that either $u = g_C$, and so the object's height is the height of the obstacle and there is contact; or $\frac{\partial u}{\partial \nu} = \psi_C$, and so the only force on the object is the background force (eg gravity) and there is no contact. (1.37f) ensures that the object cannot penetrate the obstacle and the contact force cannot be negative.

In this chapter, we focus on solving an interior Laplace problem with mixed Dirichlet–Signorini boundary conditions: Find $u \in H^1(\Delta, \Omega^-)$ such that

$$-\Delta u = 0 \quad \text{in } \Omega^-, \quad (1.37a)$$

$$u = g_D \quad \text{on } \Gamma_D, \quad (1.37c)$$

$$u \leq g_C \quad \text{and} \quad \frac{\partial u}{\partial \nu} \leq \psi_C \quad (1.37f)$$

$$\text{and} \quad \left(\frac{\partial u}{\partial \nu} - \psi_C \right) (u - g_C) = 0 \quad \text{on } \Gamma_C. \quad (1.37g)$$

We assume that $g_D \in H^{3/2}(\Gamma_D)$, $g_C \in H^{1/2}(\Gamma_C)$, and $\psi_C \in H^{-1/2}(\Gamma_C)$.

Observe that when $\Gamma_C = \emptyset$, there exists a unique solution to (1.37) by the Lax–Milgram lemma, and that $u \in H^{3/2+\epsilon}(\Omega^-)$ for some $\epsilon > 0$. In the case that $\text{meas}(\Gamma_C) > 0$, the theory of Lions and Stampacchia [53] for variational inequalities yields existence and uniqueness of solutions with the same regularity.

The application of Nitsche techniques based on FEM to deal with variational inequalities has received increasing interest recently, starting from a series of works by Chouly, Hild and Renard for elasticity problems with contact [25]. Their approach goes back to an augmented Lagrangian formulation, that has first been introduced by Alart and Curnier

[1].

Boundary element methods for Signorini type problems have first been studied by Han [41]. A variational formulation involving the Calderón projector has been presented in [42]. An alternative formulation is based on Steklov–Poincaré operators [74, 84]. The numerical approaches to solve such formulations include a penalty formulation [67], operator splitting techniques [71, 85] or semi-smooth Newton methods [74, 84]. The latter reference includes besides the usual energy norm estimates an $L^2(\Gamma)$ -error estimate based on a duality argument. Maischak and Stephan [54] presented *a posteriori* error estimates and an *hp*-adaptive algorithm for the Signorini problem. Recently, an augmented Lagrangian approach has been presented in combination with a semi-smooth Newton method [84].

In this chapter, we look at how the Nitsche-inspired method of weakly imposing boundary conditions on BEM, as proposed in chapter 3, can be extended to problems such as this. We will show how we may use arguments similar to those of Chouly, Hild and Renard [25, 26] to impose Signorini conditions seamlessly. The result is a nonlinear system to which one may apply Newton’s method or a fixed-point iteration in a straightforward manner. We prove existence and uniqueness of solutions to the nonlinear system and optimal order error estimates.

This chapter is based on the material in [21].

— 4.1 —

WEAK IMPOSITION OF SIGNORINI BOUNDARY CONDITIONS ON LAPLACE’S EQUATION

In this section, we derive formulations for an interior Laplace problem with mixed Dirichlet–Signorini boundary conditions. We follow the same approach as in chapter 3: we write the boundary condition in the form

$$R_\Gamma(u, \lambda) = 0, \tag{4.2}$$

and add a suitably weighted version of this to the multitrace equation (3.5) to obtain an equation of the form

$$\mathcal{A}[(u, \lambda), (v, \mu)] = \frac{1}{2} \langle u, \mu \rangle_\Gamma + \frac{1}{2} \langle \lambda, v \rangle_\Gamma + \langle R_\Gamma(u, \lambda), \beta_1 v + \beta_2 \mu \rangle_\Gamma. \tag{3.8}$$

To quantify the two traces we introduce the product space

$$\mathbb{V} := H^{1/2}(\Gamma) \times H^{-1/2}(\Gamma) \tag{4.3}$$

and the associated norm

$$\|(v, \mu)\|_{\mathbb{V}} := \|v\|_{H^{1/2}(\Gamma)} + \|\mu\|_{H^{-1/2}(\Gamma)}. \quad (4.4)$$

— 4.1.1 —

SIGNORINI BOUNDARY CONDITIONS

For the derivation of the formulation on the contact boundary, we will first omit the Dirichlet part and let $\Gamma = \Gamma_C$. To impose the contact conditions, we will use the following relations, introduced by Alart and Curnier [1], with $[x]_{\pm} := \pm \max(0, \pm x)$.

$$(u - g_C) = [(u - g_C) - \tau^{-1}(\lambda - \psi_C)]_- \quad \text{on } \Gamma_C, \quad (4.5)$$

$$(\lambda - \psi_C) = -[\tau(u - g_C) - (\lambda - \psi_C)]_+ \quad \text{on } \Gamma_C, \quad (4.6)$$

for all $\tau > 0$. It is straightforward [25] to show that each of these two conditions is equivalent to the contact boundary conditions (1.37f) and (1.37g).

To simplify the notation, we introduce the operators

$$P^\tau(u, \lambda) := \tau(u - g_C) - (\lambda - \psi_C), \quad (4.7)$$

$$P_0^\tau(u, \lambda) := \tau u - \lambda. \quad (4.8)$$

Using (4.5), we arrive at the following boundary term for the contact conditions

$$R_{\Gamma_C}^1(u, \lambda) = (g_C - u) + \tau^{-1} [P^\tau(u, \lambda)]_-. \quad (4.9)$$

Alternatively, by using (4.6), we arrive at the following boundary term

$$R_{\Gamma_C}^2(u, \lambda) = \tau^{-1} ((\psi_C - \lambda) - [P^\tau(u, \lambda)]_+). \quad (4.10)$$

By using the fact that $x = [x]_+ + [x]_-$, it can be shown that (4.9) and (4.10) are equivalent.

Substituting (4.9) into (3.5), and using the weights $\beta_1 = \tau$ and $\beta_2 = 1$, we obtain

$$\begin{aligned} \mathcal{A}[(u, \lambda), (v, \mu)] + \frac{1}{2} \langle \mu, u \rangle_{\Gamma_C} + \langle \tau u - \frac{1}{2} \lambda, v \rangle_{\Gamma_C} - \langle [P^\tau(u, \lambda)]_-, v + \tau^{-1} \mu \rangle_{\Gamma_C} \\ = \langle g_C, \tau v + \mu \rangle_{\Gamma_C}. \end{aligned} \quad (4.11)$$

Using (4.10), we have

$$\begin{aligned} \mathcal{A}[(u, \lambda), (v, \mu)] + \frac{1}{2} \langle \lambda, v \rangle_{\Gamma_C} + \langle \tau^{-1} \lambda - \frac{1}{2} u, \mu \rangle_{\Gamma_C} + \langle [P^\tau(u, \lambda)]_+, v + \tau^{-1} \mu \rangle_{\Gamma_C} \\ = \langle \psi_C, v + \tau^{-1} \mu \rangle_{\Gamma_C}. \end{aligned} \quad (4.12)$$

We see that (4.12) is similar to the non-symmetric version of the method proposed in [26] and (4.11) is similar to the non-symmetric Nitsche formulation for contact discussed

in [22]. As pointed out in the latter reference, the two formulations are equivalent, with the same solutions. In what follows, we focus exclusively on the variant (4.12).

Defining

$$\mathcal{B}_C[(u, \lambda), (v, \mu)] := \frac{1}{2} \langle \lambda, v \rangle_{\Gamma_C} + \langle \tau^{-1} \lambda - \frac{1}{2} u, \mu \rangle_{\Gamma_C} + \langle [P^\tau(u, \lambda)]_+, v + \tau^{-1} \mu \rangle_{\Gamma_C}, \quad (4.13)$$

$$\mathcal{L}_C(v, \mu) := \langle \psi_C, v + \tau^{-1} \mu \rangle_{\Gamma_C}, \quad (4.14)$$

we arrive at the variational formulation: Find $(u, \lambda) \in \mathbb{V}$ such that

$$(\mathcal{A} + \mathcal{B}_C)[(u, \lambda), (v, \mu)] = \mathcal{L}_C(v, \mu) \quad \forall (v, \mu) \in \mathbb{V}. \quad (4.15)$$

— 4.1.2 —

MIXED DIRICHLET AND CONTACT BOUNDARY CONDITIONS

Combining the formulations for the Dirichlet and contact conditions, we arrive at the following formulation for the problem (1.37): Find $(u, \lambda) \in \mathbb{V}$ such that

$$(\mathcal{A} + \mathcal{B}_D + \mathcal{B}_C)[(u, \lambda), (v, \mu)] = \mathcal{L}_D(v, \mu) + \mathcal{L}_C(v, \mu) \quad \forall (v, \mu) \in \mathbb{V},$$

where \mathcal{B}_D , \mathcal{L}_D , \mathcal{B}_C and \mathcal{L}_C are defined in (3.12), (3.13), (4.13) and (4.14).

For discretisation, we use the assumptions and spaces introduced in section 2.3.1. The discrete problem reads: Find $(u_h, \lambda_h) \in \mathbb{V}_h$ such that

$$(\mathcal{A} + \mathcal{B}_D + \mathcal{B}_C)[(u_h, \lambda_h), (v_h, \mu_h)] = \mathcal{L}_D(v_h, \mu_h) + \mathcal{L}_C(v_h, \mu_h) \quad \forall (v_h, \mu_h) \in \mathbb{V}_h. \quad (4.16)$$

— 4.2 —

ANALYSIS OF THE WEAK IMPOSITION OF SIGNORINI BOUNDARY CONDITIONS

In this section, we prove the existence of unique solutions to the nonlinear system of equations (4.16) as well as optimal error estimates.

Let $\mathbb{W} := H^{1/2}(\Gamma) \times (H^{-1/2}(\Gamma) \cap L^2(\Gamma_C))$ and assume that $(u, \lambda) \in \mathbb{W} \cup (H^r(\Gamma) \times H^s(\Gamma))$ for some $r \geq \frac{1}{2}$ and $s \geq -\frac{1}{2}$ solves (1.37).

We define the distance function d_C and norm $\|\cdot\|_*$, for $(v, \mu), (w, \eta) \in \mathbb{W}$, by

$$\begin{aligned} d_C[(v, \mu), (w, \eta)] &:= \|(v - w, \mu - \eta)\|_{\mathcal{B}_D} + \left\| \tau^{-\frac{1}{2}} (\mu - \eta + [P^\tau(v, \mu)]_+ - [P^\tau(w, \eta)]_+) \right\|_{L^2(\Gamma_C)} \\ \|(v, \mu)\|_* &:= \|(v, \mu)\|_{\mathcal{B}_D} + \left\| \tau^{\frac{1}{2}} v \right\|_{L^2(\Gamma_C)} + \left\| \tau^{-\frac{1}{2}} \mu \right\|_{L^2(\Gamma_C)}. \end{aligned}$$

We note that due the appearance of $[\cdot]_+$ in its second term, d_C is not a norm. d_C does provide a bound on the error however, as for all $(v, \mu) \in \mathbb{W}$, $d_C[(v, \mu), (0, 0)] \geq \|(v, \mu)\|_{\mathcal{B}_D} \geq$

$\|(v, \mu)\|_{\mathbb{V}}$. Due to this and the non-linearity of \mathcal{B}_C , the results in section 3.2 must be adapted for this problem.

When proving this section's results, we will use properties of the $[\cdot]_+$ function that are given in the following lemma.

Lemma 4.1. *Let $a, b \in \mathbb{R}$ then there holds*

$$([a]_+ - [b]_+)^2 \leq ([a]_+ - [b]_+) (a - b), \quad (4.17)$$

$$|[a]_+ - [b]_+| \leq |a - b|. \quad (4.18)$$

Proof. For a proof of these well-known properties see eg [25]. \square

We now prove a result that is analagous to assumption 3.1.

Lemma 4.2. *If there is $\beta_{\min} > 0$, independent of h , such that $\beta_D > \beta_{\min}$, then there is $\alpha > 0$ such that for all $(v, \mu), (w, \eta) \in \mathbb{W}$,*

$$\begin{aligned} \alpha (d_C[(v, \mu), (w, \eta)])^2 &\leq (\mathcal{A} + \mathcal{B}_D)[(v - w, \mu - \eta), (v - w, \mu - \eta)] \\ &\quad + \mathcal{B}_C[(v, \mu), (v - w, \mu - \eta)] - \mathcal{B}_C[(w, \eta), (v - w, \mu - \eta)]. \end{aligned}$$

Proof. From the analysis of the Dirichlet problem (proposition 3.4) we know that when $\beta_D > \beta_{\min} > 0$,

$$\alpha \|(v - w, \mu - \eta)\|_{\mathcal{B}_D}^2 \leq (\mathcal{A} + \mathcal{B}_D)[(v - w, \mu - \eta), (v - w, \mu - \eta)]. \quad (4.19)$$

Introducing the notation $\delta P := [P^\tau(v, \mu)]_+ - [P^\tau(w, \eta)]_+$, we have

$$\begin{aligned} \mathcal{B}_C[(v, \mu), (v - w, \mu - \eta)] - \mathcal{B}_C[(w, \eta), (v - w, \mu - \eta)] \\ = \tau^{-1} \|\mu - \eta\|_{L^2(\Gamma_C)}^2 + \langle \delta P, v - w + \tau^{-1}(\mu - \eta) \rangle_{\Gamma_C}. \end{aligned} \quad (4.20)$$

To estimate the expression on the right-hand side, we use

$$\tau^{-1} \|\mu - \eta + \delta P\|_{L^2(\Gamma_C)}^2 = \tau^{-1} \left(\|\mu - \eta\|_{L^2(\Gamma_C)}^2 + \|\delta P\|_{L^2(\Gamma_C)}^2 + 2 \langle \mu - \eta, \delta P \rangle_{\Gamma_C} \right).$$

Using (4.17), this implies the bound

$$\tau^{-1} \|\mu - \eta + \delta P\|_{L^2(\Gamma_C)}^2 \leq \tau^{-1} \left(\|\mu - \eta\|_{L^2(\Gamma_C)}^2 + \langle \delta P, P_0^\tau(v - w, \mu - \eta) \rangle_{\Gamma_C} + 2 \langle \mu - \eta, \delta P \rangle_{\Gamma_C} \right).$$

Observing that $P_0^\tau(v - w, \mu - \eta) + 2(\mu - \eta) = \tau(v - w) + \mu - \eta$, we infer that

$$\tau^{-1} \|\mu - \eta + \delta P\|_{L^2(\Gamma_C)}^2 \leq \mathcal{B}_C[(v, \mu), (v - w, \mu - \eta)] - \mathcal{B}_C[(w, \eta), (v - w, \mu - \eta)]. \quad (4.21)$$

We conclude the proof by noting that

$$(d_C[(v, \mu), (w, \eta)])^2 \lesssim \|(v - w, \mu - \eta)\|_{\mathcal{B}_D}^2 + \tau^{-1} \|\mu - \eta + [P^\tau(v, \mu)]_+ - [P^\tau(w, \eta)]_+\|_{L^2(\Gamma_C)}^2,$$

and applying (4.19) and (4.21). \square

Next, we prove a result analagous to assumption 3.2.

Lemma 4.3. *If there is $\beta_{\min} > 0$, independent of h , such that $\beta_D > \beta_{\min}$, then there is $\alpha > 0$ such that for all $(v_h, \mu_h) \in \mathbb{V}_h$,*

$$\begin{aligned} \alpha \left(\|(v_h, \mu_h)\|_{\mathcal{B}_D} + \left\| \tau^{-\frac{1}{2}} (\mu_h + [P^\tau(v_h, \mu_h)]_+) \right\|_{L^2(\Gamma_C)} \right)^2 \\ \leq (\mathcal{A} + \mathcal{B}_D + \mathcal{B}_C)[(v_h, \mu_h), (v_h, \mu_h)] - \langle [P^\tau(v_h, \mu_h)]_+, g_C - \tau^{-1}\psi_C \rangle_{\Gamma_C} \end{aligned}$$

Proof. The proof is similar to that of lemma 4.2, but with μ_h and v_h instead of $\mu - \eta$ and $v - w$. The appearance of the data term in the right-hand side is due to the relation

$$\begin{aligned} \tau^{-1} \|[P^\tau(v_h, \mu_h)]_+\|_{L^2(\Gamma_C)}^2 + 2\tau^{-1} \langle \mu_h, [P^\tau(v_h, \mu_h)]_+ \rangle_{\Gamma_C} + \tau^{-1} \|\mu_h\|_{L^2(\Gamma_C)}^2 \\ = \tau^{-1} \langle [P^\tau(v_h, \mu_h)]_+, P^\tau(v_h, \mu_h) \rangle_{\Gamma_C} + 2\tau^{-1} \langle \mu_h, [P^\tau(v_h, \mu_h)]_+ \rangle_{\Gamma_C} \\ + \tau^{-1} \|\mu_h\|_{L^2(\Gamma_C)}^2 \\ = \langle [P^\tau(v_h, \mu_h)]_+, u_h + \tau^{-1}\mu_h \rangle_{\Gamma_C} - \langle [P^\tau(v_h, \mu_h)]_+, g_C - \tau^{-1}\psi_C \rangle_{\Gamma_C} \\ + \tau^{-1} \|\mu_h\|_{L^2(\Gamma_C)}^2 \\ = \mathcal{B}_C[(v_h, \mu_h), (v_h, \mu_h)] - \langle [P^\tau(v_h, \mu_h)]_+, g_C - \tau^{-1}\psi_C \rangle_{\Gamma_C}. \end{aligned}$$

\square

Using lemmas 4.2 and 4.3, we may now prove that (4.16) is well-posed.

Theorem 4.1. *The finite dimensional nonlinear system (4.16) admits a unique solution.*

Proof. [79, chapter 2, lemma 1.4] states that if F is a continuous mapping from a finite dimensional Hilbert space \mathcal{H} into itself, and if F is positive, then there exists a point $\xi \in \mathcal{H}$ such that $F(\xi) = 0$.

Therefore, in order prove the existence of a solution, we show the continuity and the positivity of the nonlinear operator $\mathcal{A} + \mathcal{B}_D + \mathcal{B}_C - \mathcal{L}_D - \mathcal{L}_C$.

We define $F : \mathbb{V}_h \rightarrow \mathbb{V}_h$, for $(v_h, \mu_h) \in \mathbb{V}_h$, by

$$\langle F(v_h, \mu_h), (w_h, \eta_h) \rangle_\Gamma = (\mathcal{A} + \mathcal{B}_D + \mathcal{B}_C)[(v_h, \mu_h), (w_h, \eta_h)] - \mathcal{L}_D(w_h, \eta_h) - \mathcal{L}_C(w_h, \eta_h),$$

for all $(w_h, \eta_h) \in \mathbb{V}_h$. We may write the non-linear system (4.16) as

$$\langle F(v_h, \mu_h), (w_h, \eta_h) \rangle_\Gamma = 0 \quad \forall (w_h, \eta_h) \in \mathbb{V}_h. \quad (4.22)$$

For fixed h , by the equivalence of norms on discrete spaces, there exist $c_1, c_2 > 0$ such that for all $(v_h, \mu_h) \in \mathbb{V}_h$,

$$c_1 \|(v_h, \mu_h)\|_{L^2(\Gamma)} \leq \|(v_h, \mu_h)\|_{\mathcal{B}_D} \leq c_2 \|(v_h, \mu_h)\|_{L^2(\Gamma)}.$$

To show positivity, we let $(v_h, \mu_h) \in \mathbb{V}_h$. Using lemma 4.3, we see that

$$\begin{aligned} \langle \mathbf{F}(v_h, \mu_h), (v_h, \mu_h) \rangle_{\Gamma} &\geq \alpha \|(v_h, \mu_h)\|_{\mathcal{B}_D}^2 + \alpha \tau^{-1} \|\mu_h + [P^\tau(v_h, \mu_h)]_+\|_{L^2(\Gamma_C)}^2 \\ &\quad + \langle [P^\tau(v_h, \mu_h)]_+, g_C - \tau^{-1}\psi_C \rangle_{\Gamma_C} - \mathcal{L}_D(v_h, \mu_h) - \mathcal{L}_C(v_h, \mu_h). \end{aligned}$$

Using the Cauchy–Schwarz inequality and an arithmetic-geometric inequality, we see that there exists $C_{g_C\psi_C} > 0$ such that

$$\begin{aligned} &\langle [P^\tau(v_h, \mu_h)]_+, g_C - \tau^{-1}\psi_C \rangle_{\Gamma_C} - \mathcal{L}_D(v_h, \mu_h) - \mathcal{L}_C(v_h, \mu_h) \\ &= \langle [P^\tau(v_h, \mu_h)]_+ + \mu_h, g_C - \tau^{-1}\psi_C \rangle_{\Gamma_C} - \langle \mu_h, g_C - \tau^{-1}\psi_C \rangle_{\Gamma_C} \\ &\quad - \langle g_D, \beta_D v_h + \mu_h \rangle_{\Gamma_D} - \langle \psi_C, v_h + \tau^{-1}\mu_h \rangle_{\Gamma_C} \\ &\geq -C_{g_C\psi_C}^2 - \frac{\alpha}{2} \left(\|(v_h, \mu_h)\|_{\mathcal{B}_D}^2 + \tau^{-1} \|\mu_h + [P^\tau(v_h, \mu_h)]_+\|_{L^2(\Gamma_C)}^2 \right). \end{aligned}$$

Using norm equivalence, we obtain

$$\begin{aligned} \langle \mathbf{F}(v_h, \mu_h), (v_h, \mu_h) \rangle_{\Gamma} &\geq \frac{\alpha}{2} \left(\|(v_h, \mu_h)\|_{\mathcal{B}_D}^2 + \tau^{-1} \|\mu_h + [P^\tau(v_h, \mu_h)]_+\|_{L^2(\Gamma_C)}^2 \right) - C_{g_C\psi_C}^2 \\ &\geq C' \|(v_h, \mu_h)\|_{L^2(\Gamma)}^2 - C_{g_C\psi_C}^2, \end{aligned}$$

for some $C' > 0$. We conclude that for all $(v_h, \mu_h) \in \mathbb{V}_h$ with

$$\|(v_h, \mu_h)\|_{L^2(\Gamma)}^2 > \frac{C_{g_C\psi_C}^2}{C'} + 1,$$

there holds $\langle \mathbf{F}(v_h, \mu_h), (v_h, \mu_h) \rangle_{\Gamma} > 0$.

To show continuity, let $(v_h^1, \mu_h^1), (v_h^2, \mu_h^2) \in \mathbb{V}_h$. We have for all $(w_h, \eta_h) \in \mathbb{V}_h$,

$$\begin{aligned} &\langle \mathbf{F}(v_h^1, \mu_h^1) - \mathbf{F}(v_h^2, \mu_h^2), (w_h, \eta_h) \rangle_{\Gamma} \\ &= \left\langle [P^\tau(v_h^1, \mu_h^1)]_+ - [P^\tau(v_h^2, \mu_h^2)]_+, w_h + \tau^{-1}\eta_h \right\rangle_{\Gamma_C} \\ &\quad + \frac{1}{2} \langle \mu_h^1 - \mu_h^2, w_h + \tau^{-1}\eta_h \rangle_{\Gamma} - \frac{1}{2} \langle v_h^1 - v_h^2, \mu_h^1 - \mu_h^2 \rangle_{\Gamma_C} \\ &\quad + (\mathcal{A} + \mathcal{B}_D)[(v_h^1 - v_h^2, \mu_h^1 - \mu_h^2), (w_h, \eta_h)] \\ &\leq \left(\tau \|v_h^1 - v_h^2\|_{L^2(\Gamma_C)} + \|\mu_h^1 - \mu_h^2\|_{L^2(\Gamma_C)} \right) \left(\|w_h\|_{L^2(\Gamma_C)} + \tau^{-1} \|\eta_h\|_{L^2(\Gamma_C)} \right), \end{aligned}$$

where we have used (4.18). By norm equivalence, this means that

$$\frac{\langle \mathbf{F}(v_h^1, \mu_h^1) - \mathbf{F}(v_h^2, \mu_h^2), (w_h, \eta_h) \rangle_{\Gamma}}{\|(w_h, \eta_h)\|_{L^2(\Gamma)}} \leq C \|(v_h^1 - v_h^2, \mu_h^1 - \mu_h^2)\|_{L^2(\Gamma)}$$

showing that \mathbf{F} is continuous.

Applying [79, chapter 2, lemma 1.4] shows that there exists a solution to (4.22) and hence also to (4.16).

Uniqueness is an immediate consequence of lemma 4.2. Assume that (u_h^1, λ_h^1) and (u_h^2, λ_h^2) are solutions to (4.16). We immediately see that

$$\alpha (d_{\mathbf{C}}[(u_h^1, \lambda_h^1), (u_h^2, \lambda_h^2)])^2 = 0,$$

and we conclude that the solution is unique. \square

We now proceed to prove the following result, which is analagous to proposition 3.2

Lemma 4.4. *Let $(u, \lambda) \in \mathbb{W}$ be the solution of (1.37) and $(u_h, \lambda_h) \in \mathbb{V}_h$ the solution of (4.16). Then there holds*

$$d_{\mathbf{C}}[(u, \lambda), (u_h, \lambda_h)] \leq C \inf_{(v_h, \mu_h) \in \mathbb{V}_h} \|(u - v_h, \lambda - \mu_h)\|_*.$$

Proof. Using lemma 4.2 and Galerkin orthogonality, we see that, for arbitrary $(v_h, \mu_h) \in \mathbb{V}_h$,

$$\begin{aligned} \alpha (d_{\mathbf{C}}[(u, \lambda), (u_h, \lambda_h)])^2 &\leq (\mathcal{A} + \mathcal{B}_{\mathbf{D}})[(u - u_h, \lambda - \lambda_h), (u - u_h, \lambda - \lambda_h)] \\ &\quad + \mathcal{B}_{\mathbf{C}}[(u, \lambda), (u - u_h, \lambda - \lambda_h)] - \mathcal{B}_{\mathbf{C}}[(u_h, \lambda_h), (u - u_h, \lambda - \lambda_h)] \\ &= (\mathcal{A} + \mathcal{B}_{\mathbf{D}})[(u - u_h, \lambda - \lambda_h), (u - v_h, \lambda - \mu_h)] \\ &\quad + \mathcal{B}_{\mathbf{C}}[(u, \lambda), (u - v_h, \lambda - \mu_h)] - \mathcal{B}_{\mathbf{C}}[(u_h, \lambda_h), (u - v_h, \lambda - \mu_h)]. \end{aligned}$$

Next, we use

$$\begin{aligned} &\mathcal{B}_{\mathbf{C}}[(u, \lambda), (u - v_h, \lambda - \mu_h)] - \mathcal{B}_{\mathbf{C}}[(u_h, \lambda_h), (u - v_h, \lambda - \mu_h)] \\ &= \langle \lambda - \lambda_h + [P^\tau(u, \lambda)]_+ - [P^\tau(u_h, \lambda_h)]_+, (u - v_h) + \tau^{-1}(\lambda - \mu_h) \rangle_{\Gamma_{\mathbf{C}}} \\ &\quad - \frac{1}{2} \langle u - u_h, \lambda - \mu_h \rangle_{\Gamma_{\mathbf{C}}} - \frac{1}{2} \langle \lambda - \lambda_h, u - v_h \rangle_{\Gamma_{\mathbf{C}}} \end{aligned}$$

to show that

$$\begin{aligned} &(\mathcal{A} + \mathcal{B}_{\mathbf{D}})[(u - u_h, \lambda - \lambda_h), (u - u_h, \lambda - \lambda_h)] \\ &\quad + \mathcal{B}_{\mathbf{C}}[(u, \lambda), (u - u_h, \lambda - \lambda_h)] - \mathcal{B}_{\mathbf{C}}[(u_h, \lambda_h), (u - u_h, \lambda - \lambda_h)] \\ &= \underbrace{(\mathcal{A} + \mathcal{B}_{\mathbf{D}})[(u - u_h, \lambda - \lambda_h), (u - v_h, \lambda - \mu_h)]}_{\text{(I)}} \\ &\quad - \underbrace{\frac{1}{2} \langle u - u_h, \lambda - \mu_h \rangle_{\Gamma_{\mathbf{C}}} - \frac{1}{2} \langle \lambda - \lambda_h, u - v_h \rangle_{\Gamma_{\mathbf{C}}}}_{\text{(II)}} \\ &\quad + \underbrace{\langle \lambda - \lambda_h + [P^\tau(u, \lambda)]_+ - [P^\tau(u_h, \lambda_h)]_+, (u - v_h) + \tau^{-1}(\lambda - \mu_h) \rangle_{\Gamma_{\mathbf{C}}}}_{\text{(III)}}. \end{aligned}$$

We estimate the three parts of the right-hand separately. For the first term, we use the continuity of $\mathcal{A} + \mathcal{B}_D$ (proposition 3.4) to obtain

$$(I) \leq M \|(u - u_h, \lambda - \lambda_h)\|_{\mathcal{B}_D} \|(u - v_h, \lambda - \mu_h)\|_{\mathcal{B}_D}.$$

For the second line, we use $H^{1/2}(\Gamma)$ – $H^{-1/2}(\Gamma)$ duality and the Cauchy–Schwarz inequality to obtain

$$(II) \leq \|(u - u_h, \lambda - \lambda_h)\|_{\mathcal{B}_D} \|(u - v_h, \lambda - \mu_h)\|_{\mathcal{B}_D}.$$

For the last term, we use the Cauchy–Schwarz inequality to get

$$(III) \leq \left\| \tau^{-1/2} (\lambda - \lambda_h + [P^\tau(u, \lambda)]_+ - [P^\tau(u_h, \lambda_h)]_+) \right\|_{L^2(\Gamma_C)} \\ \cdot \left(\left\| \tau^{1/2}(u - v_h) \right\|_{L^2(\Gamma_C)} + \left\| \tau^{-1/2}(\lambda - \mu_h) \right\|_{L^2(\Gamma_C)} \right).$$

Collecting these bounds, we see that

$$d_C[(u, \lambda), (u_h, \lambda_h)]^2 \lesssim d_C[(u, \lambda), (u_h, \lambda_h)] \|(u - v_h, \lambda - \mu_h)\|_*.$$

Dividing through by $d_C[(u, \lambda), (u_h, \lambda_h)]$, and taking the infimum yields the desired result. \square

We now prove the main result of this section, an *a priori* bound on the error of the solution of (4.16). This result is analogous to corollary 3.1.

Theorem 4.2. *Let $(u, \lambda) \in H^s(\Gamma) \times H^r(\Gamma)$ for some $s \geq \frac{1}{2}, r \geq 0$ and $(u_h, \lambda_h) \in \mathbb{P}_h^k \times \mathbb{DP}_h^l$ be the solutions of (1.37) and the discrete problem (4.16), respectively. If there is $\beta_{\min} > 0$ such that $\beta_{\min} < \beta_D \lesssim h^{-1}$ and $\tau \approx h^{-1}$, then*

$$d_C[(u, \lambda), (u_h, \lambda_h)] \lesssim h^{\zeta-1/2} |u|_{H^\zeta(\Gamma)} + h^{\xi+1/2} |\lambda|_{H^\xi(\Gamma)},$$

where $\zeta = \min(k+1, s)$ and $\xi = \min(l+1, r)$. Additionally,

$$\|\tilde{u} - \tilde{u}_h\|_{H^1(\Omega^-)} \lesssim h^{\zeta-1/2} |u|_{H^\zeta(\Gamma)} + h^{\xi+1/2} |\lambda|_{H^\xi(\Gamma)},$$

where \tilde{u} and \tilde{u}_h are the solutions in Ω^- defined by (1.47).

Proof. Using lemmas 2.2 and 2.3, we see that

$$\inf_{(v_h, \mu_h) \in \mathbb{V}_h} \|(u - v_h, \lambda - \mu_h)\|_{\mathbb{V}} = \inf_{v_h \in \mathbb{P}_h^k} \|u - v_h\|_{H^{1/2}(\Gamma)} + \inf_{\mu_h \in \Lambda_h^l} \|\lambda - \mu_h\|_{H^{-1/2}(\Gamma)} \\ \lesssim h^{\zeta-1/2} |u|_{H^\zeta(\Gamma)} + h^{\xi+1/2} |\lambda|_{H^\xi(\Gamma)}, \\ \inf_{v_h \in \mathbb{P}_h^k} \|u - v_h\|_{L^2(\Gamma)} \lesssim h^\zeta |u|_{H^\zeta(\Gamma)}, \\ \inf_{\mu_h \in \mathbb{DP}_h^l} \|\lambda - \mu_h\|_{L^2(\Gamma)} \lesssim h^\xi |\lambda|_{H^\xi(\Gamma)}.$$

Applying these to the definition of $\|\cdot\|_*$ gives

$$\begin{aligned} \inf_{(v_h, \mu_h) \in \mathbb{V}_h} \|(u - v_h, \lambda - \mu_h)\|_* &\lesssim h^{\zeta-1/2} |u|_{H^\zeta(\Gamma)} + h^{\xi+1/2} |\lambda|_{H^\xi(\Gamma)} \\ &\quad + \beta_D^{1/2} h^\zeta |u|_{H^\zeta(\Gamma)} + \tau^{1/2} h^\zeta |u|_{H^\zeta(\Gamma)} + \tau^{-1/2} h^\xi |\lambda|_{H^\xi(\Gamma)}. \end{aligned}$$

In combination with lemma 4.4 and using the given choice of the parameters τ and β_D this proves the first assertion.

The estimate in the domain Ω^- follows by using the relations (1.74) and (1.76). \square

If λ is smooth enough and $k = l$, the bounds on τ can be replaced with $h \lesssim \tau \lesssim h^{-1}$ without reducing the order of convergence.

By observing that for all $(v, \mu), (w, \eta) \in \mathbb{W}$, $\|(v - w, \mu - \eta)\|_{\mathbb{V}} \leq d_C[(v, \mu), (w, \eta)]$, we arrive at the following corollary of theorem 4.2.

Corollary 4.1. *Let $(u, \lambda) \in H^s(\Gamma) \times H^r(\Gamma)$ be the solution of (1.37) for some $s \geq \frac{1}{2}$ and $r \geq 0$ and $(u_h, \lambda_h) \in \mathbb{P}_h^k \times \mathbb{DP}_h^l$ the solution of the discrete problem (4.16). If there is $\beta_{\min} > 0$ such that $\beta_{\min} < \beta_D \lesssim h^{-1}$ and $\tau \approx h^{-1}$, then*

$$\|(u - u_h, \lambda - \lambda_h)\|_{\mathbb{V}} \lesssim h^{\zeta-1/2} |u|_{H^\zeta(\Gamma)} + h^{\xi+1/2} |\lambda|_{H^\xi(\Gamma)},$$

where $\zeta = \min(k + 1, s)$ and $\xi = \min(l + 1, r)$.

Using lemma 2.4, we can derive the following result if \mathbb{V} is taken to be $\mathbb{P}_h^1(\Gamma) \times \text{DUAL}_h^0(\Gamma)$.

Corollary 4.2. *Let $(u, \lambda) \in H^s(\Gamma) \times H^r(\Gamma)$ be the solution of (1.37) for some $s \geq \frac{1}{2}$ and $r \geq 0$ and $(u_h, \lambda_h) \in \mathbb{P}_h^1 \times \text{DUAL}_h^0$ the solution of the discrete problem (4.16). If there is $\beta_{\min} > 0$ such that $\beta_{\min} < \beta_D \lesssim h^{-1}$ and $\tau \approx h^{-1}$, then*

$$\|(u - u_h, \lambda - \lambda_h)\|_{\mathbb{V}} \lesssim h^{\zeta-1/2} |u|_{H^\zeta(\Gamma)} + h^{\xi+1/2} |\lambda|_{H^\xi(\Gamma)},$$

where $\zeta = \min(2, s)$ and $\xi = \min(\frac{1}{2}, r)$.

— 4.3 —

NUMERICAL RESULTS

We now demonstrate the theory with a series of numerical examples. In this section, we consider two example problems.

For the first problem, we let $\Omega^- = [0, 1] \times [0, 1] \times [0, 1]$ be the unit cube, $\Gamma_C := \{(x, y, z) \in$

$\Gamma : z = 1\}$, and $\Gamma_D := \Gamma \setminus \Gamma_C$. Let

$$g_D = 0, \quad (4.23a)$$

$$g_C = \begin{cases} \sin(\pi x) \sin(\pi y) \sinh(\sqrt{2}\pi) & x \leq \frac{1}{2} \\ \sin(\pi y) \sinh(\sqrt{2}\pi) & x > \frac{1}{2} \end{cases}, \quad (4.23b)$$

$$\psi_C = \begin{cases} \sqrt{2}\pi \sin(\pi x) \sin(\pi y) \cosh(\sqrt{2}\pi) & x \geq \frac{1}{2} \\ \sqrt{2}\pi \sin(\pi y) \cosh(\sqrt{2}\pi) & x < \frac{1}{2} \end{cases}. \quad (4.23c)$$

It can be shown that

$$u(x, y, z) = \sin(\pi x) \sin(\pi y) \sinh(\sqrt{2}\pi z)$$

is the solution to (1.37) with these boundary conditions.

For the second problem, we let $\Omega^- = \{(x, y, z) \in \mathbb{R}^3 : x^2 + y^2 + z^2 = 1\}$ be the unit sphere, $\Gamma_C := \{(x, y, z) \in \Gamma : x > 0\}$, and $\Gamma_D := \Gamma \setminus \Gamma_C$. Let

$$g_D = x^2 - y^2, \quad (4.24a)$$

$$g_C = \begin{cases} x^2 - y^2 & y > 0 \\ x^2 & y \leq 0 \end{cases}, \quad (4.24b)$$

$$\psi_C = \begin{cases} 2x^2 - 2y^2 & y < 0 \\ 2x^2 & y \geq 0 \end{cases}. \quad (4.24c)$$

It can be shown that

$$u(x, y, z) = x^2 - y^2 \quad (4.25)$$

is the solution to (1.37) with these boundary conditions.

As in the previous chapter, we denote which problem we are solving in each plot by a small cube or sphere at the top right-hand corner of the plot.

To solve the non-linear system (4.15), we will treat the nonlinear term explicitly. Therefore, we define

$$\mathcal{B}'_C[(u, \lambda), (v, \mu)] := \frac{1}{2} \langle \lambda, v \rangle_{\Gamma_C} + \langle \tau^{-1} \lambda - \frac{1}{2} u, \mu \rangle_{\Gamma_C} \quad (4.26)$$

Note that \mathcal{B}'_C differs from \mathcal{B}_C only by the missing nonlinear term.

We pick initial guesses $(u_0, \lambda_0) \in \mathbb{V}_h$ and define $(u_{n+1}, \lambda_{n+1}) \in \mathbb{V}_h$, for $n \in \mathbb{N}$, to be the solution of

$$(\mathcal{A} + \mathcal{B}_D + \mathcal{B}'_C)[(u_{n+1}, \lambda_{n+1}), (v_h, \mu_h)] = \mathcal{L}_C(v_h, \mu_h) - \langle [P^\tau(u_n, \lambda_n)]_+, v_h + \tau^{-1} \mu_h \rangle_{\Gamma_C} \\ \forall (v_h, \mu_h) \in \mathbb{V}_h. \quad (4.27)$$

This leads us to algorithm 1, an iterative method for solving the contact problem.

In all the computations in this section, we precondition GMRES using a mass matrix preconditioner applied blockwise from the left, as we did in the previous chapter.

Algorithm 1 Iterative algorithm for solving the contact problem

```

1: function SOLVE( $(u_0, \lambda_0)$ , TOL, MAXITER)
2:   for  $n \leftarrow 0$  to MAXITER do
3:      $(u_{n+1}, \lambda_{n+1}) \leftarrow$  solution of (4.27), calculated using GMRES
4:     if  $\|(u_{n+1}, \lambda_{n+1}) - (u_n, \lambda_n)\|_{\mathbb{V}} < \text{TOL}$  then
5:       return  $(u_{n+1}, \lambda_{n+1})$ 
6:     end if
7:   end for
8: end function

```

— 4.3.1 —

NUMERICAL RESULTS ON THE UNIT CUBE

We begin by looking at the result for the problem on the unit cube with boundary conditions (4.23).

Figures 4.1 and 4.2 show how the error, number of outer iterations, and the average number of GMRES iterations inside each outer iteration for the problem on the unit cube change as the parameter τ is varied. The results in figure 4.1 are for $\mathbb{V}_h = \mathbb{P}_h^1(\Gamma) \times \text{DUAL}_h^0(\Gamma)$, and the results in figure 4.2 are for $\mathbb{V}_h = \mathbb{P}_h^1(\Gamma) \times \text{DP}_h^0(\Gamma)$. Here, we see that the error and number of outer iterations are lowest when τ is between around 1 and 10.

Motivated by figures 4.1 and 4.2 and the bounds in corollaries 4.1 and 4.2, we take $\tau = 0.5/h$, and look at the convergence as h is decreased. Figure 4.3 shows how the error and iteration counts vary as h is decreased when $\mathbb{V}_h = \mathbb{P}_h^1(\Gamma) \times \text{DUAL}_h^0(\Gamma)$. Here we observe slightly higher than the order 1 convergence predicted by corollary 4.2.

Figure 4.4 shows the error and iterations counts as h is reduced when $\mathbb{V}_h = \mathbb{P}_h^1(\Gamma) \times \text{DP}_h^0(\Gamma)$. In this case, corollary 4.1 tells us to expect order 1.5 convergence. However, we observe a slightly lower order of convergence. This appears to be due to the ill-conditioning of this system, and the mass matrix preconditioner being ineffective, leading to an inaccurate solution when using GMRES. This could be rectified by taking a lower tolerance, but in this case the increasing number of iterations required leads to this being infeasible.

As in section 3.3, we could look for $(u_n, \lambda_n) \in \mathbb{P}_h^1(\Gamma) \times \text{DP}_h^0(\Gamma)$ and test with $(v_h, \mu_h) \in \text{DUAL}_h^1(\Gamma) \times \text{DUAL}_h^0(\Gamma)$ so that we obtain the higher order convergence as in corollary 4.1, while having stable dual pairings and hence more effective mass matrix preconditioning. For these spaces, we have seen in the experiments we have run that the error and iteration counts are highly sensitive to changes in the value of the parameter τ , and so we have been unable to obtain an accurate solution to the problem. A deeper investigation of this method using these dual spaces warrants future work.

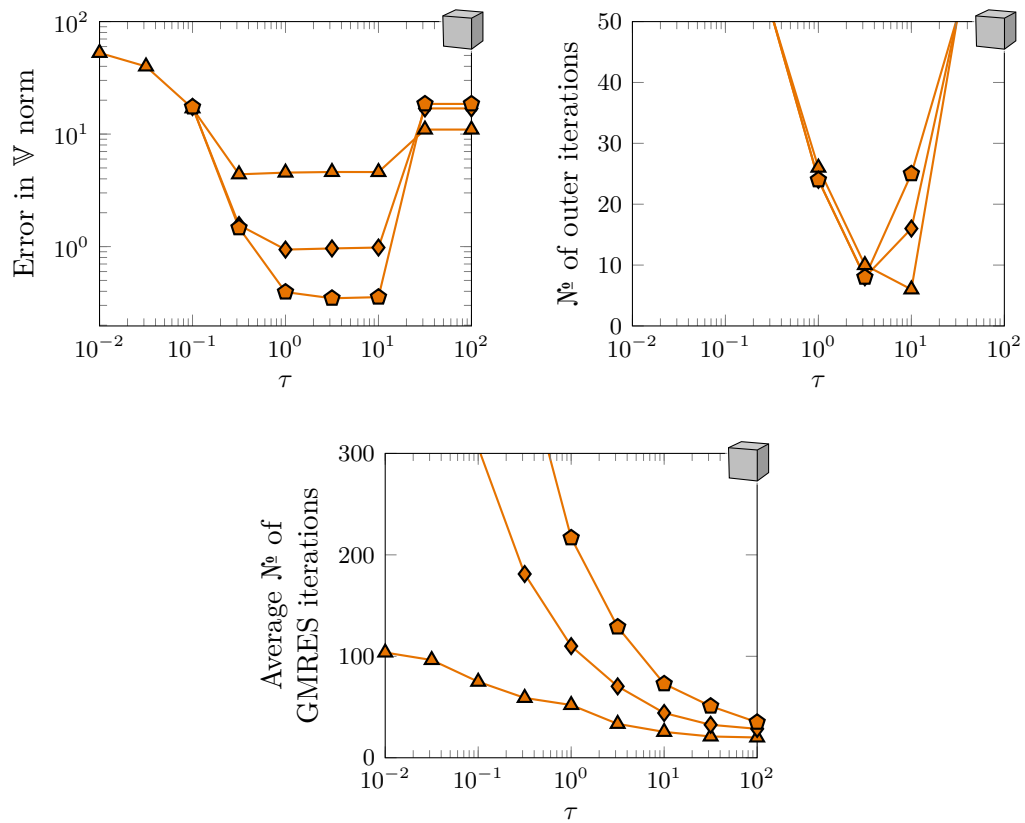


Figure 4.1: The dependence of the error, number of outer iterations, and the average number of GMRES iterations on τ , for the problem (1.37) with boundary conditions (4.23) on the unit cube with $h = 2^{-2}$ (orange triangles), $h = 2^{-3.5}$ (orange diamonds), and $h = 2^{-5}$ (orange pentagons). Here we take $(u_n, \lambda_n), (v_h, \mu_h) \in P_h^1(\Gamma) \times \text{DUAL}_h^0(\Gamma)$, $u_0 = \lambda_0 = 0$, $\beta_D = 0.01$, $\text{TOL} = 0.05$, and $\text{MAXITER} = 50$.

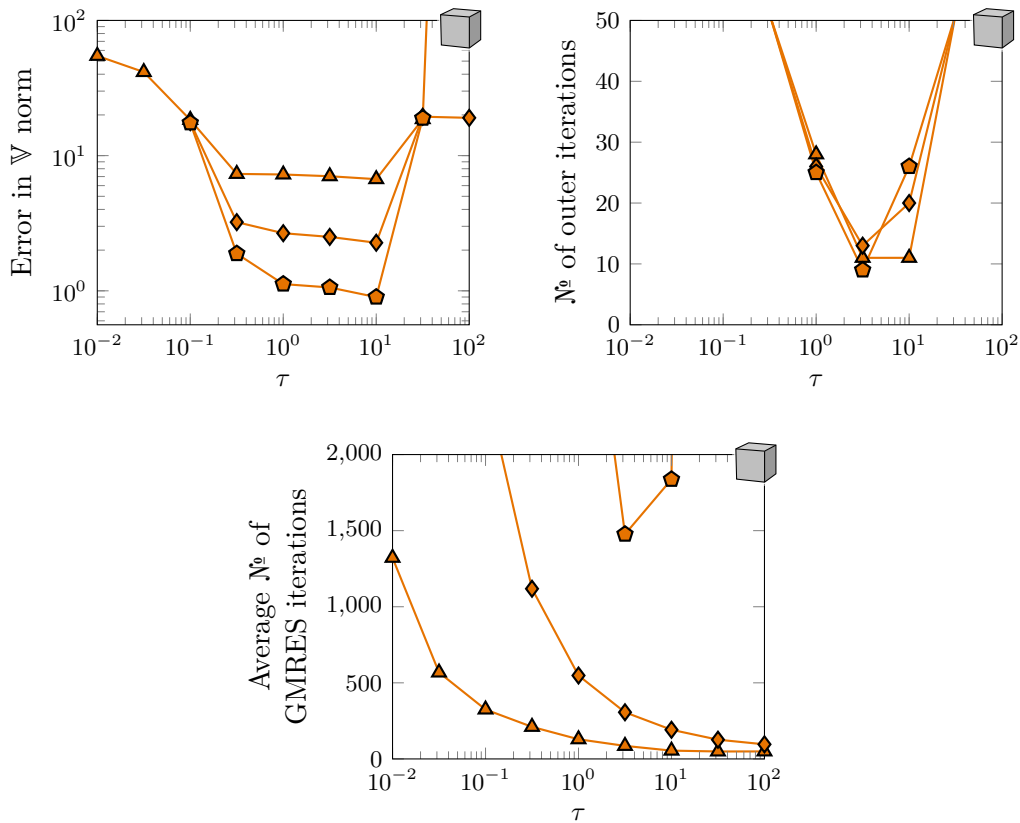


Figure 4.2: The dependence of the error, number of outer iterations, and the average number of GMRES iterations on τ , for the problem (1.37) with boundary conditions (4.23) on the unit cube with $h = 2^{-2}$ (orange triangles), $h = 2^{-3.5}$ (orange diamonds), and $h = 2^{-5}$ (orange pentagons). Here we take $(u_n, \lambda_n), (v_h, \mu_h) \in P_h^1(\Gamma) \times DP_h^0(\Gamma)$, $u_0 = \lambda_0 = 0$, $\beta_D = 0.01$, $\text{TOL} = 0.05$, and $\text{MAXITER} = 50$.

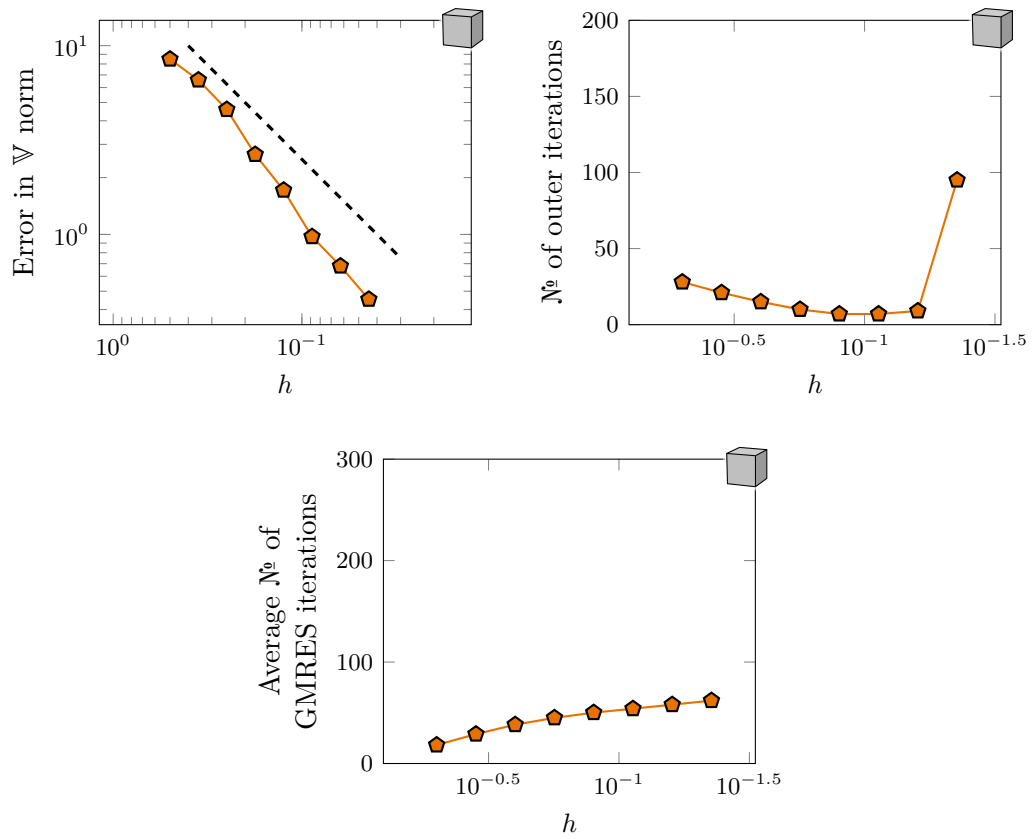


Figure 4.3: The error, number of outer iterations and average number of inner GMRES iteration for the problem (1.37) with boundary conditions (4.23) on the unit cube as h is reduced. Here we take $(u_n, \lambda_n), (v_h, \mu_h) \in P_h^1(\Gamma) \times \text{DUAL}_h^0(\Gamma)$, $u_0 = \lambda_0 = 0$, $\beta_D = 0.01$, $\text{TOL} = 0.05$, $\text{MAXITER} = 200$, and $\tau = 0.5/h$. The dashed line shows order 1 convergence.

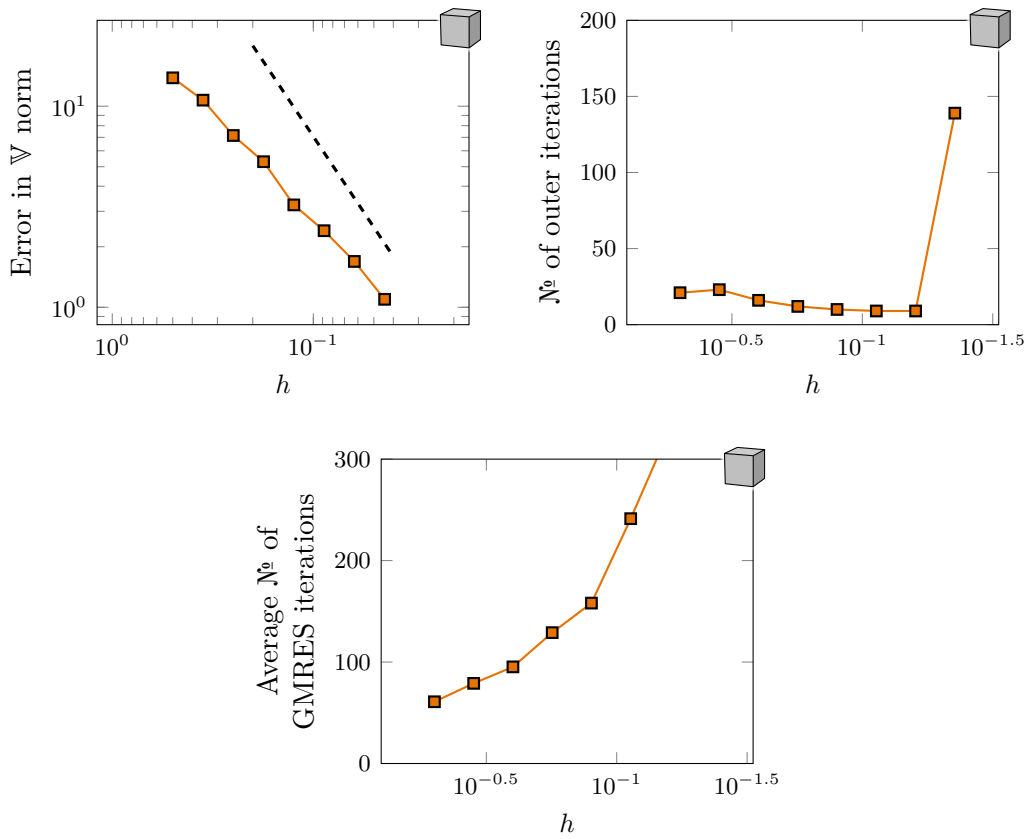


Figure 4.4: The error, number of outer iterations and average number of inner GMRES iteration for the problem (1.37) with boundary conditions (4.23) on the unit cube as h is reduced. Here we take $(u_n, \lambda_n), (v_h, \mu_h) \in P_h^1(\Gamma) \times DP_h^0(\Gamma)$, $u_0 = \lambda_0 = 0$, $\beta_D = 0.01$, $\text{TOL} = 0.05$, $\text{MAXITER} = 200$, and $\tau = 0.5/h$. The dashed line shows order 1.5 convergence.

— 4.3.2 —

NUMERICAL RESULTS ON THE UNIT SPHERE

We now look at the results for the problem on the unit sphere with boundary conditions (4.24).

In our initial experiments, we observed that for this problem and almost all choices of the parameter τ , the nonlinear outer iteration does not converge. For this problem, therefore, we use a relaxed algorithm: instead of taking (u_{n+1}, λ_{n+1}) to be the solution of (4.27), we take it to be a weighted average of the solution of (4.27) and (u_n, λ_n) . This modified algorithm is algorithm 2.

Algorithm 2 Iterative algorithm with relaxation for solving the contact problem

```

function SOLVE( $(u_0, \lambda_0)$ , TOL, MAXITER, RELAX)
2:   for  $n \leftarrow 0$  to MAXITER do
       $(u'_{n+1}, \lambda'_n) \leftarrow$  solution of (4.27), calculated using GMRES
4:    $(u_{n+1}, \lambda_{n+1}) \leftarrow$  RELAX( $u'_n, \lambda'_n$ ) + (1 - RELAX)( $u_n, \lambda_n$ )
      if  $\|(u'_n, \lambda'_n) - (u_n, \lambda_n)\|_{\mathbb{V}} <$  TOL then
6:     return ( $u_{n+1}, \lambda_{n+1}$ )
      end if
8:   end for
end function

```

Figure 4.5 shows the error and iteration counts for the problem on the sphere with $\mathbb{V}_h = P_h^1(\Gamma) \times \text{DUAL}_h^0(\Gamma)$ as h is reduced. As in the previous section, we take $\tau = 0.5/h$. A greater level of relaxation is required for smaller values of h in order to obtain good convergence. We therefore take $\text{RELAX} = h$. In figure 4.5, we observe order 1.5 convergence. This is expected as the space $\text{DUAL}_h^0(\Gamma)$ exhibits the same approximation order as $\text{DP}_h^0(\Gamma)$ on smooth surfaces.

As in the previous section, if we take $\mathbb{V}_h = P_h^1(\Gamma) \times \text{DP}_h^0(\Gamma)$, we observe a lower order of convergence than the expected 1.5. This is shown in figure 4.6. Again we see that the number of GMRES iterations greatly increases as h is reduced, suggesting that the lower convergence here is also due to the ill-conditioning of the problem, and the ineffectiveness of mass matrix preconditioning for this choice of spaces.

— — —

Now that you've finished reading chapter 4, why not take a break and snack on figure 4.7 before reading on.

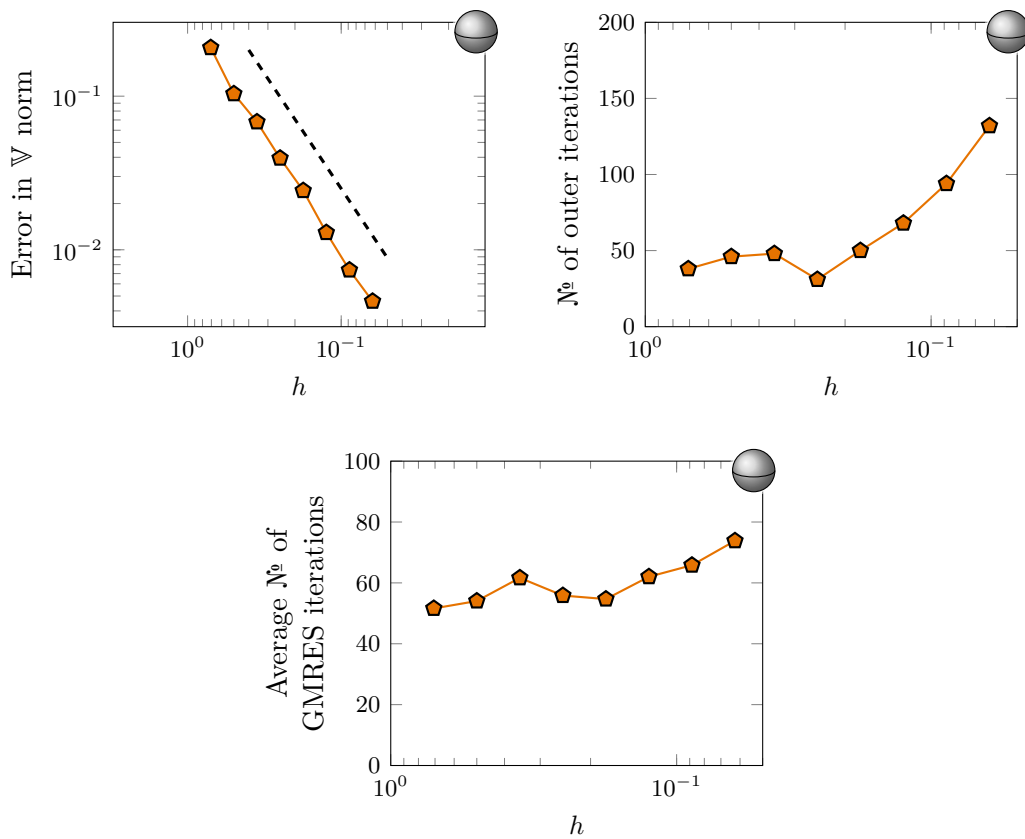


Figure 4.5: The error, number of outer iterations and average number of inner GMRES iteration for the problem (1.37) with boundary conditions (4.24) on the unit sphere as h is reduced. Here we take $(u_n, \lambda_n), (v_h, \mu_h) \in P_h^1(\Gamma) \times \text{DUAL}_h^0(\Gamma)$, $u_0 = \lambda_0 = 0$, $\beta_D = 0.01$, $\text{TOL} = 0.001$, $\text{MAXITER} = 200$, $\text{RELAX} = h$, and $\tau = 0.5/h$. The dashed line shows order 1.5 convergence.

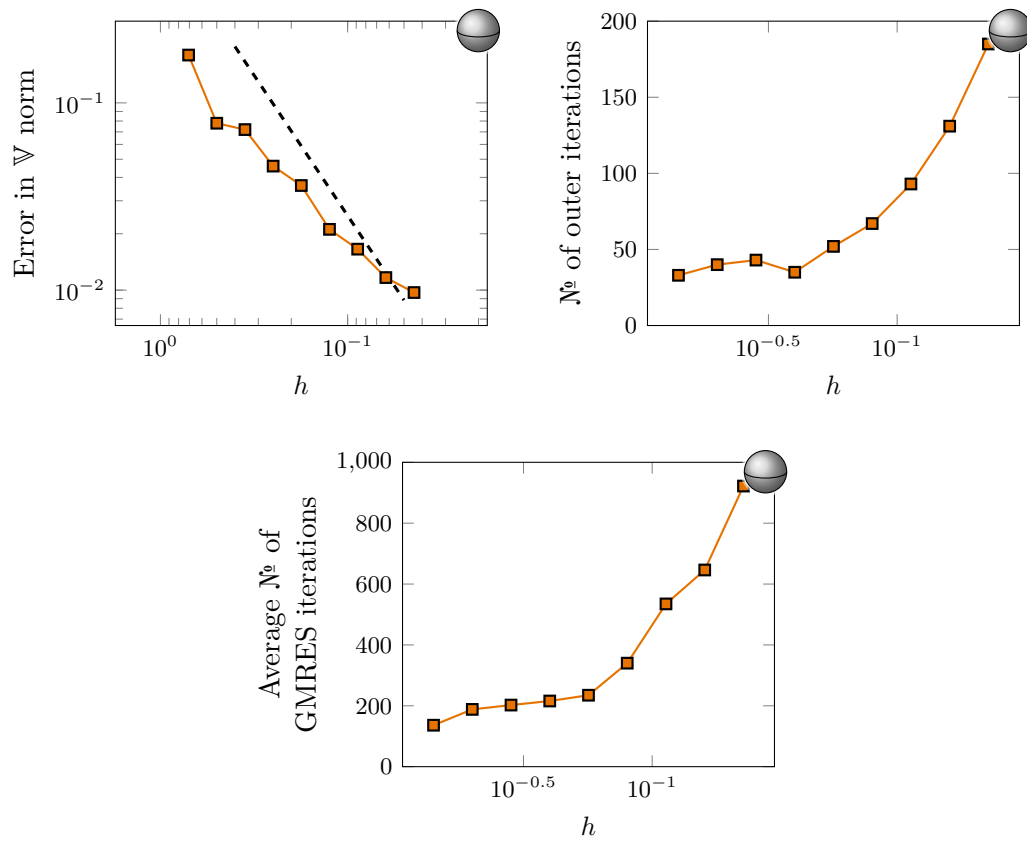


Figure 4.6: The error, number of outer iterations and average number of inner GMRES iteration for the problem (1.37) with boundary conditions (4.24) on the unit sphere as h is reduced. Here we take $(u_n, \lambda_n), (v_h, \mu_h) \in P_h^1(\Gamma) \times DP_h^0(\Gamma)$, $u_0 = \lambda_0 = 0$, $\beta_D = 0.01$, $TOL = 0.001$, $MAXITER = 200$, $RELAX = h$, and $\tau = 0.5/h$. The dashed line shows order 1.5 convergence.

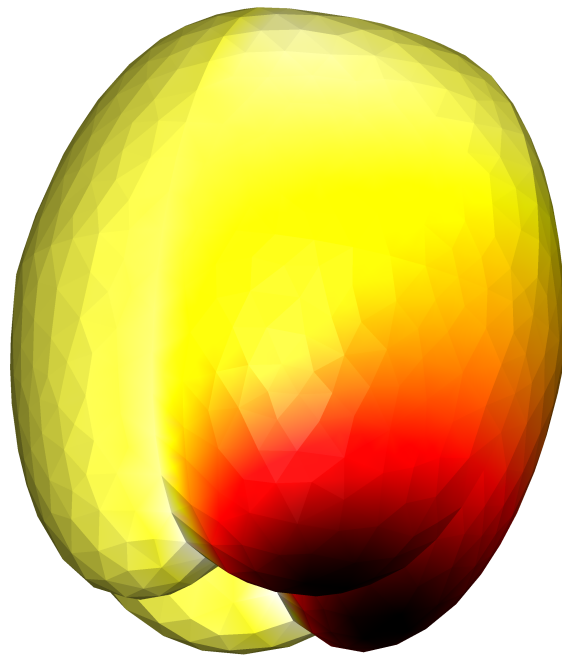


Figure 4.7: The solution, u_h , of a mixed Dirichlet–Signorini problem on the interior of an apple, solved using the penalty method with $\beta_D = 0.01$, $(u_n, \lambda_n), (v_h, \mu_h) \in P_h^1(\Gamma) \times DP_h^0(\Gamma)$, $u_0 = \lambda_0 = 0$, $\beta_D = 0.01$, $\text{TOL} = 0.001$, $\text{MAXITER} = 200$, $\text{RELAX} = 0.5$, and $\tau = 1$. The boundary conditions used are $u(\mathbf{x}) = 0$ on the bottom half of the apple and (1.37f) and (1.37g) with $g_C(\mathbf{x}) = x^3$ and $\psi_C(\mathbf{x}) = z^3$ everywhere else.

CHAPTER 5

WEAK IMPOSITION OF BOUNDARY CONDITIONS ON THE HELMHOLTZ EQUATION

In chapters 3 and 4, we focussed on the weak imposition of boundary conditions on Laplace's equation. In this chapter, we look at how this method and its analysis can be adapted to be used for the Helmholtz equation, focussing on the exterior Helmholtz problem (1.38): Find $u \in H_{\text{loc}}^1(\Delta, \Omega^+)$ such that

$$-\Delta u - k^2 u = 0 \quad \text{in } \Omega^+, \quad (1.38a)$$

$$\frac{\partial u^{\text{scat}}}{\partial |\mathbf{x}|} - iku^{\text{scat}} = o(|\mathbf{x}|^{-1}) \quad \text{as } |\mathbf{x}| \rightarrow \infty, \quad (1.38b)$$

$$u = g_{\text{D}} \quad \text{on } \Gamma_{\text{D}}, \quad (1.37c)$$

$$\frac{\partial u}{\partial \boldsymbol{\nu}} = g_{\text{N}} \quad \text{on } \Gamma_{\text{N}}, \quad (1.37d)$$

where $k \in \mathbb{R}$ is the wavenumber of the problem.

As in chapter 3, we assume that the boundary between Γ_{D} and Γ_{N} coincides with edges between the faces of Γ . We assume that $g_{\text{D}} \in H^{1/2}(\Gamma_{\text{D}})$, $g_{\text{N}} \in L^2(\Gamma_{\text{N}})$, and $u \in H^{3/2+\epsilon}(\Gamma)$ for some $\epsilon > 0$.

— 5.1 —

DERIVATION OF WEAKLY IMPOSED BOUNDARY CONDITIONS FOR THE HELMHOLTZ EQUATION

In this section, we derive formulations for the exterior Helmholtz problem with non-homogeneous Dirichlet conditions and mixed Dirichlet–Neumann boundary conditions.

For exterior problems, we see from (1.64) that

$$\mathbf{A} \begin{bmatrix} u \\ \lambda \end{bmatrix} = -\frac{1}{2} \begin{bmatrix} u \\ \lambda \end{bmatrix}. \quad (5.1)$$

Writing this using the multitrace form (3.4) for Helmholtz, we obtain

$$\mathcal{A}[(u, \lambda), (v, \mu)] = -\frac{1}{2} \langle u, \mu \rangle_{\Gamma} - \frac{1}{2} \langle \lambda, v \rangle_{\Gamma}. \quad (5.2)$$

As in chapter 3, we write the boundary condition as

$$R_{\Gamma}(u, \lambda) = 0, \quad (5.3)$$

and look to solve

$$\mathcal{A}[(u, \lambda), (v, \mu)] = -\frac{1}{2} \langle u, \mu \rangle_{\Gamma} - \frac{1}{2} \langle \lambda, v \rangle_{\Gamma} + \langle R_{\Gamma}(u, \lambda), \beta_1 v + \beta_2 \mu \rangle_{\Gamma}. \quad (5.4)$$

— 5.1.1 —

DIRICHLET BOUNDARY CONDITION

In this section, we assume that $\Gamma_{\text{D}} \equiv \Gamma$ and consider the resulting Dirichlet problem. We choose $\beta_1 = \beta_{\text{D}}^{1/2}$, $\beta_2 = -\beta_{\text{D}}^{-1/2}$, where β_{D} will be identified with a mesh-dependent penalty parameter, and

$$R_{\Gamma_{\text{D}}}(u, \lambda) := \beta_{\text{D}}^{1/2}(g_{\text{D}} - u) \quad (5.5)$$

where $g_{\text{D}} \in H^{1/2}(\Gamma)$ is the Dirichlet data. Here, β_1 and β_2 have been multiplied by negative 1 compared to the values used in chapter 3. This is because we are now formulating an exterior problem, and this parameter tweak ensures that the resulting formulation will be the antisymmetric formulation rather than the nonsymmetric formulation obtained if the other sign is used.

Inserting this into (3.8), we obtain the formulation

$$\mathcal{A}[(u, \lambda), (v, \mu)] - \frac{1}{2} \langle u, \mu \rangle_{\Gamma} + \frac{1}{2} \langle \lambda, v \rangle_{\Gamma} + \langle \beta_{\text{D}} u, v \rangle_{\Gamma} = \langle g_{\text{D}}, \beta_{\text{D}} v - \mu \rangle_{\Gamma}. \quad (5.6)$$

This leads us to the following formulation for the Helmholtz Dirichlet problem: Find $(u, \lambda) \in \mathbb{V}$ such that

$$\mathcal{A}[(u, \lambda), (v, \mu)] + \mathcal{B}_{\text{D}}^{+}[(u, \lambda), (v, \mu)] = \mathcal{L}_{\text{D}}^{+}(v, \mu) \quad \forall (v, \mu) \in \mathbb{V}, \quad (5.7)$$

where

$$\mathcal{B}_{\text{D}}^{+}[(u, \lambda), (v, \mu)] := \frac{1}{2} \langle \lambda, v \rangle_{\Gamma_{\text{D}}} - \frac{1}{2} \langle u, \mu \rangle_{\Gamma_{\text{D}}} + \langle \beta_{\text{D}} u, v \rangle_{\Gamma_{\text{D}}}, \quad (5.8)$$

$$\mathcal{L}_{\text{D}}^{+}(v, \mu) := \langle g_{\text{D}}, \beta_{\text{D}} v - \mu \rangle_{\Gamma_{\text{D}}}. \quad (5.9)$$

— 5.1.2 —

MIXED DIRICHLET–NEUMANN BOUNDARY CONDITION

We now consider the case of mixed Dirichlet–Neumann boundary conditions, when $\Gamma = \Gamma_D \cup \Gamma_N$. We note that in this case, we take $\mathbb{V} = H^{1/2}(\Gamma) \times L^2(\Gamma)$.

Proceeding as in chapter 3, with the change in sign of the parameters as in section 5.1.1, we obtain the following formulation for the Helmholtz mixed Dirichlet–Neumann problem: Find $(u, \lambda) \in \mathbb{V}$ such that

$$\mathcal{A}[(u, \lambda), (v, \mu)] + \mathcal{B}_{\text{ND}}^+[(u, \lambda), (v, \mu)] = \mathcal{L}_{\text{ND}}^+(v, \mu) \quad \forall (v, \mu) \in \mathbb{V}, \quad (5.10)$$

where

$$\begin{aligned} \mathcal{B}_{\text{ND}}^+[(u, \lambda), (v, \mu)] := & -\frac{1}{2} \langle u, \mu \rangle_{\Gamma_D} + \frac{1}{2} \langle \lambda, v \rangle_{\Gamma_D} + \langle \beta_D u, v \rangle_{\Gamma_D} \\ & - \frac{1}{2} \langle \lambda, v \rangle_{\Gamma_N} + \frac{1}{2} \langle u, \mu \rangle_{\Gamma_N} + \langle \beta_N \lambda, \mu \rangle_{\Gamma_N}, \end{aligned} \quad (5.11)$$

$$\mathcal{L}_{\text{ND}}^+(v, \mu) := \langle g_D, \beta_D v - \mu \rangle_{\Gamma_D} + \langle g_N, \beta_N \mu - v \rangle_{\Gamma_N}. \quad (5.12)$$

— 5.2 —

ANALYSIS OF WEAKLY IMPOSED BOUNDARY
CONDITIONS FOR THE HELMHOLTZ EQUATION

In this section, we present a version of the abstract analysis in section 3.2 adapted to apply to Helmholtz problems.

As in section 3.2, we let $\mathbb{V}_h = P_h^1(\Gamma) \times DP_h^0(\Gamma)$ be a finite dimensional subspace of \mathbb{V} ; we let \mathbb{W} be a product Hilbert space, such that $\mathbb{V}_h \subset \mathbb{W} \subset \mathbb{V}$; and we let $\|\cdot\|_{\mathcal{B}}$ be a norm defined on \mathbb{W} , such that for all $(v, \mu) \in \mathbb{W}$, $\|(v, \mu)\|_{\mathcal{B}} \geq \|(v, \mu)\|_{\mathbb{V}}$.

We define the projection $\pi_h^1 : H^{1/2}(\Gamma) \rightarrow P_h^1(\Gamma)$, for $v \in H^{1/2}(\Gamma)$ by

$$\langle \pi_h^1 v, w_h \rangle_{\Gamma} = \langle v, w_h \rangle_{\Gamma} \quad \forall w_h \in P_h^1(\Gamma),$$

we define $\pi_h^0 : H^{-1/2}(\Gamma) \rightarrow DP_h^0(\Gamma)$, for $\mu \in H^{-1/2}(\Gamma)$ by

$$\langle \pi_h^0 \mu, \eta_h \rangle_{H^{-1/2}(\Gamma)} = \langle \mu, \eta_h \rangle_{H^{-1/2}(\Gamma)} \quad \forall \eta_h \in DP_h^0(\Gamma).$$

By [73, (10.4) and theorem 10.4], π_h^1 and π_h^0 are well-defined. We define $\pi_h : \mathbb{W} \rightarrow \mathbb{V}_h$, for $(v, \mu) \in \mathbb{W}$, by

$$\pi_h(v, \mu) = (\pi_h^1 v, \pi_h^0 \mu).$$

It is clear from this definition that for all $(v_h, \mu_h) \in \mathbb{V}_h$, $\pi_h(v_h, \mu_h) = (v_h, \mu_h)$. As given in

the following lemma, π_h is bounded.

Lemma 5.1. *There exists $c > 0$ such that for all $(v, \mu) \in \mathbb{W}$,*

$$\|\pi_h(v, \mu)\|_{\mathbb{V}} \leq c \|(v, \mu)\|_{\mathbb{V}}.$$

Proof. Let $(v, \mu) \in \mathbb{W}$.

By [73, (10.15)], there exists $c > 0$ such that for all $v \in H^{1/2}(\Gamma)$,

$$\|\pi_h^1 v\|_{H^{1/2}(\Gamma)} \leq c \|v\|_{H^{1/2}(\Gamma)}. \quad (5.13)$$

By the triangle inequality,

$$\|\pi_h^0 \mu\|_{H^{-1/2}(\Gamma)} \leq \|\mu - \pi_h^0 \mu\|_{H^{-1/2}(\Gamma)} + \|\mu\|_{H^{-1/2}(\Gamma)}. \quad (5.14)$$

In the proof of [73, theorem 10.4], it was shown that

$$\|\mu - \pi_h^0 \mu\|_{H^{-1/2}(\Gamma)} \leq \|\mu\|_{H^{-1/2}(\Gamma)}, \quad (5.15)$$

and so

$$\|\pi_h^0 \mu\|_{H^{-1/2}(\Gamma)} \leq 2 \|\mu\|_{H^{-1/2}(\Gamma)}. \quad (5.16)$$

Combining (5.13) and (5.16) completes the proof. \square

For the following analysis, we assume that assumption 3.3 (continuity) and assumption 3.4 (approximation) hold. We also make the following additional assumptions.

Assumption 5.1 (Gårding's inequality). *There exists $\alpha > 0$, $\delta > 0$ such that $\forall (v, \mu) \in \mathbb{W}$*

$$\alpha \|(v, \mu)\|_{\mathcal{B}}^2 - \delta \|(v, \mu)\|_{\mathbb{V}}^2 \leq \mathcal{A}[(v, \mu), (v, \mu)] + \mathcal{B}[(v, \mu), (v, \mu)].$$

Assumption 5.2 (Injectivity). *Let $(w, \eta) \in \mathbb{W}$. If $\forall (v, \mu) \in \mathbb{W}$,*

$$\mathcal{A}[(w, \eta), (v, \mu)] + \mathcal{B}[(w, \eta), (v, \mu)] = 0,$$

then $(w, \eta) = 0$.

Let $(v, \mu) \in \mathbb{W}$. If $\forall (w, \eta) \in \mathbb{W}$,

$$\mathcal{A}[(w, \eta), (v, \mu)] + \mathcal{B}[(w, \eta), (v, \mu)] = 0,$$

then $(v, \mu) = 0$.

Assumption 5.3 (Quasi-continuity). *There exists $M > 0$ such that for all $(v_h, \mu_h) \in \mathbb{V}_h$*

and $(w, \eta) \in \mathbb{W}$,

$$(\mathcal{A} + \mathcal{B})[(v_h, \mu_h), (w, \eta) - \pi_h(w, \eta)] \leq M \|(v_h, \mu_h)\|_{\mathcal{B}} \|(w, \eta) - \pi_h(w, \eta)\|_{\mathbb{V}},$$

and

$$(\mathcal{A} + \mathcal{B})[(w, \eta) - \pi_h(w, \eta), (v_h, \mu_h)] \leq M \|(v_h, \mu_h)\|_{\mathcal{B}} \|(w, \eta) - \pi_h(w, \eta)\|_{\mathbb{V}}.$$

Assumption 5.4 (Asymptotic convergence). *Let $\epsilon > 0$ and $(w, \eta) \in \mathbb{W}$. There exists $h_0 > 0$ such that for all $h < h_0$,*

$$\|(w, \eta) - \pi_h(w, \eta)\|_{\mathcal{B}} < \epsilon \|(w, \eta)\|_{\mathcal{B}}.$$

We now proceed to prove that if assumptions 3.3, 3.4 and 5.1 to 5.4 hold, then assumptions 3.1 and 3.2 will hold.

Lemma 5.2 (Inf-sup condition). *If assumptions 5.1 and 5.2 hold, then assumption 3.1 holds.*

Proof. Following the proof of [52, theorem 2], we suppose (for a contradiction) that the first part assumption 3.1 does not hold. This means that for any n , there exists $(v_n, \mu_n) \in \mathbb{W}$ such that $\|(v_n, \mu_n)\|_{\mathcal{B}} = 1$ and

$$\sup_{(w, \eta) \in \mathbb{W} \setminus \{0\}} \frac{(\mathcal{A} + \mathcal{B})[(v_n, \mu_n), (w, \eta)]}{\|(w, \eta)\|_{\mathcal{B}}} \leq \frac{1}{n} \|(v_n, \mu_n)\|_{\mathcal{B}} = \frac{1}{n}. \quad (5.17)$$

The space \mathbb{W} is closed, hence the sequence $\{(v_n, \mu_n)\}_{n=1}^{\infty}$ has a convergent subsequence that converges to $(v_{\infty}, \mu_{\infty}) \in \mathbb{W}$. In the remainder of this proof, all limits refer to this convergent subsequence.

Let $(t, \kappa) \in \mathbb{W}$ with $\|(t, \kappa)\|_{\mathcal{B}} = 1$. By (5.17), we see that

$$\begin{aligned} |(\mathcal{A} + \mathcal{B})[(v_n, \mu_n), (t, \kappa)]| &\leq \sup_{(w, \eta) \in \mathbb{W} \setminus \{0\}} \frac{(\mathcal{A} + \mathcal{B})[(v_n, \mu_n), (w, \eta)]}{\|(w, \eta)\|_{\mathcal{B}}} \\ &\leq \frac{1}{n}, \end{aligned}$$

and so

$$\begin{aligned} 0 \leq |(\mathcal{A} + \mathcal{B})[(v_{\infty}, \mu_{\infty}), (t, \kappa)]| &= \lim_{n \rightarrow \infty} |(\mathcal{A} + \mathcal{B})[(v_n, \mu_n), (t, \kappa)]| \\ &\leq \lim_{n \rightarrow \infty} \frac{1}{n} \\ &= 0. \end{aligned} \quad (5.18)$$

By assumption 5.2, this implies that $(v_{\infty}, \mu_{\infty}) = 0$.

By assumption 5.1, we see that

$$\begin{aligned} (\mathcal{A} + \mathcal{B})[(v_n, \mu_n), (v_n, \mu_n)] &\geq \alpha \|(v_n, \mu_n)\|_{\mathcal{B}}^2 - \delta \|(v_n, \mu_n)\|_{\mathbb{V}}^2 \\ &= \alpha - \delta \|(v_n, \mu_n)\|_{\mathbb{V}}^2, \end{aligned}$$

and so

$$\begin{aligned} (\mathcal{A} + \mathcal{B})[(v_\infty, \mu_\infty), (v_\infty, \mu_\infty)] &= \lim_{n \rightarrow \infty} (\mathcal{A} + \mathcal{B})[(v_n, \mu_n), (v_n, \mu_n)] \\ &\geq \lim_{n \rightarrow \infty} \left(\alpha - \delta \|(v_n, \mu_n)\|_{\mathbb{V}}^2 \right) \\ &= \alpha > 0 \end{aligned} \tag{5.19}$$

Combining (5.18) and (5.19), we see that $0 > 0$, which is a contradiction; and so the first part of assumption 3.1 holds.

The second part of assumption 3.1 immediately follows from the second part of assumption 5.2. \square

In order to show that assumption 3.2 holds, we will require the following results

Lemma 5.3. *Let $(v, \mu) \in \mathbb{W}$. If assumption 3.4 holds, then for any $\epsilon > 0$, there is an $h_0 > 0$ such that for all $h < h_0$,*

$$\inf_{(w_h, \eta_h) \in \mathbb{V}_h} \|(v, \mu) - (w_h, \eta_h)\|_{\mathbb{V}} < \epsilon.$$

Proof. Let $c > 0$ and $k > 0$. Let $(v_c, \mu_c) \in H^{1/2+k}(\Gamma) \times H^{-1/2+k}(\Gamma)$ be a mollification of (v, μ) such that

$$\|(v, \mu) - (v_c, \mu_c)\|_{\mathbb{V}} \leq c.$$

Using the triangle inequality and assumption 3.4, we see that

$$\begin{aligned} \inf_{(w_h, \eta_h) \in \mathbb{V}_h} \|(v, \mu) - (w_h, \eta_h)\|_{\mathbb{V}} &\leq \|(v, \mu) - (v_c, \mu_c)\|_{\mathbb{V}} + \inf_{(w_h, \eta_h) \in \mathbb{V}_h} \|(v_c, \mu_c) - (w_h, \eta_h)\|_{\mathbb{V}} \\ &\leq c + h^k \left(|v_c|_{H^{1/2+k}(\Gamma)} + |\mu_c|_{H^{-1/2+k}(\Gamma)} \right). \end{aligned}$$

Taking $c = \epsilon/2$ and

$$h < h_0 = \left(\frac{\epsilon}{2 \left(|v_c|_{H^{1/2+k}(\Gamma)} + |\mu_c|_{H^{-1/2+k}(\Gamma)} \right)} \right)^{\frac{1}{k}},$$

we obtain the desired result. \square

Corollary 5.1. *Let $(v, \mu) \in \mathbb{W}$. If assumption 3.4 holds, then for any $\epsilon > 0$, there is an*

$h_0 > 0$ such that for all $h < h_0$,

$$\|(v, \mu) - \pi_h(v, \mu)\|_{\mathbb{V}} < \epsilon.$$

Proof. For any $(w_h, \eta_h) \in \mathbb{V}_h$, we see by the triangle inequality and lemma 5.1

$$\begin{aligned} \|(v, \mu) - \pi_h(v, \mu)\|_{\mathbb{V}} &\leq \|(v, \mu) - (w_h, \eta_h)\|_{\mathbb{V}} + \|\pi_h[(v, \mu) - (w_h, \eta_h)]\|_{\mathbb{V}} \\ &\leq (1 + c) \|(v, \mu) - (w_h, \eta_h)\|_{\mathbb{V}}. \end{aligned}$$

Therefore by lemma 5.3, the result holds. \square

We note that corollary 5.1 holds independently of assumption 5.4, and so this result may be used later when we proving that the projection for each problem satisfies assumption 5.4.

We now prove that assumption 3.2 holds.

Lemma 5.4 (Discrete inf-sup stability). *If assumptions 3.3, 3.4 and 5.1 to 5.4 hold, then assumption 3.2 holds.*

Proof. Following the proof of [11, theorem 2.2], we suppose (for a contradiction) that the first part of assumption 3.2 does not hold. This implies that there exists a sequence $(h_n)_{n \in \mathbb{N}}$ such that $\lim_{n \rightarrow \infty} h_n = 0$, and for each n there exists $(v_{h_n}, \mu_{h_n}) \in \mathbb{V}_{h_n}$ such that

$$\|(v_{h_n}, \mu_{h_n})\|_{\mathcal{B}} = 1 \tag{5.20}$$

$$\sup_{(w_{h_n}, \eta_{h_n}) \in \mathbb{V}_{h_n}} \frac{(\mathcal{A} + \mathcal{B})[(v_{h_n}, \mu_{h_n}), (w_{h_n}, \eta_{h_n})]}{\|(w_{h_n}, \eta_{h_n})\|_{\mathcal{B}}} < k_n, \tag{5.21}$$

where $k_n > 0$ and $\lim_{n \rightarrow \infty} k_n = 0$.

We define $F : \mathbb{V}_{h_n} \rightarrow \mathbb{V}_{h_n}$, for $(t_{h_n}, \kappa_{h_n}) \in \mathbb{V}_{h_n}$, by

$$\langle F(t_{h_n}, \kappa_{h_n}), (w_{h_n}, \eta_{h_n}) \rangle_{\Gamma} = (\mathcal{A} + \mathcal{B})[(t_{h_n}, \kappa_{h_n}), (w_{h_n}, \eta_{h_n})] \quad \forall (w_{h_n}, \eta_{h_n}) \in \mathbb{V}_{h_n}.$$

Let $(t, \kappa) \in \mathbb{W} \setminus \{0\}$. We use the triangle inequality, assumption 3.3 and (5.20) and (5.21) to obtain

$$L := \langle F(v_{h_n}, \mu_{h_n}), (t, \kappa) \rangle_{\Gamma} \tag{5.22}$$

$$\begin{aligned} &= |(\mathcal{A} + \mathcal{B})[(v_{h_n}, \mu_{h_n}), (t, \kappa)]| \\ &\leq |(\mathcal{A} + \mathcal{B})[(v_{h_n}, \mu_{h_n}), (t, \kappa) - \pi_{h_n}(t, \kappa)]| + |(\mathcal{A} + \mathcal{B})[(v_{h_n}, \mu_{h_n}), \pi_{h_n}(t, \kappa)]| \\ &\leq M \|(t, \kappa) - \pi_{h_n}(t, \kappa)\|_{\mathbb{V}} + k_n \|\pi_{h_n}(t, \kappa)\|_{\mathcal{B}}. \end{aligned} \tag{5.23}$$

Let $\epsilon > 0$. By corollary 5.1, there is an $N \in \mathbb{N}$ such that for all $n > N$,

$$\|(t, \kappa) - \pi_{h_n}(t, \kappa)\|_{\mathbb{V}} < \epsilon, \tag{5.24}$$

$$k_n < \epsilon. \tag{5.25}$$

Using the triangle inequality and assumption 5.4, we see that

$$\begin{aligned} \|\pi_{h_n}(t, \kappa)\|_{\mathcal{B}} &\leq \|(t, \kappa) - \pi_{h_n}(t, \kappa)\|_{\mathcal{B}} + \|(t, \kappa)\|_{\mathcal{B}} \\ &< \epsilon + \|(t, \kappa)\|_{\mathcal{B}}. \end{aligned} \quad (5.26)$$

Substituting (5.24) to (5.26) into (5.23), we obtain

$$\begin{aligned} L &< M\epsilon + k_n\epsilon + k_n \|(t, \kappa)\|_{\mathcal{B}} \\ &< M\epsilon + \epsilon^2 + \epsilon \|(t, \kappa)\|_{\mathcal{B}}, \end{aligned} \quad (5.27)$$

and so $F(v_{h_n}, \mu_{h_n}) \rightarrow 0$ (weakly). By lemma 5.2, F has a continuous inverse, and so $(v_{h_n}, \mu_{h_n}) \rightarrow 0$ (weakly).

By lemmas 1.6 and 1.7, there exists a compact operator $C : \mathbb{V}_{h_n} \rightarrow \mathbb{V}_{h_n}$ such that the operator $A + C$ is elliptic. Following the proofs for the Laplace problem in chapter 3, we see that there exists $\alpha > 0$ such that

$$\alpha \|(v_{h_n}, \mu_{h_n})\|_{\mathcal{B}} \leq \sup_{(w_{h_n}, \eta_{h_n}) \in \mathbb{V}_{h_n}} \frac{\langle (F + C)(v_{h_n}, \mu_{h_n}), (w_{h_n}, \eta_{h_n}) \rangle_{\Gamma}}{\|(w_{h_n}, \eta_{h_n})\|_{\mathcal{B}}}.$$

Since C is compact, $C(v_{h_n}, \mu_{h_n}) \rightarrow 0$ (strongly in \mathbb{V}), and so $\|C(v_{h_n}, \mu_{h_n})\|_{\mathbb{V}} \rightarrow 0$.

Using (5.21), we see that

$$\begin{aligned} \alpha \|(v_{h_n}, \mu_{h_n})\|_{\mathcal{B}} &\leq \sup_{(w_{h_n}, \eta_{h_n}) \in \mathbb{V}_{h_n}} \frac{\langle F(v_{h_n}, \mu_{h_n}), (w_{h_n}, \eta_{h_n}) \rangle_{\Gamma}}{\|(w_{h_n}, \eta_{h_n})\|_{\mathcal{B}}} + \sup_{(w_{h_n}, \eta_{h_n}) \in \mathbb{V}_{h_n}} \frac{\langle C(v_{h_n}, \mu_{h_n}), (w_{h_n}, \eta_{h_n}) \rangle_{\Gamma}}{\|(w_{h_n}, \eta_{h_n})\|_{\mathcal{B}}} \\ &\leq k_n + \sup_{(w_{h_n}, \eta_{h_n}) \in \mathbb{V}_{h_n}} \frac{\langle C(v_{h_n}, \mu_{h_n}), (w_{h_n}, \eta_{h_n}) \rangle_{\Gamma}}{\|(w_{h_n}, \eta_{h_n})\|_{\mathcal{B}}}. \end{aligned}$$

By the Cauchy–Schwarz inequality,

$$\begin{aligned} \langle C(v_{h_n}, \mu_{h_n}), (w_{h_n}, \eta_{h_n}) \rangle_{\Gamma} &\leq \|C(v_{h_n}, \mu_{h_n})\|_{\mathbb{V}} \|(w_{h_n}, \eta_{h_n})\|_{\mathbb{V}} \\ &\leq \|C(v_{h_n}, \mu_{h_n})\|_{\mathbb{V}} \|(w_{h_n}, \eta_{h_n})\|_{\mathcal{B}}. \end{aligned}$$

Taking N_ϵ large enough so that for all $n > N_\epsilon$, $k_n < \frac{\epsilon}{2}$ and $\|C(v_{h_n}, \mu_{h_n})\|_{\mathbb{C}} < \frac{\epsilon}{2}$, we see that

$$\alpha \|(v_{h_n}, \mu_{h_n})\|_{\mathcal{B}} < \epsilon.$$

This contradicts (5.20), and so the first part of assumption 3.2 holds.

To prove the second part of assumption 3.2, we suppose (for a contradiction) that it does not hold, and so there exists $(w_h, \eta_h) \in \mathbb{V}_h$ with $\|(w_h, \eta_h)\|_{\mathcal{B}} = 1$ such that

$$(\mathcal{A} + \mathcal{B})[(v_h, \mu_h), (w_h, \eta_h)] = 0 \quad \forall (v_h, \mu_h) \in \mathbb{V}_h. \quad (5.28)$$

By lemma 5.2, there exists $(t, \kappa) \in \mathbb{W}$ such that

$$L := |(\mathcal{A} + \mathcal{B})[(t, \kappa), (w_h, \eta_h)]| > 0. \quad (5.29)$$

By (5.28) and assumption 5.3,

$$\begin{aligned} L &= |(\mathcal{A} + \mathcal{B})[(t, \kappa) - \pi_h(t, \kappa), (w_h, \eta_h)]| \\ &\leq M \|(t, \kappa) - \pi_h(t, \kappa)\|_{\mathbb{V}} \end{aligned} \quad (5.30)$$

Using corollary 5.1, we see that taking h small enough, we can bound this above by any $\epsilon > 0$, and so $L = 0$. This is a contradiction, and so the second part of assumption 3.2 holds. \square

Having shown that assumptions 3.3, 3.4 and 5.1 to 5.4 imply assumptions 3.1 and 3.2, we now restate the results of section 3.2 with these alternative assumptions.

Proposition 5.1. *If assumptions 5.1 and 5.2 hold, then the linear system defined by (3.32) is invertible. If, in addition, we assume that*

- *assumption 3.3 hold,*
- *there exists $L > 0$ such that $\mathcal{L}(w, \eta) \leq L \|(w, \eta)\|_{\mathcal{B}} \quad \forall (w, \eta) \in \mathbb{W},$*
- *the norms $\|\cdot\|_{\mathcal{B}}$ and $\|\cdot\|_*$ are equivalent,*

then the formulation (3.31) admits a unique solution in \mathbb{W} .

Proof. This follows from proposition 3.1 and lemma 5.2. \square

Proposition 5.2. *Assume that $(u, \lambda) \in \mathbb{V}$ is the solution to a boundary value problem of the form (1.38) satisfying the abstract form (3.31). Let $(u_h, \lambda_h) \in \mathbb{V}_h$ be the solution of (3.32). If assumptions 3.3, 3.4 and 5.1 to 5.4 are satisfied then*

$$\|(u - u_h, \lambda - \lambda_h)\|_{\mathcal{B}} \lesssim \inf_{(v_h, \mu_h) \in \mathbb{V}_h} \|(u - v_h, \lambda - \mu_h)\|_*. \quad (5.31)$$

Proof. This follows from proposition 3.2 and lemmas 5.2 and 5.4. \square

Corollary 5.2. *Let $(u, \lambda) \in H^s(\Gamma) \times H^r(\Gamma)$, for some $s \geq \frac{1}{2}$ and $r \geq -\frac{1}{2}$, satisfy the abstract form (3.31). Under the assumptions of proposition 5.2,*

$$\|(u - u_h, \lambda - \lambda_h)\|_{\mathcal{B}} \lesssim h^{\zeta-1/2} |u|_{H^\zeta(\Gamma)} + h^{\xi+1/2} |\lambda|_{H^\xi(\Gamma)},$$

where $\zeta = \min(k + 1, s)$ and $\xi = \min(l + 1, r)$.

Proof. Apply assumption 3.4 to the right hand side of (5.31). \square

Proposition 5.3. *Assume that $(u, \lambda) \in \mathbb{V}$ is the solution to a boundary value problem of the form (1.38) satisfying the abstract form (3.31) and that the assumptions of proposition 5.2 are satisfied. Let $(u_h, \lambda_h) \in \mathbb{V}_h$. Let $\tilde{u} : \Omega^+ \rightarrow \mathbb{R}$ be the reconstruction obtained using (1.47), with $u = \lambda$ and $u = u$; and $\tilde{u}_h : \Omega^+ \rightarrow \mathbb{R}$ be the reconstruction obtained using (3.34). Then there holds*

$$\|\tilde{u} - \tilde{u}_h\|_{H_{\text{loc}}^1(\Omega^+)} \lesssim \frac{M}{\alpha} \inf_{v_h, \mu_h \in \mathbb{V}_h} \|(u - v_h, \lambda - \mu_h)\|_*.$$

Proof. This follows from proposition 3.3 and lemmas 5.2 and 5.4. \square

Corollary 5.3. *Under the same assumptions of proposition 5.3,*

$$\|\tilde{u} - \tilde{u}_h\|_{H_{\text{loc}}^1(\Omega^+)} \lesssim h^{\zeta-1/2} |u|_{H^\zeta(\Gamma)} + h^{\xi+1/2} |\lambda|_{H^\xi(\Gamma)},$$

where $\zeta = \min(k+1, s)$ and $\xi = \min(l+1, r)$.

Proof. Apply assumption 3.4 to (3.40) in the proof of proposition 3.3. \square

— 5.2.1 —

APPLICATION OF THE THEORY TO THE HELMHOLTZ DIRICHLET PROBLEM

For a Dirichlet problem, the discretised formulation is: Find $(u_h, \lambda_h) \in \mathbb{V}_h$ such that

$$\mathcal{A}[(u_h, \lambda_h), (v_h, \mu_h)] + \mathcal{B}_D^+[(u_h, \lambda_h), (v_h, \mu_h)] = \mathcal{L}_D^+(v_h, \mu_h) \quad \forall (v_h, \mu_h) \in \mathbb{V}_h, \quad (5.32)$$

where \mathcal{B}_D^+ and \mathcal{L}_D^+ are defined in (5.8) and (5.9).

As in chapter 3, we define the norm

$$\|(v, \mu)\|_{\mathcal{B}_D} := \|(v, \mu)\|_{\mathbb{V}} + \beta_D^{1/2} \|v\|_{L^2(\Gamma_D)},$$

we let $\|\cdot\|_* = \|\cdot\|_{\mathcal{B}_D}$, and we let $\mathbb{W} = \mathbb{V}$.

We now proceed to verify that assumptions 3.3, 3.4 and 5.1 to 5.4 hold for this formulation.

Proposition 5.4 (Continuity). *Assumption 3.3 is satisfied for the Helmholtz Dirichlet problem.*

Proof. The proof is the same as the proof of proposition 3.6. \square

Proposition 5.5 (Approximation). *Assumption 3.4 is satisfied for the Helmholtz Dirichlet problem if $0 \leq \beta_D \lesssim h^{-1}$.*

Proof. The proof is the same as the proof of proposition 3.7. \square

Proposition 5.6 (Gårding's inequality). *Assumption 5.1 is satisfied for the Helmholtz Dirichlet problem.*

Proof. Let $(v, \mu) \in \mathbb{W}$. Using lemmas 1.6 and 1.7, we see that

$$\begin{aligned} (\mathcal{A} + \mathcal{B}_D^+)[(v, \mu), (v, \mu)] &= \langle \mathbf{V}\mu, \mu \rangle_\Gamma + \langle \mathbf{W}v, v \rangle_\Gamma + \langle \beta_D v, v \rangle_\Gamma \\ &\geq \alpha_V \|\mu\|_{H^{-1/2}(\Gamma)}^2 + \alpha_W \|v\|_{H^{1/2}(\Gamma)}^2 + \beta_D \|v\|_{L^2(\Gamma_D)}^2 - \langle \mathbf{C}_1 \mu, \mu \rangle_\Gamma - \langle \mathbf{C}_2 v, v \rangle_\Gamma, \end{aligned}$$

where the operators $\mathbf{C}_1 : H^{-1/2}(\Gamma) \rightarrow H^{1/2}(\Gamma)$ and $\mathbf{C}_2 : H^{1/2}(\Gamma) \rightarrow H^{-1/2}(\Gamma)$ are compact.

Compact operators are bounded, and so

$$\langle \mathbf{C}_1 \mu, \mu \rangle_\Gamma \leq c_1 \|\mu\|_{H^{-1/2}(\Gamma)}^2 \quad (5.33)$$

$$\langle \mathbf{C}_2 v, v \rangle_\Gamma \leq c_2 \|v\|_{H^{1/2}(\Gamma)}^2, \quad (5.34)$$

for some $c_1, c_2 \in \mathbb{R}$. Therefore,

$$\begin{aligned} (\mathcal{A} + \mathcal{B}_D^+)[(v, \mu), (v, \mu)] &\geq \alpha_V \|\mu\|_{H^{-1/2}(\Gamma)}^2 + \alpha_W \|v\|_{H^{1/2}(\Gamma)}^2 + \beta_D \|v\|_{L^2(\Gamma_D)}^2 - c_1 \|\mu\|_{H^{-1/2}(\Gamma)}^2 - c_2 \|v\|_{H^{1/2}(\Gamma)}^2 \\ &\geq \alpha \|(v, \mu)\|_{\mathcal{B}_D}^2 - \delta \|(v, \mu)\|_{\mathbb{V}}^2, \end{aligned}$$

where $\alpha = \min(\alpha_V, \alpha_W, 1)$ and $\delta = \max(c_1, c_2)$. \square

Proposition 5.7 (Injectivity). *Assumption 5.2 is satisfied for the Helmholtz Dirichlet problem if k^2 is not a solution l of the exterior Laplace Dirichlet eigenvalue problem*

$$-\Delta u = lu \quad \text{in } \Omega^+, \quad \text{in } \Omega^+, \quad (5.35a)$$

$$\|u\|_{L^2(S)} > 0 \quad \text{for some } S \subset \Omega^+ \quad (5.35b)$$

$$\gamma_D^+ u = 0 \quad \text{on } \Gamma, \quad (5.35c)$$

$$u(\mathbf{x}) \rightarrow 0 \quad \text{as } |\mathbf{x}| \rightarrow \infty \quad (1.37b)$$

Proof. Suppose that $(v, \mu) \in \mathbb{W}$ such that

$$(\mathcal{A} + \mathcal{B}_D^+)[(v, \mu), (w, \eta)] = 0 \quad \forall (w, \eta) \in \mathbb{W}.$$

Taking $w = 0$, we see that

$$-\langle \mathbf{K}v, \eta \rangle_\Gamma + \langle \mathbf{V}\mu, \eta \rangle_\Gamma - \frac{1}{2} \langle v, \eta \rangle_\Gamma = 0 \quad \forall \eta \in H^{-1/2}(\Gamma),$$

and so $-\mathbf{K}v + \mathbf{V}\mu - \frac{1}{2}\text{Id}v = 0$. Let $\tilde{u} := \mathcal{K}v - \mathcal{V}\mu$. Then by (1.83) and (1.84),

$$-\Delta \tilde{u} - k^2 \tilde{u} = 0.$$

Using the definition of the Green's function for Helmholtz (1.42), we see that for $\mathbf{y} \in \Gamma$ and as $|\mathbf{x}| \rightarrow \infty$, $G(\mathbf{x}, \mathbf{y}) \rightarrow 0$, and therefore $\tilde{u}(\mathbf{x}) \rightarrow 0$. We also see that

$$\begin{aligned}\gamma_{\mathbb{D}}^+ \tilde{u} &= \left(\frac{1}{2}\text{Id} + \mathbf{K}\right)v - \mathbf{V}\mu \\ &= 0.\end{aligned}$$

Therefore either k^2 is a solution of (5.35), or $(v, \mu) = 0$ and hence the first part of assumption 5.2 holds.

To prove the second part of assumption 5.2, suppose that $(w, \eta) \in \mathbb{W}$ such that

$$(\mathcal{A} + \mathcal{B}_{\mathbb{D}}^+)[(v, \mu), (w, \eta)] = 0 \quad \forall (v, \mu) \in \mathbb{W}.$$

Talking $v = 0$ and proceeding as above, we find that either k^2 is a solution of (5.35) or $(w, -\eta) = 0$. Therefore the second part of assumption 5.2. \square

Proposition 5.8 (Quasi-continuity). *Assumption 5.3 is satisfied for the Helmholtz Dirichlet problem if $\beta_{\mathbb{D}} \lesssim h^{-1}$.*

Proof. Let $(v_h, \mu_h) \in \mathbb{V}_h$ and $(w, \eta) \in \mathbb{W}$. By the boundedness of the boundary operators (lemma 1.8), we know that

$$\mathcal{A}[(v_h, \mu_h), (w, \eta) - \pi_h(w, \eta)] \lesssim \|(v_h, \mu_h)\|_{\mathbb{V}} \|(w, \eta) - \pi_h(w, \eta)\|_{\mathbb{V}}. \quad (5.36)$$

By the definition of $\mathcal{B}_{\mathbb{D}}^+$,

$$\begin{aligned}\mathcal{B}_{\mathbb{D}}^+[(v_h, \mu_h), (w, \eta) - \pi_h(w, \eta)] &= \frac{1}{2} \langle \mu_h, w - \pi_h^1 w \rangle_{\Gamma} - \frac{1}{2} \langle v_h, \eta - \pi_h^0 \eta \rangle_{\Gamma} + \beta_{\mathbb{D}} \langle v_h, w - \pi_h^1 w \rangle_{\Gamma} \\ &\lesssim \|(v_h, \mu_h)\|_{\mathbb{V}} \|(w, \eta) - \pi_h(w, \eta)\|_{\mathbb{V}} + \beta_{\mathbb{D}} \langle v_h, w - \pi_h^1 w \rangle_{\Gamma}.\end{aligned} \quad (5.37)$$

To bound the final term of this, we note that due to the definition of π_h^1 ,

$$\begin{aligned}\beta_{\mathbb{D}} \langle v_h, w - \pi_h^1 w \rangle_{\Gamma} &= \beta_{\mathbb{D}} \langle v_h - \pi_h^1 v_h, w - \pi_h^1 w \rangle_{\Gamma} \\ &= \beta_{\mathbb{D}} \langle v_h - \pi_h^1 v_h, w - \pi_h^1 w - \pi_h^1(w - \pi_h^1 w) \rangle_{\Gamma}.\end{aligned} \quad (5.38)$$

Applying the Cauchy–Schwarz inequality and standard approximation results [73, theorems 10.4 and 10.9], we deduce that

$$\begin{aligned}\beta_{\mathbb{D}} \langle v_h, w - \pi_h^1 w \rangle_{\Gamma} &\leq \beta_{\mathbb{D}} \|v_h - \pi_h^1 v_h\|_{L^2(\Gamma)} \|w - \pi_h^1 w - \pi_h^1(w - \pi_h^1 w)\|_{L^2(\Gamma)} \\ &\leq \beta_{\mathbb{D}} h^{1/2} \|v_h\|_{H^{1/2}(\Gamma)} h^{1/2} \|w - \pi_h^1 w\|_{H^{1/2}(\Gamma)} \\ &= \beta_{\mathbb{D}} h \|v_h\|_{H^{1/2}(\Gamma)} \|w - \pi_h^1 w\|_{H^{1/2}(\Gamma)} \\ &\lesssim \|(v_h, \mu_h)\|_{\mathbb{V}} \|(w, \eta) - \pi_h(w, \eta)\|_{\mathbb{V}}.\end{aligned} \quad (5.39)$$

Combining (5.36) and (5.39) proves first part of assumption 5.3.

The second part of assumption 5.3 can be proved in the same way. \square

Proposition 5.9 (Asymptotic convergence). *Assumption 5.4 is satisfied for the Helmholtz Dirichlet problem if $\beta_D \lesssim h^{-1}$.*

Proof. Let $\epsilon > 0$. By the definition of $\|\cdot\|_{\mathcal{B}_D}$ and corollary 5.1, there exists $h_0 > 0$ such that for all $h < h_0$,

$$\begin{aligned} \|(w, \eta) - \pi_h(w, \eta)\|_{\mathcal{B}_D} &= \|(w, \eta) - \pi_h(w, \eta)\|_{\mathbb{V}} + \beta_D^{1/2} \|w - \pi_h w\|_{L^2(\Gamma)} \\ &\lesssim \epsilon + h^{-1/2} \|w - \pi_h w\|_{L^2(\Gamma)}. \end{aligned} \quad (5.40)$$

By standard approximation results [73, theorems 10.4 and 10.9] and corollary 5.1, we see that

$$\begin{aligned} \|w - \pi_h w\|_{L^2(\Gamma)}^2 &\leq h \|w - \pi_h w\|_{H^{1/2}(\Gamma)}^2 \\ &\leq h\epsilon^2. \end{aligned} \quad (5.41)$$

Combining (5.40) and (5.41) leads to the desired result \square

We have shown that assumptions 3.3, 3.4 and 5.1 to 5.4 are satisfied. Additionally the extra assumptions in proposition 5.1 are satisfied, so we conclude that the results of propositions 5.1 to 5.3 and corollaries 5.2 and 5.3 apply to the Dirichlet problem. This is summarised in the following result.

Theorem 5.1. *If k^2 is not a Dirichlet eigenvalue of the exterior Laplace problem, the Helmholtz Dirichlet problem (5.7) has a unique solution $(u, \lambda) \in H^s(\Gamma) \times H^r(\Gamma)$, for some $s \geq \frac{1}{2}$ and $r \geq -\frac{1}{2}$. The discrete Dirichlet problem (5.32) is invertible. If $0 < \beta_D \lesssim h^{-1}$, then its solution $(u_h, \lambda_h) \in P_h^1(\Gamma) \times DP_h^0(\Gamma)$ satisfies*

$$\|(u - u_h, \lambda - \lambda_h)\|_{\mathcal{B}_D} \lesssim h^{\zeta-1/2} |u|_{H^\zeta(\Gamma)} + h^{\xi+1/2} |\lambda|_{H^\xi(\Gamma)},$$

where $\zeta = \min(2, s)$ and $\xi = \min(1, r)$. Additionally,

$$\|\tilde{u} - \tilde{u}_h\|_{H_{\text{loc}}^1(\Omega^+)} \lesssim h^{\zeta-1/2} |u|_{H^\zeta(\Gamma)} + h^{\xi+1/2} |\lambda|_{H^\xi(\Gamma)},$$

where \tilde{u} and \tilde{u}_h are the solutions in Ω^+ computed using (1.49).

— 5.2.2 —

APPLICATION OF THE THEORY TO THE HELMHOLTZ MIXED
DIRICHLET–NEUMANN PROBLEM

For a mixed Dirichlet–Neumann problem, the discretised formulation is: Find $(u, \lambda) \in \mathbb{V}_h$ such that

$$\mathcal{A}[(u_h, \lambda_h), (v_h, \mu_h)] + \mathcal{B}_{\text{ND}}^+[(u_h, \lambda_h), (v_h, \mu_h)] = \mathcal{L}_{\text{ND}}^+(v_h, \mu_h) \quad \forall (v_h, \mu_h) \in \mathbb{V}_h. \quad (5.42)$$

For simplicity in this section, we assume that Γ_{D} and Γ_{N} are two disjoint closed objects, as in problems involving multiple scatterers. We expect the analysis of the general problem to be similar to that presented here.

As in chapter 3, we introduce the following norms.

$$\begin{aligned} \|(v, \mu)\|_{\mathcal{B}_{\text{ND}}} &:= \|(v, \mu)\|_{\mathbb{V}} + \beta_{\text{D}}^{1/2} \|v\|_{L^2(\Gamma_{\text{D}})} + \beta_{\text{N}}^{1/2} \|\mu\|_{L^2(\Gamma_{\text{N}})} \\ \|(v, \mu)\|_* &:= \|(v, \mu)\|_{\mathbb{V}} + \beta_{\text{D}}^{1/2} \|v\|_{L^2(\Gamma)} + \beta_{\text{N}}^{1/2} \|\mu\|_{L^2(\Gamma)}. \end{aligned}$$

We let $\mathbb{W} = H^{1/2}(\Gamma) \times L^2(\Gamma)$.

We now proceed to show that assumptions 3.3, 3.4 and 5.1 to 5.4 hold for the mixed Dirichlet–Neumann problem.

Proposition 5.10 (Continuity). *Assumption 3.3 is satisfied for the Helmholtz mixed Dirichlet–Neumann problem if $\exists \beta_{\text{min}} > 0$, independent of h , such that $\beta_{\text{D}}^{1/2} \beta_{\text{N}}^{1/2} > \beta_{\text{min}}$.*

Proof. The proof is the same as the proof of proposition 3.12. □

Proposition 5.11 (Approximation). *Assumption 3.4 is satisfied for the Helmholtz mixed Dirichlet–Neumann problem if $0 < \beta_{\text{D}} \lesssim h^{-1}$ and $0 < \beta_{\text{N}} \lesssim h$.*

Proof. The proof is the same as the proof of proposition 3.13. □

Proposition 5.12 (Gårding’s inequality). *Assumption 5.1 is satisfied for the Helmholtz mixed Dirichlet–Neumann problem.*

Proof. Let $(v, \mu) \in \mathbb{W}$. Using lemmas 1.6 and 1.7, we see that

$$\begin{aligned} \mathcal{A}[(v, \mu), (v, \mu)] + \mathcal{B}_{\text{ND}}^+[(v, \mu), (v, \mu)] &= \langle \mathbf{V}\mu, \mu \rangle_{\Gamma} + \langle \mathbf{W}v, v \rangle_{\Gamma} + \langle \beta_{\text{D}}v, v \rangle_{\Gamma_{\text{D}}} + \langle \beta_{\text{N}}\mu, \mu \rangle_{\Gamma_{\text{N}}} \\ &\geq \alpha_{\mathbf{V}} \|\mu\|_{H^{-1/2}(\Gamma)}^2 + \alpha_{\mathbf{W}} \|v\|_{H^{1/2}(\Gamma)}^2 + \beta_{\text{D}} \|v\|_{L^2(\Gamma_{\text{D}})}^2 + \beta_{\text{N}} \|\mu\|_{L^2(\Gamma_{\text{N}})}^2 - \langle \mathbf{C}_1\mu, \mu \rangle_{\Gamma} - \langle \mathbf{C}_2v, v \rangle_{\Gamma}, \end{aligned}$$

where the operators $\mathbf{C}_1 : H^{-1/2}(\Gamma) \rightarrow H^{1/2}(\Gamma)$ and $\mathbf{C}_2 : H^{1/2}(\Gamma) \rightarrow H^{-1/2}(\Gamma)$ are compact.

Proceeding as in the proof of proposition 5.6, we see that

$$\mathcal{A}[(v, \mu), (v, \mu)] + \mathcal{B}_{\text{ND}}^+[(v, \mu), (v, \mu)] \geq \alpha \|(v, \mu)\|_{\mathcal{B}_{\text{ND}}}^2 - \delta \|(v, \mu)\|_{\mathbb{V}}^2,$$

where $\alpha = \min(\alpha_V, \alpha_W, 1)$ and $\delta = \max(c_1, c_2)$. \square

Proposition 5.13 (Injectivity). *Assumption 5.2 is satisfied for the Helmholtz mixed Dirichlet–Neumann problem if k^2 is not a solution l of the exterior Laplace mixed eigenvalue problem*

$$-\Delta u = lu \quad \text{in } \Omega^+, \quad (5.43a)$$

$$\gamma_D^+ u = 0 \quad \text{on } \Gamma_D, \quad (5.43b)$$

$$\gamma_N^+ u = 0 \quad \text{on } \Gamma_N, \quad (5.43c)$$

$$u(\mathbf{x}) \rightarrow 0 \quad \text{as } |\mathbf{x}| \rightarrow \infty. \quad (1.37b)$$

Proof. Suppose that $(v, \mu) \in \mathbb{W}$ such that

$$(\mathcal{A} + \mathcal{B}_N^+)[(v, \mu), (w, \eta)] = 0 \quad \forall (w, \eta) \in \mathbb{W}. \quad (5.44)$$

Taking $w = \begin{cases} 0 & \text{in } \Gamma_D \\ w & \text{in } \Gamma_N \end{cases}$ and $\eta = \begin{cases} 0 & \text{in } \Gamma_N \\ \eta & \text{in } \Gamma_D \end{cases}$, we see that

$$\begin{aligned} -\langle \mathcal{K}_D v_D, \eta \rangle_{\Gamma_D} + \langle \mathcal{V}_D \mu_D, \eta \rangle_{\Gamma_D} - \frac{1}{2} \langle v_D, \eta \rangle_{\Gamma_D} &= 0 & \forall \eta \in H^{-1/2}(\Gamma_D), \\ \langle \mathcal{W}_N v_N, w \rangle_{\Gamma_N} + \langle \mathcal{K}'_N \mu_N, w \rangle_{\Gamma_N} - \frac{1}{2} \langle \mu_N, w \rangle_{\Gamma_N} &= 0 & \forall w \in H^{1/2}(\Gamma_N), \end{aligned}$$

where \mathcal{K}_D , \mathcal{V}_D , v_D , μ_D , \mathcal{W}_N , \mathcal{K}'_N , v_N , and μ_N are the operators and function restricted to the disjoint surfaces Γ_D and Γ_N . We deduce that $(\frac{1}{2}\text{Id}_D + \mathcal{K}_D)v_D - \mathcal{V}_D \mu_D = 0$ and $(\frac{1}{2}\text{Id}_N - \mathcal{K}'_N)\mu_N - \mathcal{W}_N v_N = 0$ on Γ_N .

Let $\tilde{u} := \mathcal{K}_D v_D - \mathcal{V}_D \mu_D + \mathcal{K}'_N v_N - \mathcal{W}_N \mu_N$. Then by (1.83) and (1.84),

$$-\Delta \tilde{u} - k^2 \tilde{u} = 0.$$

Using the definition of the Green's function for Helmholtz (1.42), we see that for $\mathbf{y} \in \Gamma$ and as $|\mathbf{x}| \rightarrow \infty$, $G(\mathbf{x}, \mathbf{y}) \rightarrow 0$, and therefore $\tilde{u}(\mathbf{x}) \rightarrow 0$. We also see that, on Γ_D ,

$$\begin{aligned} \gamma_D^+ \tilde{u} &= (\frac{1}{2}\text{Id}_D + \mathcal{K}_D)v_D - \mathcal{V}_D \mu_D \\ &= 0; \end{aligned}$$

and on Γ_N ,

$$\begin{aligned} \gamma_N^+ \tilde{u} &= -\mathcal{W}_N v_N + (\frac{1}{2}\text{Id}_N - \mathcal{K}'_N)\mu_N \\ &= 0. \end{aligned}$$

Therefore either k^2 is a solution of (5.43), or $(v, \mu) = 0$ and hence the first part of assumption 5.2 holds.

The second part of assumption 5.2 can be proved in the same way with the roles of

(v, μ) and (w, η) reversed. \square

Proposition 5.14 (Quasi-continuity). *Assumption 5.3 is satisfied for the Helmholtz mixed Dirichlet–Neumann problem if $\beta_D \approx h^{-1}$ and $\beta_N \approx h$.*

Proof. Let $(v_h, \mu_h) \in \mathbb{V}_h$ and $(w, \eta) \in \mathbb{W}$. By the boundedness of the boundary operators (lemma 1.8), we know that

$$\mathcal{A}[(v_h, \mu_h), (w, \eta) - \pi_h(w, \eta)] \lesssim \|(v_h, \mu_h)\|_{\mathbb{V}} \|(w, \eta) - \pi_h(w, \eta)\|_{\mathbb{V}}. \quad (5.45)$$

By the definition of $\mathcal{B}_{\text{ND}}^+$,

$$\begin{aligned} L &:= \mathcal{B}_{\text{ND}}^+[(v_h, \mu_h), (w, \eta) - \pi_h(w, \eta)] \\ &= \frac{1}{2} \langle \mu_h, w - \pi_h^1 w \rangle_{\Gamma_D} - \frac{1}{2} \langle v_h, \eta - \pi_h^0 \eta \rangle_{\Gamma_D} + \beta_D \langle v_h, w - \pi_h^1 w \rangle_{\Gamma_D} \\ &\quad - \frac{1}{2} \langle \mu_h, w - \pi_h^1 w \rangle_{\Gamma_N} + \frac{1}{2} \langle v_h, \eta - \pi_h^0 \eta \rangle_{\Gamma_N} + \beta_N \langle \mu_h, \eta - \pi_h^0 \eta \rangle_{\Gamma_N} \\ &= \frac{1}{2} \langle \mu_h, w - \pi_h^1 w \rangle_{\Gamma} + \frac{1}{2} \langle v_h, \eta - \pi_h^0 \eta \rangle_{\Gamma} + \beta_D \langle v_h, w - \pi_h^1 w \rangle_{\Gamma_D} \\ &\quad - \langle \mu_h, w - \pi_h^1 w \rangle_{\Gamma_N} - \langle v_h, \eta - \pi_h^0 \eta \rangle_{\Gamma_D} + \beta_N \langle v_h, w - \pi_h^1 w \rangle_{\Gamma_N} \\ &\lesssim \|(v_h, \mu_h)\|_{\mathbb{V}} \|(w, \eta) - \pi_h(w, \eta)\|_{\mathbb{V}} \\ &\quad + \underbrace{h^{-1} \langle v_h, w - \pi_h^1 w \rangle_{\Gamma_D}}_{\text{(I)}} + \underbrace{h \langle \mu_h, \eta - \pi_h^0 \eta \rangle_{\Gamma_N}}_{\text{(II)}} - \underbrace{\langle \mu_h, w - \pi_h^1 w \rangle_{\Gamma_N}}_{\text{(III)}} - \underbrace{\langle v_h, \eta - \pi_h^0 \eta \rangle_{\Gamma_D}}_{\text{(IV)}}. \end{aligned} \quad (5.46)$$

In order to bound these terms, we note that

$$\begin{aligned} \|w - \pi_h^1 w\|_{L^2(\Gamma)}^2 &= \langle w - \pi_h^1 w, w - \pi_h^1 w \rangle_{\Gamma} \\ &= \langle w - \pi_h^1 w, w - \pi_h^1 w - \pi_h^1(w - \pi_h^1 w) \rangle_{\Gamma} \\ &= \langle w - \pi_h^1 w - \pi_h^1(w - \pi_h^1 w), w - \pi_h^1 w - \pi_h^1(w - \pi_h^1 w) \rangle_{\Gamma} \\ &= \|w - \pi_h^1 w - \pi_h^1(w - \pi_h^1 w)\|_{L^2(\Gamma)}^2, \end{aligned} \quad (5.47)$$

and so, by a standard approximation result [73, theorem 10.9],

$$\|w - \pi_h^1 w\|_{L^2(\Gamma)} \lesssim h^{1/2} \|w - \pi_h^1 w\|_{H^{1/2}(\Gamma)}. \quad (5.48)$$

By [39, theorem 3.5, remark 3.6], we see that

$$\|\eta - \pi_h^0 \eta\|_{L^2(\Gamma)} \leq h^{-1/2} \|\eta - \pi_h^0 \eta\|_{H^{-1/2}(\Gamma)}. \quad (5.49)$$

Using the Cauchy–Schwarz inequality, (5.48) and (5.49), we can now bound each of

the terms in (5.46).

$$\begin{aligned}
\text{(I)} &\leq h^{-1} \|v_h\|_{L^2(\Gamma_D)} \|w - \pi_h^1 w\|_{L^2(\Gamma)} \\
&\lesssim h^{-1/2} \|v_h\|_{L^2(\Gamma_D)} \|w - \pi_h^1 w\|_{H^{1/2}(\Gamma)} \\
&\lesssim \beta_D^{1/2} \|v_h\|_{L^2(\Gamma_D)} \|w - \pi_h^1 w\|_{H^{1/2}(\Gamma)}, \tag{5.50}
\end{aligned}$$

$$\begin{aligned}
\text{(II)} &\leq h \|\mu_h\|_{L^2(\Gamma_N)} \|\eta - \pi_h^0 \eta\|_{L^2(\Gamma)} \\
&\leq h^{1/2} \|\mu_h\|_{L^2(\Gamma_N)} \|\eta - \pi_h^0 \eta\|_{H^{-1/2}(\Gamma)} \\
&\lesssim \beta_N^{1/2} \|\mu_h\|_{L^2(\Gamma_N)} \|\eta - \pi_h^0 \eta\|_{H^{-1/2}(\Gamma)}, \tag{5.51}
\end{aligned}$$

$$\begin{aligned}
\text{(III)} &\leq \|\mu_h\|_{L^2(\Gamma_N)} \|w - \pi_h^1 w\|_{L^2(\Gamma)} \\
&\lesssim h^{1/2} \|\mu_h\|_{L^2(\Gamma_N)} \|w - \pi_h^1 w\|_{H^{1/2}(\Gamma)} \\
&\lesssim \beta_N^{1/2} \|\mu_h\|_{L^2(\Gamma_N)} \|w - \pi_h^1 w\|_{H^{1/2}(\Gamma)}, \tag{5.52}
\end{aligned}$$

$$\begin{aligned}
\text{(IV)} &\leq \|v_h\|_{L^2(\Gamma_D)} \|\eta - \pi_h^0 \eta\|_{L^2(\Gamma)} \\
&\leq h^{-1/2} \|v_h\|_{L^2(\Gamma_D)} \|\eta - \pi_h^0 \eta\|_{H^{-1/2}(\Gamma)} \\
&\lesssim \beta_D^{1/2} \|v_h\|_{L^2(\Gamma_D)} \|\eta - \pi_h^0 \eta\|_{H^{-1/2}(\Gamma)}, \tag{5.53}
\end{aligned}$$

and so

$$L \lesssim \|(v_h, \mu_h)\|_{\mathcal{B}_{\text{ND}}} \|(w, \eta) - \pi_h(w, \eta)\|_{\mathbb{V}}. \tag{5.54}$$

Combining (5.45) and (5.54) proves first part of assumption 5.3.

The second part of assumption 5.3 can be proved in the same way. \square

Proposition 5.15 (Asymptotic convergence). *Assumption 5.4 is satisfied for the Helmholtz mixed Dirichlet–Neumann problem if $\exists \beta_{\text{max}} > 0$ such that $\beta_D \lesssim h^{-1}$ and $\beta_N \lesssim h$.*

Proof. Let $\epsilon > 0$. By the definition of $\|\cdot\|_{\mathcal{B}_{\text{ND}}}$ and corollary 5.1, there exists $h_0 > 0$ such that for all $h < h_0$,

$$\begin{aligned}
\|(w, \eta) - \pi_h(w, \eta)\|_{\mathcal{B}_{\text{ND}}} &= \|(w, \eta) - \pi_h(w, \eta)\|_{\mathbb{V}} + \beta_D^{1/2} \|w - \pi_h^1 w\|_{L^2(\Gamma_D)} + \beta_N^{1/2} \|\eta - \pi_h^0 \eta\|_{L^2(\Gamma_N)} \\
&\lesssim \epsilon + h^{-1/2} \|w - \pi_h^1 w\|_{L^2(\Gamma)} + h^{1/2} \|\eta - \pi_h^0 \eta\|_{L^2(\Gamma)}. \tag{5.55}
\end{aligned}$$

By (5.48) and corollary 5.1, we see that

$$\begin{aligned}
\|w - \pi_h^1 w\|_{L^2(\Gamma)} &\lesssim h^{1/2} \|w - \pi_h^1 w\|_{H^{1/2}(\Gamma)} \\
&\leq h^{1/2} \epsilon. \tag{5.56}
\end{aligned}$$

By (5.49) and corollary 5.1, we see that

$$\begin{aligned} \|\eta - \pi_h^0 \eta\|_{L^2(\Gamma)} &\leq h^{-1/2} \|\eta - \pi_h^0 \eta\|_{H^{-1/2}(\Gamma)} \\ &\leq h^{-1/2} \epsilon. \end{aligned} \quad (5.57)$$

Combining (5.55) to (5.57) leads to the desired result \square

We have shown that assumptions 3.3, 3.4 and 5.1 to 5.4 are satisfied. Additionally the extra assumptions in proposition 5.1 are satisfied, so we conclude that the results of propositions 5.1 to 5.3 and corollaries 5.2 and 5.3 apply to the mixed Dirichlet–Neumann problem. This is summarised in the following result.

Theorem 5.2. *Let $(u, \lambda) \in H^s(\Gamma) \times H^r(\Gamma)$, for some $s \geq \frac{1}{2}$ and $r \geq 0$, be the unique solution to the Helmholtz mixed Dirichlet–Neumann problem. This solution satisfies (5.10). Let $(u_h, \lambda_h) \in P_h^1(\Gamma) \times DP_h^0(\Gamma)$ be the solution of (5.42). If k^2 is not a eigenvalue of the exterior mixed Laplace problem, $\beta_D \approx h^{-1}$, $\beta_N \approx h$ and $\exists \beta_{\min} > 0$ such that $\beta_D^{1/2} \beta_N^{1/2} > \beta_{\min}$, then*

$$\|(u - u_h, \lambda - \lambda_h)\|_{\mathcal{B}_{ND}} \lesssim h^{\zeta-1/2} |u|_{H^\zeta(\Gamma)} + h^{\xi+1/2} |\lambda|_{H^\xi(\Gamma)},$$

where $\zeta = \min(2, s)$ and $\xi = \min(1, r)$.

— 5.3 —

NUMERICAL RESULTS FOR THE HELMHOLTZ EQUATION

In this section, we demonstrate the theory with a series of numerical examples. All linear systems used are preconditioned with blocked mass matrix preconditioners, as described in sections 2.2.4 and 2.2.5.

— 5.3.1 —

DIRICHLET AND MIXED DIRICHLET–NEUMANN PROBLEMS

Define

$$g_D(\mathbf{x}) = \frac{e^{ik|\mathbf{x}|}}{|\mathbf{x}|} + \frac{e^{ik|\mathbf{r}|}}{|\mathbf{r}|}, \quad (5.58)$$

$$g_N(\mathbf{x}) = \frac{(ik|\mathbf{x}| - 1)e^{ik|\mathbf{x}|}}{|\mathbf{x}|^3} \mathbf{x} \cdot \boldsymbol{\nu} + \frac{(ik|\mathbf{r}| - 1)e^{ik|\mathbf{r}|}}{|\mathbf{r}|^3} \mathbf{r} \cdot \boldsymbol{\nu}, \quad (5.59)$$

where $\mathbf{r} = \mathbf{x} - (\frac{1}{2}, \frac{1}{2}, 0)$. It is easy to check that for any wavenumber $k > 0$ and any bounded domain Ω^- with $(0, 0, 0), (\frac{1}{2}, \frac{1}{2}, 0) \in \Omega^-$ and $\Omega^+ := \mathbb{R}^3 \setminus \Omega^-$, $u(\mathbf{x}) = \frac{e^{ik|\mathbf{x}|}}{|\mathbf{x}|} + \frac{e^{ik|\mathbf{r}|}}{|\mathbf{r}|}$

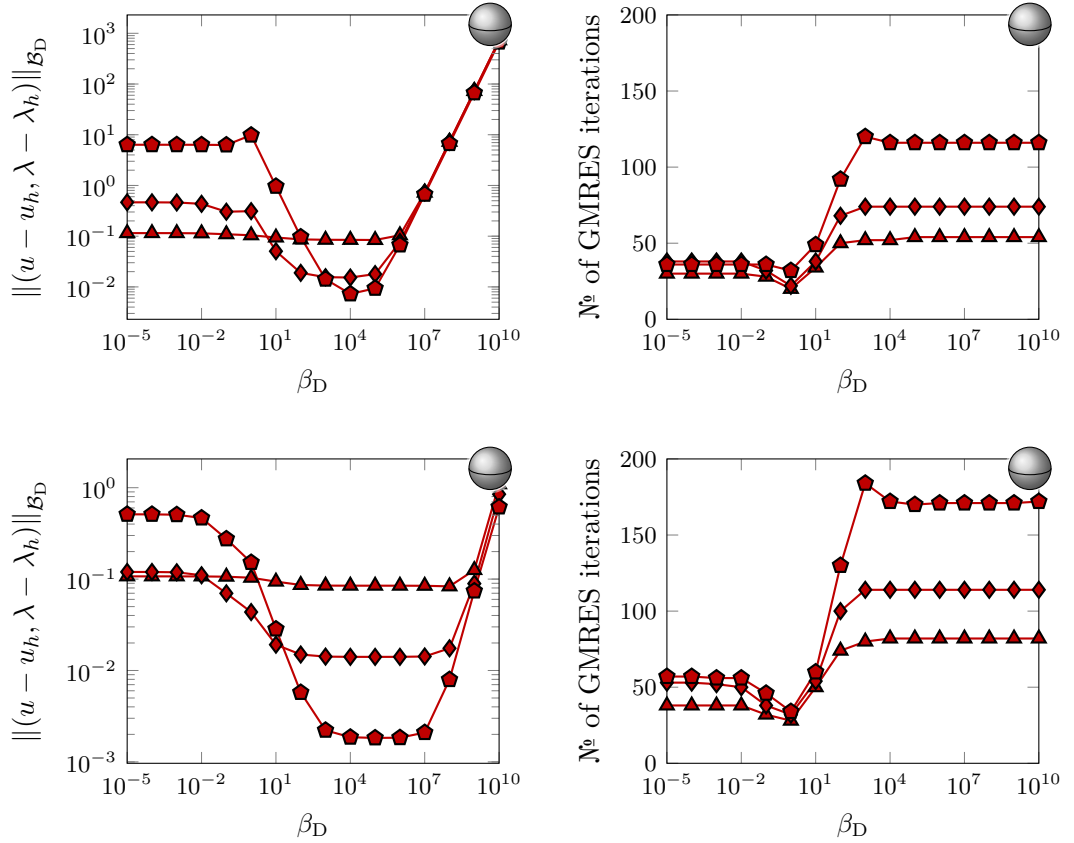


Figure 5.1: The error (left) and GMRES iteration counts (right) as β_D is varied for the penalty method for the Helmholtz Dirichlet problem with $k = 2$ on the unit sphere with $h = 2^{-2}$ (red triangles) $h = 2^{-3.5}$ (red diamonds) $h = 2^{-5}$ (red pentagons), solved to a GMRES tolerance of 10^{-8} (top) and 10^{-11} (bottom). Here we take $(u_h, \lambda_h), (v_h, \mu_h) \in P_h^1(\Gamma) \times \text{DUAL}_h^0(\Gamma)$.

is the solution of the exterior Helmholtz problem

$$-\Delta u - k^2 u = 0 \quad \text{in } \Omega^+, \quad (1.38a)$$

$$\frac{\partial u^{\text{scat}}}{\partial |\mathbf{x}|} - iku^{\text{scat}} = o(|\mathbf{x}|^{-1}) \quad \text{as } |\mathbf{x}| \rightarrow \infty, \quad (1.38b)$$

$$u = g_D \quad \text{on } \Gamma_D, \quad (1.37c)$$

$$\frac{\partial u}{\partial \boldsymbol{\nu}} = g_N \quad \text{on } \Gamma_N, \quad (1.37d)$$

with $u^{\text{inc}} = 0$ (and so $u = u^{\text{scat}}$).

DIRICHLET BOUNDARY CONDITIONS

In this section, we let Ω^- be the unit sphere and $\Gamma_D = \Gamma$, and solve the resulting Dirichlet problem with $\mathbb{V}_h = P_h^1(\Gamma) \times \text{DUAL}_h^0(\Gamma)$. Figure 5.1 shows the error compared to the exact solution and number of GMRES iteration required for a range of values of the parameter β_D for this problem with $k = 2$ discretised on grids with $h = 2^{-2}$, $h = 2^{-3.5}$ and $h = 2^{-5}$.

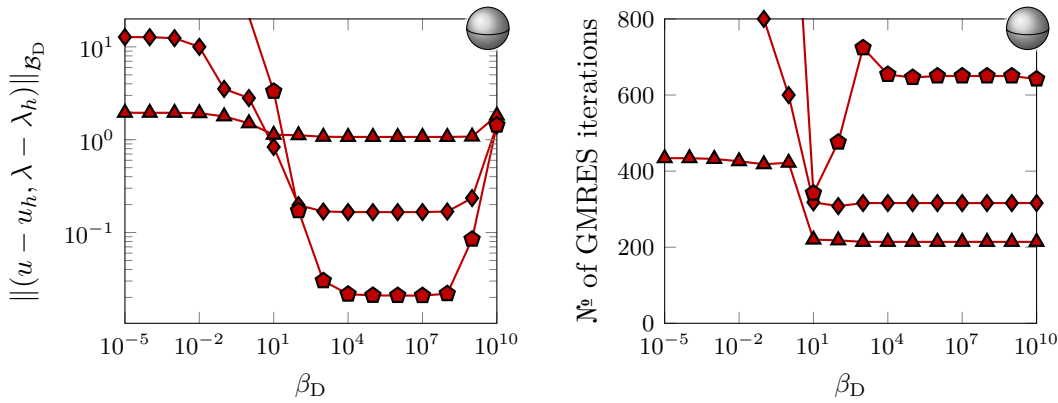


Figure 5.2: The error (left) and GMRES iteration counts (right) as β_D is varied for the penalty method for the Helmholtz Dirichlet problem with $k = 10$ on the unit sphere with $h = 2^{-2}$ (red triangles) $h = 2^{-3.5}$ (red diamonds) $h = 2^{-5}$ (red pentagons), solved to a GMRES tolerance of 10^{-11} . Here we take $(u_h, \lambda_h), (v_h, \mu_h) \in P_h^1(\Gamma) \times \text{DUAL}_h^0(\Gamma)$.

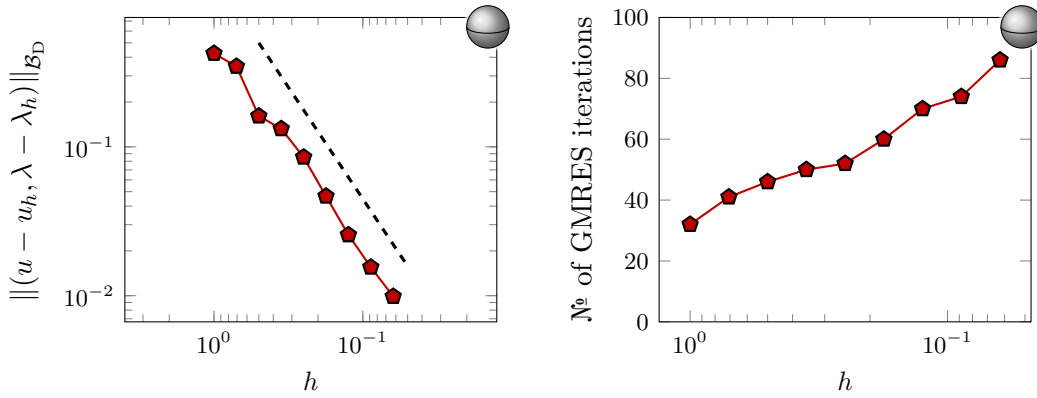


Figure 5.3: The convergence (left) and GMRES iteration counts (right) of the penalty method for the Helmholtz Dirichlet problem with $k = 2$ on the unit sphere with $\beta_D = 90/h$, solved to a GMRES tolerance of 10^{-9} . Here we take $(u_h, \lambda_h), (v_h, \mu_h) \in P_h^1(\Gamma) \times \text{DUAL}_h^0(\Gamma)$. The dashed line shows order 1.5 convergence.

As in chapters 3 and 4, the ill-conditioning of this system is an issue. Due to this we must take a small GMRES tolerance to obtain good results, so that the GMRES algorithm will only exit once the residuals very small. As the matrices involved here have a high condition number, an approximate solution with a quite small (but not small enough) GMRES residual could still have a high error. Solving with a SciPy’s default tolerance of 10^{-5} (figure 5.1, top) leads to limited convergence, while solving with a tolerance of 10^{-11} (figure 5.1, bottom) leads to good convergence for values of β_D between around 10^2 and 10^5 . As in the Laplace case, the development of better preconditioners warrants future work.

Figure 5.2 shows the error compared to the exact solution and number of GMRES iterations required for a range of values of β_D for this problem with $k = 10$, solved to a GMRES tolerance of 10^{-11} . It can be seen here that values of β_D in a similar range to those for $k = 2$ lead to good convergence, although the problem at this higher wavenumber has worse conditioning so requires more iterations to solve.

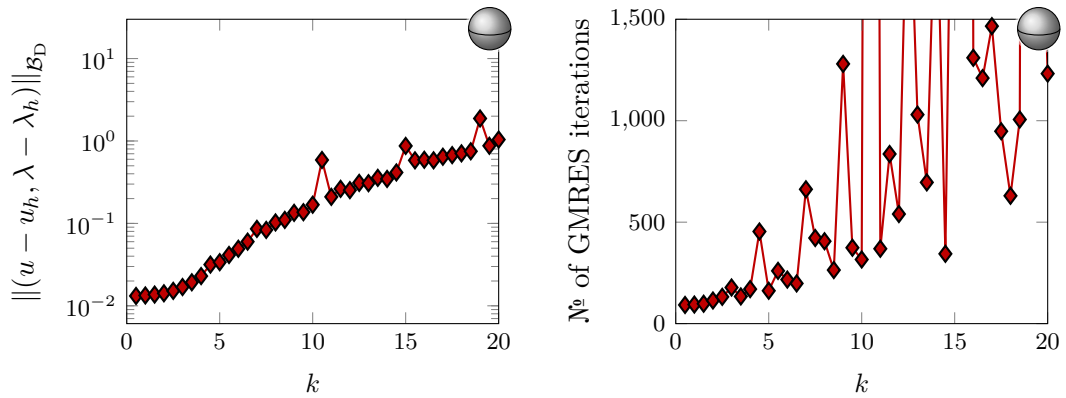


Figure 5.4: The error (left) and GMRES iteration counts (right) as the wavenumber k is varied for the penalty method for the Helmholtz Dirichlet problem with $\beta_D = 90/h$ on the unit sphere with $h = 2^{-3.5}$, solved to a GMRES tolerance of 10^{-11} . Here we take $(u_h, \lambda_h), (v_h, \mu_h) \in P_h^1(\Gamma) \times \text{DUAL}_h^0(\Gamma)$.

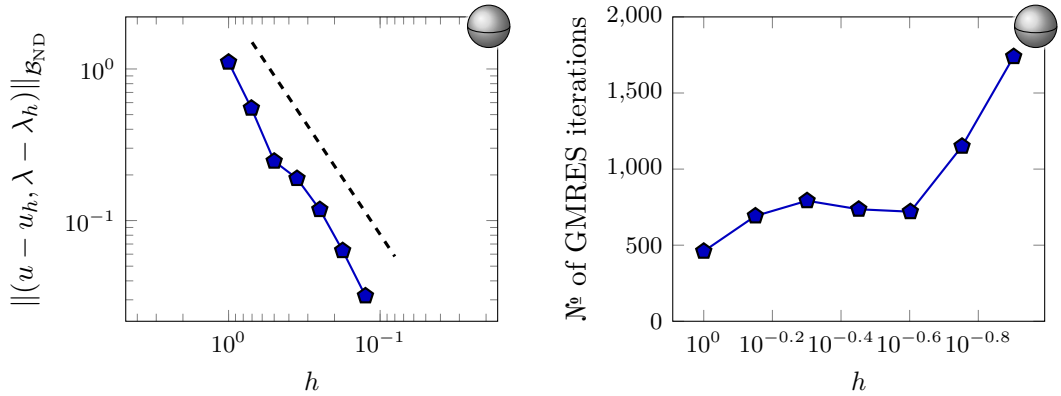


Figure 5.5: The convergence (left) and GMRES iteration counts (right) of the penalty method for the Helmholtz mixed Dirichlet–Neumann problem with $k = 2$ on the unit sphere with $\beta_D = 90/h$ and $\beta_N = 90h$, solved to a GMRES tolerance of 10^{-9} . Here we take $(u_h, \lambda_h), (v_h, \mu_h) \in P_h^1(\Gamma) \times \text{DUAL}_h^0(\Gamma)$. The dashed line shows order 1.5 convergence.

In figure 5.3, we take $\beta_D = 90/h$ and look at the convergence as h is reduced. We observe order 1.5 convergence in agreement with theorem 5.1.

Figure 5.4 shows how the error and iteration count change as the wavenumber k is increased. It can be seen that the error gradually increases as the wavenumber increases, with some spikes in the error near resonances. At higher wavenumbers, the system is more prone to ill-conditioning, and the iteration counts are very high for the majority of larger wavenumbers.

MIXED DIRICHLET–NEUMANN BOUNDARY CONDITIONS

In this section, we let Ω^- be the unit sphere, $\Gamma_D = \{(x, y, z) \in \Gamma : x < 0\}$, $\Gamma_N = \Gamma \setminus \Gamma_D$, and solve the resulting mixed Dirichlet–Neumann problem with $\mathbb{V}_h = P_h^1(\Gamma) \times \text{DUAL}_h^0(\Gamma)$.

Figure 5.5 shows the error and iteration count for this problem as h is reduced, with $\beta_D = 90/h$ and $\beta_N = 90h$. We observe order 1.5 convergence in agreement with theo-

rem 5.2.

— 5.3.2 —

APPLICATION TO MULTIPLE SCATTERERS

We now look at an application of this method to wave scattering problems. Let u^{inc} be an incident wave that satisfies

$$-\Delta u^{\text{inc}} - k^2 u^{\text{inc}} = 0 \quad \text{in } \Omega^+. \quad (5.60)$$

Typically, we take $u^{\text{inc}}(\mathbf{x}) = Ae^{ik\mathbf{x}\cdot\mathbf{d}}$, where \mathbf{d} is a unit vector representing the direction of the wave and $A \in \mathbb{R}$ is constant. Splitting total wave u^{tot} into the scattered wave u^{scat} and the incident wave u^{inc} leads us to the following problem.

$$-\Delta u^{\text{scat}} - k^2 u^{\text{scat}} = 0 \quad \text{in } \Omega^+, \quad (5.61a)$$

$$\frac{\partial u^{\text{scat}}}{\partial |\mathbf{x}|} - ik u^{\text{scat}} = o(|\mathbf{x}|^{-1}) \quad \text{as } |\mathbf{x}| \rightarrow \infty, \quad (1.38b)$$

$$u^{\text{scat}} = -u^{\text{inc}} + g_{\text{D}} \quad \text{on } \Gamma_{\text{D}}, \quad (5.61b)$$

$$\frac{\partial u^{\text{scat}}}{\partial \boldsymbol{\nu}} = -\frac{\partial u^{\text{inc}}}{\partial \boldsymbol{\nu}} + g_{\text{N}} \quad \text{on } \Gamma_{\text{N}}. \quad (5.61c)$$

For sound-soft scattering, we take $g_{\text{D}} = 0$ and $\Gamma = \Gamma_{\text{D}}$ (and so $\gamma_{\text{D}}^+ u^{\text{tot}} = 0$); for sound-hard scattering, we take $g_{\text{N}} = 0$ and $\Gamma = \Gamma_{\text{N}}$ (and so $\gamma_{\text{N}}^+ u^{\text{tot}} = 0$).

This method of weak imposition gives us a natural way of dealing with problems involving multiple scatterers, with the scatterers having different properties. As an example, let Γ be comprised of two unit spheres, Γ_1 and Γ_2 , centred at $(0, 0, 0)$ and $(2.5, 1.2, 0.5)$ respectively. Let Γ_1 be a sound-soft scatterer and Γ_2 be a sound-hard scatterer, and so set $\Gamma_{\text{D}} = \Gamma_1$ and $\Gamma_{\text{N}} = \Gamma_2$.

To solve this problem using weak imposition, we assemble the global multitrace operator on the whole of $\Gamma = \Gamma_1 \cup \Gamma_2$, then add the terms on the first row of (5.11) for the sound-soft scatterer Γ_1 , and the terms on the second row of (5.11) for the sound-hard scatterer Γ_2 . The right-hand side is defined by (5.12) with the appropriate terms for each scatterer.

Figure 5.6 shows two slices through solution of this problem with an incident wave given by $u^{\text{inc}} = e^{ik\mathbf{x}\cdot\mathbf{d}}$, where $\mathbf{d} = (\frac{1}{\sqrt{5}}, \frac{2}{\sqrt{5}}, 0)$ and $k = 2$. The values of u^{tot} in Ω^+ in this diagram were computed using (1.49).

A greater number of scatterers could be implemented by adding the appropriate sparse terms for each scatterer. Figure 5.7 shows the incident wave $u^{\text{inc}}(x, y, z) = e^{iky}$, where $k = 2$, scattering off an array of 25 spheres that are a mixture of sound-hard and sound-soft. In order to solve this problem with objects of the same shape but with different material properties would only require the reassembly of the sparse terms that implement the boundary conditions. Therefore this method is well suited to inverse problems where

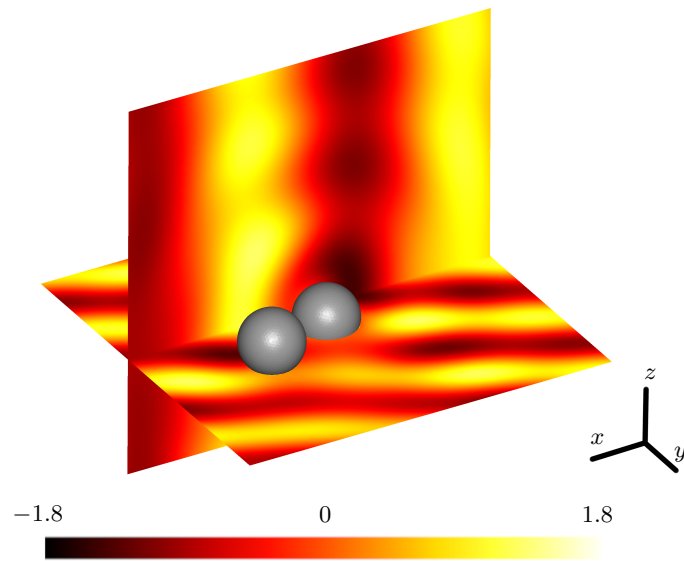


Figure 5.6: The incident wave $u^{\text{inc}} = e^{ik\mathbf{x}\cdot\mathbf{d}}$, where $\mathbf{d} = (\frac{1}{\sqrt{5}}, \frac{2}{\sqrt{5}}, 0)$ and $k = 2$, scattering off two spheres. The sphere on the left is sound-hard and the sphere on the right is sound-soft. Here, we took $\mathbb{V}_h = P_h^1(\Gamma) \times \text{DUAL}_h^0(\Gamma)$, $\beta_D = 90/h$, $\beta_N = 90h$, and used a GMRES tolerance of 10^{-11} .

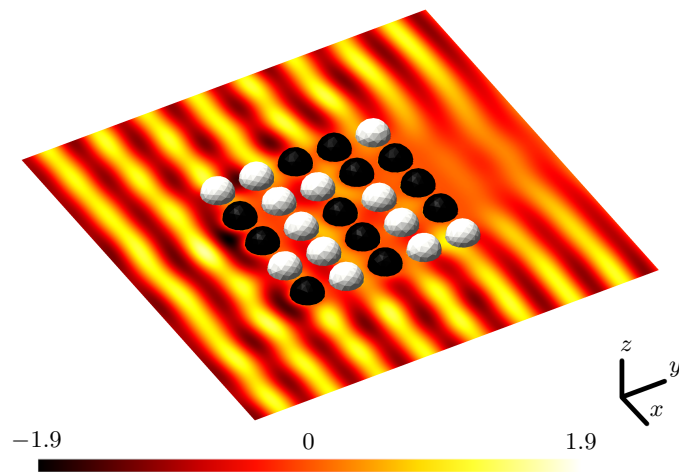


Figure 5.7: The incident wave $u^{\text{inc}} = e^{ik\mathbf{x}\cdot\mathbf{d}}$, where $\mathbf{d} = (0, 1, 0)$ and $k = 2$, scattering off 25 spheres. The white spheres are sound-hard and the black spheres are sound-soft. Here, we took $\mathbb{V}_h = P_h^1(\Gamma) \times \text{DUAL}_h^0(\Gamma)$, $\beta_D = 90/h$, $\beta_N = 90h$, and used a GMRES tolerance of 10^{-11} .

the type of material is unknown, such as the design of metamaterials.

— 5.4 —

CONCLUDING REMARKS

In this chapter, we have derived and analysed the weak imposition of Dirichlet and mixed Dirichlet–Neumann boundary conditions on the Helmholtz equation. Both the formulations derived in this chapter bear a close resemblance to the formulations for Laplace in chapter 3, and the corresponding formulations for Neumann and Robin problems can be easily derived. We expect the analysis of these formulations to follow the same outline as the Dirichlet and mixed Dirichlet–Neumann formulations analysed here.

For Maxwell’s equations, formulations for Dirichlet, Neumann, and mixed problems can be derived in the same way as for Laplace and Helmholtz problems, and closely resemble those in this chapter. The analysis of these formulations, however, looks likely to be very different to the analysis for Laplace and Helmholtz.

In the tests we have run to experiment with weak imposition for Maxwell’s equations, we have been unable to obtain good solutions in a reasonable amount of time. As we saw in section 2.4, Maxwell problems are prone to being strongly ill-conditioned, and this appears to be a major issue for this method. Therefore, we believe that it is necessary to design more powerful preconditioners for these weak formulations in order to make this method feasible for Maxwell problems.



Now that you’ve finished reading chapter 5, the final chapter of this thesis, why not celebrate by cracking open figure 5.8 before reading the conclusions and appendices.

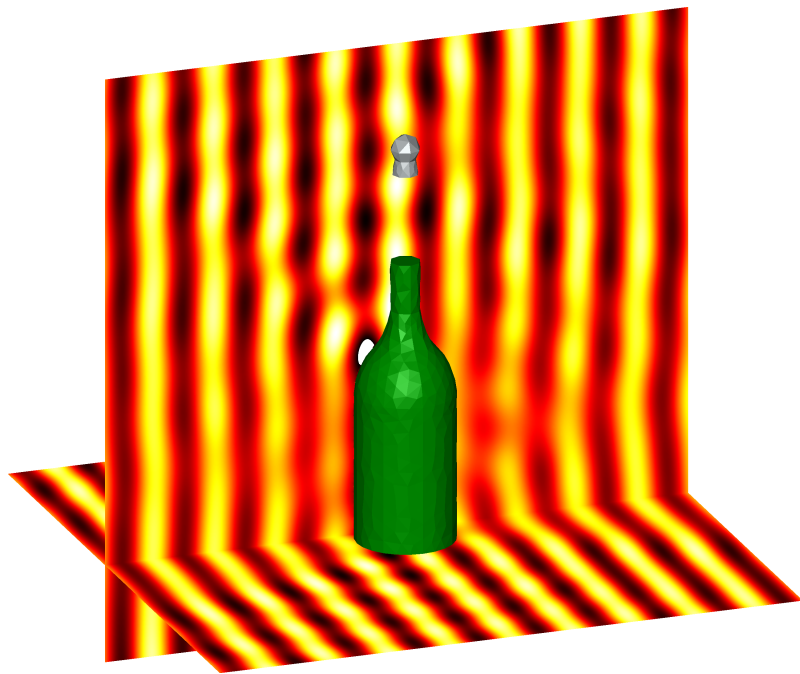


Figure 5.8: An acoustic wave scattering off a sound-hard champagne bottle and a sound-soft cork.

CONCLUDING REMARKS

In this thesis, we have looked at a method of weakly imposing boundary conditions and operator preconditioning methods, both derived from properties of the Calderón projector.

We have derived and analysed formulations for the weak imposition of Dirichlet, Neumann, mixed Dirichlet–Neumann, Robin, and Signorini boundary conditions on Laplace’s equation (chapters 3 and 4); and Dirichlet, and mixed Dirichlet–Neumann conditions on the Helmholtz equation (chapter 5).

Perhaps the most obvious area for future work is the extension of this theory to other boundary conditions and problems. The extension of the theory to Maxwell’s equations would be of particular interest, and elements of the theory differ greatly from that presented here. The weak imposition of Signorini boundary conditions for elasticity would also be of particular interest, as this was the application for which these conditions were first introduced in [69].

As we saw throughout chapters 3 to 5, the ill-conditioning of the linear systems arising from the formulations for weakly imposed boundary conditions limits the use of such methods. Hence, the development of better preconditioners for such systems presents itself as an important area of future work.

It would be desirable to design a blocked operator preconditioner that exploits properties of the Calderón projector to give a better conditioned system on the continuous level, similar to the Calderón preconditioners we used in chapter 2. Alternatively, formulations could be derived by adding the weighted penalty terms to a Calderón projector that has already had a preconditioner applied. If a carefully chosen preconditioner is used here, it may be that the resulting linear system is well conditioned, or an operator preconditioner for the final system may be easier to design.

As we remarked in section 3.3, the penalty terms that are added to the Calderón projector are sparse and only have non-zero entries for nearby triangles, and so methods such as hierarchical LU can be used with limited algorithmic changes. An investigation of hierarchical LU preconditioners, or the use of direct hierarchical LU solvers as an alternative to preconditioned GMRES for the systems arising from weak imposition would be an interesting area for future work.

One final avenue of future interest would be the formulation of coupled BEM-BEM and FEM-BEM within the framework of weak imposition. This would allow the extension of the method described in section 5.3.2 to problems involving penetrable objects, or a mixture of penetrable and non-penetrable objects.

<APPENDICES>

APPENDIX A

NOTATION

In this appendix, we list the notation used throughout this thesis as a useful reference.

DOMAINS, SURFACES, ETC.

Symbol(s)	Meaning
Ω^-	An interior domain
Ω^+	An exterior domain
Γ	The boundary of a domain
Γ_D	The Dirichlet part of a boundary
Γ_N	The Neumann part of a boundary
Γ_R	The Robin part of a boundary
Γ_C	The contact part of a boundary
ν	The outward pointing normal to the surface Γ
ν_x	The outward pointing normal to the surface Γ at the point x
θ	The number of smooth faces of Γ
$\Gamma^1, \dots, \Gamma^\theta$	The smooth faces of Γ

TRIANGULATIONS OF SURFACES

Symbol(s)	Meaning
\mathcal{T}_h	A triangulation of Γ with largest triangle diameter h
T_i	The i th triangle in the triangulation \mathcal{T}_h
n	The number of vertices in a triangulation of Γ
m	The number of edges in a triangulation of Γ
o	The number of triangles in a triangulation of Γ
v_1, \dots, v_n	The vertices of a triangulation
u_1, \dots, u_m	The midpoints of the edges of a triangulation
w_1, \dots, w_o	The midpoints of the faces of a triangulation

POINTS, VECTORS, ETC.

Symbol(s)	Meaning
Bold lowercase: $\mathbf{x}, \mathbf{y}, \dots$	A point in 3D space
x, y and z	The three components of a point \mathbf{x}

DIFFERENTIAL OPERATORS

Symbol(s)	Meaning
∇	The vector derivative, $\left(\frac{\partial}{\partial x}, \frac{\partial}{\partial y}, \frac{\partial}{\partial z}\right)$
Δ	The Laplacian, $\frac{\partial^2}{\partial x^2} + \frac{\partial^2}{\partial y^2} + \frac{\partial^2}{\partial z^2}$
div	The divergence, $\nabla \cdot$
curl	The curl, $\nabla \times$
div_Γ	The scalar surface divergence
div_Γ	The vector surface divergence
curl_Γ	The scalar surface curl
curl_Γ	The vector surface curl

OPERATORS AND MATRICES

Symbol(s)	Meaning
Curly capitals: $\mathcal{K}, \mathcal{V}, \dots$	Potential operators
Sans-serif capitals: $\mathbf{K}, \mathbf{V}, \dots$	Boundary operators
Bold serif capitals: $\mathbf{K}, \mathbf{V}, \dots$	Matrices
C^-, C^+	Interior and exterior Calderón projectors
A	Multitrace operator
Id, M	Identity operator/mass matrix
$\mathcal{V}, \mathbf{V}, \mathbf{V}$	Single layer operator/matrix
$\mathcal{K}, \mathbf{K}, \mathbf{K}$	Double layer operator/matrix
\mathbf{K}', \mathbf{K}'	Adjoint double layer operator/matrix
\mathbf{W}, \mathbf{W}	Hypersingular operator/matrix
$\mathcal{E}, \mathbf{E}, \mathbf{E}$	Electric field operator/matrix
$\mathcal{H}, \mathbf{H}, \mathbf{H}$	Magnetic field operator/matrix

FUNCTIONS

Symbol(s)	Meaning
G	The Green's function
Lowercase letters: ϕ, ψ, u, f, \dots	Scalar valued functions
Bold lowercase letters: $\boldsymbol{\phi}, \boldsymbol{\psi}, \boldsymbol{u}, \boldsymbol{f}, \dots$	Vector valued functions
Greek letters with subscripts: $\phi_i, \psi_i, \phi_i, \dots$	Basis functions of a discrete space

FUNCTION SPACES

Symbol(s)	Meaning
$\mathcal{H}_X^{\text{dom}}$	The domain of an operator X
$\mathcal{H}_X^{\text{ran}}$	The range of an operator X
$\mathcal{H}_X^{\text{dual}}$	The dual to the range of an operator X
$L^2(\Upsilon)$	The space of square integrable functions on the domain Υ
$L_{\text{loc}}^2(\Upsilon)$	The space of locally square integrable functions on the domain Υ
$H^s(\Upsilon)$	The order s Sobolev space on the domain Υ of functions whose mean value is 0
$H_*^s(\Upsilon)$	The order s Sobolev space on the domain Υ
$H_{\text{loc}}^s(\Upsilon)$	The locally order s Sobolev space on the domain Υ
$H^s(\text{op}, \Upsilon)$	The order s Sobolev space of op-conforming functions on the domain Υ
$H_{\text{loc}}^s(\text{op}, \Upsilon)$	The locally order s Sobolev space of op-conforming functions on the domain Υ
$\mathbf{L}^2(\Upsilon)$	The space of square integrable vector functions on the domain Υ
$\mathbf{L}_{\text{loc}}^2(\Upsilon)$	The space of locally square integrable vector functions on the domain Υ
$\mathbf{H}^s(\Upsilon)$	The order s vector Sobolev space on the domain Υ
$\mathbf{H}_{\text{loc}}^s(\Upsilon)$	The locally order s vector Sobolev space on the domain Υ
$\mathbf{H}^s(\mathbf{op}, \Upsilon)$	The order s vector Sobolev space of op -conforming functions on the domain Υ
$\mathbf{H}^s(\text{op}, \Upsilon)$	The order s vector Sobolev space of op-conforming functions on the domain Υ
$\mathbf{H}_{\text{loc}}^s(\mathbf{op}, \Upsilon)$	The locally order s vector Sobolev space of op -conforming functions on the domain Υ
$\mathbf{H}_{\text{loc}}^s(\text{op}, \Upsilon)$	The locally order s vector Sobolev space of op-conforming functions on the domain Υ

$\mathbf{L}_t^2(\Gamma)$	The space of square integrable tangential vector functions on the surface Γ
$\mathbf{H}_\times^s(\Gamma)$	The tangential order s vector Sobolev space on the surface Γ
$\mathbf{H}_\times^s(\text{op}, \Gamma)$	The tangential order s vector Sobolev space of op-conforming functions on the surface Γ
$\mathbf{H}_\times^s(\mathbf{op}, \Gamma)$	The tangential order s vector Sobolev space of \mathbf{op} -conforming functions on the surface Γ
\mathbf{H}	An order 0 vector Sobolev space, eg $\mathbf{H}(\Omega^-) = \mathbf{H}^0(\Omega^-)$
\mathbb{V}	The product space $H^{1/2}(\Gamma) \times H^{-1/2}(\Gamma)$ in the scalar case, or $[\mathbf{H}_\times^{-1/2}(\text{div}_\Gamma, \Gamma)]^2$ in the vector case
\mathbb{V}^*	The product space $H_*^{1/2}(\Gamma) \times H^{-1/2}(\Gamma)$

DISCRETE SPACES

Symbol(s)	Meaning
$\mathbf{P}_h^k(\Gamma)$	The space of continuous piecewise order k polynomials
$\mathbf{DP}_h^l(\Gamma)$	The space of discontinuous piecewise order l polynomials
$\mathbf{DUAL}_h^1(\Gamma)$	The space of continuous piecewise linear polynomials on the dual grid
$\mathbf{DUAL}_h^0(\Gamma)$	The space of discontinuous piecewise constant polynomials on the dual grid
$\mathbf{RT}_h^0(\Gamma)$	The space of Raviart–Thomas vector functions
$\mathbf{NC}_h^0(\Gamma)$	The space of Nédélec vector functions
$\mathbf{RWG}_h^0(\Gamma)$	The space of Rao–Wilton–Glisson vector functions
$\mathbf{SNC}_h^0(\Gamma)$	The space of scaled Nédélec vector functions
$\mathbf{BC}_h^0(\Gamma)$	The space of Buffa–Christiansen vector functions
$\mathbf{RBC}_h^0(\Gamma)$	The space of rotated Buffa–Christiansen vector functions
ϕ_i	The i th basis function of $\mathbf{P}_h^1(\Gamma)$
ψ_i	The i th basis function of $\mathbf{DP}_h^0(\Gamma)$
ξ_i	The i th basis function of $\mathbf{DUAL}_h^1(\Gamma)$
χ_i	The i th basis function of $\mathbf{DUAL}_h^0(\Gamma)$
ϕ_i	The i th basis function of $\mathbf{RT}_h^0(\Gamma)$
ψ_i	The i th basis function of $\mathbf{NC}_h^0(\Gamma)$
ζ_i	The i th basis function of $\mathbf{RWG}_h^0(\Gamma)$
ς_i	The i th basis function of $\mathbf{SNC}_h^0(\Gamma)$
ξ_i	The i th basis function of $\mathbf{BC}_h^0(\Gamma)$

χ_i	The i th basis function of $\mathbf{RBC}_h^0(\Gamma)$
\mathbb{V}_h	A discrete subspace of the product space \mathbb{V}
\mathbb{V}_h^*	A discrete subspace of the product space \mathbb{V}^*

TRACES

Symbol(s)	Meaning
$\gamma_{\mathbb{D}}^-$ and $\gamma_{\mathbb{D}}^+$	Interior and exterior Dirichlet traces
$\gamma_{\mathbb{N}}^-$ and $\gamma_{\mathbb{N}}^+$	Interior and exterior Neumann traces
$\gamma_{\mathbb{T}}^-$ and $\gamma_{\mathbb{T}}^+$	Interior and exterior tangential traces
$\gamma_{\mathbb{N},k}^-$ and $\gamma_{\mathbb{N},k}^+$	Interior and exterior (vector) Neumann traces
$\gamma_{\mathbb{V}}^-$ and $\gamma_{\mathbb{V}}^+$	Interior and exterior normal traces
$\llbracket \gamma_* \rrbracket_{\Gamma}$	The jump between the interior and exterior traces γ_*^- and γ_*^+
$\{\gamma_*\}_{\Gamma}$	The average of the interior and exterior traces γ_*^- and γ_*^+

LAPLACE'S EQUATION

Symbol(s)	Meaning
u	The solution
u	The Dirichlet trace of the solution, $\gamma_{\mathbb{D}}^{\pm} u$
λ	The Neumann trace of the solution, $\gamma_{\mathbb{N}}^{\pm} u$

THE HELMHOLTZ EQUATION

Symbol(s)	Meaning
k	The wavenumber
u^{inc}	The incident field
u^{scat}	The scattered field
u^{tot}	The total field
u	The Dirichlet trace of the total field, $\gamma_{\mathbb{D}}^{\pm} u^{\text{tot}}$
λ	The Neumann trace of the total field, $\gamma_{\mathbb{N}}^{\pm} u^{\text{tot}}$

MAXWELL'S EQUATIONS

Symbol(s)	Meaning
k	The wavenumber
ω	The wave's frequency
ϵ_0	The electric permittivity
μ_0	The electric permeability
e^{inc}	The incident field
e^{scat}	The scattered field
e^{tot}	The total field
e	The tangential trace of the total field, $\gamma_t^\pm e^{\text{tot}}$
h	The Neumann trace of the total field, $\gamma_{N,k}^\pm e^{\text{tot}}$

APPENDIX B

CONVERGENCE RESULTS FOR FUNCTIONS ON THE DUAL GRID

In this appendix, we present a proof of lemma 2.4. The proofs presented here are based on those in [73, chapter 10], and heavily use results from [16].

Throughout this appendix, we assume that the triangulations of Γ are quasi-uniform with shape regular elements.

— B.1 —

ORDER 0 DUAL SPACES, $\text{DUAL}_h^0(\Gamma)$

We define the projector $\pi_h^0 : L^2(\Gamma) \rightarrow \text{DUAL}_h^0(\Gamma)$, for $\mu \in L^2(\Gamma)$, by

$$\langle \pi_h^0 \mu, \eta_h \rangle_\Gamma = \langle \mu, \eta_h \rangle_\Gamma \quad \forall \eta_h \in \text{DUAL}_h^0(\Gamma). \quad (\text{B.1})$$

In the proof of the results in this appendix, we will use the following trace inequalities.

Lemma B.1. *Let $T_i \subset \mathbb{R}^2$ be a triangle in a triangulation \mathcal{T}_h of Γ . Let $E \subset \partial T_i$ be an edge of T_i . For any $\eta_h \in \text{DP}_h^0(\Gamma)$,*

$$\|\eta_h\|_{L^2(T_i)} \lesssim h_i^{1/2} \|\gamma_{T_i} \eta_h\|_{L^2(E)},$$

where h_i is the diameter of T_i , and γ_{T_i} is the trace on E from the interior T_i .

Proof. η_h is constant in T_i , so $\eta_h = \gamma_{[T_i]} \eta_h = k$ for some $k \in \mathbb{R}$. Hence,

$$\begin{aligned} \|\eta_h\|_{L^2(T_i)}^2 &= k^2 |T_i| \\ \|\gamma_{T_i} \eta_h\|_{L^2(E)}^2 &= k^2 |E|. \end{aligned}$$

By our regularity assumptions, it follows that

$$\|\eta_h\|_{L^2(T_i)}^2 \lesssim h \|\gamma_{T_i} \eta_h\|_{L^2(E)}^2.$$

□

Lemma B.2. *Let $T_i \subset \mathbb{R}^2$ be a triangle in a triangulation \mathcal{T}_h of Γ . Let $E \subset \partial T_i$ be an edge of T_i . For any $\eta \in H^1(\Gamma)$,*

$$\|\gamma_{T_i} \eta\|_{L^2(E)} \lesssim h_i^{-1/2} \|\eta\|_{L^2(T_i)} + h_i^{1/2} |\eta|_{H^1(T_i)},$$

where h_i is the diameter of T_i , and γ_{T_i} is the trace on E from the interior of T_i .

Proof. [61, corollary 6.1]. □

We now prove the following approximation result

Lemma B.3. *For all $\mu \in H^1(\Gamma)$,*

$$\|\pi_h^0 \mu - \mu\|_{L^2(\Gamma)} \lesssim h |\mu|_{H^1(\Gamma)} + h^{1/2} \|\mu\|_{H^{1/2}(\Gamma)}.$$

Proof. Let H_i be the face in the dual grid centred around the vertex \mathbf{v}_i of the coarse grid. Note that $H_i = H_i^1 \cup \dots \cup H_i^{n_i}$, where $H_i^1, \dots, H_i^{n_i}$ are triangles in the barycentrically refined grid adjacent to \mathbf{v}_i .

Let $\mu \in H^1(\Gamma)$. Consider the error on H_i ,

$$\|\pi_h^0 \mu - \mu\|_{L^2(H_i)}^2 = \sum_{j=1}^{n_i} \|\pi_h^0 \mu - \mu\|_{L^2(H_i^j)}^2. \quad (\text{B.2})$$

For each triangle H_i^j , we define $\pi_{h,i,j}^0 : L^2(\Gamma) \rightarrow \text{DUAL}_h^0(\Gamma)$, for $\mu \in L^2(\Gamma)$, by

$$\pi_{h,i,j}^0 \mu = |H_i^j|^{-1} \int_{H_i^j} \mu.$$

We now consider a fixed triangle H_i^j . Using the triangle inequality, we see that the error on H_i^j satisfies

$$\|\pi_h^0 \mu - \mu\|_{L^2(H_i^j)} \leq \|\pi_{h,i,j}^0 \mu - \mu\|_{L^2(H_i^j)} + \|\pi_{h,i,j}^0 \mu - \pi_h^0 \mu\|_{L^2(H_i^j)}. \quad (\text{B.3})$$

To bound the first term of (B.3), we note that the definition of $\pi_{h,i,j}^0$ implies that

$$\int_{H_i^j} \pi_{h,i,j}^0 \mu - \mu = 0.$$

We can then apply the Poincaré–Wirtinger inequality [63] on H_i^j (as H_i^j is convex) to obtain

$$\|\pi_{h,i,j}^0 \mu - \mu\|_{L^2(H_i^j)} \lesssim h |u|_{H^1(H_i^j)}. \quad (\text{B.4})$$

To bound the second term of (B.3), observe that in H_i ,

$$\pi_h^0 \mu = |H_i|^{-1} \left(\sum_{k=1}^n |H_i^k| \pi_{h,i,k}^0 \mu \right),$$

and so,

$$\begin{aligned} \pi_{h,i,j}^0 \mu - \pi_h^0 \mu &= |H_i|^{-1} \left(|H_i| \pi_{h,i,j}^0 \mu - \sum_{k=1}^n |H_i^k| \pi_{h,i,k}^0 \mu \right) \\ &= \sum_{\substack{k=1 \\ k \neq j}}^n |H_i^k| |H_i|^{-1} (\pi_{h,i,j}^0 \mu - \pi_{h,i,k}^0 \mu). \end{aligned}$$

Using lemma B.1, we see that

$$\begin{aligned} \|\pi_{h,i,j}^0 \mu - \pi_h^0 \mu\|_{L^2(H_i^j)} &\leq \sum_{\substack{k=1 \\ k \neq j}}^n |H_i^k| |H_i|^{-1} \|\pi_{h,i,j}^0 \mu - \pi_{h,i,k}^0 \mu\|_{L^2(H_i^j)} \\ &\leq h_i^{1/2} \sum_{\substack{k=1 \\ k \neq j}}^n \|\pi_{h,i,j}^0 \mu - \pi_{h,i,k}^0 \mu\|_{L^2(E_i^j)}, \end{aligned} \quad (\text{B.5})$$

where $E_i^j := \overline{H_i} \setminus \overline{H_i^j} \cap \overline{H_i^j}$ is the 1D boundary between H_i^j and the rest of H_i ,

By the triangle inequality,

$$\begin{aligned} \|\pi_{h,i,j}^0 \mu - \pi_{h,i,k}^0 \mu\|_{L^2(E_i^j)} &\leq \|\pi_{h,i,j}^0 \mu - \gamma_i^j \mu\|_{L^2(E_i^j)} + \|\pi_{h,i,k}^0 \mu - \gamma_i^{-j} \mu\|_{L^2(E_i^j)} + \|\gamma_i^j \mu - \gamma_i^{-j} \mu\|_{L^2(E_i^j)}, \end{aligned} \quad (\text{B.6})$$

where

$$\begin{aligned} \gamma_i^j \mu(\mathbf{x}) &:= \lim_{H_i^j \ni \mathbf{x}' \rightarrow \mathbf{x} \in E_i^j} \mu(\mathbf{x}'), \\ \gamma_i^{-j} \mu(\mathbf{x}) &:= \lim_{H_i \setminus H_i^j \ni \mathbf{x}' \rightarrow \mathbf{x} \in E_i^j} \mu(\mathbf{x}'). \end{aligned}$$

Combining (B.5) and (B.6), we obtain

$$\begin{aligned} \|\pi_{h,i,j}^0 \mu - \pi_h^0 \mu\|_{L^2(H_i^j)} &\lesssim \underbrace{h_i^{1/2} \|\pi_{h,i,j}^0 \mu - \gamma_i^j \mu\|_{L^2(E_i^j)}}_{\text{(I)}} + \underbrace{\sum_{\substack{k=1 \\ k \neq j}}^n h_i^{1/2} \|\pi_{h,i,k}^0 \mu - \gamma_i^{-j} \mu\|_{L^2(E_i^j)}}_{\text{(II)}} \\ &\quad + \underbrace{h_i^{1/2} \|\gamma_i^j \mu - \gamma_i^{-j} \mu\|_{L^2(E_i^j)}}_{\text{(III)}}. \end{aligned} \quad (\text{B.7})$$

To bound the first term of (B.7), we use lemma B.2 and the approximation properties

of piecewise constant functions on the barycentric grid [73, corollary 10.3] to obtain

$$\begin{aligned}
(\text{I}) &\lesssim \|\pi_{h,i,j}^0 \mu - \mu\|_{L^2(H_i^j)} + h_i |\pi_{h,i,j}^0 \mu - \mu|_{H^1(H_i^j)} \\
&= h_i \left(h_i^{-1} \|\pi_{h,i,j}^0 \mu - \mu\|_{L^2(H_i^j)} + |\pi_{h,i,j}^0 \mu - \mu|_{H^1(H_i^j)} \right) \\
&\lesssim h_i |\mu|_{H^1(H_i^j)}.
\end{aligned}$$

To bound the second term of (B.7), let H_i^l be a triangle that borders H_i^j . Let E_1 be the edge between H_i^l and H_i^j , and let E_2 be the other edge of H_i^l that is adjacent to the vertex \mathbf{v}_i . Using lemma B.2 and the triangle inequality, we see that

$$\begin{aligned}
(\text{II}) &= h_i^{1/2} \left\| \pi_{h,i,k}^0 \mu - \gamma_i^{-j} \mu \right\|_{L^2(E_1)} \\
&\lesssim \|\pi_{h,i,k}^0 \mu - \mu\|_{L^2(H_i^l)} + h_i |\pi_{h,i,k}^0 \mu - \mu|_{H^1(H_i^l)} \\
&\leq \|\pi_{h,i,k}^0 \mu - \pi_{h,i,l}^0 \mu\|_{L^2(H_i^l)} + \|\pi_{h,i,l}^0 \mu - \mu\|_{L^2(H_i^l)} + h_i |\pi_{h,i,k}^0 \mu|_{H^1(H_i^l)} + h_i |\mu|_{H^1(H_i^l)}
\end{aligned}$$

Using lemma B.1, the same approximation result as above [73, corollary 10.3], and noting that $\pi_{h,i,k}^0 \mu$ being constant implies that $|\pi_{h,i,k}^0 \mu|_{H^1(H_i^l)} = 0$, we see that

$$(\text{II}) \lesssim h_i^{1/2} \|\pi_{h,i,k}^0 \mu - \pi_{h,i,l}^0 \mu\|_{L^2(E_2)} + h_i |\mu|_{H^1(H_i^l)}. \quad (\text{B.8})$$

If $k = l$, then the first term of this will be zero. If not, we repeat the above steps until we obtain $k = l$, and so

$$(\text{II}) \lesssim h_i \sum_l |\mu|_{H^1(H_i^l)}. \quad (\text{B.9})$$

Combining all the above, we obtain

$$\|\pi_h^0 \mu - \mu\|_{L^2(\Gamma)} \lesssim h |\mu|_{H^1(\Gamma)} + h^{1/2} \sum_{k=1}^{\tilde{m}} \left\| \llbracket \gamma \rrbracket_{E_k} \mu \right\|_{L^2(E_k)}, \quad (\text{B.10})$$

where $E_1, \dots, E_{\tilde{m}}$ are the edges of the barycentrically refined grid and $\llbracket \gamma \rrbracket_{E_k} \mu$ is the jump of μ over the edge E_k . As μ is in $H^1(F_i^\Gamma)$, for each polygonal face F_i^Γ of the domain Γ , the only terms of the final sum that are non-zero are those that correspond to edges between the faces of Γ . This means that

$$h^{1/2} \sum_{k=1}^{\tilde{m}} \left\| \llbracket \gamma \rrbracket_{E_k} \mu \right\|_{L^2(E_k)} \lesssim h^{1/2} \sum_{k=1}^{m_\Gamma} \left\| \llbracket \gamma \rrbracket_{E_k^\Gamma} \mu \right\|_{L^2(E_k^\Gamma)}, \quad (\text{B.11})$$

where $E_1^\Gamma, \dots, E_{m_\Gamma}^\Gamma$ are the edges between the faces of Γ . To bound this, let E_k^Γ be the edge

between the faces F_i^Γ and F_j^Γ , let

$$\begin{aligned}\gamma_{k,i}^\Gamma \mu(\mathbf{x}) &:= \lim_{F_i^\Gamma \ni \mathbf{x}' \rightarrow \mathbf{x} \in E_k^\Gamma} \mu(\mathbf{x}') \\ \gamma_{k,j}^\Gamma \mu(\mathbf{x}) &:= \lim_{F_j^\Gamma \ni \mathbf{x}' \rightarrow \mathbf{x} \in E_k^\Gamma} \mu(\mathbf{x}')\end{aligned}$$

and observe that using the triangle inequality and [73, theorem 2.21],

$$\begin{aligned}\|[\![\gamma]\!]_{E_k^\Gamma} \mu\|_{L^2(E_k^\Gamma)} &\leq \|\gamma_{k,i}^\Gamma \mu\|_{L^2(E_k^\Gamma)} + \|\gamma_{k,j}^\Gamma \mu\|_{L^2(E_k^\Gamma)} \\ &\leq \|\mu\|_{H^{1/2}(F_i^\Gamma)} + \|\mu\|_{H^{1/2}(F_j^\Gamma)},\end{aligned}$$

and so

$$\|\pi_h^0 \mu - \mu\|_{L^2(\Gamma)} \lesssim h |\mu|_{H^1(\Gamma)} + h^{1/2} \|\mu\|_{H^{1/2}(\Gamma)}.$$

□

If μ is continuous, the following higher order approximation result holds.

Corollary B.1. *For all $\mu \in H^1(\Gamma) \cap C^0(\Gamma)$,*

$$\|\pi_h^0 \mu - \mu\|_{L^2(\Gamma)} \lesssim h |\mu|_{H^1(\Gamma)}.$$

Proof. If μ is continuous, then the final term in (B.10) will be 0. □

We now prove the following approximation result in $H^{1/2}(\Gamma)$.

Lemma B.4. *For all $\mu \in H^{1/2}(\Gamma)$,*

$$\|\pi_h^0 \mu - \mu\|_{L^2(\Gamma)} \lesssim h^{1/2} \|\mu\|_{H^{1/2}(\Gamma)}.$$

Proof. As in the proof of lemma B.3, let H_i^j be a triangle in the barycentric refinement. Observe by the definition of $\pi_{h,i,j}^0$ and the Cauchy–Schwarz inequality that

$$\begin{aligned}\|\pi_{h,i,j}^0 \mu - \mu\|_{L^2(H_i^j)}^2 &= \langle \pi_{h,i,j}^0 \mu - \mu, \pi_{h,i,j}^0 \mu - \mu \rangle \\ &= \langle \pi_{h,i,j}^0 \mu - \mu, -\mu \rangle \\ &\leq \|\pi_{h,i,j}^0 \mu - \mu\|_{L^2(\Gamma)} \|\mu\|_{L^2(\Gamma)},\end{aligned}\tag{B.12}$$

and so

$$\|\pi_{h,i,j}^0 \mu - \mu\|_{L^2(H_i^j)} \leq \|\mu\|_{L^2(\Gamma)}.\tag{B.13}$$

Using interpolation, we see that for all $s \in [0, \frac{1}{2}]$,

$$\|\pi_{h,i,j}^0 \mu - \mu\|_{L^2(H_i^j)} \leq h^{1/2} \|\mu\|_{H^{1/2}(\Gamma)}. \quad (\text{B.14})$$

Using this in the place of (B.4), plus the fact that $|1|_{H^{1/2}(\Gamma)} = 0$, the desired result can be proven in the same way as lemma B.3. \square

Using interpolation, we can prove a more general approximation result.

Corollary B.2. *Let $\sigma \in [0, \frac{1}{2}]$ and let $\mu \in H^s(\Gamma)$, for some $s \in [0, \frac{1}{2}]$.*

$$\|\pi_h^0 \mu - \mu\|_{H^\sigma(\Gamma)} \lesssim h^{s-\sigma} \|\mu\|_{H^s(\Gamma)}$$

Proof. Let $\eta \in L^2(\Gamma)$. By [39, theorem 3.5, remark 3.6],

$$\|\pi_h^0 \eta - \eta\|_{H^\sigma(\Gamma)} \lesssim h^{-\sigma} \|\pi_h^0 \eta - \eta\|_{L^2(\Gamma)}.$$

Using lemma B.4 gives

$$\|\pi_h^0 \eta - \eta\|_{H^\sigma(\Gamma)} \lesssim h^{1/2-\sigma} \|\eta\|_{H^{1/2}(\Gamma)}. \quad (\text{B.15})$$

Applying [39, theorem 3.5, remark 3.6] gives

$$\|\pi_h^0 \eta - \eta\|_{H^\sigma(\Gamma)} \lesssim h^{-\sigma} \|\eta\|_{L^2(\Gamma)}. \quad (\text{B.16})$$

We define the norm of an operator $F : H^a(\Gamma) \rightarrow H^b(\Gamma)$ by

$$\|F\|_{a,b} := \sup_{\eta \in H^a(\Gamma) \setminus \{0\}} \frac{\|F\eta\|_{H^b(\Gamma)}}{\|\eta\|_{H^a(\Gamma)}}. \quad (\text{B.17})$$

Let $v \in H^s(\Gamma)$. Using (B.16), we see that

$$\begin{aligned} \|\text{Id} - \pi_h^0\|_{0,\sigma} &= \sup_{\eta \in L^2(\Gamma) \setminus \{0\}} \frac{\|\eta - \pi_h^0 \eta\|_{H^\sigma(\Gamma)}}{\|\eta\|_{L^2(\Gamma)}} \\ &\lesssim h^{-\sigma}. \end{aligned} \quad (\text{B.18})$$

Using (B.15), we see that

$$\begin{aligned} \|\text{Id} - \pi_h^0\|_{1/2,\sigma} &= \sup_{\eta \in H^{1/2}(\Gamma) \setminus \{0\}} \frac{\|\eta - \pi_h^0 \eta\|_{H^\sigma(\Gamma)}}{\|\eta\|_{H^{1/2}(\Gamma)}} \\ &\lesssim h^{1/2-\sigma} \end{aligned} \quad (\text{B.19})$$

Therefore by [73, theorem 2.18, remark 2.23],

$$\begin{aligned} \|\text{Id} - \pi_h^0\|_{s,\sigma} &\leq \|\text{Id} - \pi_h^0\|_{0,\sigma}^{1-2s} \|\text{Id} - \pi_h^0\|_{1,\sigma}^{2s} \\ &\lesssim (h^{-\sigma})^{1-2s} (h^{1/2-\sigma})^{2s} \\ &= h^{s-\sigma}. \end{aligned} \tag{B.20}$$

Finally, we see that

$$\begin{aligned} \|\mu - \pi_h^0 \mu\|_{H^\sigma(\Gamma)} &\leq \|\text{Id} - \pi_h^0\|_{s,\sigma} \|\mu\|_{H^s(\Gamma)} \\ &\lesssim h^{s-\sigma} \|\mu\|_{H^s(\Gamma)}. \end{aligned} \tag{B.21}$$

□

For negative order norms, we have the following result.

Corollary B.3. *Let $\sigma \in [-\frac{1}{2}, 0]$ and let $\mu \in H^s(\Gamma)$, for some $s \in [0, \frac{1}{2}]$.*

$$\|\pi_h^0 \mu - \mu\|_{H^\sigma(\Gamma)} \lesssim h^{s-\sigma} \|\mu\|_{H^s(\Gamma)}$$

Proof. Using the definitions of $\|\cdot\|_{H^\sigma(\Gamma)}$ and π_h^0 , we see that

$$\begin{aligned} \|\pi_h^0 \mu - \mu\|_{H^\sigma(\Gamma)} &= \sup_{w \in H^{-\sigma}(\Gamma)} \frac{\langle w, \pi_h^0 \mu - \mu \rangle}{\|w\|_{H^{-\sigma}(\Gamma)}} \\ &= \sup_{w \in H^{-\sigma}(\Gamma)} \frac{\langle \pi_h^0 w - w, \mu \rangle}{\|w\|_{H^{-\sigma}(\Gamma)}}. \end{aligned}$$

Using the duality of $H^s(\Gamma)$ and $H^{-s}(\Gamma)$, and corollary B.2 gives

$$\begin{aligned} \|\pi_h^0 \mu - \mu\|_{H^\sigma(\Gamma)} &\leq \sup_{w \in H^{-\sigma}(\Gamma)} \frac{\|\pi_h^0 w - w\|_{H^{-s}(\Gamma)} \|\mu\|_{H^s(\Gamma)}}{\|w\|_{H^{-\sigma}(\Gamma)}} \\ &\leq \sup_{w \in H^{-\sigma}(\Gamma)} \frac{h^{s-\sigma} \|w\|_{H^{-\sigma}(\Gamma)} \|\mu\|_{H^s(\Gamma)}}{\|w\|_{H^{-\sigma}(\Gamma)}} \\ &= h^{s-\sigma} \|\mu\|_{H^s(\Gamma)}. \end{aligned}$$

□

Using this, we may now prove the first part of lemma 2.4.

Lemma B.5. $\forall \mu \in H^s(\Gamma)$,

$$\inf_{\eta_h \in \text{DUAL}_h^1(\Gamma)} \|\mu - \eta_h\|_{H^{-1/2}(\Gamma)} \lesssim h^{\xi+1/2} \|\mu\|_{H^\xi(\Gamma)}$$

where $\xi = \min(\frac{1}{2}, s)$.

Proof. Use corollary B.3 with $\sigma = -\frac{1}{2}$. \square

Note that if μ is continuous, then corollary B.1 can be used to prove that the above result holds with $\xi = \min(1, s)$.

— B.2 —

ORDER 1 DUAL SPACES, $\text{DUAL}_h^1(\Gamma)$

We define the interpolator $\iota_h^1 : L^2(\Gamma) \rightarrow \text{DUAL}_h^1(\Gamma)$, for $v \in L^2(\Gamma)$, by

$$\iota_h^1 v(\mathbf{w}_i) = v(\mathbf{w}_i) \quad \forall i \in \{1, \dots, o\}, \quad (\text{B.22})$$

where $\mathbf{w}_1, \dots, \mathbf{w}_o$ are the vertices of the triangulation \mathcal{T}_h . We now prove the following lemma.

Lemma B.6. *Let $\sigma \in [0, 1]$ and let $v \in H^s(\Gamma)$ for some $s \in (1, \frac{3}{2})$.*

$$\|v - \iota_h^1 v\|_{H^\sigma(\Gamma)} \lesssim h^{s-\sigma} \|v\|_{H^s(\Gamma)}. \quad (\text{B.23})$$

Proof. We define the norm of an operator $\mathbf{F} : H^a(\Gamma) \rightarrow H^b(\Gamma)$ by

$$\|\mathbf{F}\|_{a,b} := \sup_{w \in H^a(\Gamma) \setminus \{0\}} \frac{\|\mathbf{F}w\|_{H^b(\Gamma)}}{\|w\|_{H^a(\Gamma)}}. \quad (\text{B.24})$$

Let $v \in H^s(\Gamma)$. By [16, theorem 3.2], we know that

$$\begin{aligned} \|v - \iota_h^1 v\|_{H^1(\Gamma)} &\lesssim h^{s-1} \|v\|_{H^s(\Gamma)} \\ \|v - \iota_h^1 v\|_{L^2(\Gamma)} &\lesssim h^s \|v\|_{H^s(\Gamma)}. \end{aligned} \quad (\text{B.25})$$

Using these, we see that

$$\begin{aligned} \|\text{Id} - \iota_h^1\|_{s,0} &= \sup_{w \in H^s(\Gamma) \setminus \{0\}} \frac{\|w - \iota_h^1 w\|_{L^2(\Gamma)}}{\|w\|_{H^s(\Gamma)}} \\ &\lesssim h^s \end{aligned} \quad (\text{B.26})$$

$$\begin{aligned} \|\text{Id} - \iota_h^1\|_{s,1} &= \sup_{w \in H^s(\Gamma) \setminus \{0\}} \frac{\|w - \iota_h^1 w\|_{H^1(\Gamma)}}{\|w\|_{H^s(\Gamma)}} \\ &\lesssim h^{s-1} \end{aligned} \quad (\text{B.27})$$

Therefore by [73, theorem 2.18, remark 2.23],

$$\begin{aligned} \|\text{Id} - \iota_h^1\|_{s,\sigma} &\leq \|\text{Id} - \iota_h^1\|_{s,0}^{1-\sigma} \|\text{Id} - \iota_h^1\|_{s,1}^\sigma \\ &\lesssim (h^s)^{1-\sigma} (h^{s-1})^\sigma \\ &= h^{s-\sigma} \end{aligned} \tag{B.28}$$

Finally, we see that

$$\begin{aligned} \|v - \iota_h^1 v\|_{H^\sigma(\Gamma)} &\leq \|\text{Id} - \iota_h^1\|_{s,\sigma} \|v\|_{H^s(\Gamma)} \\ &\lesssim h^{s-\sigma} \|v\|_{H^s(\Gamma)}. \end{aligned} \tag{B.29}$$

□

Using this, we may now prove the second part of lemma 2.4.

Lemma B.7. *Let $\epsilon > 0$. $\forall v \in H^s(\Gamma)$,*

$$\inf_{w_h \in \text{DUAL}_h^1(\Gamma)} \|v - w_h\|_{H^{1/2}(\Gamma)} \lesssim h^{\zeta-1/2} \|v\|_{H^\zeta(\Gamma)}$$

where $\zeta = \min(\frac{3}{2}, s)$.

Proof. Use lemma B.6 with $\sigma = \frac{1}{2}$.

□

APPENDIX C

WEAK IMPOSITION OF BOUNDARY CONDITIONS WITH DUAL DISCRETE SPACES

All the methods introduced in section 3.1 are written as the sum of the multitrace operator \mathcal{A} and a boundary condition operator \mathcal{B} . We write this generally as: Find $(u, \lambda) \in \mathbb{V}$ such that

$$\mathcal{A}[(u, \lambda), (v, \mu)] + \mathcal{B}[(u, \lambda), (v, \mu)] = \mathcal{L}(v, \mu) \quad \forall (v, \mu) \in \mathbb{V}. \quad (3.31)$$

In this appendix, we consider this general problem when the test and trial spaces are discretised using different finite dimensional spaces. In particular, we look to solve: Find $(u_h, \lambda_h) \in \mathbb{V}_h$ such that

$$\mathcal{A}[(u_h, \lambda_h), (v'_h, \mu'_h)] + \mathcal{B}[(u_h, \lambda_h), (v'_h, \mu'_h)] = \mathcal{L}(v'_h, \mu'_h) \quad \forall (v'_h, \mu'_h) \in \mathbb{V}'_h, \quad (3.41)$$

where $\mathbb{V}_h = \mathbb{P}_h^1(\Gamma) \times \text{DP}_h^0(\Gamma)$ and $\mathbb{V}'_h = \text{DUAL}_h^1(\Gamma) \times \text{DUAL}_h^0(\Gamma)$ as in chapter 3.

Let \mathbb{W} be a product Hilbert space for the primal and flux variables, such that $\mathbb{V}_h \subset \mathbb{W} \subset \mathbb{V}$ and $\mathbb{V}'_h \subset \mathbb{W} \subset \mathbb{V}$. Let $\|\cdot\|_{\mathcal{B}}$ be a norm defined on \mathbb{W} , such that for all $(v, \mu) \in \mathbb{W}$, $\|(v, \mu)\|_{\mathcal{B}} \geq \|(v, \mu)\|_{\mathbb{V}}$.

To prove the results in this appendix, we will use assumptions 3.1, 3.3 and 3.4 and the following version of assumption 3.2.

Assumption C.1 (Discrete inf-sup stability). *There exists $\alpha > 0$ such that $\forall (v_h, \mu_h) \in \mathbb{V}_h$*

$$\alpha \|(v_h, \mu_h)\|_{\mathcal{B}} \leq \sup_{(w'_h, \eta'_h) \in \mathbb{V}'_h \setminus \{0\}} \frac{\mathcal{A}[(v_h, \mu_h), (w'_h, \eta'_h)] + \mathcal{B}[(v_h, \mu_h), (w'_h, \eta'_h)]}{\|(w'_h, \eta'_h)\|_{\mathcal{B}}},$$

and $\forall (w'_h, \eta'_h) \in \mathbb{V}'_h \setminus \{0\}$

$$\sup_{(v_h, \mu_h) \in \mathbb{V}_h} |\mathcal{A}[(v_h, \mu_h), (w'_h, \eta'_h)] + \mathcal{B}[(v_h, \mu_h), (w'_h, \eta'_h)]| > 0.$$

Propositions 3.1 to 3.3 and corollaries 3.1 and 3.2 can be proved with assumption C.1 in the place of assumption 3.2 in the same way as in section 3.2.

In order to prove that assumption C.1 holds, we must assume the following approxima-

tion result in \mathbb{V}'_h . This can be proved for each problem in the same way as assumption 3.4 is proved in chapter 3 and using the results in appendix B.

Assumption C.2 (Approximation). $\forall (v, \mu) \in H^s(\Gamma) \times H^r(\Gamma)$,

$$\inf_{(w'_h, \eta'_h) \in \mathbb{V}'_h} \|(v - w'_h, \mu - \eta'_h)\|_* \lesssim h^{\zeta-1/2} |v|_{H^\zeta(\Gamma)} + h^{\xi+1/2} |\mu|_{H^\xi(\Gamma)},$$

where $\zeta = \min(k + \frac{1}{2}, s)$, $\xi = \min(l + \frac{1}{2}, r)$, $s \geq \frac{1}{2}$ and $r \geq -\frac{1}{2}$.

We define π_h as in chapter 5. Analogously to chapter 5, we define the projections $\tilde{\pi}_h^1 : H^{1/2}(\Gamma) \rightarrow \text{DUAL}_h^1(\Gamma)$ and $\tilde{\pi}_h^0 : H^{-1/2}(\Gamma) \rightarrow \text{DUAL}_h^0(\Gamma)$, for $v \in H^{1/2}(\Gamma)$ and $\mu \in H^{-1/2}(\Gamma)$ by

$$\begin{aligned} \langle \tilde{\pi}_h^1 v, w_h \rangle_\Gamma &= \langle v, w_h \rangle_\Gamma & \forall w_h \in \text{DUAL}_h^1(\Gamma), \\ \langle \tilde{\pi}_h^0 \mu, \eta_h \rangle_{H^{-1/2}(\Gamma)} &= \langle \mu, \eta_h \rangle_{H^{-1/2}(\Gamma)} & \forall \eta_h \in \text{DUAL}_h^0(\Gamma), \end{aligned}$$

and we define $\pi'_h : \mathbb{W} \rightarrow \mathbb{V}'_h$, for $(v, \mu) \in \mathbb{W}$, by

$$\pi'_h(v, \mu) = (\tilde{\pi}_h^1 v, \tilde{\pi}_h^0 \mu).$$

It is clear from this definition that for all $(v'_h, \mu'_h) \in \mathbb{V}'_h$, $\pi'_h(v'_h, \mu'_h) = (v'_h, \mu'_h)$. As given in the following lemma, π'_h is bounded.

Lemma C.1. *There exists $c > 0$ such that for all $(v, \mu) \in \mathbb{W}$,*

$$\|\pi'_h(v, \mu)\|_{\mathbb{V}} \leq c \|(v, \mu)\|_{\mathbb{W}}.$$

Proof. This can be proved in the same way as lemma 5.1. □

In order to prove that that results in chapter 3 apply in this case, we must assume the following additional assumptions.

Assumption C.3 (Quasi-continuity). *There exists $M > 0$ such that for all $(v_h, \mu_h) \in \mathbb{V}_h$ and $(w, \eta) \in \mathbb{W}$,*

$$(\mathcal{A} + \mathcal{B})[(v_h, \mu_h), (w, \eta) - \pi'_h(w, \eta)] \leq M \|(v_h, \mu_h)\|_{\mathcal{B}} \|(w, \eta) - \pi'_h(w, \eta)\|_{\mathbb{V}}.$$

There exists $M > 0$ such that for all $(v'_h, \mu'_h) \in \mathbb{V}'_h$ and $(w, \eta) \in \mathbb{W}$,

$$(\mathcal{A} + \mathcal{B})[(w, \eta) - \pi_h(w, \eta), (v'_h, \mu'_h)] \leq M \|(v'_h, \mu'_h)\|_{\mathcal{B}} \|(w, \eta) - \pi_h(w, \eta)\|_{\mathbb{V}}.$$

Assumption C.4 (Asymptotic convergence). *Let $\epsilon > 0$ and $(w, \eta) \in \mathbb{W}$. There exists $h_0 > 0$ such that for all $h < h_0$,*

$$\|(w, \eta) - \pi'_h(w, \eta)\|_{\mathcal{B}} < \epsilon.$$

We expect that these can be proved for each problem in the same way that assumptions 5.3 and 5.4 were shown to hold in chapter 5

We can prove that the following results analagous to lemma 5.3 and corollary 5.1 in chapter 5.

Lemma C.2. *Let $(v, \mu) \in \mathbb{W}$. If assumption C.2 holds, then for any $\epsilon > 0$, there is an $h_0 > 0$ such that for all $h < h_0$,*

$$\inf_{(w'_h, \eta'_h) \in \mathbb{V}'_h} \|(v, \mu) - (w'_h, \eta'_h)\|_{\mathbb{V}} < \epsilon.$$

Proof. This can be proved in the same was as lemma 5.3. \square

Corollary C.1. *Let $(v, \mu) \in \mathbb{W}$. If assumption 3.4 holds, then for any $\epsilon > 0$, there is an $h_0 > 0$ such that for all $h < h_0$,*

$$\|(v, \mu) - \pi_h(v, \mu)\|_{\mathbb{V}} < \epsilon.$$

Proof. This can be proved in the same way as corollary 5.1, using lemma C.1 in the place of lemma 5.1. \square

We would now like to prove that assumption C.1 holds. We have yet to complete this proof, so we leave the following as a conjecture.

Conjecture C.1 (Discrete inf-sup stability). *If assumptions 3.1, 3.3 and C.2 hold, then assumption C.1 holds.*

As we did when proving lemma 5.4, we attempt to prove this by following the proof of [11, theorem 2.2]. We suppose (for a contradiction) that the first part of assumption C.1 does not hold. This implies that there exists a sequence $(h_n)_{n \in \mathbb{N}}$ such that $\lim_{n \rightarrow \infty} h_n = 0$, and for each n there exists $(v_{h_n}, \mu_{h_n}) \in \mathbb{V}_{h_n}$ such that

$$\|(v_{h_n}, \mu_{h_n})\|_{\mathcal{B}} = 1 \tag{C.1}$$

$$\sup_{(w'_{h_n}, \eta'_{h_n}) \in \mathbb{V}'_{h_n}} \frac{(\mathcal{A} + \mathcal{B})[(v_{h_n}, \mu_{h_n}), (w'_{h_n}, \eta'_{h_n})]}{\|(w'_{h_n}, \eta'_{h_n})\|_{\mathcal{B}}} < k_n, \tag{C.2}$$

where $k_n > 0$ and $\lim_{m \rightarrow \infty} k_n = 0$.

Let $(t, \kappa) \in \mathbb{W} \setminus \{0\}$. We use the triangle inequality, assumption C.3 and (C.1) and (C.2) to obtain

$$\begin{aligned} L &:= |(\mathcal{A} + \mathcal{B})[(v_{h_n}, \mu_{h_n}), (t, \kappa)]| \\ &\leq |(\mathcal{A} + \mathcal{B})[(v_{h_n}, \mu_{h_n}), (t, \kappa) - \pi'_{h_n}(t, \kappa)]| + |(\mathcal{A} + \mathcal{B})[(v_{h_n}, \mu_{h_n}), \pi'_{h_n}(t, \kappa)]| \\ &\leq M \|(t, \kappa) - \pi'_{h_n}(t, \kappa)\|_{\mathcal{B}} + k_n \|\pi'_{h_n}(t, \kappa)\|_{\mathcal{B}}. \end{aligned} \tag{C.3}$$

Let $\epsilon > 0$. By corollary C.1, that there is an $N \in \mathbb{N}$ such that for all $n > N$,

$$\|(t, \kappa) - \pi'_{h_n}(t, \kappa)\|_{\mathcal{B}} < \epsilon, \quad (\text{C.4})$$

$$k_n < \epsilon. \quad (\text{C.5})$$

Using the triangle inequality and assumption C.4, we see that

$$\begin{aligned} \|\pi'_{h_n}(t, \kappa)\|_{\mathcal{B}} &\leq \|(t, \kappa) - \pi'_{h_n}(t, \kappa)\|_{\mathcal{B}} + \|(t, \kappa)\|_{\mathcal{B}} \\ &< \epsilon + \|(t, \kappa)\|_{\mathcal{B}}. \end{aligned} \quad (\text{C.6})$$

Substituting (C.4) to (C.6) into (C.3), we obtain

$$\begin{aligned} L &\leq M\epsilon + k_n\epsilon + k_n \|(t, \kappa)\|_{\mathcal{B}} \\ &\leq M\epsilon + \epsilon^2 + \epsilon \|(t, \kappa)\|_{\mathcal{B}}. \end{aligned} \quad (\text{C.7})$$

We would like to now use assumption 3.1 to show that

$$\begin{aligned} \alpha \|(v_{h_n}, \mu_{h_n})\|_{\mathcal{B}} &\leq \sup_{\substack{(t, \kappa) \in \mathbb{W} \\ \|(t, \kappa)\|_{\mathcal{B}}=1}} (\mathcal{A} + \mathcal{B})[(v_{h_n}, \mu_{h_n}), (t, \kappa)] \\ &\leq M\epsilon + \epsilon^2 + \epsilon. \end{aligned} \quad (\text{C.8})$$

However, doing so requires that h is smaller than the value of h_0 for each $(t, \kappa) \in \mathbb{W}$. There is no guarantee that the infimum of these values of h_0 is greater than 0, and so we cannot do this.

When proving lemma 5.4, we used the fact that the Helmholtz multitrace operator is a compact perturbation of an elliptic operator, then used the results we proved in chapter 3 on this perturbation. This approach does not appear to work here, however, as the difference between the formulation here and in chapter 3 is in the spaces and not the operators.

</APPENDICES>

BIBLIOGRAPHY

- [1] P. Alart and A. Curnier. A mixed formulation for frictional contact problems prone to Newton like solution methods. *Computer Methods in Applied Mechanics and Engineering*, 92(3):353–375, 1991.
- [2] F. P. Andriulli, K. Cools, H. Bağci, F. Olyslager, A. Buffa, S. Christiansen, and E. Michielssen. A multiplicative Calderón preconditioner for the electric field integral equation. *IEEE Transactions on Antennas and Propagation*, 56(8):2398–2412, 2008.
- [3] I. Babuška. The finite element method with penalty. *Mathematics of Computation*, 27(122):221–228, 1973.
- [4] I. Babuška and A. K. Aziz. Survey lectures on the mathematical foundations of the finite element method. In *The mathematical foundations of the finite element method with applications to partial differential equations*, pages 1–359. Academic Press, 1972. With the collaboration of G. Fix and R. B. Kellogg.
- [5] H. Bagci, F. Andriulli, K. Cools, F. Olyslager, and E. Michielssen. A Calderón Multiplicative Preconditioner for the Combined Field Integral Equation. *IEEE Transactions on Antennas and Propagation*, 57(10):3387–3392, 2009.
- [6] L. Baratchart, L. Bourgeois, and J. Leblond. Uniqueness results for inverse Robin problems with bounded coefficient. *Journal of Functional Analysis*, 270(7):2508–2542, 2016.
- [7] M. Bebendorf. Hierarchical LU decomposition-based preconditioners for BEM. *Computing*, 74(3):225–247, 2005.
- [8] R. Becker, P. Hansbo, and R. Stenberg. A finite element method for domain decomposition with non-matching grids. *M2AN. Mathematical Modelling and Numerical Analysis*, 37(2):209–225, 2003.
- [9] T. Betcke, E. Burman, and M. W. Scroggs. Boundary element methods with weakly imposed boundary conditions. *SIAM Journal on Scientific Computing*, 41(3):A1357–A1384, 2019.
- [10] T. Betcke, M. W. Scroggs, and W. Śmigaj. Product algebras for Galerkin discretizations of boundary integral operators and their applications. submitted to *ACM Transactions on Mathematical Software*, 2019.
- [11] A. S. Bonnet-Ben Dhia, P. Ciarlet Jr., and C. M. Zwölf. Time harmonic wave diffraction problems in materials with sign-shifting coefficients. *Journal of Computational and Applied Mathematics*, 234:1912–1919, 2010.
- [12] S. Börm, L. Grasedyck, and W. Hackbusch. Hierarchical matrices. Technical report, Max-Planck-Institut für Mathematik in den Naturwissenschaften, 2003.

-
- [13] H. Brezis and P. Mironescu. Gagliardo-Nirenberg, composition and products in fractional Sobolev spaces. *Journal of Evolution Equations*, 1(4):387–404, 2001. Dedicated to the memory of Tosio Kato.
- [14] O. Bruno, T. Elling, and C. Turc. Regularized integral equations and fast high-order solvers for sound-hard acoustic scattering problems. *International Journal for Numerical Methods in Engineering*, 91:1045–1072, 2012.
- [15] A. Buffa. Trace theorems on non-smooth boundaries for functional spaces related to Maxwell equations: an overview. In P. Monk, C. Carstensen, S. Funken, W. Hackbusch, and R. H. W. Hoppe, editors, *Computational electromagnetics*, volume 28 of *Lecture Notes in Computational Science and Engineering*, pages 23–34. Springer, 2003.
- [16] A. Buffa and S. H. Christiansen. A dual finite element complex on the barycentric refinement. *Mathematics of Computation*, 76(260):1743–1769, 2007.
- [17] A. Buffa and P. Ciarlet. On traces for functional spaces related to Maxwell’s equations Part I: An integration by parts formula in Lipschitz polyhedra. *Mathematical Methods in the Applied Sciences*, 24(1):9–30, 2001.
- [18] A. Buffa and P. Ciarlet. On traces for functional spaces related to Maxwell’s equations Part II: Hodge decompositions on the boundary of Lipschitz polyhedra and applications. *Mathematical Methods in the Applied Sciences*, 24(1):31–48, 2001.
- [19] A. Buffa, M. Costabel, and D. Sheen. On traces for $\mathbf{H}(\mathbf{curl}, \Omega)$ in Lipschitz domains. *Journal of Mathematical Analysis and Applications*, 276(2):845–867, 2002.
- [20] A. Buffa and R. Hiptmair. Galerkin boundary element methods for electromagnetic scattering. In M. Ainsworth, P. Davies, D. Duncan, B. Rynne, and P. Martin, editors, *Topics in Computational Wave Propagation: Direct and Inverse Problems*, volume 31 of *Lecture Notes in Computational Science and Engineering*, pages 83–124. Springer, 2003.
- [21] E. Burman, S. Frei, and M. W. Scroggs. Weak imposition of Signorini boundary conditions on the boundary element method. submitted to *SIAM Journal on Numerical Analysis*, 2019.
- [22] E. Burman, P. Hansbo, and M. G. Larson. The penalty free Nitsche method and nonconforming finite elements for the Signorini problem. *ArXiv e-prints*, 2016.
- [23] A. Chernov and P. Hansbo. Nonconforming hp-FE/BE coupling for interface problems based on Nitsche’s method. Unpublished.
- [24] F. Chouly and N. Heuer. A Nitsche-based domain decomposition method for hyper-singular integral equations. *Numerische Mathematik*, 121(4):705–729, 2012.
- [25] F. Chouly and P. Hild. A Nitsche-based method for unilateral contact problems: numerical analysis. *SIAM Journal on Numerical Analysis*, 51(2):1295–1307, 2013.
- [26] F. Chouly, P. Hild, and Y. Renard. Symmetric and non-symmetric variants of Nitsche’s method for contact problems in elasticity: theory and numerical experiments. *Mathematics of Computation*, 84(293):1089–1112, 2015.

- [27] S. H. Christiansen and J.-C. Nédélec. A preconditioner for the electric field integral equation based on Calderón formulas. *SIAM Journal on Numerical Analysis*, 40(3):1100–1135, 2002.
- [28] D. Colton and R. Kress. *Integral Equation Methods in Scattering Theory*. Wiley, 1983.
- [29] H. Contopanagos, B. Dembart, M. Epton, J. J. Ottusch, V. Rokhlin, J. L. Visher, and S. M. Wandzura. Well-conditioned boundary integral equations for three-dimensional electromagnetic scattering. *IEEE transactions on antennas and propagation*, 50(12):1824–1830, 2002.
- [30] K. Cools, F. P. Andriulli, D. De Zutter, and E. Michielssen. Accurate and conforming mixed discretisation of the MFIE. *IEEE antennas and wireless propagation letters*, 10:528–531, 2011.
- [31] M. Costabel. Boundary integral operators on Lipschitz domains: Elementary results. *Siam Journal on Mathematical Analysis*, 19:613–626, 1988.
- [32] M. Costabel and E. Stephan. Boundary integral equations for mixed boundary value problems in polygonal domains and Galerkin approximation. *Banach Center Publications*, 15(1):175–251, 1985.
- [33] E. Di Nezza, G. Palatucci, and E. Valdinoci. Hitchhiker’s guide to the fractional Sobolev spaces. *Bulletin des Sciences Mathématiques*, 136(5):521–573, 2012.
- [34] A. Ern and J.-L. Guermond. *Theory and Practice of Finite Elements*, volume 159 of *Applied Mathematical Sciences*. Springer-Verlag, 2004.
- [35] D. Fleisch. *A Student’s Guide to Maxwell’s Equations*. Student’s Guides. Cambridge University Press, 2008.
- [36] W. Fong and E. Darve. The black-box fast multipole method. *Journal of Computational Physics*, 228(23):8712–8725, 2009.
- [37] G. Gatica, M. Healey, and N. Heuer. The boundary element method with Lagrangian multipliers. *Numerical Methods for Partial Differential Equations*, 25(6):1303–1319, 2009.
- [38] Google Scholar. Citation count. <https://scholar.google.co.uk/scholar?cites=17530791602214284423,11433496395088984366>. [Online; accessed 2019-05-10].
- [39] I. G. Graham, W. Hackbusch, and S. Sauter. Discrete boundary element methods on general meshes in 3D. *Numerische Mathematik*, 86(1):103–137, 2000.
- [40] W. Hackbusch. *Hierarchical matrices: algorithms and analysis*, volume 49 of *Springer Series in Computational Mathematics*. Springer, 2015.
- [41] H. Han. The boundary finite element methods for Signorini problems. In Y. Zhu and B. Guo, editors, *Numerical Methods for Partial Differential Equations*, number 1297 in *Lecture Notes in Mathematics*, pages 38–49. Springer, 1987.
- [42] H. Han. A direct boundary element method for Signorini problems. *Mathematics of Computation*, 55(191):115–128, 1990.

-
- [43] M. R. Hestenes and E. Stiefel. Methods of conjugate gradients for solving linear systems. *Journal of research of the National Bureau of Standards*, 49:409–436, 1952.
- [44] R. Hiptmair. Operator preconditioning. *Computers and Mathematics with Applications*, 52:699–706, 2006.
- [45] B. Jin and J. Zou. Numerical estimation of the Robin coefficient in a stationary diffusion equation. *IMA Journal of Numerical Analysis*, 30(3):677–701, 2010.
- [46] E. Jones, T. Oliphant, P. Peterson, et al. SciPy: Open source scientific tools for Python. <http://www.scipy.org/>, 2001. [Online; accessed 2019-05-10].
- [47] M. Juntunen and R. Stenberg. Nitsche’s method for general boundary conditions. *Mathematics of Computation*, 78(267):1353–1374, 2009.
- [48] R. C. Kirby. From Functional Analysis to Iterative Methods. *SIAM Review*, 52(2):269–293, 2010.
- [49] R. C. Kirby, A. Logg, M. E. Rognes, and A. R. Terrel. Common and unusual finite elements. In A. Logg, K.-A. Mardal, and G. Wells, editors, *Automated Solution of Differential Equations by the Finite Element Method: The FEniCS Book*, pages 95–119. Springer, 2012.
- [50] U. Langer and O. Steinbach. Boundary element tearing and interconnecting methods. *Computing. Archives for Scientific Computing*, 71(3):205–228, 2003.
- [51] U. Langer and O. Steinbach. Coupled boundary and finite element tearing and interconnecting methods. In T. J. Barth, M. Griebel, D. E. Keyes, R. M. Nieminen, D. Roose, T. Schlick, R. Kornhuber, R. Hoppe, J. Périaux, O. Pironneau, O. Widlund, and J. Xu, editors, *Domain Decomposition Methods in Science and Engineering*, volume 40 of *Lecture Notes in Computational Science and Engineering*, pages 83–97. Springer, 2005.
- [52] R. Lazarov. Inf-sup condition and Banach–Nečas–Babuška theorem. http://www.math.tamu.edu/~raytcho.lazarov/access/Sofia_L_04.pdf, 2013. [Online; accessed 2019-05-10].
- [53] J.-L. Lions and G. Stampacchia. Variational inequalities. *Communications on Pure and Applied Mathematics*, 20:493–519, 1967.
- [54] M. Maischak and E. P. Stephan. Adaptive hp-versions of BEM for Signorini problems. *Applied Numerical Mathematics*, 54(3):425–449, 2005. Selected papers from the 16th Chemnitz Finite Element Symposium 2003.
- [55] W. McLean. *Strongly elliptic systems and boundary integral equations*. Cambridge University Press, 2000.
- [56] P. Meury. *Stable finite element boundary element Galerkin schemes for acoustic and electromagnetic scattering*. PhD thesis, ETH Zurich, 2007.
- [57] J.-C. Nédélec. Mixed finite elements in \mathbb{R}^3 . *Numerische Mathematik*, 35(3):315–341, 1980.

- [58] J.-C. Nédélec. *Acoustic and electromagnetic equations*, volume 144 of *Applied Mathematical Sciences*. Springer-Verlag, 2001. Integral representations for harmonic problems.
- [59] J. Nečas. Sur une méthode pour résoudre les équations aux dérivées partielles du type elliptique, voisine de la variationnelle. *Annali della Scuola Normale Superiore di Pisa - Classe di Scienze*, 16(4):305–326, 1962.
- [60] J. Nitsche. Über ein Variationsprinzip zur Lösung von Dirichlet-Problemen bei Verwendung von Teilräumen, die keinen Randbedingungen unterworfen sind. *Abhandlungen aus dem Mathematischen Seminar der Universität Hamburg*, 36:9–15, 1971. Collection of articles dedicated to Lothar Collatz on his sixtieth birthday.
- [61] R. H. Nochetto, S. K. G., and A. Veiser. Theory of adaptive finite element methods: an introduction. In *Multiscale, Nonlinear, and Adaptive Approximation*, pages 409–542. Springer, 2009.
- [62] C. Paige and M. Saunders. Solution of sparse indefinite systems of linear equations. *SIAM Journal on Numerical Analysis*, 12(4):617–629, 1975.
- [63] L. E. Payne and H. F. Weinberger. An optimal Poincaré inequality for convex domains. *Archive for Rational Mechanics and Analysis*, 5(1):286–292, 1960.
- [64] S. M. Rao, D. R. Wilton, and A. W. Glisson. Electromagnetic scattering by surfaces of arbitrary shape. *IEEE Transactions on antennas and propagation*, 30(3):409–418, 1982.
- [65] P.-A. Raviart and J.-M. Thomas. A mixed finite element method for 2nd order elliptic problems. In I. Galligani and E. Magenes, editors, *Mathematical aspects of finite element methods*, volume 606 of *Lecture Notes in Mathematics*, pages 292–315. Springer, 1977.
- [66] Y. Saad and M. H. Schultz. GMRES: A generalized minimal residual algorithm for solving nonsymmetric linear systems. *SIAM Journal on Scientific and Statistical Computing*, 7(3):856–869, 1986.
- [67] H. Schmit and G. Schneider. Boundary element solution of the Dirichlet–Signorini problem by a penalty method. *Applicable Analysis*, 51(1–4):175–186, 1993.
- [68] M. W. Scroggs, T. Betcke, E. Burman, W. Śmigaj, and E. van ’t Wout. Software frameworks for integral equations in electromagnetic scattering based on Calderón identities. *Computers & Mathematics with Applications*, 74(11):2897–2914, 2017. Proceedings of the International Conference on Computational Mathematics and Inverse Problems, On occasion of the 60th birthday of Prof. Peter Monk.
- [69] A. Signorini. Questioni di elasticità non linearizzata e semilinearizzata. *Rendiconti di Matematica e delle sue Applicazioni*, 5(18):95–139, 1959.
- [70] W. Śmigaj, T. Betcke, S. Arridge, J. Phillips, and M. Schweiger. Solving boundary integral problems with BEM++. *ACM Transactions on mathematical software*, 41(2):6:1–6:40, 2015.
- [71] W. Spann. On the boundary element method for the Signorini problem of the Laplacian. *Numerische Mathematik*, 65(1):337–356, 1993.

-
- [72] O. Steinbach. On a generalized L_2 projection and some related stability estimates in Sobolev spaces. *Numerische Mathematik*, 90:775–786, 2002.
- [73] O. Steinbach. *Numerical approximation methods for elliptic boundary value problems*. Springer-Verlag, 2008. Translated from the 2003 German original.
- [74] O. Steinbach. Boundary element methods for variational inequalities. *Numerische Mathematik*, 126(1):173–197, 2014.
- [75] O. Steinbach and W. L. Wendland. The construction of some efficient preconditioners in the boundary element method. *Advances in Computational Mathematics*, 9(1):191–216, 1998.
- [76] O. Steinbach and M. Windisch. Stable boundary element domain decomposition methods for the Helmholtz equation. *Numerische Mathematik*, 118(1):171–195, 2011.
- [77] E. Stephan. Boundary integral equations for mixed boundary value problems in \mathbb{R}^3 . *Mathematische Nachrichten*, 134(1):21–53, 1987.
- [78] L. Tartar. On the characterization of traces of a Sobolev space used for Maxwell’s equation. In A.-Y. Le Roux, editor, *Proceedings of a Meeting Held in Bordeaux, in Honour of Michel Artola*, 1997.
- [79] R. Temam. *Navier–Stokes equations. Theory and numerical analysis*, volume 2 of *Studies in Mathematics and its Applications*. North-Holland, 1979.
- [80] T. Von Petersdorff and R. Leis. Boundary integral equations for mixed Dirichlet, Neumann and transmission problems. *Mathematical Methods in the Applied Sciences*, 11(2):185–213, 1989.
- [81] T. Von Petersdorff and E. P. Stephan. Regularity of mixed boundary value problems in \mathbb{R}^3 and boundary element methods on graded meshes. *Mathematical Methods in the Applied Sciences*, 12(3):229–249, 1990.
- [82] A. C. Woo, H. T. G. Wang, M. J. Schuh, and M. L. Sanders. Benchmark radar targets for the validation of computational electromagnetics programs. *IEEE antennas and propagation magazine*, 35(1):84–89, 1993.
- [83] J. Xu and L. Zikatanov. Some observations on Babuška and Brezzi theories. *Numerische Mathematik*, 94(1):195–202, 2003.
- [84] S. Zhang and X. Li. An augmented Lagrangian method for the Signorini boundary value problem with BEM. *Boundary Value Problems*, 2016(1):62, 2016.
- [85] S. Zhang and J. Zhu. A projection iterative algorithm boundary element method for the Signorini problem. *Engineering Analysis with Boundary Elements*, 37(1):176–181, 2013.